An investigation into the effects of *ex vivo* antioxidant treatment on the regenerative potential of mesenchymal stem cells following prolonged exposure to a pathological microenvironment associated with diabetes mellitus *in vivo*.

by

Yashar Mehrbani Azar

Dissertation presented for the degree of
PhD in Internal Medicine in the
Faculty of Medicine and Health Sciences at
Stellenbosch University

Supervisor: Dr Mari van de Vyver

Co-supervisor: Prof Carola Ulrike Niesler

December 2019

Declaration

By submitting this dissertation electronically, I declare that the entirety of the work contained therein is my own, original work, that I am the sole author thereof (save to the extent explicitly otherwise stated), that reproduction and publication thereof by Stellenbosch University will not infringe any third party rights and that I have not previously in its entirety or in part submitted it for obtaining any qualification.

December 2019

Abstract

Obesity-associated type-2 diabetes mellitus (T2DM) is a multifactorial disease that causes severe co-morbidities such as non-healing wounds. Non-healing diabetic wounds affect 15-25% of all diabetic patients and are responsible for nearly 50% of all diabetes-related hospital admissions.

Mesenchymal stem cell (MSC) therapy is a promising therapeutic option, as MSCs can 'sense' the clinical status of the wound and restore the micro-environment through paracrine signalling to promote regeneration. However, the pathological nature of the niche micro-environment does limit the use of autologous MSC therapy in diabetic patients, since prolonged exposure of endogenous MSCs to the diabetic environment *in vivo* reduces their ability to respond to environmental cues. Thus, the advancement of autologous cell therapy depends on (a) a better understanding of how the pathogenesis of T2DM affects the multifunctional properties of MSCs, and (b) the development of new strategies to restore the function of these impaired MSCs before they are used for transplantation.

This study investigated whether *ex vivo* antioxidant [N-acetylcysteine (7.5 mM NAC) and ascorbic acid 2-phosphate (0.6 mM AAP)] treatment could restore the paracrine responsiveness, growth rate, migration ability and viability of impaired diabetic MSCs, and, if so, whether this restored state could be maintained in the presence of diabetic wound fluid (DWF).

Bone marrow-derived MSCs were isolated from eight-week-old wild-type C57BL/6J mice (healthy control: MSC^{WT}) (n = 24) and obese diabetic B6.Cg-Lep^{ob}/J mice (impaired/dysfunctional: MSC^{ob}) (n = 24). The *ex vivo* treatment groups (MSC^{WT} *vs* MSC^{ob}) were (a) no treatment (baseline phenotype), (b) DWF-stimulated (baseline response), (c) antioxidant-preconditioned (preconditioned phenotype), and (d) antioxidant-preconditioned with subsequent DWF stimulation (preconditioned response). For these *ex vivo* experiments, DWF was harvested over a period of 28 days from bilateral, dorsal, full-thickness excisional wounds created on obese diabetic mice (B6.Cg-Lep^{ob}/J) (n = 7). The optimum concentration of antioxidants was determined using a dose-response experiment in immortalised C3H10/T1/2 cells.

This study demonstrated that the expansion of primary MSCs (MSC^{WT} and MSC^{ob}) in the presence of antioxidants improved the *ex vivo* viability of cells and had a protective effect against the toxicity of DWF. The paracrine responsiveness of MSC^{WT} and MSC^{ob} (with and without antioxidant preconditioning) was furthermore determined at both the molecular level (mRNA expression of 84 cytokines and receptors, qPCR microarray) and protein level (23-plex bead-array Luminex assay). At baseline, 31 genes were overexpressed (more than twofold) and 39 genes were under-expressed (more than twofold) in MSC^{ob} versus MSC^{WT}. In conditioned medium, significant baseline differences ($p < 0.05$) were detected for two pro-inflammatory cytokines (TNFα and IFNγ), four chemokines (KC, G-CSF, Eotaxin and MCP1) and one anti-inflammatory cytokine (IL10). Following DWF stimulation, significant differences ($p < 0.05$) were detected in the secretion of two chemokines (GM-CSF and Eotaxin), three pro-inflammatory cytokines (TNFα, IFNγ and IL9) and four anti-inflammatory cytokines (IL10, IL4, IL13 and IL3). Antioxidant preconditioning significantly dampened the excessive TNFα

response observed in MSC^{ob} and improved the secretion of IL10. This suggests that combined *ex vivo* treatment of autologous MSCs with NAC and AAP could potentially be an effective strategy to restore the paracrine function of impaired diabetic MSCs before transplantation. However, despite improved viability and a restored paracrine response, antioxidant preconditioning could not rescue the proliferation and migration capacity of severely impaired diabetic MSCs.

Opsomming

Obesiteitsverwante tipe 2-diabetes mellitus (T2DM) is ’n komplekse siekte wat verskeie ko-morbiditeite veroorsaak, waaronder wonde wat sukkel om te genees. Sowat 15-25% van alle diabetespasiënte het las van sulke wonde, en bykans 50% van alle diabetesverwante hospitaalopnames kan hieraan toegeskryf word.

Mesenchimale stamsel- (MSS-)terapie is ’n belowende behandelingsmoontlikheid omdat MSS’e die kliniese status van ’n wond kan ‘aanvoel’ en die mikro-omgewing deur parakriene seine kan herstel om regenerasie te bevorder. Die patologiese aard van die nis-mikro-omgewing beperk egter die gebruik van outoloë MSS-terapie by diabetespasiënte omdat verlengde blootstelling van endogene MSS’e aan die diabetiese omgewing *in vivo* die selle se vermoë aantas om op omgewingseine te reageer. Daarom berus die verdere ontwikkeling van outoloë selterapie op (a) ’n beter begrip van hoe die patogenese van T2DM die multifunksionele eienskappe van MSS’e beïnvloed, en (b) die ontwikkeling van nuwe strategieë om die funksie van hierdie aangetaste MSS’e te herstel voordat dit vir oorplanting gebruik word.

Hierdie studie ondersoek of *ex vivo*-antioksidant- [N-asetielsisteïen (7.5 mM NAC) en askorbiensuur-2-fosfaat-behandeling (0.6 mM AAP)] die parakriene responsiwiteit, groeitempo, migrasievermoë en lewensvatbaarheid van aangetaste diabetiese MSS’e kan herstel, en, indien wel, of hierdie herstelde toestand in die teenwoordigheid van diabetiese wondvog (DWV) gehandhaaf kan word.

Beenmurgafkomstige MSS’e is op die ouderdom van agt weke geïsoleer by wildetipe-C57BL/6J-muise (gesonde kontrole: MSC^{WT}) (n = 24) en vetsugtige diabetiese B6.Cg-Lep^{ob}/J-muise (aangetas/disfunksioneel: MSC^{ob}) (n = 24). Die *ex vivo*-behandelingsgroepe (MSC^{WT} teenoor MSC^{ob}) het bestaan uit (a) geen behandeling (basislynfenotipe), (b) DWV-gestimuleer (basislynreaksie), (c) vooraf met antioksidante gekondisioneer (voorafgekondisioneerde fenotipe), en (d) vooraf met antioksidante gekondisioneer, met daaropvolgende DWV-stimulering (voorafgekondisioneerde reaksie). DWV vir hierdie *ex vivo*-proefnemings is oor ’n tydperk van 28 dae bekom uit bilaterale, dorsale eksisiewonde van volle dikte wat op diabetiese muise (B6.Cg-Lep^{ob}/J) (n = 7) aangebring is. Die optimale konsentrasie antioksidante is met behulp van ’n dosisreaksieproefneming met geïmmortaliseerde C3H10/T1/2-selle bepaal.

Hierdie studie toon dat die uitbreiding van primêre MSS’e (MSC^{WT} en MSC^{ob}) in die teenwoordigheid van antioksidante die *ex vivo*-lewensvatbaarheid van selle verbeter en ’n beskermende uitwerking teen die toksisiteit van DWV het. Daarbenewens is die parakriene responsiwiteit van MSC^{WT} en MSC^{ob} (met en sonder voorafkondisionering met antioksidante) op molekulêre vlak (mRNA-uitdrukking van 84 sitokiene en reseptors, qPCR-mikrorangskikking) sowel as proteïenvlak bereken (Luminex-essai, 23-pleks, kraalrangskikking). Op die basislyn is ooruitdrukking van 31 gene (meer as tweevoudig) en onderuitdrukking van 39 gene (meer as tweevoudig) by MSC^{ob} teenoor MSC^{WT} opgemerk. In gekondisioneerde media is beduidende basislynverskille ($p < 0.05$) opgemerk vir twee pro-inflammatoriese sitokiene (TNFα en IFNγ), vier chemokiene (KC, G-CSF, Eotaxin en MCP1) en

een anti-inflammatoriese sitokien (IL10). Ná DWV-stimulering is beduidende verskille ($p < 0.05$) opgemerk in die uitskeiding van twee chemokiene (GM-CSF en Eotaxin), drie pro-inflammatoriese sitokiene (TNFα, IFNγ en IL9) en vier anti-inflammatoriese sitokiene (IL10, IL4, IL13 en IL3). Voorafkondisionering met antioksidante het die waargenome TNFα-oorreaksie by MSC^{ob} aansienlik gedemp en die uitskeiding van IL10 verbeter. Dít dui daarop dat gekombineerde *ex vivo*-behandeling van outoloë MSS'e met NAC en AAP moontlik 'n doeltreffende strategie kan wees om die parakriene funksie van aangetaste MSS'e voor oorplanting te herstel. Ondanks beter lewensvatbaarheid en 'n herstelde parakriene reaksie, kon voorafkondisionering met antioksidante egter nie die proliferasie- en migrasievermoë van ernstig aangetaste diabetiese MSS'e red nie.

Acknowledgements

This research project was supported by grants from the **National Research Foundation (NRF)** (grant no. 105921) and the **Harry Crossley Foundation**. I was supported by an NRF bursary as well as a bursary from the **Faculty of Medicine and Health Sciences** (FMHS), Stellenbosch University.

I would like to express my very great appreciation to **Dr Mari van de Vyver** (my supervisor) for the opportunity, valuable guidance and continues support, without whom this would not have been possible.

I would like to offer my special thanks to **Prof. Carola Niesler** (my co-supervisor) for her valuable and constructive suggestions during this research.

I would like to thank **Prof. Rafique Moosa** (Head of Department) for his continues support and **Prof. William Ferris** for the support and the jokes which helped ease my anxieties.

Assistance provided by **Dr Sven Parsons** and **Mr Noel Markgraaff** (Animal Research Facility) was greatly appreciated.

I am particularly grateful for the guidance given by **Dr Jyothi Chabilall** (doctoral office) and valuable support from International and registrar offices.

I wish to acknowledge the help provided by colleagues **(Stephen Hough Laboratory)** and thank them for the companionship and welcoming environment.

Finally, I wish to thank my parents for their unhesitating support and encouragement throughout my life and studies.

Abbreviations

AAP: ascorbic acid 2-phosphate

Abcg1: ATP-binding cassette sub-family G member 1

ADP: adenosine diphosphate

ADSC: adipose tissue-derived stem cell

AGE: advanced glycation end-products

AGER1: AGE receptor 1

AIF: apoptosis inducing factor

Akt: serine/threonine protein kinase

allo-acd-mMSCs: cellular derivatives of allogeneic bone marrow mesenchymal stem cells

***Ang1*:** angiopoietin 1

ANOVA: Analysis of variance

Apaf1: Apoptotic protease activating factor 1

App: amyloid precursor protein

ATP: adenosine triphosphate

AVMA: American Veterinary Medical Association

B6Cg-Lep^{ob}/J: obese prediabetic mouse *(ob/ob)*

BAK: BCL2 antagonist/killer 1

BAX: BCL2 associated X protein

***Bcl*:** B-cell lymphoma

B-cell: B lymphocyte

bFGF: basic fibroblast growth factor

BM: bone marrow

BMI: body mass index

BM-MSC: bone marrow-derived mesenchymal stem cell

BM-MNCs: bone marrow mononuclear cells

Bmp2: bone morphogenetic protein 2

BrdU: Bromodeoxyuridine / 5-bromo-2'-deoxyuridine

BSA: bovine serum albumin

C57BL/6J: wild type healthy mouse

C3H10T1/2: mouse, immortalized MSC cell-line

Ca^{2+}: Calcium ion

caspase: cysteine-aspartic proteases

CBS: cord blood serum

***Ccl*:** Chemokine (C-C motif) ligand

***Ccr*:** Chemokine (C-C motif) receptor

CD: cluster of differentiation

cDNA: Complementary DNA

cm: centimetre

cm²: centimetre squared

CM: conditioned medium

CML: carboxymethyl lysine

CO_2: Carbon dioxide

CRP: C-reactive protein

CS: chondroitin sulphate

***Csf*:** Colony stimulating factor

CST: serum-free media growth supplement

CV: crystal violet

***Cxcl*:** Chemokine (C-X3-C motif) ligand

***Cxcr*:** Chemokine (C-X-C motif) receptor

d: day

DAMPs: tissue-damage associated molecular patterns

db/db: obese/ type 2 diabetes mouse

DCCT: diabetes control and complications trial

DFU: diabetic foot ulcer

dH_2O: distilled water

dl: decilitre

DMSO: dimethyl sulfoxide

DMEM: Dulbecco's modified Eagle medium

DNA: deoxyribonucleic acid

DPP-4: dipeptidyl peptidase 4

Drp1: Dynamin-related protein-1

DWF: diabetic wound fluid

EC: endothelial cell

ECM: extracellular matrix

EDTA: Ethylenediaminetetraacetic acid

EGF: epidermal growth factor

ELISA: Enzyme-linked Immunosorbent Assay

Eotaxin: eosinophil chemoattractant protein

EPC: endothelial progenitor cell

ER: endoplasmic reticulum

ERK: signal-regulated kinase

EtOH: ethanol

EV: extracellular vesicle

FACS: fluorescence-activated cell sorting

FBS: foetal bovine serum

FGF: fibroblast growth factor

FITC: Fluorescein isothiocyanate

FMO: fluorochrome minus one
FMHS: Faculty of Medicine and Health Sciences
FOXO1: Forkhead box protein O1
FSC: forward scatter
***FTO*:** fat mass and obesity associated gene
FU: fluorescence units
g: gram
GAGs: glycosaminoglycans
G-CSF: granulocyte – colony stimulating factor
GFP: green fluorescent protein
GLUT: glucose transporter
GLO: L-gulonolactone oxidase
GM-CSF: granulocyte macrophage – colony stimulating factor
GSK3β: glycogen synthase kinase-3β
GWAS: genome-wide association studies
h: hour
H2AX: histone family member X
H_2O_2: hydrogen peroxide
HA: hyaluronic acid
HbA1c: glycated haemoglobin
HBO: Hyperbaric oxygen therapy
HDL: high-density lipoprotein
HGF: hepatocyte growth factor
***HHEX*:** haematopoietically expressed homeobox
HLA: human leukocyte antigen
***HOOK2*:** protein hook homolog 2
HPC: hematopoietic progenitor cells
HRP: horseradish peroxidase
HS: heparan sulphate
HSCs: hematopoietic stem cells
Hsp90ab1: heat shock protein 90α class B member 1
IDF: International Diabetes Federation
***Ifi202b*:** interferon-achievable protein gene
IFNγ: Interferon gamma
Ig: Immunoglobulin
IGF1: insulin like growth factor 1
IL: interleukin
IL1ra: Interleukin-1 receptor antagonist
iPSCs: induced pluripotent stem cells
IRS: insulin receptor substrate

ISCT: International Society for Cellular Therapy
JNK: c-Jun N-terminal kinase
JAK: Janus Kinase
KC: Keratinocyte chemoattractant
KCl: Potassium chloride
***KCNJ11*:** potassium inwardly rectifying channel, subfamily J, member 11
kg: kilogram
KH_2PO_4: Monopotassium phosphate
L: litre
LDL: low density lipoprotein
Lepr: Leptin receptor
Lisch-like-2: immunoglobulin like domain containing receptor 2
M1: pro-inflammatory type macrophage
M2: anti-inflammatory type macrophage
MAPK: mitogen activated protein kinase
MCP: monocyte chemoattractant protein
MCs: mononuclear cells
mg: milligram
MG: methylglyoxal
M-CSF: macrophage-colony stimulating factor
MGDC: mouse genomic DNA contamination
miRNA: micro-RNA
miR: miRNA
MIP: Macrophage inflammatory protein
***Mif*:** Macrophage migration inhibitory factor
min: minutes
ml: millilitre
MLKL: Mixed lineage kinase domain like pseudo-kinase
mm: millimetre
mm^2: millimetre square
mM (mmol): millimole
MMPs: matrix metalloproteinases
mRNA: messenger ribonucleic acid
MSC: mesenchymal stem cell
MSC^{WT}: isolated MSC from wild type mouse
MSC^{ob}: isolated MSC from obese mouse
mTORC1: mammalian target of rapamycin complex 1
mTOR: mammalian target of rapamycin
MTT: methyl-thiazolyl-tetrazolium
NAC: N-acetylcysteine

NaCl: Sodium chloride

Na_2HPO_4: Disodium phosphate

NADPH: nicotinamide adenine dinucleotide phosphate

NEP: neural endopeptidase

NFκB: nuclear factor kappa B

ng: nanogram

NGF: neural growth factor

NK-1R: neurokinin receptor

NLRP3: NOD-like receptor family pyrin domain containing 3

nm: nanometre

Nmu2R: neuromedin U receptor 2

Nnt: nicotinamide nucleotide transhydrogenase

NorLeu3: N-ethoxycarbonyl, (S)-1-phenylethylamide

NOD: Non-Obese diabetic

NRF: National Research Foundation

nt: nucleotide

NZO: New Zealand obese mouse

NZW: New Zealand white

ob/ob: obese prediabetic mouse (B6 Cg-Lep^{ob}/J)

***Oct*:** octamer-binding transcription factor

OD: optical density

OOR: out of measurable range

OSM: Oncostatin M

PARP: poly ADP ribose polymerase

PBS: phosphate buffered saline

PBN: alpha -phenyl-t-butyl nitrone

PCR: Polymerase chain reaction

***Pctp*:** phosphatidylcholine transfer protein gene

PDGF: platelet derived growth factor

PDEGF: platelet derived endothelial cell growth factor

PE: phycoerythrin

pen/strep: penicillin streptomycin

pg: picogram

PhP: microscope photographic objective

PI3K: phosphoinositide 3-kinases

PKC: protein kinase C

PPARG: peroxisome proliferator activated receptor gamma

PPC: positive PCR control

PGs: proteoglycans

pmol: per mole

PVA: Polyvinyl Alcohol

qPCR: quantitative polymerase chain reaction

RAGE: receptor for advanced glycation end-products

RANTES: Regulated on Activation, Normal T Cell Expressed and Secreted

RGB: (red, green, and blue) image

RIN: RNA integrity

RIPK: Receptor-interacting serine/threonine-protein kinase

RNA: ribonucleic acid

ROS: reactive oxygen species

RPM: revolutions per minute

RT: reverse transcriptase

RTC: reverse transcriptase control

S: standard

SA: South Africa

SAVC: South African Veterinary Council

Sca-1: stem cell marker

SCF: stem cell factor

SD: standard deviation

SDF1α: stromal derived factor 1 alpha

SDS-PAGE: Sodium dodecyl sulfate-polyacrylamide gel electrophoresis

SE: standard error

SFM: serum free media

SGM: standard growth medium

SIRT1: Sirtuin 1

SLC: Solute carrier

SOCS: suppressor of cytokine signalling

SOD: superoxide dismutase

Sorcs1: sortilin related VPS10 domain containing receptor

SOX: Sry-related HMG box

SP: Substance P

SPF: specific pathogen free

SSC: side scatter

STAT: signal transducer and activator of transcription

STZ: streptozotocin

SU: University of Stellenbosch

SVCT: sodium coupled ascorbic acid transporters

T2DM: type 2 diabetes mellitus

Tbc1d1*:* TBC1 domain family member 1

TBR: T-box brain transcription factor

TCF7L2: transcription factor 7 like 2

T-cell: lymphocyte T

TG: triglyceride

TGF*β*: transforming growth factor beta

Th: T helper lymphocyte

TIMP1: tissue inhibitor of metalloproteinase 1

Tomosyn-2: syntaxin-binding protein gene

TLR: Toll-Like Receptor

TNFα: tumour necrosis factor α

T reg: Regulatory T-cell

Tsc2: Tuberous sclerosis

Ube2l6: Ubiquitin conjugating enzyme

USA: United States of America

VEGF: vascular endothelial growth factor

***Vegfa*:** vascular endothelial growth factor alpha

VLDL: very-low-density lipoprotein

***vs*:** versus

WNT: Wingless-related integration site

WT: wild type

WRN: Werner syndrome

Zfp69: zinc finger protein gene

°C: degrees Celsius

µg: microgram

µl: microlitre

µM: micromole

µm²: micrometre square

3T3: 3-day transfer, inoculum 3×10^5 cells

11β-Hsd1: 11β-Hydroxysteroid dehydrogenase type 1

Table of Contents

List of Figures

List of Tables

Chapter 1: Introduction

The research presented in this thesis combines the complex aspects of diabetology, regenerative medicine (wound healing) and mesenchymal stem cell (MSC) biology. Type 2 diabetes mellitus (T2DM) is the most common type of diabetes, accounting for approximately 90% of all diabetes cases (World Health Organization, 1999) and is associated with debilitating co-morbidities such as non-healing wounds (foot ulcers). Diabetic patients have a 25% lifetime risk of developing foot ulcers with lower-limb amputations occurring in 12% of patients with ulcers (Mulder et al., 2012; Polonsky and Burant, 2016; Sen et al., 2009; World Health Organization, 1999).

Obesity is the most prominent risk factor for T2DM (Lin et al., 2018b) with disease progression from obesity to metabolic syndrome and ultimately T2DM being related to the progressive decrease in insulin secretion and simultaneous rise in insulin resistance (Abdullah et al., 2010; Bhowmik et al., 2015; Golay and Ybarra, 2005). As consequence, uncontrolled high blood glucose levels (hyperglycaemia) (Polonsky and Burant, 2016) leads to the formation and accumulation of advanced glycation end products (AGEs), which in turn activate multiple signalling cascades with widespread physiological implications (Singh et al., 2014). AGEs are associated with the excessive generation of reactive oxygen species (ROS) and production of pro-inflammatory factors (Kim et al., 2017; Nowotny et al., 2015; Okura et al., 2017). If persistent, the resultant tissue inflammation and oxidative damage contribute to the development of comorbidities whilst suppressing the body's natural repair processes by impairing the function of cellular regenerative mediators (such as MSCs).

The literature review *(chapter 2, p.3)* gives an integrated overview of the complexity and physiological interaction between these different aspects and highlight previous work, albeit in other contexts that have shown the potential protective effects of antioxidants. The purpose of this research project as described in the aims & objectives *(Chapter 3, p.28)* was to broaden our insight into the sensitivity of MSCs to the pathological diabetic environment (systemic and local wound) and to better our understanding of how to counteract MSC impairment by manipulating their phenotype *in vitro* (through the use of antioxidants) to improve the predictability and success of stem cell-based treatments.

The functional alterations evident in diabetic MSCs include impaired viability, reduced multilineage differentiation capacity and refractory mobility which is evident despite the removal of these cells to a more optimal *in vitro* environment (Frykberg and Banks, 2015; Shin and Peterson, 2012; van de Vyver et al., 2016). To study the molecular, paracrine and functional responsiveness of these MSCs (with and without treatments aimed at restoring function) it was thus necessary to create an *in vitro* microenvironment that would mimic the chronic wound post-transplantation.

The project, therefore, involved three studies using 3 different models in order to investigate our hypothesis *(Chapter 3, p.28)* in a physiologically relevant setting.

The first challenge was to establish a chronic wound model that mimics the pathological microenvironment of a non-healing wound in the clinical setting *(Chapter 4, p.30).* This was necessary for the harvesting of diabetic wound fluid (DWF) that represents the pathological microenvironment within a non-healing diabetic wound. Wound fluid is generated by enhanced capillary leakage and local activity of a variety of resident and migratory cell types and its composition is therefore broadly assumed to reflect the clinical condition of a wound (Trengove et al., 1996; Yager et al., 2007). The excisional wound model was established in animals with an obese prediabetic phenotype (B6Cg-Lep^{ob}/J Male) with known defects in the healing response. The model was further optimised by injecting a neural endopeptidase (NEP) around the wound edges at concentrations similar to that previously detected in the ulcer margins of diabetic patients (Antezana et al., 2002). As part of this first study *(Chapter 4, p.30)*, the inflammatory cytokine profile and total protein content of the harvested DWF was analysed to ensure that it represented the microenvironment of an inflammatory diabetic wound *(Refer to Addendum A, p.115 for the ethical approval letters).*

The second study *(Chapter 5, p.43),* involved the determination of the safest, non-toxic dosages of the antioxidants [N-acetylcysteine (NAC) and ascorbic acid 2-phosphate (AAP)] to be used as potential agents to counteract MSC impairment. As part of the refinement and replacement criteria (to limit the number of animals used) and due to the limited viability of primary mouse derived MSCs *in vitro*, this second study was performed using an embryonic mouse MSC line (C3H10T1/2) *(chapter 5, p.43).*

In the final study, a model of primary isolated healthy control (source: wild type, C57BL/6J mice/Male) and impaired diabetic (source: obese diabetic, B6.Cg-Lep^{ob}/J mice/Male) bone marrow-derived MSC was used *(Chapter 6, p.57)*. This enabled a direct comparison of the inflammatory/regenerative phenotype of healthy and impaired diabetic MSCs at baseline under standard culture conditions. Preconditioning of these cells with the optimum concentrations of antioxidants *(as determined in Chapter 5, p.43)* prior to stimulation with DWF *(harvested in Chapter 4, p.30)* furthermore enabled in-depth investigations into the responsiveness of MSCs and the efficacy of antioxidants to either restore the function of impaired MSCs or protect them against the toxicity of DWF *(Chapter 6, p.57).*

The results of the molecular and paracrine responsiveness of healthy *vs* impaired diabetic MSCs (with and without antioxidant preconditioning) were recently published in the Journal: Stem Cells & Development (Mehrbani Azar et al., 2018) *(Refer to Addendum B, p.117 for published paper)* and a second manuscript containing the results of the functional responses are currently under preparation. The final chapter of this thesis *(Chapter 7, p.90)* highlights the future perspectives and limitations of the research presented.

Chapter 2: Literature review

2.1 Obesity-associated Type 2 diabetes mellitus

T2DM is the most common type of diabetes, accounting for approximately 90% of all diabetes cases (World Health Organization, 1999). According to the International Diabetes Federation (IDF), the global prevalence of diabetes amongst adults (20-79 years) was 425 million in 2017 and it is predicted to increase to 629 million by 2045 (IDF, 8th edition, 2017). Furthermore, treatment costs of diabetes are significant and in 2017 was already amounting to $348 billion in the United States alone. Several risk factors have been associated with T2DM such as family history of diabetes, overweight/obesity, high blood pressure, unhealthy diet, physical inactivity, ethnicity, age, history of gestational diabetes or poor nutrition during pregnancy and impaired glucose tolerance (Polonsky and Burant, 2016).

Obesity is, however, the most significant risk factor for T2DM, with body mass index (BMI) being directly correlated to insulin secretion and metabolic disease progression (Lin et al., 2018b). Disease progression from obesity to metabolic syndrome and ultimately T2DM is related to the progressive decrease in insulin secretion and a simultaneous rise in insulin resistance (Abdullah et al., 2010; Bhowmik et al., 2015; Golay and Ybarra, 2005). Given the nature of this metabolic disease, important preventative measures for T2DM are focussed on improving glucose metabolism through lifestyle modifications (Lin et al., 2018b).

Insulin resistance causes higher circulating levels of glucose which in turn triggers the overproduction of insulin that eventually exhausts the pancreas. This leads to lower insulin production causing even higher blood glucose levels, termed hyperglycaemia (Polonsky and Burant, 2016). Uncontrolled hyperglycaemia leads to the formation and accumulation of glycated proteins and lipids also known as AGEs, which in turn activate multiple signalling cascades with widespread physiological implications that include but are not limited to cellular dysfunction and/or tissue destruction (Singh et al., 2014). AGEs are also associated with excessive accumulation of ROS and the production of pro-inflammatory factors (Kim et al., 2017; Nowotny et al., 2015; Okura et al., 2017). If persistent, the resultant tissue inflammation and injury eventually leads to comorbidities. T2DM patients therefore have a shorter life expectancy due to increased risk of microvascular and cardiovascular disease (ischemic heart disease and stroke), development of chronic wounds leading to lower limb amputations, non-traumatic blindness (retinopathy), kidney failure, acanthosis nigricans, sexual dysfunction, and frequent infections (Polonsky and Burant, 2016; World Health Organization, 1999).

2.1.1 Symptoms, diagnosis and predisposition

Common symptoms of diabetes are polydipsia (abnormal thirst), polyuria (excessive production of dilute urine), polyphagia (excessive appetite) and weight loss. Other symptoms include blurred vision, itchiness, peripheral neuropathy, recurrent vaginal infections, and fatigue (Polonsky and Burant, 2016; World Health Organization, 1999).

The diagnosis of T2DM is based on the measurement of glycaemia (the level of glucose in the blood). A positive diagnosis is usually made based on fasting plasma glucose ≥ 7.0 mmol/l (126 mg/dl); a glucose tolerance test with plasma glucose ≥ 11.1 mmol/l (200 mg/dl) at 2 hours following oral ingestion of a glucose bolus (75g) and/or glycated haemoglobin (HbA1c) of ≥ 48 mmol/mol (≥ 6.5 DCCT %) (American diabetes association, 2010; M. Nathan, 2009; Polonsky and Burant, 2016; World Health Organization, 1999).

Despite obesity being the major risk factor, a combination of modifiable (lifestyle) and non-modifiable (genetic predisposition) factors are involved in the development of T2DM. Genetics, ageing and gender are the most prominent risk factors that cannot be managed (Polonsky and Burant, 2016). A family history of T2DM doubles an individual's risk of becoming obese and has been shown to increase susceptibility to metabolic impairment (Cederberg et al., 2015; Scott et al., 2014). Meta-analysis and other studies indicate that whilst BMI-associated genetic variants are significantly associated with T2DM risk, there are also numerous genetic variants that predispose an individual to T2DM independent of obesity (Huang et al., 2015b; Xi et al., 2014).

Initially (2007-2011), the number of loci thought to be associated with T2DM were related to 36 genes (Herder and Roden, 2011). In 2015, Genome-Wide Association Studies (GWAS) had however already identified more than 250 genetic loci related to T2DM and/or obesity. Investigations into the overlap between loci for obesity-related traits and T2DM have highlighted the potential mechanisms that affect T2DM susceptibility (Joost and Schürmann, 2014; Karaderi et al., 2015). For instance, in European populations six variants are known to be prominently associated with T2DM and include: *TCF7L2* (transcription factor 7 like 2), *HHEX* (haematopoietically expressed homeobox), *PPARG* (peroxisome proliferator-activated receptor gamma), *KCNJ11* (potassium inwardly rectifying channel, subfamily J, member 11), and *FTO* (fat mass and obesity associated gene). Patterns of cell-type dependent epigenetic markers (DNA methylation, histone tail modifications, and chromatin remodeling) are furthermore present in individuals with T2DM and obesity (Martínez et al., 2014). For example, a differential methylation profile of the *HOOK2* (protein hook homolog 2) gene is evident in individuals with T2DM and obesity compared to healthy controls; a significant correlation between hypermethylated regions on the gene body and the presence of T2DM have thus been demonstrated (Rodríguez-Rodero et al., 2017). In animal models (specifically mice), the strong gene candidates involved in the T2DM phenotype includes *Pctp* (phosphatidylcholine transfer protein), *Tbc1d1* (TBC1 domain family member 1), *Zfp69* (zinc finger protein), and *Ifi202b* (interferon-achievable protein) for NZO (New Zealand obese mouse)-derived obesity and *Sorcs1* (sortilin related VPS10 domain containing receptor), *Lisch-like-2* (immunoglobulin-like domain containing receptor 2), *Tomosyn-2* (syntaxin binding protein), *App* (amyloid precursor protein), *Tsc2* (Tuberous sclerosis), and *Ube2l6* (Ubiquitin conjugating enzyme) for obesity caused by the ob or db mutation (Joost and Schürmann, 2014). Refer to Figure 2.1 for an overview of gene regulation in the pathophysiology of diabetes.

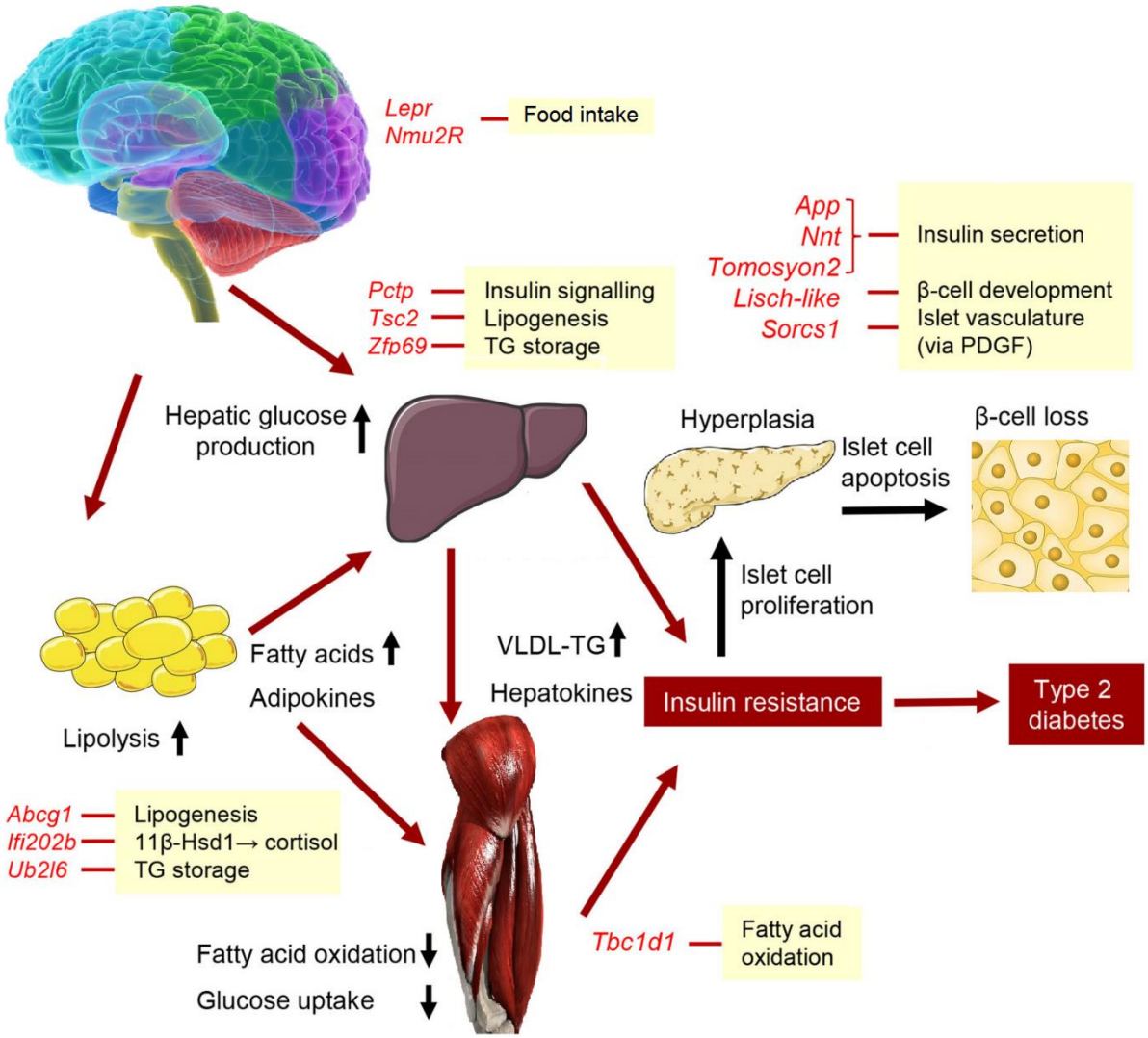

Figure 2.1 Site of action of candidate genes (red) and their relationship with symptoms of T2DM. The identification of the adipogenic/diabetogenic alleles of *Tbc1d1, Zfp69, and Ifi202b* supports the idea that fat oxidation and fat storage are essential determinants of obesity and diabetes (adapted from Joost and Schürmann, 2014). **Abbreviations:** ***Abcg1*****:** ATP-binding cassette sub-family G member 1**, App:** amyloid precursor protein, ***Ifi202b:*** interferon-achievable protein gene, ***Lepr:*** Leptin receptor, **Lisch-like**: immunoglobulin like domain containing receptor, ***Nmu2R:*** neuromedin U receptor-2, ***Nnt:*** nicotinamide nucleotide transhydrogenase, ***Pctp:*** phosphatidylcholine transfer protein gene, ***Sorcs1:*** sortilin related VPS10 domain containing receptor, ***Tbc1d1:*** TBC1 domain family member 1, **TG:** triglyceride, ***Tomosyn-2:*** syntaxin-binding protein gene, ***Tsc2:*** Tuberous sclerosis, ***Ube2l6:*** Ubiquitin conjugating enzyme, **VLDL:** very-low-density lipoprotein, ***Zfp69:*** zinc finger protein gene, **11β-Hsd1:** 11β-Hydroxysteroid dehydrogenase type 1.

2.1.2 Lifestyle changes

Preventive strategies against T2DM such as physical activity, dietary changes, and insulin-sensitising agents are beneficial in preventing disease progression and are most cost-effective (Haw et al., 2017; Lee et al., 2012). Even though the effectiveness of exercise and dietary changes in decreasing the incidence of T2DM has been confirmed, lifestyle modification on its own cannot completely reduce all-cause mortality in patients who already have T2DM (J. O'Gorman and Krook, 2011; Schellenberg et al., 2013). Nonetheless, investigations into the interplay between lifestyle factors and genetic

predisposition on T2DM risk showed that body weight, diet, and physical activity have a greater impact on glycaemic traits than genetic predisposition (Walker et al., 2015).

Increased dietary use of oils containing large amounts of trans fatty acids, saturated fats, sugar and refined carbohydrates combined with low intake of protein and fibre contributes to metabolic disease (elevated blood glucose levels, serum insulin, lipids, inflammatory markers and hepatic fat) (Gulati and Misra, 2017). Excessive fatty acids not only influence glucose metabolism but also alters cell membrane function, enzyme activity and gene expression (Risérus et al., 2009) leading to dysregulation of cellular metabolism.

Other lifestyle factors such as reducing social networking, seven hours of uninterrupted sleep at night and taking antioxidant and/or food supplements such as zinc, lipoic acid, carnitine, cinnamon, green tea, vitamin D3 and vitamin C plus E have shown slight benefits in managing obesity associated hyperglycaemia (Abdali et al., 2015; Raghavan et al., 2016; Seida et al., 2014; Touma and Pannain, 2011). Despite these cost-effective preventative strategies, T2DM is still a major health challenge globally and its incidence is continuing to rise (Haw et al., 2017).

2.1.3 Pathophysiology

T2DM is a multifactorial disease involving a complex interplay between tissues on various levels that lead to dysregulation of molecular signalling pathways, tissue/cellular damage and ultimately the development of severe co-morbidities. The key aspects underlying the pathogenesis of T2DM is discussed below:

2.1.3.1 Insulin resistance

The major mechanisms involved in metabolic disease progression include (1) Resistance to the action of insulin in peripheral tissues (muscle, fat, and liver); (2) Unresponsiveness to glucose stimulus leading to insufficient insulin secretion (pancreas), and (3) Increased glucose production by the liver. The cause and dysregulation of these mechanisms do however differ amongst individuals (Polonsky and Burant, 2016).

The underlying mechanism associated with the excessive caloric intake (obesity) includes an increased breakdown of lipids within adipose tissue due to impaired insulin signalling (Joost and Schürmann, 2014; Staiano et al., 2015; Zhang et al., 2014). Simultaneously, the release of glucose and very-low-density lipoprotein (VLDL) from the liver is triggered, fatty acid oxidation is decreased and glucose uptake by the skeletal muscle is reduced. To compensate for these excessive products in circulation due to lack of insulin action, β-cell hyperplasia occurs in the pancreatic islets in an attempt to increase insulin production but leads to β-cell dysfunction and apoptosis instead (Abderrahmani et al., 2018; Firneisz, 2014). Furthermore, hyperglycaemia-induced glucose toxicity and hyperinsulinemia are also known to induce an autoimmune response against β-cells (Kahn et al.,

2014; Tfayli and Arslanian, 2009; Zaccardi et al., 2016). Disrupting metabolic homeostasis even further and contribute to the development of T2DM (Bellan et al., 2014; Zaccardi et al., 2016).

2.1.3.2 Chronic systemic inflammation

Chronic low-grade inflammation and activation of the immune system are prominent in metabolic syndrome and T2DM (Finegood, 2003; van Greevenbroek et al., 2013; Luft et al., 2013). The hypertrophic state of adipocytes due to nutrient overload leads to hypoxia and endoplasmic reticulum (ER) stress (accumulation of unfolded or misfolded proteins) within adipose tissue and induces a pro-inflammatory response (Esser et al., 2014). The stressed adipocytes produce a wide range of pro-inflammatory cytokines/chemokines *[tumour necrosis factor alpha (TNFα), interleukin (IL-) 6, IL1β, monocyte chemotactic protein 1 (MCP1 also known as CCL2)]* and saturated fatty acids which attract M1 macrophages (pro-inflammatory) and T cells to infiltrate the tissue (Dahlén et al., 2014; DeFuria et al., 2013; Fadini et al., 2013a; van Greevenbroek et al., 2013).

This inflammatory signalling occurs *via* the phosphoinositide 3-kinases (PI3K), c-Jun N-terminal kinase (JNK) and nuclear factor kappa beta (NFκB) pathways. In response, the suppressor of cytokine signalling (SOCS1 and SOCS3) pathway is activated and downstream inhibits insulin signalling by promoting insulin receptor substrate (IRS) degradation (Babon and Nicola, 2012; van Greevenbroek et al., 2013), resulting in further metabolic deterioration (Paul, 2018; Schuster, 2010). In addition to these key pathways, the intracellular inflammasome protein complex: NOD-like receptor family pyrin domain containing 3 (NLRP3), that functions to detect either pathogenic micro-organisms or sterile stressors, have been proposed as a central regulator of adipose tissue inflammation (Lee, 2013; Paul, 2018).

The excessive release of adipokine and pro-inflammatory cytokines together with lower levels of anti-inflammatory cytokines *[such as transforming growth factor beta (TGFβ1) and IL10]* is a contributing factor in T2DM complications such as coronary artery disease, retinopathy, cardiovascular disease and overall reduced quality of life in diabetic patients (Rajkovic et al., 2014; Rodrigues et al., 2015; Slagter et al., 2015; Strissel et al., 2014; Tomić et al., 2013).

Refer to Figure 2.2 below for an overview of the role of pro-inflammatory cytokines in hypertrophic adipocytes.

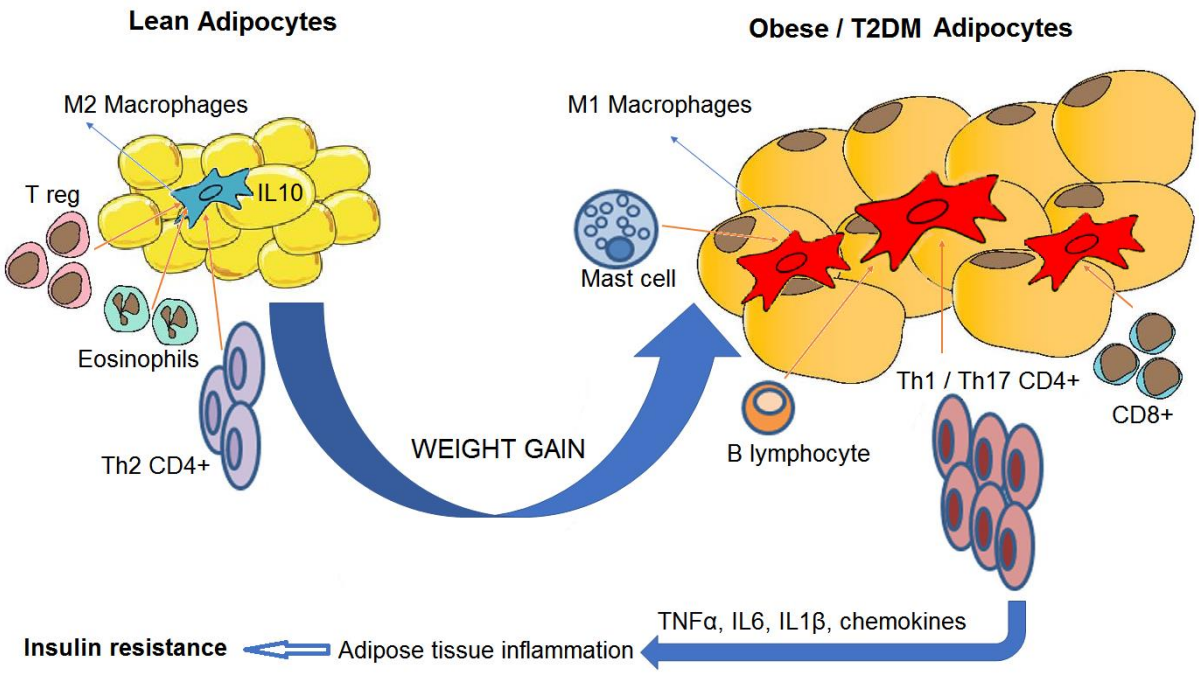

Figure 2.2 The overexpression of pro-inflammatory cytokines in hypertrophic adipose tissue during obesity. Pro-inflammatory cytokines such as IL1β, IL6, and TNFα are overexpressed whilst the expression of anti-inflammatory cytokines such as IL10 is downregulated, inducing a state of chronic inflammation. IL1β produced by macrophages is an essential pro-inflammatory cytokine and contributes to the pathogenesis by activating NFκB signalling which in turn amplifies inflammation through the production of inflammatory mediators, such as TNFα (adapted from Esser et al., 2014). **Abbreviations: CD**: cluster of differentiation**, IL**: interleukin, **NFκB**: nuclear factor kappa B, **T2DM**: type 2 diabetes mellitus, **Th**: T helper lymphocyte, **T reg**: Regulatory T-cell.

2.1.3.3 Hyperglycaemia and advanced glycation end products (AGEs)

Several metabolic signalling pathways that lead to inflammation are triggered by hyperglycaemia, leading to diabetic complications. Persistent hyperglycaemia causes the formation and accumulation of AGEs. AGEs are proteins or lipids that are glycated when exposed to sugars (Okura et al., 2017). They are assumed to be a major cause of insulin resistance, oxidative stress, β-cell injury and cellular dysfunction (Nowotny et al., 2015). AGEs mostly consist of dicarbonyl derivatives such as carboxymethyl lysine (CML), pentosidine, or derivatives of methylglyoxal (MG) (Singh et al., 2014; Vlassara and Uribarri, 2014). The accumulation of AGEs, triggers the non-enzymatic modification of extracellular matrix (ECM) components, plasma proteins (albumin, fibrinogen and globulins) and lipids through the Maillard reaction (denaturation and functional decline of the target protein and/or lipid). In addition to altering cellular functions, it generates oxidative and carbonyl stress (Duran-Jimenez et al., 2009; Nowotny et al., 2015; Singh et al., 2014).

Interaction between AGEs and their cellular receptors (receptor for advanced glycation end products) (RAGE) activate a cascade of downstream signalling pathways that play an important role in the pathogenesis of diabetic complications. RAGE signalling is activated due to the intracellular glycation of mitochondrial respiratory chain proteins that leads to the excessive production of ROS (Litwinoff et

al., 2015; Volpe et al., 2018). On the cellular level, the negative effect of AGEs has been demonstrated in β-cells, macrophages, endothelial progenitors and bone marrow MSC (Kume et al., 2005; Lu et al., 2012; Weinberg et al., 2014; Yang et al., 2010). In β-cells, chronic exposure to AGEs downregulates the AGE receptor 1 (AGER1) and Sirtuin 1 (SIRT1) that normally function to suppress AGE signalling and as result, intracellular AGE accumulation triggers oxidative stress and eventually β-cell dysfunction or destruction (Nowotny et al., 2015). AGEs further impair insulin secretion by inhibiting cytochrome-c oxidase and reducing adenosine triphosphate (ATP) production (Nowotny et al., 2015; Vlassara and Uribarri, 2014). In macrophages, RAGE signalling stimulates M1 (pro-inflammatory) polarization and activates NFκB signalling *via* mitogen-activated protein kinase (MAPK). This activation increases the production of pro-inflammatory cytokines such as TNFα, which in turn not only amplifies inflammation but also leads to enhanced ROS production and tissue damage (Guo et al., 2016; Uribarri et al., 2011). In bone marrow-derived endothelial progenitors and MSCs, the downstream effects of this combined oxidative stress and excessive inflammatory response (due to the accumulation of AGEs) result in DNA damage, mitochondrial fragmentation, defects in membrane repair, cellular senescence, impaired viability, proliferation and migration capacity (van de Vyver, 2017).

2.1.3.4 Excessive production of reactive oxygen species (ROS)

Continuous high levels of oxidative stress is associated with cell death *via* either autophagy, necroptosis or apoptosis (Saisho, 2014). Autophagy involves catabolic and homeostatic processes responsible for the lysosomal degradation of damaged organelles, whereas apoptosis occurs *via* either activation of the mammalian target of rapamycin complex 1 (mTORC1) / protein kinase C (PKC) pathway or Toll-Like Receptor 4 (TLR4) signalling (Volpe et al., 2018). Even though ROS generation occurs *via* enzymatic [nicotinamide adenine dinucleotide phosphate (NADPH)-oxidase] and non-enzymatic pathways involving the mitochondrial respiratory chain enzymes (Fakhruddin et al., 2017; Volpe et al., 2018), signalling pathways such as NFκB and mTORC1 [downstream of serine/threonine protein kinase (Akt) signalling] play a critical role in ROS-induced apoptosis (Kaneto et al., 2010; Pieme et al., 2017; Singh et al., 2009).

The physiological consequences of ROS-mediated cellular damage are wide-spread. In peripheral tissues (skeletal muscle), ROS generation causes a decrease in the expression of glucose transporters (glucose transporter type 4, GLUT4) on the cellular membrane and together with the inflammatory response contributes to insulin resistance (Coughlan et al., 2009; Hurrle and Hsu, 2017; Lin et al., 2018a). This metabolic dysregulation characterized by excessive free fatty acids and pro-inflammatory cytokines released from adipose tissue triggers the over activation of NADPH-oxidase which in turn further amplifies the accumulation of ROS (Hurrle and Hsu, 2017; Sindhu et al., 2018). ROS have also been shown to cause ER stress by producing unfolded protein responses leading to autophagy (Restaino et al., 2017; Ridzuan et al., 2016; Schiffer and Friederich-Persson, 2017). In the vascular system, increased ROS in the arterial environment has been shown to decrease adiponectin secretion from adipose tissue and as result, fatty acid breakdown is impaired and contributes to the

development of vascular complications (Padilla et al., 2015). Similarly, changes in the bone marrow microenvironment caused by combination of excessive ROS, inflammatory cytokines and AGEs lead to microangiopathy and inadequate perfusion of the endosteum within the bone. Thus, the failure of sinusoidal barrier function due to microangiopathy disrupts bone marrow resident progenitor cell (haematopoietic, endothelial, MSC) homeostasis (Mangialardi et al., 2014). The impaired progenitor cell homeostasis has a direct effect on the mobilization and regenerative capacity of these stem/progenitor cells (Denu and Hematti, 2016; Mangialardi et al., 2014).

Taking together, therapeutic strategies to prevent the development of comorbidities, should therefore not only focus on glucose control but also on limiting the excessive oxidative stress and inflammation in order to protect against cellular and tissue damage.

2.2 Chronic non-healing diabetic wounds

2.2.1 Prevalence and approaches in wound management

Diabetic foot ulcers (DFU) affect approximately 25% of all diabetic patients and are responsible for nearly 50% of all diabetes-related hospital admissions. This is a serious and debilitating condition leading to >80,000 amputations per year in the United States alone (Ahmad, 2016; Dinh et al., 2012) and the incidence of these wounds increase even further with ageing (Sen et al., 2009). The recurrence rate of diabetic wounds is between 20-80% (Ahmad, 2016; Sen et al., 2009) and due to the current lack of effective treatment strategies places a large financial burden on national health services (van Acker et al., 2014; Järbrink et al., 2016).

There are numerous risk factors that increase a diabetic patient's likelihood to develop a foot ulcer. These include peripheral neuropathy, microvascular disease, foot deformities, arterial insufficiency, trauma and/or small injuries to lower limb extremities (Noor et al., 2015). Among these risk factors, peripheral neuropathy is the most significant, accounting for approximately 66% of DFUs (Noor et al., 2015; Volmer-Thole and Lobmann, 2016). Peripheral neuropathy develops as a result of persistent hyperglycaemia (AGE accumulation), abnormalities in fatty acid metabolism and production of antibodies against neural tissues and can result in foot deformities (Noor et al., 2015; Volmer-Thole and Lobmann, 2016). Peripheral neuropathy is furthermore associated with impaired nociception which in turn affects paracrine signalling and inhibits the mobilization of stem/progenitor cells from the bone marrow (Dang et al., 2015; Fadini et al., 2017). Dang et al. (2015) demonstrated that a reduced number of nociceptive fibres in the bone marrow of T2DM patients resulted in the defective mobilization of stem/progenitor cells even in the presence of stimulants such as granulocyte colony stimulating factor (G-CSF) or ischemia. The authors indicated that this phenomenon was associated with an altered gradient of the nociceptor, Substance P, between the bone marrow, peripheral circulation and the ischemic wounded area (Dang et al., 2015). Together with neuropathy, peripheral microvascular disease (leading to ischemia) is another major risk factor and is responsible for the

development of DFUs in approximately 50% of patients (Noor et al., 2015; Zhao et al., 2016). Managing and treatment of these wounds are thus complex and difficult.

Refer to Figure 2.3 below for an illustration of the most common anatomical location that develops DFUs.

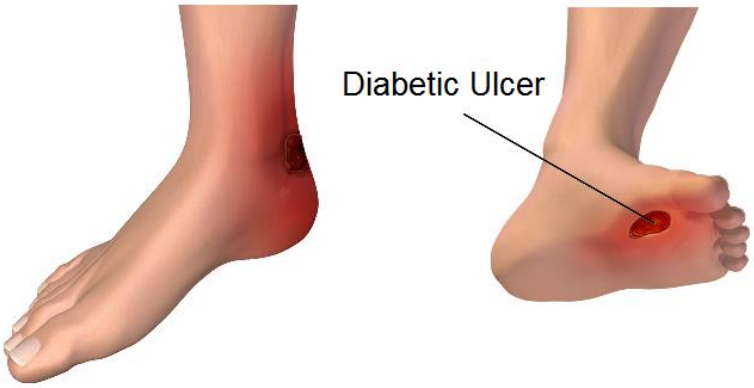

Figure 2.3 Representative image illustrating a diabetic foot ulcer (© https://commons.wikimedia.org/wiki/File:Diabetes_Foot_Ulcers.png).

Wound management in diabetes follows a standard wound care/management protocol. Usually, the procedure starts with debridement, infection control and maintaining a moist wound environment whilst preserving adequate blood flow. This is achieved through one of the following: moist or wet gauze/foam dressings, silver dressings, transparent films, hydrocolloid dressings, alginates, hydro fibres /hydro polymers and/or antimicrobial dressings; each of which has its own advantages and disadvantages (Andrews et al., 2015; Baltzis et al., 2014). Several new adjunctive treatment options have emerged during the last few years and mostly involve the application of either bioengineered skin substitutes, ECM proteins, growth factors, hyperbaric oxygen therapy (HBO), negative pressure wound dressings or electrical stimulation. Unfortunately, the currently available treatments are inadequate with very low success rates. Novel treatment strategies are therefore focussed on the underlying causes and aim to correct the factors that lead to impaired wound healing (Andrews et al., 2015; Markakis et al., 2016). Some of these future therapeutic perspectives include: gene therapy (delivery of genes which encoding growth factors), molecular approaches (micro-RNA application) and topical application of factors promoting angiogenesis (NorLeu3-angiotensin), neuropeptides (to counteract neuropathy), cytokine inhibition (to counteract persistent inflammation) and stem cell therapies (utilizing their pro-regenerative paracrine properties) (Baltzis et al., 2014; Frykberg and Banks, 2015; Jhamb et al., 2016).

In order to optimise therapeutic approaches, it is however essential that the regenerative process is fully understood and that deficiency that occur during each stage of healing is adequately addressed.

2.2.2 Phases of wound healing

Wound healing is a highly organised process that involves many cell types and mediators which interact in a coordinated sequence of events. The phases of wound healing include Haemostasis (humans) or contraction (animals), inflammation, cellular proliferation/migration and remodelling (Mutsaers et al., 1997; Sorg et al., 2017). A normal progression through these phases is essential for regeneration and is governed by paracrine signalling (cytokines, chemokines, growth factors). Any pathological changes that disrupt this progression (such as cellular microenvironmental changes during diabetes) are detrimental to the healing process.

Wound healing starts with haemostasis (phase I: blood clotting) and is followed by an acute inflammatory response (phase II: phagocytic). During phase I, vasoconstriction occurs followed by platelet aggregation and leukocyte infiltration (Sorg et al., 2017). Following haemostasis, molecular and/or pathogen-specific patterns function to initiate an immune response. During the inflammatory response (phase II), chemoattractant release recruits neutrophils, pro-inflammatory macrophages (M1) and T-cells to the injured area for phagocytosis of bacteria, dead cells and tissue debris. An increasing gradient of chemokines *MCP2, Macrophage inflammatory protein (MIP)-1α, Regulated on Activation Normal T Cell Expressed and Secreted (RANTES), Keratinocyte chemoattractant (KC), G-CSF]* promote immune cell migration towards the site of injury and the additional release of pro-inflammatory cytokines *[TNFα, Interferon gamma (IFNγ), IL1, IL8, IL6, IL12]* by neutrophils and M1 macrophages amplifies the inflammatory response (Behm et al., 2012; Martin and Nunan, 2015; Ridiandries et al., 2018). Members of the toll-like receptor family (TLR), specifically TLR2 plays an integral role in initiating the inflammatory response through mediators such as tissue-damage associated molecular patterns (DAMPs) and interferons (IFN) (Martin and Nunan, 2015; Sorg et al., 2017). Although acute inflammation, is essential to the healing process, chronic persistent inflammation can attenuate healing and is evident in non-healing wounds (Zhao et al., 2016).

Under normal circumstances, M1 macrophages will switch phenotype to become M2 pro-regenerative and healing will progress to the proliferation phase (phase III) through the release of growth factors *[platelet derived growth factor (PDGF), epidermal growth factor (EGF), fibroblast growth factor (FGF), TGFβ, vascular endothelial growth factor (VEGF)]* and anti-inflammatory cytokines *(IL10, IL4, IL13)* (Behm et al., 2012; Opal and DePalo, 2000; Qi et al., 2018; Zhao et al., 2016).

The proliferative phase is characterized by fibroblast proliferation, collagen synthesis, ECM reorganization, angiogenesis, granulation tissue formation, and re-epithelialization (Dreifke et al., 2015; Mutsaers et al., 1997). During this phase, the vascular network is restored (endothelial cell-mediated angiogenesis), fibroblasts and myofibroblasts are responsible for ECM production and keratinocytes repair dermal barriers. Fibroplasia and ECM deposition involve the secretion of locally produced PDGF, TGFβ and granulocyte macrophage-colony stimulating factor (GM-CSF) (Dreifke et al., 2015; Jhamb et al., 2016; Qi et al., 2018). It is thought that in T2DM, hyperglycaemia inhibits ECM formation by upregulating matrix metalloproteinases (MMPs) due to persistently increased levels of

pro-inflammatory cytokines such as TNFα and IL1β (Zhao et al., 2016). As a consequence, ECM dysfunction prevents keratinocyte migration and dermal repair. In diabetic wounds, chronic inflammation furthermore creates an environment that favours proteolysis (increased ROS, abnormally high level of MMPs and pro-inflammatory cytokines) which negatively influence cellular proliferation and migration during phase III (Jhamb et al., 2016; Zhao et al., 2016).

Under healthy conditions, the healing process is completed during the remodelling phase (phase IV). This phase is characterized by the completion of epithelialization, ECM remodelling and increased tensile strength within the wounded area (Dreifke et al., 2015; Mutsaers et al., 1997). Mechanical tension and PDGF stimulates dermal fibroblasts at wound margins to turn into myofibroblasts. Remodelling occurs when MMPs breakdown disorganised collagen (type III) and it is replaced with fibroblast-derived type I collagen. Apoptosis also occurs within the cell-rich granulation tissue forming either normal functional tissue or collagen filled scar (Schultz et al., 2011; Sorg et al., 2017).

Refer to Table 2.1 below for an overview of the paracrine factors involved in each stage of wound healing and how this is altered in diabetic wounds. From table, it is clear that differences exist in the paracrine secretion of both inflammatory and regenerative mediators within the diabetic wound microenvironment that can affect the natural progression of healing.

Table 2.1 Diabetes associated alterations in the levels of cytokines, chemokines and growth factors.

Factor	Altered expression in DFUs	Wound healing phase	Function during wound repair	Ref.
G-CSF	↑	II	Chemoattractant, cellular recruitment	(Dinh et al., 2012)
MIP1α	↓	II	Chemoattractant for inflammatory cells, recruitment of macrophages, promote angiogenesis	(Dinh et al., 2012; Ridiandries et al., 2018)
MCP1	↑	II	Chemoattractant for inflammatory cells, recruitment of macrophages, promote angiogenesis	(Dinh et al., 2012; Ridiandries et al., 2018)
TNFα	↑	II	Pro-inflammatory, mitogen for fibroblasts	(Dinh et al., 2012; Trengove et al., 2000)
IL8	↑	II	Attracts macrophages (M1)	(Dinh et al., 2012)
IL1α/β	↑	II, III, IV	Pro-inflammatory, angiogenesis, re-epithelialization, tissue remodelling	(Behm et al., 2012; Trengove et al., 2000)
IL6	↑	II, III, IV	Angiogenesis, re-epithelialization, collagen deposition, tissue remodelling	(Behm et al., 2012; Dinh et al., 2012; Trengove et al., 2000)
IL10	↓	II, III	Anti-inflammatory, inhibition of monocyte/macrophage (M1) and neutrophil cytokine production	(Opal and DePalo, 2000)
IL13	↓	II, III	Attenuation of monocyte/macrophage function	(Opal and DePalo, 2000)
IL4	↓	III, IV	Anti-inflammatory (promote Th2), Collagen synthesis	(Behm et al., 2012; Opal and DePalo, 2000)
PDGF	↓	II, III, IV	Re-epithelialization, collagen deposition, tissue remodelling	(Behm et al., 2012; Dinh et al., 2012)
TGFβ	↓	II, III, IV	Anti-inflammatory, angiogenesis, granulation tissue formation, collagen synthesis, tissue remodelling	(Behm et al., 2012; Dinh et al., 2012; Opal and DePalo, 2000)
VEGF	↑	II, III	Angiogenesis, recruitment of endothelial progenitors	(Behm et al., 2012; Dinh et al., 2012)
EGF	↑	III	Stimulates fibronectin synthesis, angiogenesis, fibroplasia, and collagenase activity	(Dinh et al., 2012; Qing, 2017)
FGF	↑	III, IV	Granulation, tissue formation, re-epithelialization, detoxification of ROS	(Behm et al., 2012; Dinh et al., 2012)
MMP9	↑	II, IV	Breaking down of matrix proteins	(Ben David et al., 2008; Dinh et al., 2012)

Footnote: This table gives a limited overview of the major growth factors, cytokines and chemokines known to be altered in DFUs and is not a comprehensive list. **Phases of wound healing:** Phase (II): Inflammation, Phase (III): Proliferation, Phase (IV): Remodelling. **↑:** Increase, **↓:** Decrease compared to acute wounds. **Abbreviations: DFU:** diabetic foot ulcer, **EGF:** epidermal growth factor, **FGF:** fibroblast growth factor, **G-CSF:** granulocyte colony stimulating factor, **IL-:** Interleukin, **M1:** Pro-inflammatory macrophages, **MCP1:** monocyte chemoattractant protein, **MIP1α**: macrophage inflammatory protein 1 alpha, **MMP9:** matrix metalloproteinase 9, **PDGF:** platelet derived growth factor, **Th2:** T cell helper 2, **TGF*β*:** Transforming growth factor beta, **TNFα:** tumour necrosis factor alpha, **VEGF:** vascular endothelial derived growth factor.

2.3 Stem cell therapy in diabetic wounds

Given the complex nature of diabetic wounds, various treatment strategies are being investigated. HBO is an example of one therapeutic strategy that showed potential in initial investigations. It was hypothesized that HBO will improve the mobilization of endothelial and other stem/progenitor cells from the bone marrow by establishing hyperoxia in the wound tissue (Heublein et al., 2015). Unfortunately, HBO was unable to decrease the likelihood of amputation. The ineffectiveness of HBO could be explained by either the ineffective mobilization of stem/progenitor cells in diabetic patients and/or the functional impairment of mobilized endogenous stem/progenitor cells. This defect is thought to be a consequence of long-term exposure of stem cells to the pathological microenvironment within the bone marrow niche.

Allogeneic MSC therapy has therefore emerged as a very promising treatment strategy over the past few years, however despite having enormous potential, there are still numerous challenges that have to be overcome before successful implementation in the clinical setting. There are various safety concerns associated with allogeneic therapy and the lack of available donors, especially in low-resource settings. Autologous cell therapy is, therefore, a much more attractive option. In both instances (allogeneic and autologous), translating the results of *in vitro* and *in vivo* (animal) models to human clinical trials is still in its early days (Glenn and Whartenby, 2014; Horwitz et al., 2006). Challenges include systematic *vs* local delivery methods, a poor understanding of MSC biology (paracrine responses) and long-term safety/follow-up post-transplantation.

MSCs are the preferred candidates for cell therapy since they can “sense” the clinical status of the wound and respond accordingly (through cell receptors and/or sensors and their downstream signalling pathways) to restore a pro-regenerative microenvironment through paracrine signalling (Chen et al., 2008; Hocking and Gibran, 2010; Jiang and Papoutsakis, 2013; Otero-Viñas and Falanga, 2016). MSCs have homing potential and the capacity to migrate to the wounded area. The release of a wide array of soluble growth factors, extracellular vesicles, soluble extracellular matrix glycoproteins, and trophic cytokines regulate cellular responses and promote tissue repair (Si et al., 2011; Stephen et al., 2016). The multifactorial functions of MSCs within the context of wound healing, therefore, include anti-inflammatory, pro-angiogenic, anti-fibrotic, and anti-apoptotic signalling (Hocking and Gibran, 2010; Isakson et al., 2015; Marfia et al., 2015). There are furthermore no ethical concerns with the use of autologous MSCs (Song et al., 2017; Townsend et al., 2016).

The Mesenchymal and Tissue Stem Cell Committee of the International Society for Cellular Therapy (ISCT) has assigned minimal criteria (2006) for characterizing human MSCs suitable for transplantation: (i) plastic adherent, (ii) express cluster of differentiation (CD)-73, CD90, and CD105 surface markers and lack the expression of the hematopoietic markers $CD34^-$, $CD45^-$, $CD14^-$, $CD79^-$, and human leukocyte antigen (HLA)-DR^-, and (iii) have multi-lineage differentiation potential into osteoblasts, adipocytes, and chondroblasts (Dominici et al., 2006; Hocking and Gibran, 2010; Klimczak and Kozlowska, 2016; Si et al., 2011). However, the surface marker expression of

endogenous MSCs derived from mice are less well defined with recommended expression of CD90, CD73, CD105, and Sca-1, but they do not express CD11b, CD31, CD34, or CD45 (Huang et al., 2015a; Qian et al., 2012; Yan et al., 2012).

2.3.1 MSC therapy: Animal models vs Clinical cases

Exogenous application of MSCs in myocardial infarction, connective tissue disorders, liver diseases, parkinsonism, chronic non-healing ulcers, spinal cord injury, critical leg ischemia and musculoskeletal disorders have demonstrated some promise in regenerative medicine during the past decade (Davey et al., 2014; Glenn and Whartenby, 2014; Horwitz et al., 2006; Mangialardi and Madeddu, 2016). Initially, the regenerative properties of MSCs was thought to be a function of their multilineage differentiation capabilities, but it is now known that the migration of MSCs to the sites of injury, and their humoral and secretory factors play a vital role in repairing damaged tissue by modulating inflammation and promoting the regenerative function of numerous cell types within tissue (Cao et al., 2017; Laurent Maranda et al., 2016; Otero-Viñas and Falanga, 2016; Wu et al., 2007a).

In animal models, allogeneic MSC therapy for the treatment of non-healing wounds has been reported in several studies with promising results (Table 2.2). Despite various methods of applications and the use of MSCs derived from different sources, the studies summarised in Table 2.2 all demonstrate an overall improvement in healing in both the non-pathological (acute) models and pathological (delayed healing) models. The successful healing outcomes were mainly related to increased cellularity, epithelialization, vascularity, angiogenesis and collagen deposition in the wounded area. These models, unfortunately, do not perfectly replicate chronic non-healing wounds in diabetic patients.

In the clinical setting, the data that shows promise for the use of autologous MSCs are mainly derived from case studies and little data is available about the metabolic profile of these patients (Table 2.3). For instance, Badiavas & Falanga (2003) demonstrated that application of autologous bone marrow derived MSCs in three patients with no responses to other therapies such as bioengineered skin application and autologous skin grafting could effectively close chronic surgical wounds. However, none of these patients had a metabolic disease or T2DM as the underlying cause. Falanga et al. (2007) indicated that in patients with neuropathic DFUs, autologous bone marrow MSC therapy could only improve healing by 40% and was unable to completely close the wounds (Badiavas and Falanga, 2003; Falanga et al., 2007). Similarly, other studies demonstrated slight improvements (ranging 50-83%) in diabetic wound closure (Badiavas et al., 2007; Dash et al., 2009; Debin et al., 2008; Jain et al., 2011) with reductions in the risk for amputation (Amann et al., 2009; Lu et al., 2011) but could not observe complete healing following autologous MSC therapy. Combination therapies therefore seem to be required to improve healing outcomes in patients, as is evident in the study by Ravari et al. (2011). The authors demonstrated that in a handful of patients, complete healing occurred when autologous MSC therapy was combined with collagen matrices (Ravari et al., 2011) (Table 2.3).

Despite having promise, the underlying diabetic pathology (*as described in sections 2.1.3, p.6)* hampers the advancement of autologous MSC therapy in T2DM patients and strategies are thus needed to overcome this obstacle.

Table 2.2 Allogenic MSC therapy in animal wound models.

Wound model	Delivery method / cell type	Observations	Healing outcome	Ref.
Acute wound models				
Rat (Sprague–Dawley) incisional wounds	Systemic or local injection/ allogeneic BM-MSCs	Both delivery methods increased collagen content	↑ wound healing in 14 days	(McFarlin et al., 2006)
Rat (Wistar) excisional wounds	Intravenous injection/ BrdU labelled human BM-MSCs	MSCs localized in specific sites around the wound	↑ wound healing after 28 days	(Li et al., 2006)
Mouse (Balb/C) excisional splinted wounds	Topical delivery and subcutaneous injection/ allogenic BM-MSC-conditioned medium	Increased numbers of macrophages and endothelial progenitors	↑ wound closure in 14 days	(Chen et al., 2008)
Mouse (C57BL/6) excisional wounds	Systemic delivery/ allogenic BM-derived GFP^+MSCs	Increased cellular differentiation in the wound bed	↑ wound healing after 8 days	(Sasaki et al., 2008)
Mouse Balb/C (allogeneic) or C57BL/6 (syngeneic) excisional wounds	Topical delivery in Matrigel and four intradermal injections/ allogeneic or syngeneic BM GFP^+MSCs	Increased epithelialization, cellularity and angiogenesis	↑ wound closure in 14 days	(Chen et al., 2009)
Rabbit (NZW) excisional wounds	Topical delivery grafted with human amniotic membranes loaded with allogenic BM-MSCs	Mature differentiation and collagen bundle deposition	↑ wound closure in 15 days	(Kim et al., 2009)
Rabbit (NZW) incisional wounds	Intradermal injection/ human BM-MSCs	Increased wound tensile strength and reduced scarring	↑ cutaneous wound healing in 21 days	(Stoff et al., 2009)
Diabetic wound models with delayed healing				
Mouse *(db/db)* excisional wound	Topical delivery using fibrin spray / autologous BM GFP^+MSCs	Stimulated wound healing in diabetic mice	↑ wound closure in 25 days	(Falanga et al., 2007)
Mouse *(db/db)* excisional wound	Topical delivery/ allogeneic BM stromal progenitors	Enhanced reepithelialisation, granulated tissue formation and angiogenesis	Complete wound closure in 28 days	(Javazon et al., 2007)
Mouse *(db/db)* excisional splinted wounds	Topical delivery and four intradermal injections in wound bed/ allogeneic BM GFP^+MSCs	Increased epithelialization, differentiation and angiogenesis	Complete wound closure in 28 days	(Wu et al., 2007b)
STZ induced (type 1 diabetes) rat (Sprague–Dawley) with incisional wounds	Systemic injection *via* tail vein and wound edges/ allogenic BM-MSCs	Improved the wound-tensile strength and increased the expression of growth factors	↑ healing in day 7	(Kwon et al., 2008)
STZ induced (type 1 diabetes) mice (C57BL／6) with excisional wounds	Applied directly to the lesion/ autologous BM-MSCs plus platelet-rich plasma	wounds treated with MSCs alone had a similar level of re-epithelialization to those treated with MSC plus platelet-rich plasma	↑ healing in 30 days	(Argôlo Neto et al., 2012)
STZ induced (type 1 diabetes) mice (C57BL／6) with ischemic excisional wounds	Solid collagen carrier/ human BM-MSCs	Increased capillary density	Complete closure in 14 days of wound treated with preconditioned MSC with Cobalt protoporphyrin	(Hou et al., 2013)

Continued on next page

STZ induced (type 1 diabetes) Rat (Wistar) with Ischemic Wound	Injected directly into the derma of wounds/ autologous BM-Mononuclear Cells (MCs) and allogenic Cord Blood Serum (CBS)	Increased vascularity	Complete wound healing in 13 days with BM-MCs+CBS	(Ulus et al., 2014)
STZ induced (type 1 diabetes) Rat (Sprague–Dawley) with foot ulceration	Injected around the wound/ allogenic BM-MSCs	Increased reepithelialisation	Complete wound healing in 20 days	(Kato et al., 2014)
STZ induced (type 1 diabetes) Non-Obese diabetic (NOD) mice with excisional skin wound	Intradermal injection around wounds/ allogeneic BM-MSCs and their cellular derivatives (allo-acd-mMSCs)	Increased granulation tissue formation and density of collagen fibres	Administration of (allo-acd-mMSCs) is more effective in wound healing than allogeneic BM-MSC and wound closed in 10 days	(de Mayo et al., 2017)

Footnote: The table represents studies that used bone marrow derived MSCs to treat wounds in animal models. **Abbreviations: allo-acd-mMSCs**: cellular derivatives of allogeneic MSCs, **BrdU**: Bromodeoxyuridine / 5-bromo-2'-deoxyuridine, **BM:** Bone marrow, **CBS:** cord blood serum, ***db/db:*** obese/ type 2 diabetes mouse, **EPCs**: endothelial progenitor cells, **GFP**: green fluorescent protein, **MCs:** mononuclear cells, **MSC**: mesenchymal stem cell, **NOD:** Non-Obese diabetic, **NZW:** New Zealand white rabbit, **PVA**: Polyvinyl Alcohol, **SCF**: stem cell factor, **STZ:** streptozotocin.

Table 2.3 Autologous cell therapy for chronic wounds: clinical cases.

Condition	Patient characteristics	Delivery method /cell type	Observation	Healing outcome	Ref.
Chronic wounds	Surgical abdominal hernia (n=1); arterial disease (n=1); arterial and venous disease (n=1); (>1 year)	Injected into the edges / Autologous BM-MSCs	Dermal building, reduced scarring	Complete wound closure (100%)	(Badiavas and Falanga, 2003)
Chronic wounds	Lower extremity chronic wounds due to venous insufficiency or diabetic neuropathy (n=6); (>1 year)	Topical delivery using fibrin spray / Autologous BM-MSCs	↓ in wound size	Closure in lower extremity wounds (100%) / neuropathic ulcers (40%)	(Falanga et al., 2007)
Chronic wounds	DFU (n=1); scleroderma ulcer (n=1); ischemic surgical wound (n=1); pressure ulcer paraplegic (n=1); (>3 years)	Injected to the wounds / Autologous BM-MSCs	↑ wound healing	DFU=50% closure; scleroderma=10% closure; Ischemic surgical wound =100% closure; pressure ulcer=81% closure	(Badiavas et al., 2007)
Chronic wounds	Burn wound (n=3); skin ulcers (n=5); DFU (n=1); pressure ulcers (n=11)	Collagen sponge with artificial dermis / Autologous BM-MSCs	Wounds mostly healed in 18 of the 20 patients	100% closure except burn wounds (skin grafts)	(Yoshikawa et al., 2008)
Lower limb ischemia	T2DM (n=50)	Intramuscular and hypodermic injections / Autologous BM-MSC	↓ ischemic symptoms and amputation rate	↑ in the ulcer healing rate by 83%	(Debin et al., 2008)
Severe critical limb ischemia	Diagnosed amputation (n=51) with diabetes diagnosis (n=28)	Intramuscular injections / Autologous BM-MSCs	↑ leg perfusion, ↓ analgesics consumption, ↑ in pain-free walking distance	↓ major amputations with 71% wound closure	(Amann et al., 2009)
Chronic lower extremity wounds	DFU (n=24) (>1 year) in diabetes	Injected into ulcer margins / Autologous BM-MSCs	↓ ulcer size at 12 weeks, ↑ in pain-free walking distance	75% closure	(Dash et al., 2009)
Limb ischemia	foot ulcer (n=96) with diagnosed diabetes (n=89)	Injection into the ischemic limb / Autologous BM-MSCs	Facilitated wound healing	79% limb salvage in patients	(Procházka et al., 2010)
Chronic lower limb wounds	Diabetes (n=48)	Injected in the wound / Autologous BM-MNCs+ peripheral blood cells	↑ perfusion status and angiogenesis	Wound healing 80% in 20 weeks	(Jain et al., 2011)
Diabetic critical limb ischemia and foot ulcer	T2DM (n=41)	Intramuscular injections / Autologous BM-MNCs and BM-MSCs	BM-MSCs therapy is more effective than BM-MNCs for ↑ lower limb perfusion	Reduced amputation rate	(Lu et al., 2011)
Chronic lower extremity wounds	Diabetes (n=8)	Topical injection with impregnate collagen matrix / Autologous BM aspirates	↑ healing process	Complete wound healing in a few patients and some with improvements	(Ravari et al., 2011)
Limb ischemia	Diabetes (type 1&2) (n=22)	Intramuscular injection / Autologous BM-MNCs	↑microcirculation, revascularization	Complete wound healing in most of the cases	(Kirana et al., 2012)
Chronic wounds	Critical limb ischemia ulcer (n=7) in diabetes	Directly applied to wound / Autologous BM-MNCs mobilised by G-CSF	↓ pain and neurological signs	↓ wound size	(Mohammadzadeh et al., 2013)

Footnote: Table represents examples of clinical studies that utilized autologous bone marrow derived MSC for the treatment of chronic wounds. **Abbreviations: BM-MNCs:** Bone marrow mononuclear cells, **BM-MSCs:** Bone marrow Mesenchymal stem cells, **DFU:** diabetic foot ulcer, **G-CSF:** granulocyte colony stimulating factor, **T2DM:** type 2 diabetes mellitus**.**

2.4 MSCs dysfunction in the diabetic environment

The pathogenesis of T2DM is linked to a poor bone microenvironment, which constitutes the MSCs niche and disrupts not only the recruitment and mobilization of MSCs but also significantly alters their secretome (Chang et al., 2015; Kusuma et al., 2017; Li et al., 2007).

2.4.1 MSC niche and bone marrow remodelling

The stem cell niches within the bone marrow are specific areas that provide the microenvironment in which the stem cells are maintained in an undifferentiated and self-renewable state. The bone marrow compartment contains two types of stem cell niches: 1) the endosteal niche, where primitive hematopoietic stem cells (HSCs), MSCs and macrophages reside and 2) the vascular niche that is located in close proximity to sinusoidal vessels where committed HSCs, endothelial progenitors and perivascular cells reside (Moore and Lemischka, 2006; Votteler et al., 2010).

Refer to Figure 2.4 below for an illustration of the stem cell niches within bone marrow.

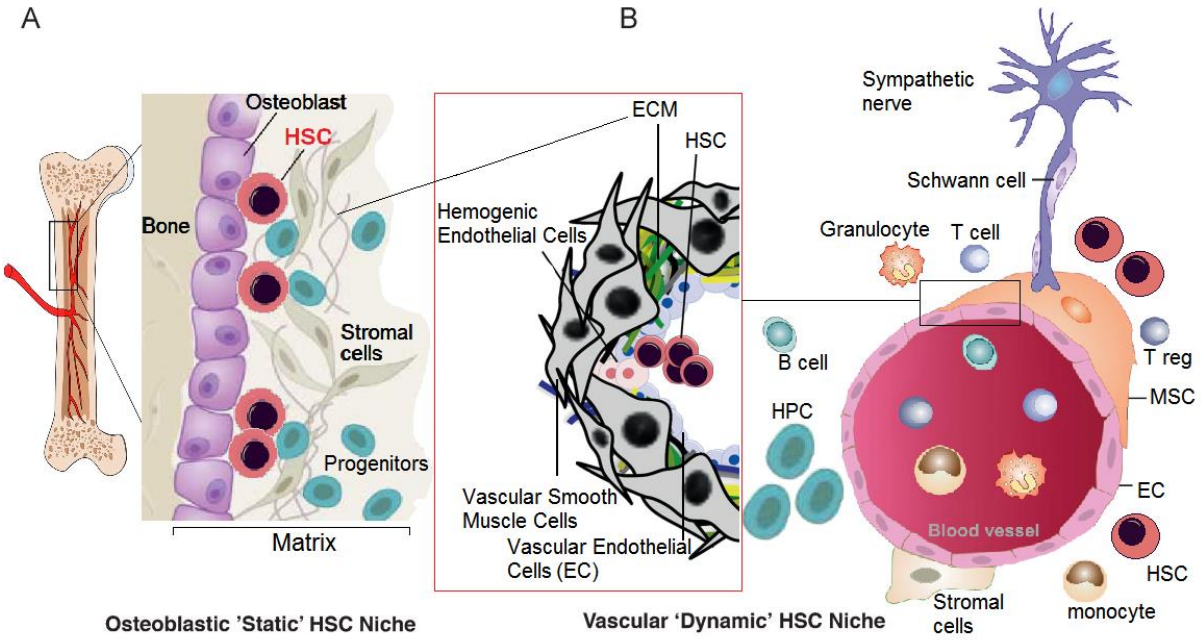

Figure 2.4 An illustration of the stem cell niches within the bone marrow. (A) Endosteal static niche containing hematopoietic stem and progenitor cells and MSCs **(B)** The vascular dynamic niche composed of vascular cells and specialized ECM structures (Adapted from votteler et al., 2010). **Abbreviations: B-cell**: B lymphocyte, **EC**: endothelial cell, **ECM**: extracellular matrix, **HPC**: hematopoietic progenitor cells, **HSC**: hematopoietic stem cells, **MSC**: mesenchymal stem cell, **T-cell**: lymphocyte T, **T reg**: Regulatory T-cell.

The bone marrow microenvironment is thus ultimately responsible for the maintenance of MSC populations, their activation, proliferation, and differentiation (Rojas-Ríos and González-Reyes, 2014; Singh, 2012). The niche consists of supporting cells, growth-modulating soluble factors and the ECM

that provides MSCs with specific signals and physical support. Niche activity is therefore influenced by local signals, systemic factors, nutritional status, developmental changes, circadian oscillations as well as physiological and pathological conditions (Metallo et al., 2007; Ra'em and Cohen, 2012).

The ECM is a cell-secreted three-dimensional complex mixture of various molecules and consist of two groups (1) structural proteins which include collagens, elastin, laminin and fibronectin and (2) proteoglycans (PGs) such as glycosaminoglycans (GAGs). PGs consist of a core protein and covalently attached sulphate GAGs, that include chondroitin sulphate (CS) and heparan sulphate (HS). GAGs together with hyaluronic acid (HA) offer a large water holding and growth factor binding capacity and have therefore a significant impact on cellular adhesion, migration, differentiation, and morphogenesis (Votteler et al., 2010).

The pathogenesis of T2DM does however cause remodelling of the bone marrow and has a negative effect on the niche microenvironment. This remodelling is characterized by an altered bone architecture (increased lipid accumulation and alveolar bone loss), micro-angiopathy (increased vascular permeability, sinusoidal rarefaction and hypoperfusion of stem cell niches) and neuropathy (reduction in the number of terminal nerve endings) (Duran-Jimenez et al., 2009; Spinetti et al., 2013). As a consequence, the mobilization of stem/progenitor cells is impaired by altered perivascular neural function and nociception-mediated defects in stromal derived factor 1 alpha (CXCL12/SDF1α) signalling that occurs via the dipeptidyl peptidase-4 (DPP-4) axis (Fadini et al., 2017; Rojas-Ríos and González-Reyes, 2014; Singh, 2012). This defect is known as mobilopathy, and eventually modulates physiologic haematopoiesis and tissue regeneration negatively (Fadini et al., 2017; Lucas, 2017). The MSCs trapped within the pathological bone marrow compartment are further subjected to the increased accumulation of AGEs, oxidative stress and persistent inflammation leading to cellular damage and apoptosis which in turn depletes the stem cell pool (Duran-Jimenez et al., 2009; Moore and Lemischka, 2006; Pérez et al., 2018).

2.4.2 Mobilopathy and MSCs recruitment

The G protein-coupled receptor, chemokine (c-x-c motif) receptor (CXCR)-4, and its ligand chemokine (c-x-c motif) ligand 12 (CXCL12)/SDF1α play a crucial role in transducing various signals such as cellular survival, proliferation, chemotaxis, apoptosis and the homing of progenitor cells to ischemic tissues (Cheng et al., 2015; Karimabad and Hassanshahi, 2015; Katsumoto and Kume, 2013; Kitaori et al., 2009; Soghra Bahmanpour, 2016). SDF1α acts as a retention signal for stem cells within the bone marrow and mobilization is only achieved when a chemotactic SDF1α gradient is established towards the peripheral blood. This occurs when SDF1α is degraded within the bone marrow by the protease activity of DPP-4, whilst SDF1α is released from ischemic/injured tissues into the circulation (Albiero et al., 2013; Fadini et al., 2013b). SDF1α, therefore, recruits CXCR4 positive stem cells into hypoxic tissue and its activity is also thought to be essential for endothelial cell survival, vascular branching and pericyte recruitment (Fadini et al., 2017; Yeboah et al., 2017). In addition to the activity of SDF1α, VEGF (a potent pro-angiogenic factor) has also been shown to play a key role in the

mobilization of stem/progenitor cells through amplification of the paracrine cascade of other chemokines and by preventing apoptosis (Albiero et al., 2013; Lewellis and Knaut, 2012; Zisa et al., 2011). Other downstream pathways involved in mobilization include PI3K/Akt signalling (Ling et al., 2018; Wang and Knaut, 2014) and the signal transducer and activator of transcription (STAT)-5 pathway (Honczarenko et al., 2006). Upon mobilization, cell migration and homing is an essential process in regeneration and in addition to the chemotactic gradient which is guided by ECM components (Goetsch and Niesler, 2011; Moissoglu et al., 2014; Venkiteswaran et al., 2013).

In T2DM, this whole process is dysregulated. Hyperglycaemia has been shown to activate glycogen synthase kinase-3β (GSK3β) leading to inhibition of the SDF1α receptor (CXCR4) on stem/progenitor cells (Zhang et al., 2016a). Furthermore, SDF1α is a dominant chemokine in bone marrow (Kitaori et al., 2009), but its degradation (required for mobilization to occur) is hampered in T2DM due to a maladaptive DPP-4/CD26 axis (Fadini et al., 2013c, 2013b) and a reduction in the density of nerve terminals (Fadini et al., 2017). This together with decreased release of SDF1α from epithelial cells and myofibroblasts in diabetic wounds (Heublein et al., 2015), prevents the chemotactic gradient from forming and retains stem cells within the bone marrow.

Stem cell retention is furthermore exacerbated by the imbalance of macrophage polarization within bone marrow that is skewed to favour a pro-inflammatory (M1) phenotype in diabetes (Albiero et al., 2013). M1 macrophages release Oncostatin M (OSM) that in turn induces SDF1α expression by MSCs through a p38 MAPK/ STAT3 dependent pathways and impairs mobilisation (Albiero et al., 2015). Clinical approaches aimed at reversing mobilopathy are mainly focussed on targeting the SDF1α/DPP4 axis but this has had limited success (Albiero et al., 2013).

2.4.3 MSC paracrine activity and mechanisms of impairment

The individual components of the T2DM pathological microenvironment are all known to negatively affect MSC function. *In vitro* studies have shown that the culture of rat bone marrow MSCs in the presence of high glucose concentrations (16.5 mM) compared to physiological concentrations (5.5 mM) interfere with the proliferation capacity of these cells by activating GSK3β signalling (Zhang et al., 2016a). High glucose levels in culture have furthermore been shown to induce cellular senescence, upregulate autophagy (Chang et al., 2015; Rezabakhsh et al., 2017) and impair the migration and multilineage differentiation capacity of MSCs (Januszyk et al., 2014; Li et al., 2007; Saki et al., 2013; Silva et al., 2015; Zhang et al., 2016a). Similarly, *in vitro* studies indicated that AGEs can inhibit the growth and migration of MSCs through activation of ROS-mediated p38 signalling (Kume et al., 2005; Weinberg et al., 2014; Yang et al., 2010) whilst increasing cellular senescence and favouring adipogenic differentiation (Denu and Hematti, 2016; Kume et al., 2005). In the presence of excessive inflammation, MSCs have been shown to have refractory mobility and increased rates of apoptosis (Katagi et al., 2014; Ko et al., 2015). Few studies have shown the interaction between these individual components. Gallagher et al. (2015) indicated that epigenetic changes and histone methylation in bone marrow MSCs resulting from exposure to a high glucose environment in a mouse model of diet-induced obesity can affect the inflammatory phenotype of macrophages by modulating

the release of IL12 from these immune cells (Gallagher et al., 2015). It is however still unclear how exactly the paracrine activity of MSCs are affected in T2DM but given the functional alterations (growth, migration and differentiation impairment) evident, the secretome is likely to also be negatively affected.

The paracrine activity of MSCs play an important role in healing and is the key aspect of their pro-regenerative properties. The MSC secretome consists of released growth factors, cytokines, chemokines as well as microvesicles and exosomes containing micro-RNAs and lipids as cargo (Ferreira et al., 2018; Nawaz et al., 2016). The constituents of the secretome are however variable and depend on the source of the stem cells (Pawitan, 2014) as well as the microenvironment or stimuli they are exposed to.

Table 2.4 below gives an overview of the most prominent factors known to be secreted by bone marrow MSCs that influence regenerative processes.

Table 2.4 Trophic and immunomodulatory factors secreted by bone marrow MSCs.

Factors	Action	Ref.
VEGF, HGF, TGFβ, bFGF, IGF1, PDGF, EGF, PDEGF, NGF	Growth factor, Anti-apoptotic, immunomodulatory, anti-scarring	(Cantinieaux et al., 2013; da Silva Meirelles et al., 2009)
IL6, IL10, IL27, IL13, IL1ra	Anti-inflammatory	(Murphy et al., 2013; Pawitan, 2014)
IL8, IL9, IL1α, IL17E, IL12p70	Pro-inflammatory	(Murphy et al., 2013; Pawitan, 2014)
GM-CSF, M-CSF, SDF1α, MCP1, G-CSF	Chemoattractant, Promote proliferation and migration	(Kusuma et al., 2017; da Silva Meirelles et al., 2009)
leptin, angiogenin, endostatin, thrombospondins, TIMP1	Angiogenic and various trophic actions	(Pawitan, 2014)
Extracellular vesicles (miRNAs, exosomes, mRNA, micro vesicles)	Anti-inflammatory, Anti-fibrosis, tissue regeneration	(Nawaz et al., 2016; Ozdemir and Feinberg, 2019; Phinney and Pittenger, 2017)

Footnote: Abbreviations: bFGF: basic fibroblast growth factor, **EGF:** epidermal growth factor, **G-CSF:** granulocyte colony stimulating factor, **GM-CSF:** granulocyte macrophage colony stimulating factor, **HGF:** hepatocyte growth factor, **IGF1:** insulin like growth factor 1, **IL1ra:** Interleukin-1 receptor antagonist, **M-CSF:** macrophage colony stimulating factor, **MCP1:** monocyte chemoattractant protein 1, **mRNA:** messenger ribonucleic acid RNA, **miRNA:** micro RNA, **NGF:** neural growth factor, **PDEGF:** platelet derived endothelial cell growth factor, **PDGF:** platelet derived growth factor, **SDF1α:** stem cell-derived factor 1 alpha, **TGF*β*:** Transforming growth factor beta, **TIMP1:** tissue inhibitor of metalloproteinase-1, **VEGF:** vascular endothelial derived growth factor.

In the context of wound healing, MSCs combat the newly presented antigens at the site of injury (Murphy et al., 2013) whilst the secreted anti-inflammatory cytokines supports the wound's ability to progress beyond the inflammatory phase to the proliferative and remodelling phases avoiding regression into a chronic inflammatory state (Dash et al., 2013). This occurs in part *via* integrin signalling, that enables cells to receive mechanical information and exhibit immunomodulatory effects on the cellular components of the innate immune system (Kusuma et al., 2017; Le Blanc and Davies, 2015). MSCs furthermore provide support for angiogenesis by secreting factors such as SDF1α, VEGF and basic fibroblast growth factor (bFGF) into the wounded area (da Silva Meirelles et al.,

2009), and by doing so promotes the expression of angiopoietin-1 (Ang1) to reinforce vascular supply (Zimmerlin et al., 2013). MSCs ability to secrete trophic factors is thus crucial for therapeutic approaches aimed at promoting growth and regeneration (Sassoli et al., 2012). Disruption of this paracrine responsiveness to environmental cues could thus be detrimental to the overall regenerative properties of MSCs.

2.5 Antioxidant treatment as a preventative strategy against stem cell impairment.

The underlying pathogenesis of T2DM that leads to stem cell dysfunction and the development of co-morbidities involve cellular damage induced through hyperglycaemia mediated oxidative stress and subsequent persistent inflammation *(section 2.1.3.2, p.7 and 2.1.3.4, p.9).* A therapeutic approach focussing on limiting oxidative stress and inflammation should thus have a protective effect and could possibly even restore the function of impaired diabetic MSCs. Specific antioxidants that have been shown to have protective effects against cellular damage in a variety of acute *in vitro* models are indicated in Table 2.5.

Table 2.5 *In vitro* studies demonstrating the protective effects of antioxidants on MSCs.

Source	Cell type	Effects	Antioxidant	Concentration	Ref.
Transgenic mice TBR-B cells	BM-MSCs	↑ smooth muscle cell differentiation	L-Ascorbic acid/ 2-phosphate	30 μM	(Arakawa et al., 2000)
Human bone marrow	BM-MSC	↑ proliferation and osteogenic differentiation	L-Ascorbic acid/ 2-phosphate	50 μg/ml	(Wang et al., 2006)
Rat/bone marrow	BM-MSC	↑ osteoblastic differentiation	Ascorbic acid	50 μg/ml	(Wan et al., 2008)
Human bone marrow	BM-MSCs	Dose-dependent ↑ on proliferation and differentiation	L-Ascorbic acid 2-phosphate	250 μM	(Choi et al., 2008)
Human adipose tissue	ADSCs	↑ proliferation and pluripotency markers: *Oct4* and SOX 2	Ascorbic acid	250 μM	(Potdar and D'souza, 2010)
Human Periodontal tissue, bone marrow, umbilical cord	MSCs	↑ MSC Sheet Formation and Tissue Regeneration	Vitamin C	20-50 μg/ml	(Wei et al., 2012)
Human umbilical cord blood	MSCs	↑ proliferation	L-Ascorbic acid	250 μM	(Mekala et al., 2013)
Human bone marrow	BM-MSCs	Reverted the decline in differentiation	Ascorbic acid	500 μM	(Jeong and Cho, 2015)
MSC/ WRN gene knockout /Werner syndrome	Human MSCs	alleviated aging defects	Vitamin C	280–560 μM	(Li et al., 2016b)
Human/ Gingiva	MSCs	↑ proliferation and expression of pluripotent markers	Ascorbic acid	50 μM	(Van Pham et al., 2016)

Continued on next page

Human adipose tissue	ADSCs	↑ proliferation	Vitamin C	30 mg/ml	(Zhang et al., 2016b)
Zucker diabetic fatty rat	ADSCs	↑ ECM secretion and ADSC sheet synthesis	Ascorbic acid	16.4 µg/ml	(Kato et al., 2017)
Wistar rat	BM-MSCs	Induced differentiation along with other osteogenic factors	Ascorbic acid and collagen-glycosaminoglycan scaffold	50 µg/ml	(Farrell et al., 2006)
Human bone marrow	BM-MSCs	↑ smooth muscle cell differentiation	TGFβ1 and ascorbic acid	30 µM AA	(Narita et al., 2008)
Human bone marrow	BM-MSCs	↑ proliferation	L-Ascorbic acid 2-phosphate and fibroblast growth factor-2	250 µM	(Bae et al., 2015)
Human bone marrow	BM-MSCs	↑ collagen mimetic peptide content and relevant gene expression and protein production	Bone morphogenetic protein-13 (BMP-13) and L-Ascorbic acid 2-phosphate	50 µg/ml AA	(Rehmann et al., 2016)
Mouse/female infarcted myocardium	Satellite cells	↑ cardiac tissue regeneration capacity	N-acetylcysteine	10 mM	(Drowley et al., 2010)
db/db Mice hind-limb ischemia	BM-MSCs	↓ oxidative stress and adipogenesis	N-acetylcysteine	-	(Yan et al., 2012)
Human embryonic MSCs	MSCs	↓ oxidative stress and ↑ cell adhesion	N-acetylcysteine	2 mM	(Wang et al., 2013a)
Rat bone marrow (type 1 diabetes)	BM stromal cells	Prevented apoptosis	N-acetylcysteine	2 mM	(Weinberg et al., 2014)
Human bone marrow / hyperglycaemia	BM-MSCs	Prevented hyperglycaemia induced autophagy and senescence	N-acetylcysteine	5 mM	(Chang et al., 2015)
Mouse adipose tissue and 3T3-L1 preadipocytes	ADSCs	Protected ADMSC from oxidative stress and ↑ cell survival	N-acetylcysteine	60 µM	(Gillis et al., 2015)
Induced diabetic mouse	BM-MSCs	↑ cell viability and upregulated pro-survival genes (Akt and *Bcl*-2)	N-acetylcysteine	30mM	(Ali et al., 2016)
Mouse bone marrow	BM-MSCs	↓ DNA damage and ↑ proliferation	alpha-phenyl-t-butyl nitrone and N-acetylcysteine	5 mM NAC	(Fan et al., 2011)
Human adipose tissue	ADSCs	↑ growth and prolong lifespan	L-Ascorbic acid 2-phosphate + N-acetylcysteine	2 mM NAC+ 0.2 mM AAP	(Lin et al., 2005)
Human adipose tissue	ADSCs	↑ proliferation	L-Ascorbic acid 2-phosphate + N-acetylcysteine/ fibroblast growth factor 2	2 mM NAC+ 0.2 mM AAP	(Sun et al., 2013)
Human adipose tissue	ADSCs	NAC+AAP protected mitochondria from oxidative stress and rescued MSCs from apoptosis	L-Ascorbic acid 2-phosphate + N-acetylcysteine	3 mM NAC+ 0.2mM AAP & 7mM NAC or 0.8mM AAP	(Li et al., 2015)

Footnote: Abbreviations: 3T3: 3-day transfer, inoculum 3×10^5 cells, **AAP:** ascorbic acid 2-phosphate, **ADSCs:** adipose tissue-derived stem cell, **Akt:** serine/threonine protein kinase, ***Bcl*:** B-cell lymphoma, **ECM:** extracellular matrix, **NAC:** N-acetylcysteine, **SOX:** Sry-related HMG box, ***Oct*:** octamer-binding transcription factor, **TBR:** T-box brain transcription factor, **TGF:** Transforming growth factor, **WRN:** Werner syndrome.

The physiological function of intracellular ROS is crucial in maintaining biological processes through redox signalling (André-Lévigne et al., 2017; Mangialardi et al., 2014), however excessive accumulation thereof causes damage to DNA, proteins, and lipids which in turn leads to gene expression malfunction, mitochondrial dysfunction, tissue inflammation, and premature cellular aging (Ali et al., 2016; Jeong and Cho, 2015). The mechanisms behind the natural anti-oxidation defence of cells involve several key pathways, which enables the efficient removal of excessive oxidants and therefore protects cellular organelles from ROS-induced damage. This regulation is mediated by antioxidant enzymes (such as superoxide dismutase, catalase, and glutathione peroxidase) and other non-enzymatic molecules (ergothioneine, vitamin C) or microelements, which altogether prevent cellular senescence and apoptosis (Chen et al., 2017).

Sustained oxidative stress overrides the natural antioxidant defence mechanisms and consequently decreases cellular proliferation, promotes senescence, apoptosis and even tumour formation by regulating the expression of apoptosis related genes and proteins such as *Bcl-2, Bax, p53* (Chen et al., 2017; D'Aniello et al., 2017). From the table, it is clear that antioxidants such as ascorbic acid (vitamin C) and NAC have beneficial effects in promoting cellular proliferation/differentiation and preventing cell death. This protective effect is mainly a result of the combined antioxidant and anti-inflammatory actions that contribute to the maintenance of mitochondrial function as indicated in Figure 2.5 below.

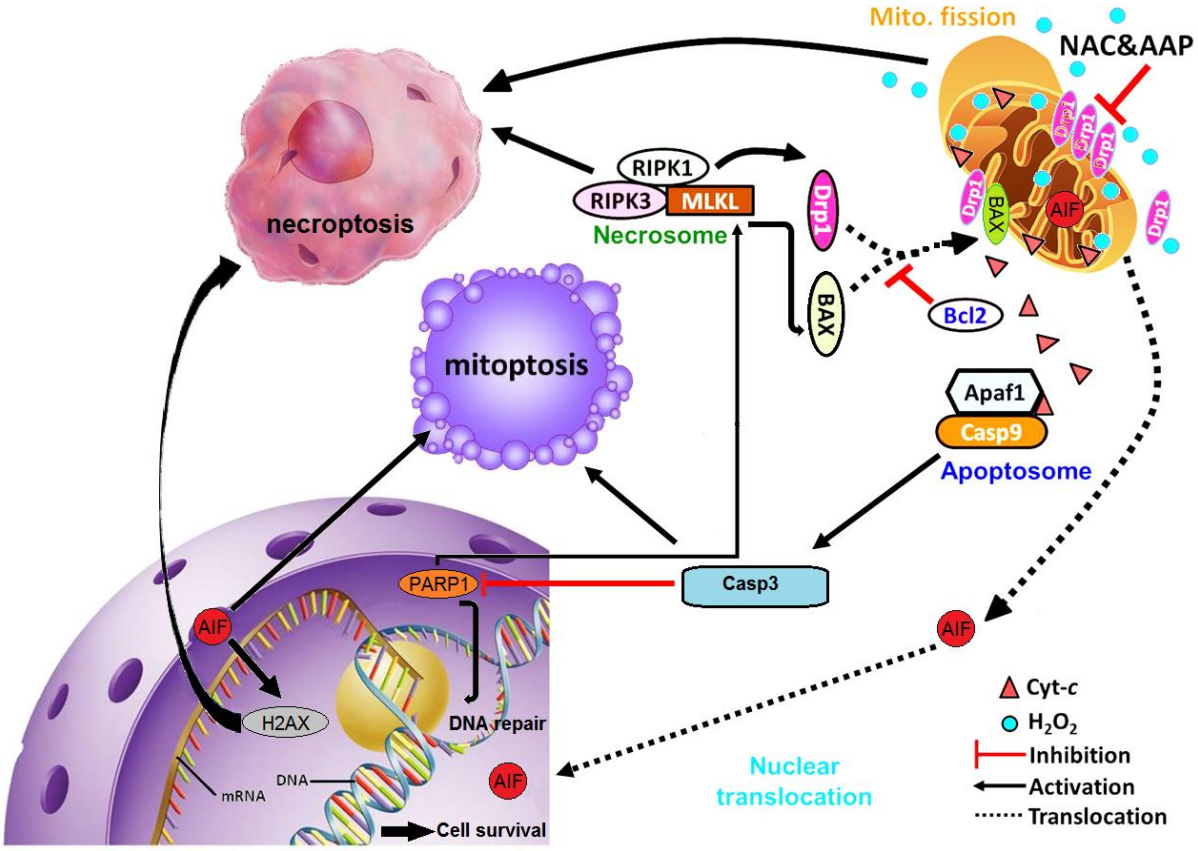

Figure 2.5 An illustration of NAC and AAP mitochondrial protection, against oxidative damage. Both NAC and AAP protect cells from oxidative stress-induced cell death *via* inhibiting mitoptosis (mitochondrial programmed cell death) by decreasing the activation of BAX, Drp1 and increasing the expression of BCL2. Thus, stabilized mitochondria will also prevent AIF induced necroptosis *via* H2AX pathway. As result, the caspase (cysteine-aspartic proteases) dependent or independent formation of necrosomes are inhibited and the secretion of apoptotic factors within the mitochondria prevented (adapted from Li et al., 2015). **Abbreviations: AAP**: ascorbic acid 2-phosphate, **AIF**: apoptosis inducing factor, **Apaf1**: Apoptotic protease activating factor 1, **BAX**: BCL2 associated X protein, **BCL2**: B-cell lymphoma 2 protein, **caspase**: cysteine-aspartic proteases, **DNA**: deoxyribonucleic acid, **Drp1**: Dynamin-related protein-1, **H2AX**: histone family member X, **Mito.**: mitochondria, **MLKL**: Mixed lineage kinase domain like pseudo-kinase, **mRNA**: messenger ribonucleic acid, **NAC**: N-acetylcysteine, **PARP**: poly ADP ribose polymerase, **RIPK**: Receptor-interacting serine/threonine-protein kinase.

It is therefore hypothesized that these protective antioxidant agents could potentially restore the function of impaired diabetic MSCs following prolonged exposure to hyperglycaemia-induced oxidative stress.

Chapter 3: Aims & Objectives

The main purpose of this research was to broaden our insight into the sensitivity of MSCs to pathological environments and to better our understanding of how to counteract stem cell impairment and manipulate their phenotype *in vitro* in order to improve the predictability and success of stem cell-based treatments.

It is ***hypothesized*** that prolonged exposure of bone marrow MSCs to a pathological diabetic microenvironment *in vivo* reduces the ability of these cells to respond to environmental cues in order to promote healing. MSC dysfunction is thought to be related to disrupted paracrine signalling that is skewed towards a pro-inflammatory and destructive instead of a pro-regenerative phenotype.

The overall aim of this research was furthermore to assess the efficacy of *ex vivo* antioxidant AAP and NAC preconditioning to restore the paracrine and functional responses of severely impaired diabetic MSCs prior to transplantation and asses its protective effect against the hostile wound micro-environment.

In order to test our hypothesis, the research study was divided into the following aims and objectives:

Aim 1: Establish and optimise a full-thickness excisional wound model for collection of diabetic wound fluid to represent the pathological micro-environment of a diabetic wound *in vitro*.

- ✓ *Objective 1.1:* Optimise and establish the standard operating procedure for induction of bilateral full-thickness excisional wounds on obese prediabetic mice (B6Cg-Lep^{ob}/J).
- ✓ *Objective 1.2:* Inject NEP, an inhibitor of substance P, around the wound edges to prevent wound contraction and further delay healing.
- ✓ *Objective 1.3:* Collect and store DWF over a period of 27 days post wounding.
- ✓ *Objective 1.4:* Determine the protein concentration within diabetic wound fluid and assess its cytokine profile.

Aim 2: Determination of the safest, non-toxic dose of NAC and AAP as potential antioxidants to counteract MSC impairment.

- ✓ *Objective 2.1:* Using an immortalized mouse stem cell line (C3H10T1/2) identify the optimum individual dose of either AAP or NAC that will maintain cell viability whilst promoting cellular proliferation under standard culture conditions.
- ✓ *Objective 2.2:* Determine the synergistic effect of the optimum combined doses of AAP+NAC on MSC viability and proliferation under standard culture conditions.
- ✓ *Objective 2.3:* Determine the optimum combined dose of AAP+NAC to be used in subsequent experiments.

Aim 3: Investigate the efficacy of antioxidant (AAP+NAC) preconditioning to restore the molecular/paracrine and functional responses of bone marrow MSCs upon stimulation with DWF.

- ✓ *Objective 3.1*: Isolation of primary bone marrow-derived MSCs from healthy control (source: wild type, C57BL/6J) and obese prediabetic (source: obese pre-diabetic, B6Cg-Lep^{ob}/J) *(ob/ob)* mice and confirm their identity by flowcytometry.
- ✓ *Objective 3.2*: Determine the *ex vivo* growth rate and viability (with and without antioxidant preconditioning) of healthy control MSCs and impaired diabetic MSCs over a period of 16 days after isolation.
- ✓ *Objective 3.3*: Assess the molecular (mRNA expression) and paracrine (secretome) responses of healthy and impaired diabetic MSCs at baseline and with antioxidant preconditioning upon stimulation with diabetic wound fluid.
- ✓ *Objective 3.4*: Assess the efficacy of antioxidant preconditioning to improve the survival (viability) and functional responsiveness (proliferation, migration) of healthy and impaired diabetic MSCs at baseline and in the presence of DWF.

Chapter 4: Diabetic wound model: Induction of full-thickness excisional wounds, collection, and characterization of diabetic wound fluid.

4.1 Introduction

The pathogenesis of chronic diabetic wounds is complex and involve numerous tissues (skin, muscle, nerves, micro-vascular system) and cell types, which following injury have failed to initiate and progress through the regular tissue repair processes to restore structural and functional integrity to the damaged area *(Chapter 2.2, p.10).* The most predictive models for studying wound healing *in vivo,* are animal models that mimic the healing environment and represent similar cell types, micro-environmental cues, and paracrine interactions.

The *full-thickness mouse excisional skin wounding technique* is well-established in the literature (Wong et al., 2011) and is used to gain a better understanding of regenerative mechanisms. This technique is beneficial for researchers because of its simplicity and reproducibility. It furthermore provides, easy access to the wound bed to (a) apply topical therapeutic agents, and (b) harvest diabetic wound fluid (DWF) and tissue samples for histological analysis. This model is thus an essential tool for research into cutaneous wound healing disorders (Reid et al., 2004; Wong et al., 2011). Although mouse skin is similar to that of humans and consists of the same three main layers (epidermis, dermis, and hypodermis), it differs in the initial response to injury. Human skin heals *via* scab formation, re-epithelialization, and granulation, whereas mouse skin produces rapid wound contraction *via* the *Panniculus carnosus* layer immediately after injury prior to re-epithelialization (Chen et al., 2013). Therefore, wound diameter is a representative factor of wound contraction and healing. Despite this difference in the initial response to injury, normal healing (wild-type mice and humans) occurs within 7-10 days (Seitz et al., 2010). These wounds do however not mimic non-healing/chronic wounds; researchers, therefore, developed various transgenic murine disease models with metabolic phenotypes similar to that observed in obese diabetic patients in which this excisional skin wound technique would generate a wound with impaired healing characteristics.

One such model uses B.6.Cg-Lep^{ob}/J (*ob/ob*) mice (JAX® #000632, USA). The obese prediabetic phenotype exhibited in *ob/ob* mice is a consequence of a spontaneous mutation in the Lep^{ob} gene that encodes a 16-kDa protein Leptin, which plays an essential role in energy homeostasis. These mice develop a complex metabolic syndrome that includes hyperphagia, hyperglycemia and glucose intolerance leading to severe healing disorders (Goren et al., 2003; Ring et al., 2000; Stallmeyer et al., 2001). The *ob/ob* mouse model is therefore commonly used to investigate impaired healing associated with metabolic dysfunction (Goren et al., 2003; Seitz et al., 2010). In the current study, the *ob/ob* wound model was further optimized to limit wound contraction and delay healing to a greater extent by applying a zinc metalloprotease (neural endopeptidase, NEP) to the wound edges at similar concentrations detected in the ulcer margins of diabetic wound patients (Antezana et al., 2002). NEP

functions to degrade, the pro-regeneration factor, substance P, and by doing so exacerbates the abnormal healing responses (Delgado et al., 2005; Spenny et al., 2002).

This optimized diabetic wound model was used in this study to collect diabetic wound fluid for subsequent application in *in-vitro* experiments *(Chapter 6, p.57*) focussed on the paracrine and functional responsiveness of mesenchymal stem cells (MSCs) to a pathological wound microenvironment. This approach enables molecular investigations in an *ex vivo* setting that simulates wound conditions.

4.2 Material and Methods

4.2.1 Ethics approval statement

This study was approved by the animal research ethics committee at Stellenbosch University (#SU-ACUD17-00016/ 23 June 2017) and complied with the South African Animal Protection Act (Act no 71, 1962). All experimental procedures were conducted according to the ethical guidelines and principles of the declaration of Helsinki *(Refer to Addendum A, p.115 for the ethical approval letters)*.

As provided for in the Veterinary and Para-Veterinary Professions Act, 1982, all researchers that were involved in the animal work were registered with or have been authorized by the South African Veterinary Council (SAVC) to perform the procedures on animals. All procedures were under the direct and continuous supervision of a SAVC-registered veterinary professional who was acting within the scope of practice for their profession.

4.2.2 Animal housing and husbandry

A specific pathogen-free (SPF) B6.Cg-Lep^{ob}/J (Fig. 4.1) strain of mice (weight 40-60g), that is homozygous for the obese spontaneous mutation (the gene responsible for the production of leptin), was used in this study. Homozygous mutant mice were first recognizable at about four weeks of age; these animals gain weight rapidly and at 6-8 weeks (40-60g) may reach three times the normal weight of wild-type controls (C57BL/6J) (17-25g). In addition to obesity, mutant mice exhibit hyperphagia, a diabetes-like syndrome of hyperglycemia, glucose intolerance and, elevated plasma insulin levels.

Mice were housed under standard conditions (12h light / 12h dark cycle at a controlled temperature of 21°C) and had free access to drinking water and chow (Rat and Mouse Breeder Feed, Animal Specialties, Pty, Ltd., Klapmuts, SA).

Figure 4.1 Representative images of the wild type (left) **C57BL/6J and *ob/ob*** (right) **B6.Cg-Lep^{ob}/J mice** (© https://www.jax.org/strain/000632).

4.2.3 Overview of Study design and experimental procedures

Refer to Figure 4.2 below for an overview of the study design. At the end of the study, on day 27, all mice were euthanized *via* cervical dislocation. Euthanasia was, performed by a well-trained SAVC-registered para-veterinary professional according to the American Veterinary Medical Association (AVMA) Guidelines on Euthanasia (Leary et al., 2013).

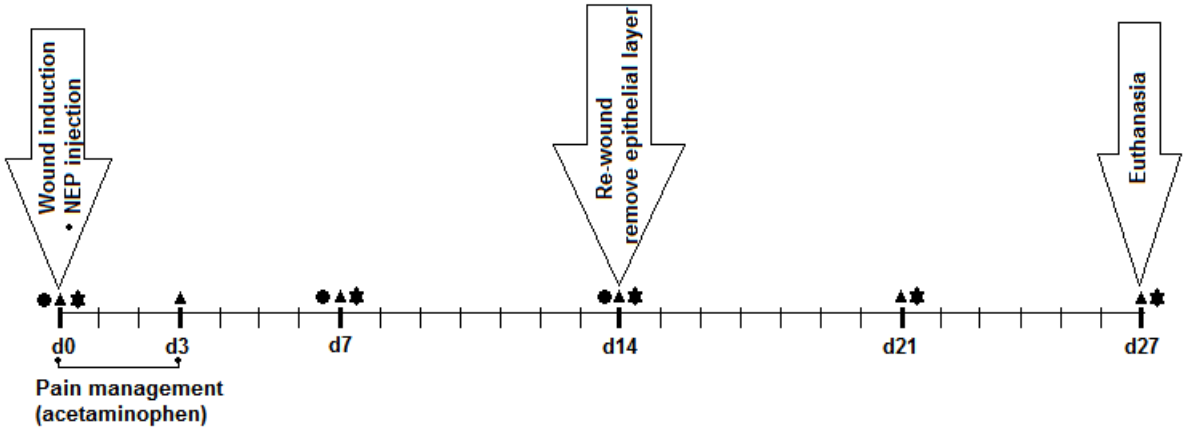

Figure 4.2 Overview of study design. Two bilateral full-thickness dorsal skin excisions were made on male B6.Cg-Lep^{ob}/J (n=7) mice on day 0. Mouse CD10 / Neprilysin (NEP, 0.330 µg/mL) was injected around the wound edges on days 0, 7 and 14. Animal wellness was monitored daily and the animals weighed twice weekly. Diabetic wound fluid was harvested from the wounds by needle puncture on days 7, 14, 21 and 27**. Legend: ★ :** collection of diabetic wound fluid, **▲ :** weight assessment, **I:** daily animal wellness monitoring and **● :** NEP injection.

4.2.3.1 Induction of full-thickness excisional wounds

Mice (n=7, 6-8 weeks old) were weighed (43±2g) and anesthetized *via* an open system inhalation anesthesia (Fig. 4.3B) using Isoflurane chamber (3% for induction and 2% for maintenance) (Safeline Pharmaceuticals (Pty), Ltd, SA). Dorsal hair was shaved, and the skin cleaned with povidone-iodine (Mundipharma (Pty) Ltd, South Africa) prior to making two identical contra-lateral full-thickness skin excisions (Fig. 4.3A). Excisional wounds were made by applying outward retraction of the skin using sterile forceps and a scissor-sharp cut (Chen et al., 2013), 1cm below the base of the skull and 1cm

on either side of the midline (Fig. 4.3C). The underlying layers (including the *panniculus carnosus*) were removed in a similar manner to achieve a full-thickness wound. The diameter of each wound was approximately 6mm. Immediately after wounding, local anesthetic, 7 mg/kg lignocaine 2% (Bodene Pty, Ltd, SA) was injected around the wound edges and the sedation maintained for a period of 3 days by administrating oral 300 mg/kg Acetaminophen (Paracetamol 120mg, GSK, SA) in drinking water. Both the excisional wounds were covered (Fig. 4.3D) by a vapor-permeable polyurethane film (Hydro-film, Paul Hartmann AG, Germany). After recovery from the anesthesia, mice were individually housed for a period of 27 days. Wounded mice were monitored closely and marked daily for signs of distress and pain to ensure the welfare of animals.

To prevent wound contraction, 75µl (0.330 µg/mL) recombinant CD10 / Neprilysin (also known as NEP) (SRP 6450, SIGMA, USA) was injected (dosage was determined based on enzyme activity: 50 pmol/hour/µg) around the wound edges at days 0, 7 and, 14. In the case of NEP inefficacy and re-epithelization, the wounds were physically reopened by removing the epithelial layer and widening the edges on day 14 to maintain exudate collection. During re-wounding, the same sedation procedure was maintained, and animal wellness monitored closely.

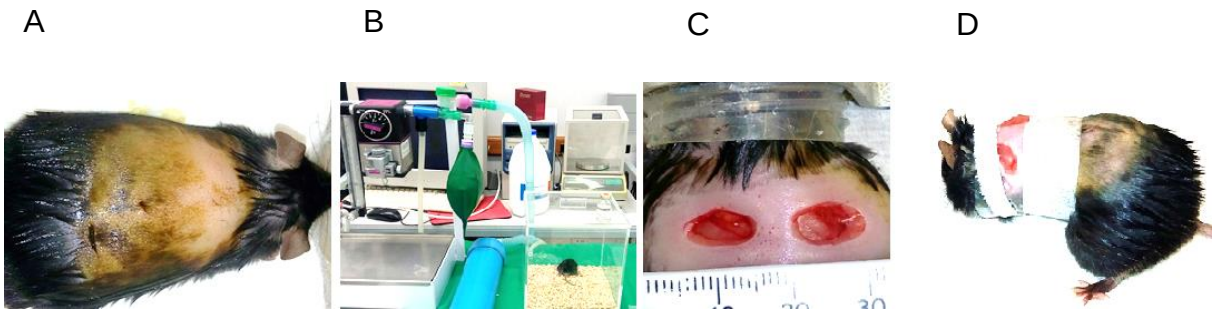

Figure 4.3 Representative images illustrating the experimental procedures: A- Male B6.Cg-Lep^{ob}/J mouse with hair shaved and skin cleaned. **B-** open system inhalation anesthesia to restrain mice during the procedure. **C-** two identical contra-lateral full-thickness skin excisions. **D-** wounds covered with a vapor-permeable polyurethane film.

4.2.3.2 Wound size calculation

The percentage of wound closure (based on the wound contraction) over time was used as an indication of healing. Wound images were captured directly from above on days 0, 7, 14, 21 and 27 post-wounding. A ruler (1cm) was placed at the wound edge prior to taking each image as a point of reference for size calculations. The surface area of each wound (mm^2) was measured by tracing along the border of the wound using Image J software (version 1.46, NIH.gov, USA).

Image J analysis: 1) After opening and selecting the appropriate image, the *Straight-line tool* was used to measure the number of pixels on the 1cm point of reference. 2) This information was then used to set the image scale (distance in pixels = length measured in *Straight line tool*; known distance =1, unit of length =cm). 3) Finally, using the *freehand tool* the outer wound edges were traced, and

the surface area of each wound automatically calculated. The percentage of wound closure over time was calculated according to the following formula:

$$\% \text{ wound closure} = \frac{[\text{wound area (d0)} - \text{wound area (dx)}]}{\text{wound area (d0)}} \times 100$$

The comparison with the initial wound area, on day 0, eliminates any discrepancies created by small differences in initial wound size (Goetsch and Niesler, 2011).

4.2.3.3 Collection of diabetic wound fluid

Accumulated exudate was harvested from the wounds by needle (25-30G, BD Micro-Fine™ Plus, USA) puncture at days 7, 14, 21 and 27 post-wounding. First, the exudate accumulated under the vapor-permeable polyurethane film was collected using a needle and syringe. Secondly, 100µl saline solution was injected under the vapor-permeable polyurethane film onto the wounded area (the volume of saline injected was consistent for each wound) and recollected after 30 seconds. After each collection, the DWF was immediately stored at -80°C.

To ensure that sufficient fluid is collected for subsequent experiments, the exudates collected from all animals and all the time points were pooled together. It was centrifuged (1000, 2000 and 3000 RPM for 10 min, x3 repeats) to eliminate all cellular debris and sterile filtered (GVS 0.2µm, USA). The sterile DWF was aliquoted and stored in eppies at -80°C. Repeat freeze-thaw cycles were avoided.

4.2.4 Characterization of collected diabetic wound fluid

The purpose for characterizing the collected DWF was to (a) confirm that the exudate is representative of a chronic wound microenvironment (cytokine profile), and (b) to determine the concentration of DWF to be used in subsequent experiments.

4.2.4.1 Protein concentration

The total protein concentration in the collected DWF was determined using a standardized Bradford protein assay. Bovine serum albumin (1%) (Hyclone BSA, Thermo, USA) was used as a standard for calibration. BSA concentrations of 1, 5, 10, 15, 20, 25, 30, 35 and 40 µg/µl were used as standard protein dilutions and one µl of each sample analyzed to determine the protein concentration (µg/µl). Depending on the protein content within samples, color changes occurred in Bradford reagent (1x) and the absorption shifts (96 well plate, standard clear flat bottom) were read at 595 nm using Multi-scan spectrophotometer (GO®, Thermo Fisher, Finland). Total protein concentration (µg/µl) within each sample was calculated based on optical density (OD) /µl measurement:

Calculation is based on OD/µl of the BSA-dilution (1µg/µl) series:

$$\sum\left(\frac{(OD(5\mu l))}{5\mu l}+\frac{(OD(10\mu l))}{10\mu l}+\frac{(OD(15\mu l))}{15\mu l}+\cdots/n\right)=OD/\mu l$$

$$\left(\frac{OD\ (protein)}{\sum(OD\mu l\ BSA\ Dilutions)*1(\mu l\ of\ sample)}\right)*X\ (Dilution\ factor)=Protein\ conc.\mu g/\mu l$$

To determine the optimal concentration of DWF to be used in subsequent *in vitro* experiments, the total protein concentration was compared to that of foetal bovine serum (FBS, growth supplement for MSC cultures) (Biochrom GmbH, Germany) and CST (serum-free media growth supplement) (StemPro® MSC SFM, Gibco Life Technologies, USA).

4.2.4.2 SDS-PAGE

Sodium dodecyl sulfate-polyacrylamide gel electrophoresis (SDS-PAGE) assay was used to denature the proteins and estimate protein size in the harvested exudate. A total of 20 or 30µg protein from each sample (DWF, FBS and CST) was denatured and loaded in pre-casted SDS-PAGE gels (Mini-protean® 4-15% Stain-free, BIO-RAD, USA). Electrophoresis started at 80V (10 min) and continued at 120V (50 min). Proteins were transferred (30min) from the gel to a nitrocellulose blotting membrane (Mini Trans-Blot® Turbo Transfer pack, BIO-RAD, USA) using a semi-dry transfer system (Trans-Blot® Turbo, BIO-RAD, USA). To visualize the proteins, the membrane was stained for 2 min using Ponceau S solution (Sigma, Germany). Pre-stained protein ladder (Pageruler™, Fermentas, USA) was used as an indication of protein size.

4.2.4.3 Cytokine profile in diabetic wound fluid

The cytokine profile of the collected DWF was assessed as an indication of the inflammatory stage of the wounds. DWF was analyzed using the Bio-Plex Pro™ Mouse 23-plex bead-array assay (BIO-RAD, USA) and quantified using the Multiplex reader and Bio-Plex Manager™ MP software (Bio-Plex® MAGPIX™ BIO-RAD, USA) according to the manufacturer's instruction. The Bio-Plex assay system is based on sandwich immunoassay, formatted on magnetic beads (Fluorescently dyed microspheres) with a distinct color code to permit discrimination and are coated with a specific panel of antibodies. This assay simultaneously measures multiple analytics in a single sample that included the following cytokines: IL1α, IL1β, IL2, IL3, IL4, IL5, IL6, IL9, IFNγ, KC, MCP1, MIP1α, MIP1β, RANTES, TNFα, IL10, IL12(p40), IL12(p70), IL13, IL17A, Eotaxin, G-CSF, GM-CSF CSF indicating inflammatory stage of the wound.

4.2.5 Statistical Analysis

Values are presented as mean ± standard error (mean±SE). All data analysis was performed using Statistica program (V. 13, StatSoft). Repeated measures ANOVA with Bonferroni post hoc test was used to assess animal weight and wound closure over time. Level of significance was accepted at $p<0.05$.

4.3 Results

4.3.1 Mice recovery and weight loss

Most of the mice recovered in a good condition after wounding with only 1 animal dying in the 27 days from initial wounding. (Fig. 4.4A). No sign of pain, anxiety or deviation (wellness score = 0) was observed in most cases during this period (Fig. 4.4B). No significant weight loss was apparent in the wounded animals (start weight: 43±2g; end weight: 40±3g) for the duration of the study (Fig. 4.4C), however due to the effect of the anaesthesia no weight gain was observed either. Only a moderate decline in weight was observed in the first 3 days post wounding.

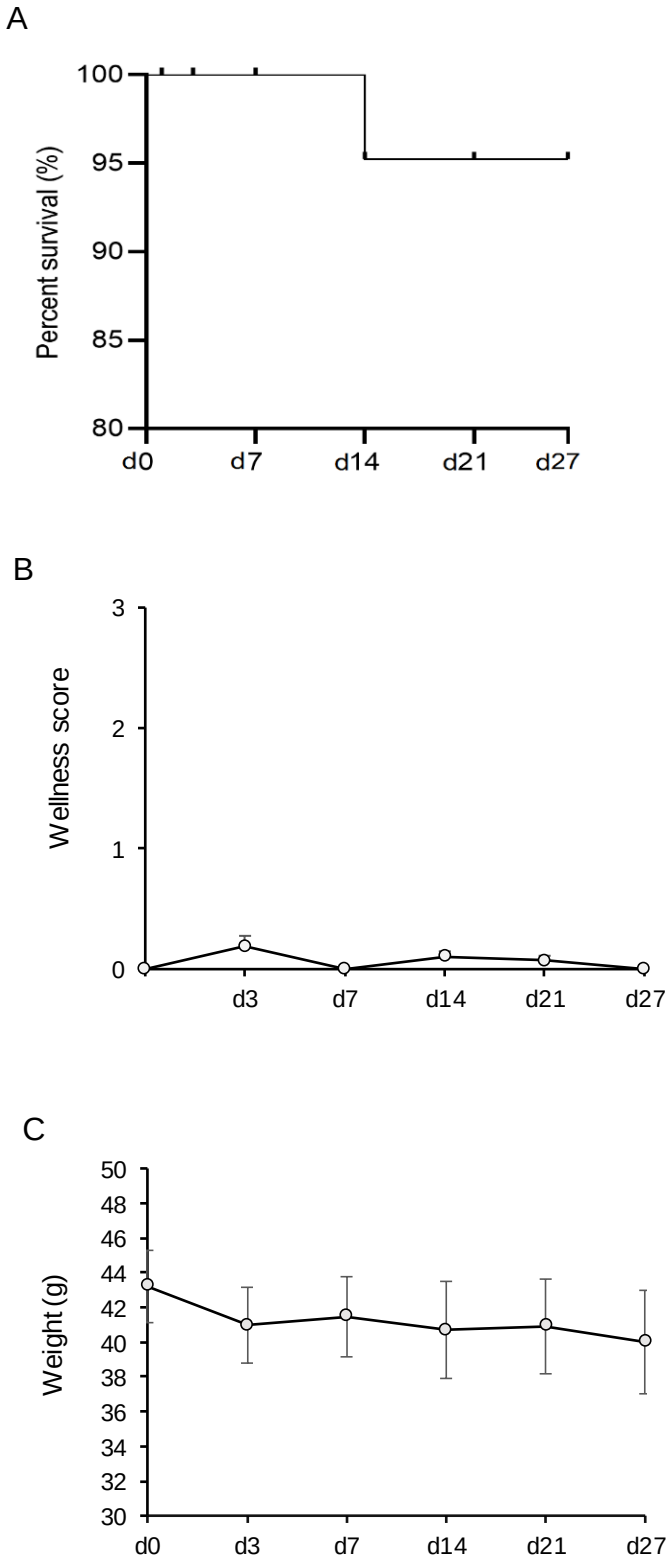

Figure 4.4 Animal wellness and recovery during the 27 days post-wounding. A- Kaplan-Meier survival curve indicating the percentage (%) survival. **B-** Animal wellness scores: (0) within normal limits and no signs of distress, (1) Appearance and behaviour shows slight or intermittently deviation from normal, (2) Appearance and behaviour shows a moderate deviation from normal, (3) Appearance and behaviour has significantly deviated from normal or animal is clearly distressed. **C-** Animal weight (mean±SD) over the 27-day period. **Statistical analysis:** Repeated measures ANOVA with Bonferroni post hoc test; no significant effect was observed over time ($p<0.05$).

4.3.2 Wound closure

Refer to Figure 4.5 for representative images of the wounds at each time point for each animal. From the seven animals wounded, one animal (#6) was not re-wounded on day 14 due to signs of distress and one animal (#7) died under anaesthesia on day 14. In this model for all the animals wounded (n=7), macroscopic wound closure was 33±7% on day 7 and 77±4% on day 14. In the subsequent period after re-wounding (from day 14 onwards), wound closure was 48±7% at day 21 (n=5, excluding mouse #6 & 7) (Fig. 4.6). Although healing was delayed, a significant effect of time ($p<0.05$) was evident between days 7 to 14 (initial wound) and days 14 to 27 (re-wounding). (Fig. 4.5).

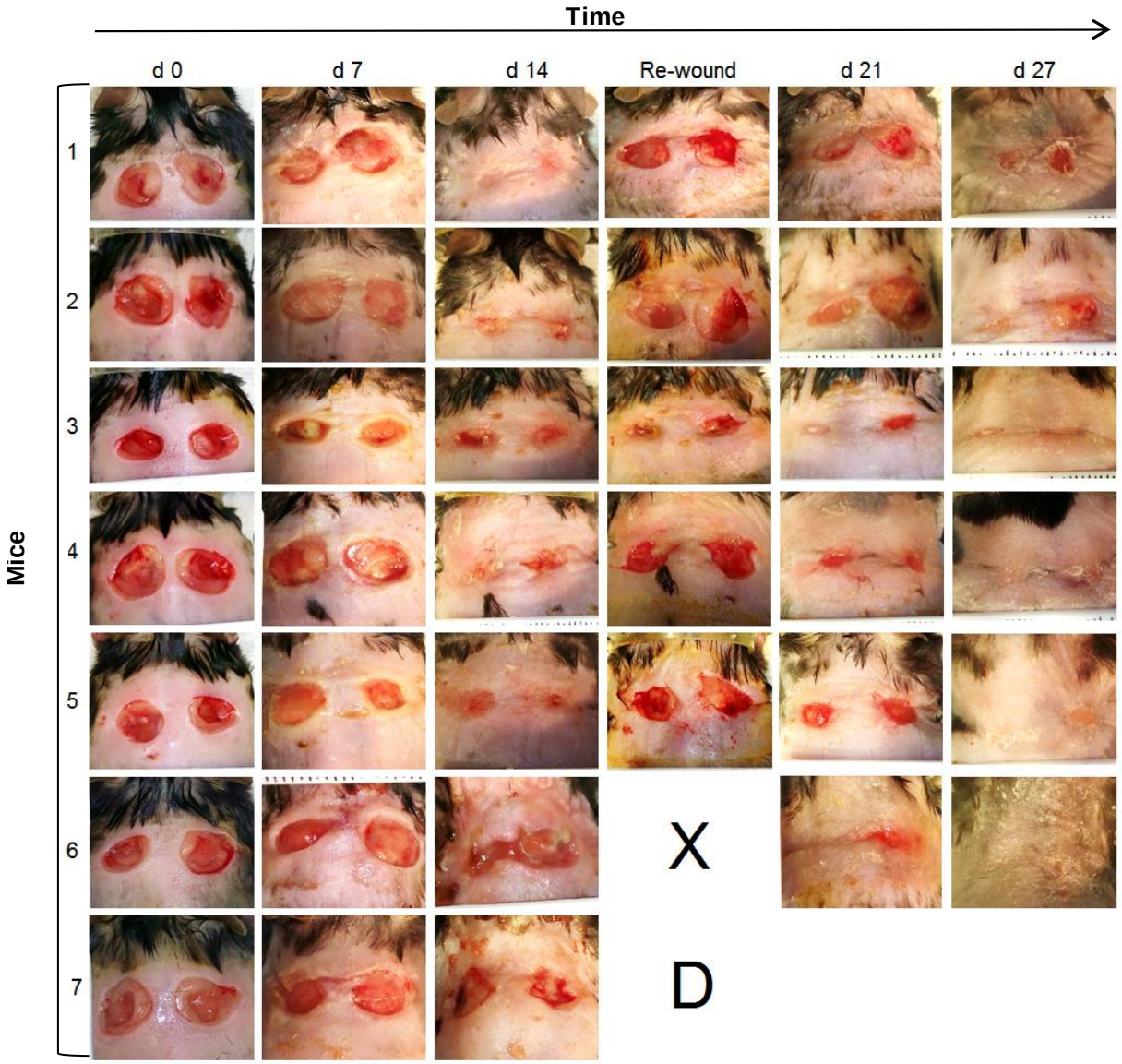

Figure 4.5 Representative images of full-thickness bilateral wounds over time. (X): Animal #6 was not re-wounded due to signs of distress. **(D):** Animal #7 died under analgesia on day 14. For these two animals diabetic wound fluid was collected until day 14.

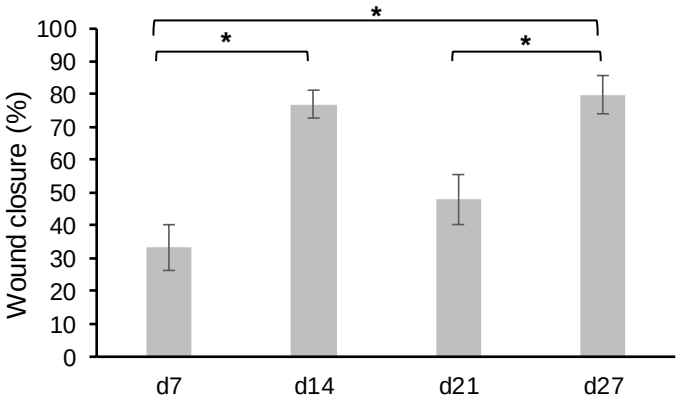

Figure 4.6 Percentage of wound closure. Wound surface area at each time point was determined using ImageJ software (version 1.46, nih.gov) and the percentage wound closure calculated using the following formula: [(wound area d0 – wound area dn)/ (wound area d0) x 100]. **Statistical analysis:** Repeated measures ANOVA with Bonferroni post hoc test. * $p < 0.05$ indicates a significant difference between time points.

4.3.3 Protein concentration of exudate and Electrophoresis

Results from Bradford assay (Fig. 4.7) revealed a total protein concentration of 9.6 µg/µl in collected DWF, whereas the protein content in FBS and CST were 27.9 µg/µl and 35 µg/µl respectively. Standard cell culture growth media, therefore, has a total protein content that is x3 fold higher than that observed in DWF. Stained Nitrocellulose membrane visualized exudate proteins at the same range of FBS or CST cell culture protein supplement.

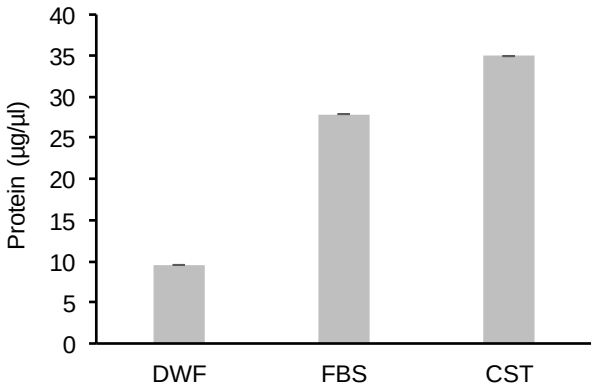

Figure 4.7 Protein concentration in 1µl of either pooled diabetic wound fluid, FBS or CST. DWF: diabetic wound Fluid, **FBS:** Foetal Bovine Serum and **CST:** StemPro® supplement.

4.3.4 Cytokine profile

The concentrations (pg/mL) of 23 cytokines detected in the DWF are presented in Table 4.1. Pro-inflammatory cytokines (IL1α, IL1β, IL6, IL12(p40), IL12(p70), IL17A and TNFα) and chemokines (Eotaxin, G-CSF, GM-CSF, KC, MCP1, MIP1α, and MIP1β) were present in high concentrations; whereas anti-inflammatory cytokines (IL2, IL3, IL4, IL5, IL13 and IL10) had much lower levels within the DWF despite re-opening wound at day 14. Suggesting that the microenvironment within wounds had a persistent pro-inflammatory profile even after re-wounding.

Table 4.1 Cytokine concentrations (pg/ml) in collected diabetic wound fluid.

Pro-inflammatory cytokines	DWF	Chemokines	DWF	Anti-inflammatory cytokines	DWF
IL1α	6992.7	**MIP1α**	OOR>7288 (S1)	**IL10**	262.8
IL1β	3360.8	**MIP1β**	1186.6	**IL13**	328.7
IL6	1004.2	**Eotaxin**	571.8	**IL2**	22.8
IL9	127.2	**G-CSF**	OOR>47590 (S1)	**IL3**	26.8
IL12(p40)	4961.6	**GM-CSF**	671.6	**IL4**	90.5
IL12(p70)	598.2	**KC**	OOR>21315 (S1)	**IL5**	26.7
IL17A	360.5	**MCP1**	18568.2		
RANTES	128.2				
TNFα	932.1				
IFNγ	43.5				

Footnote: DWF were collected from #7 mice in 4 time points and pooled together and its cytokines were analyzed by Bio-Plex assay system, **OOR:** out of measurable range (very high), **pg:** picogram, **S1:** standard one (Highest concentration of standard curve – upper detection limit).

4.4 Discussion

Despite advances in technology, clinical outcomes in managing chronic wounds are not promising. Studies suggest that MSCs may promote tissue regeneration, however further *in vitro* studies are required to clarify and understand their mechanisms of action in response to a chronic wound environment (Otero-Viñas and Falanga, 2016; Satija et al., 2009). To enable more insight into underlying mechanisms related to MSC response to the pathological microenvironment, an *in vivo* delayed-healing wound was created to mimic the diabetic wound conditions more closely; DWF was subsequently collected over a period of 27 days. Despite the NEP application, our model did not perfectly mimic a non-healing wound since re-epithelialization was evident after day 14; this necessitated the reopening of wounds. Nonetheless, analysis of DWF indicated a chronic inflammatory profile that is characteristic of diabetic wounds.

In cutaneous injuries, the epidermis produces neuropeptides such as Substance P from C-fibres, which induces pro-inflammatory effects and improves mitogenesis and migration of the surrounding keratinocytes, fibroblasts and endothelial cells (Antezana et al., 2002; Spenny et al., 2002). SP stimulates (a) nitric oxide release, vasodilatation and microvascular permeability, (b) expression of

adhesion molecules on endothelial cells and (c) monocyte chemotaxis leading to cell proliferation and repair (Antezana et al., 2002; Delgado et al., 2005; Leal et al., 2015). Substance P action is mediated primarily through a neurokinin receptor, NK-1R, a G-protein coupled receptor with a regulatory mechanism in enzymatic degradation; NK-1R is expressed in nervous and peripheral tissues (Turner et al., 2001).

NEP, a zinc metalloprotease, is present in the cell membrane of the same cells that express NK-1R. NEP competes with NK-1R and its hydroxylation of peptide bonds on the amino-terminal end of hydrophobic substrates such as Substance P and causes a disruption in neural signaling pathways. Studies indicate that there is an abnormality in neural signaling pathway in diabetes and a higher NEP activity in diabetic wounds (Antezana et al., 2002; Leal et al., 2015; Spenny et al., 2002). There is furthermore a correlation between Substance P degradation and abnormal healing responses in diabetes, whilst inhibiting NEP causes inflammation and regeneration (Delgado et al., 2005; Spenny et al., 2002).

In previous studies, NEP enzyme activity of 20.6 ±4.5 pmol/hour/µg was identified in diabetic unwounded mouse skin (Spenny et al., 2002), and an activity of 47.5 pmol /hour/ µg in the margins of DFUs in patients (Antezana et al., 2002). This is significantly higher than the baseline NEP enzyme activity (3.65 pmol/hr/µg) in non-diabetic patients (Antezana et al., 2002). Based on this information, a NEP concentration (0.330 µg/ml) equal to 50 pmol/hour/µg enzyme activity was injected at the wound edges on day 0, 7 and 14 post-wounding in the current study.

Diabetic wound fluid is considered an exudate with a high protein concentration (total protein: 26-51 µg/µl) in which albumin is the major protein consisting of 14-28 µg/µl of the total protein content (Trengove et al., 1996). This fluid is generated by enhanced capillary leakage and activity of a variety of resident and/or migratory cell types. Diabetic wound fluid, therefore, has a biochemical composition equivalent to extracellular fluid, reflects the clinical condition of the wound and is not significantly altered by the collection process (Schmohl et al., 2012). In the current study, the protein concentration of collected DWF (9.6 µg/µl), was 3-fold less than that of FBS (27.9 µg/µl) that is usually used as a growth supplement for cells in culture. Thus, to standardize the culture conditions for subsequent *in vitro* experiments, this study suggests that the 10% FBS in standard culture media be replaced with 30% DWF to mimic in the extrinsic wound environment in a cell culture dish. A limitation of the current model is the limited volume of wound fluid that could be collected from each animal that necessitated pooling of the DWF (following the initial injury and after re-wounding). This did not allow the assessment of individual variations or variation over time.

Delayed wound healing is a result of several contributing factors such as vascular disease, infection, pressure, cellular senescence, hyperglycemia and obesity (Mulder et al., 2012). Persistent inflammation is a key characteristic of chronic wounds (Lee, 2013; Paul, 2018; Qing, 2017; Ridiandries et al., 2018; Trengove et al., 2000). Therefore, fluid from these wounds contains elevated levels of pro-inflammatory cytokines, MMPs, and neutrophil collagenase (Löffler et al., 2013; Yager et al., 2007). The collected exudate from the *ob/ob* mice in this study had a cytokine profile that

mimicked these pro-inflammatory clinical characteristics of a non-healing diabetic wound. The observed overexpression of pro-inflammatory cytokines such as IL1, IL12, and TNFα as well as chemokines (KC, G-CSF and MIP1α) in collected DWF indicates a state of chronic inflammation (Esser et al., 2014; Fivenson et al., 1997; Löffler et al., 2011; Yager et al., 2007). IL1β produced by macrophages is an essential pro-inflammatory cytokine and contributes to T2DM pathogenesis by activating NFκB pathway and the subsequent production of other inflammatory mediators, such as TNFα (Esser et al., 2014; Löffler et al., 2011; Qing, 2017; Zhao et al., 2016). Moreover, proteolytic activity of ROS in the wound environment degrades and/or denatures some of the growth factors (such as EGF) released by the ECM and by doing so impairs regeneration (Hardwicke et al., 2011; Schürmann et al., 2014; Stern et al., 2009). The regulatory effect of ECM is therefore altered in non-healing wounds *via* changes in the secretome and protein profile, which together with persistent inflammation, downregulate proliferation and could negatively affect the regenerative potential of transplanted MSCs (Otero-Viñas and Falanga, 2016). Investigations into the responsiveness of MSC upon exposure to inflammatory DWF is thus necessary for the advancement of cell therapy approaches. This was the focus of the subsequent experiments presented in Chapter 6, p.57.

Chapter 5: Determination of the safest, non-toxic dose of N-acetylcysteine (NAC) and Ascorbic acid 2-phosphate (AAP)

5.1 Introduction

MSCs are considered a promising tool in regenerative medicine; therapeutic success in clinical applications has however been limited (Heublein et al., 2015; Mancuso et al., 2019). MSC impairment observed in diabetic patients may contribute to their limited success for autologous transplantation purposes (Ali et al., 2016). This impairment is a consequence of long-term exposure to pathological changes in the stem cell niche microenvironment. Characteristics of uncontrolled diabetes such as hyperglycaemia, the accumulation of AGEs, oxidative stress and chronic inflammation, all negatively affect the multifunctional properties of MSCs (van de Vyver, 2017). Strategies are thus needed to restore the function of impaired MSCs before autologous cell therapy can be considered a viable option.

The protective effects of some antioxidants, and their ability to promote the proliferation of healthy MSCs have already been demonstrated *in vitro* under stress conditions (Wang et al., 2013a; Yan et al., 2012). For instance, under long-term culture conditions usually associated with cellular senescence, 250µM AAP, in combination with FGF2, was able to maintain proliferation of human bone marrow-derived MSCs for up to two months in culture (Bae et al., 2015). In a different model, 1mM NAC was shown to reduce the oxidative stress (intracellular ROS and NO accumulation) associated with prolonged culture conditions and by doing so protected induced pluripotent stem cells (iPSCs) from apoptosis and senescence (Berniakovich et al., 2012). This is supported by a mouse study that demonstrated that 30mM NAC can protect diabetic bone marrow MSCs *in vitro,* against acute hydrogen peroxide (H_2O_2)-induced oxidative stress and subsequent cellular damage and apoptosis (Ali et al., 2016). Based on these and other studies, AAP and NAC are thus thought to play essential roles in cell cycle regulation, the epigenetic signature, redox status and the formation of ECM, all of which can impact stem cell fate (Ali et al., 2016; Berniakovich et al., 2012; D'Aniello et al., 2017; Li et al., 2015). To date, evidence indicating the positive effects of antioxidants on MSC proliferation is largely based on non-pathologic conditions, with only a few studies illustrating a protective effect against severe acute oxidative damage in a diabetic model.

The purpose of this study was therefore to identify (a) the optimum individual dose of either AAP or NAC that will maintain MSC viability whilst promoting proliferation and (b) to determine the effect of the optimum combined doses of AAP+NAC on MSC viability and proliferation under standard culture conditions. The identified optimum combined treatment will then be used in subsequent studies investigating the effectiveness of antioxidant preconditioning on restoring the paracrine and functional responses of diabetic MSCs *(Chapter 6, p.57).*

5.2 Material and Methods

5.2.1 Cell line and culture

As part of the refinement criteria, designed to limit the required number of animals, this study was performed using a mouse, immortalized MSC cell-line (C3H10T1/2, Clone 8 ATCC® CCL226TM). The C3H10T1/2 cell line consists of clonal mouse embryonic stem cells which are not tumorigenic when injected into irradiated or non-irradiated C3H mice; they can differentiate to all the mesodermal sub-lineages (Pinney and Emerson, 1989).

The C3H10T1/2 MSCs were preserved in liquid nitrogen and thawed (Passage 7) in a 37ºC water bath for one minute. Cells were seeded (2000 cells/cm^2) into 100mm culture dishes (Corning, New York, USA) containing 10ml standard growth medium (SGM) and maintained at 37ºC, in 90% humidified air with 5% CO_2. SGM consisted of high-glucose (4.5 g/L) Dulbecco's modified Eagle medium (DMEM) with ultra-glutamine 2mM (BioWittaker, Lonza, Basel, Switzerland), 1% penicillin (100 U/ml) /streptomycin (100 µg/ml) (BioWittaker, Lonza, Basel, Switzerland) and 10% foetal bovine serum (FBS) (Biochrom, Berlin, Germany). Media was changed every 96h until the cells reached 70-80% confluence (Fig. 5.1).

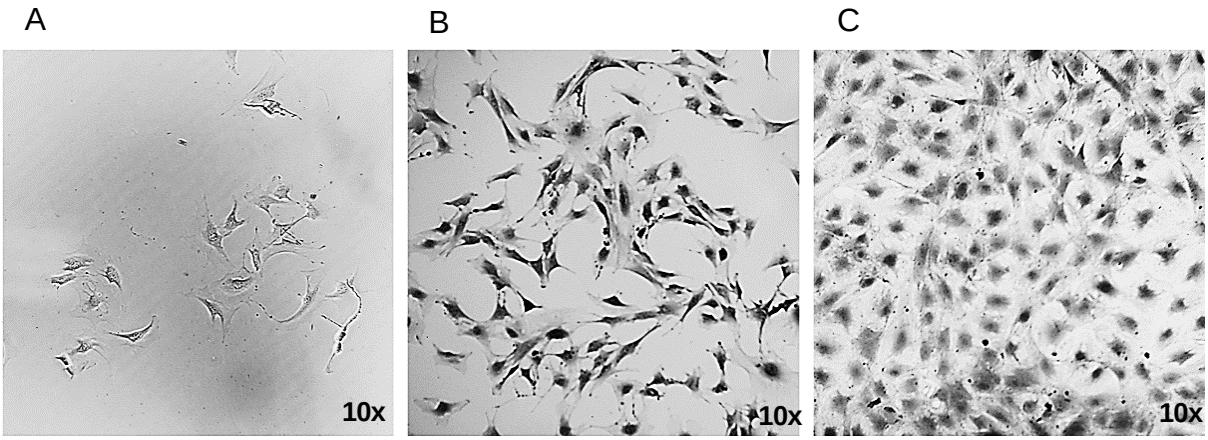

Figure 5.1 Representative images (10x/0.25 PhP objective) of C3H10T1/2 cells in culture. A-24h after seeding. **B-** 48h after seeding. **C -** 6 days after seeding (70-80% confluent).

5.2.2 Seeding and sub-culture

MSCs that reached 70% confluence (passage 7) were sub-cultured as follow: Cell culture medium was aspirated, and cells washed in pre-warmed phosphate buffered saline (PBS, containing 8g NaCl, 0.2g KCl, 1.44g Na_2HPO_4, 0.24g KH_2PO_4 in 1L dH_2O). Adherent cells were detached from the culture dish through enzymatic digestion using 0.05% trypsin-EDTA (200 mg/L Versene EDTA, Lonza, Belgium). Dishes were gently tapped until the cells were floating when viewed under a light microscope (Olympus CKX41, CachN 10x/0.25 PhP objective). SGM was added to the detached cells to inactivate the Trypsin-EDTA activity and the cell suspension transferred into 15ml Falcon tubes

(Corning, Tarnaulipas, Mexico) prior to centrifugation at 1000 RPM for 5 min (Eppendorf centrifuge 5804, Germany). After centrifugation, the cell pellet was re-suspended in 1ml fresh SGM. A cell count was performed on 20µl of the cell suspension using a haemocytometer (Fuchs-Rosenthal, Western Germany). The number of cells in four (A, B, C, and D) squares (Fig. 5.2) of the haemocytometer were counted and the density (cells/ml) calculated according to the following formula:

$$\text{Total cells/ml} = \text{Total cells counted} \times \frac{\text{dilution factor}}{\text{\# of Squares}} \times 10{,}000 \text{ cells/ml}$$

For further expansion of cell number, MSCs were seeded into a 100mm petri dish (Nest, China) at a seeding density of 2000 cells/cm^2 and sub-cultured in SGM until passage 8. For experimental procedures, cells in passage 9 were seeded into 96 well plates (Nest, China) at a seeding density of 2000 cells/cm^2.

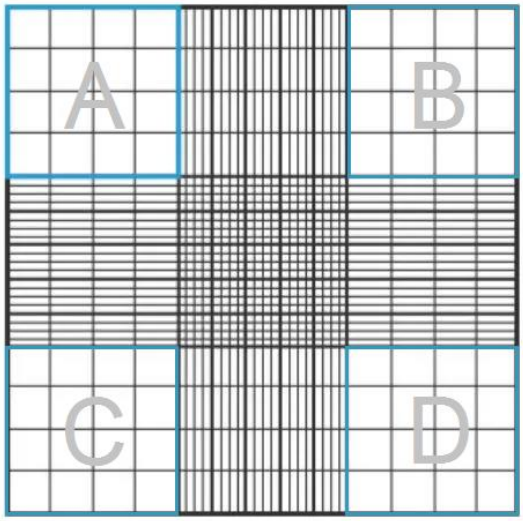

Figure 5.2 A Haemocytometer counting grid. A, B, C and D represent the respective squares used for cell counting.

5.2.3 N-acetylcysteine (NAC) and ascorbic acid 2-phosphate (AAP) concentrations

Stock solutions of NAC (60mM) (Sigma-Aldrich®, A9165-100G, St. Louis MO, USA) and AAP (0.6mM) (Sigma-Aldrich®, 49752-10G, St. Louis MO, USA) were prepared using PBS, sterile filtered (GVS 0.2µm, USA) and stored at -20ºC according to manufacturer instruction. Repeat freeze/thaw cycles were avoided and fresh stock solutions were used for subsequent serial dilutions for the dose-response experiments.

NAC (molecular weight: 163.19 g/mol) was initially diluted with PBS at a concentration of 9.79 mg/ml (60mM stock solution), and then further diluted using SGM to provide final working concentrations as indicated in Table 5.1. AAP (molecular weight: 322.05 g/mol) was diluted using DMEM at a concentration of 200µg/mL (0.6mM stock solution) and then further diluted using SGM to obtain the

final working solutions (Table 5.1). For the combination treatments, to avoid volume/volume effects of concentration reduction, the following formula was used for calculations:

$$C1V1 = C2V2$$

Table 5.1 Concentrations of NAC and AAP used in the dose-response assays.

Antioxidant	High (mM)	Medium (mM)	Low (mM)	Very low (mM)
NAC	60	30	15	7.5
AAP	0.6	0.3	0.15	-
AAP+NAC	0.6	-	15	-
AAP+NAC	0.6	-	-	7.5
AAP+NAC	-	0.3	15	-
AAP+NAC	-	0.3	-	7.5

Footnote: The medium concentration was selected based on the literature and then a higher and lower concentration chosen (based on serial dilution) to be tested in our model.

5.2.4 Cellular proliferation

Effects of NAC and/or AAP treatment on MSC proliferation was assessed using a 5-bromo-2-deoxyuridine (BrdU) ELISA assay (11669915001 Roche, Mannheim, Germany) according to the manufacturer's instructions. In the assay, BrdU incorporates into the DNA of proliferating cells during DNA synthesis. The extent of BrdU incorporation is measured using spectrophotometry and is thus directly proportional to the number of proliferating cells.

Cells were seeded (2000 cells/cm^2, in triplicate wells of a 96 well plate) in 100µl SGM and incubated for 24h at 37ºC and 5% CO_2 to allow for cell attachment. After 24h, the medium from each well was removed and 100µl of SGM containing either a high (0.6mM AAP or 60mM NAC), medium (0.3mM AAP or 30mM NAC), low (0.15mM AAP or 15mM NAC) or very low (7.5mM NAC) dose of NAC or AAP, added to each specified well (Fig. 5.3).

Plates were incubated at 37ºC for either 24h, 48h or 6 days with media being changed on day 3 since NAC has a half-life of 3-4 days. Four hours before the specified endpoints (i.e. 20h, 44h and 5 days 20h), 10µl of BrdU labelling solution (1000x Roche, Mannheim, Germany) was added to each well.

At the specified endpoints (following 4h of incubation in the presence of BrdU), the experiment was stopped by removing all the medium from each well and the plates were stored in foil at 4°C for no more than a week. This enabled the performance of the enzyme-linked immunosorbent assay ELISA for analysis of all the plates on the same day (i.e. after the 6-day time point). The assay was performed according to the manufacturer's instructions and the absorbance read at 370nm with a designated reference wavelength of 492nm (Multiskan GO plate reader, Thermo Fisher, Finland). The

assay was repeated 3 times (n=3) for each time point, with each repeat containing 3 internal replicates (3 wells).

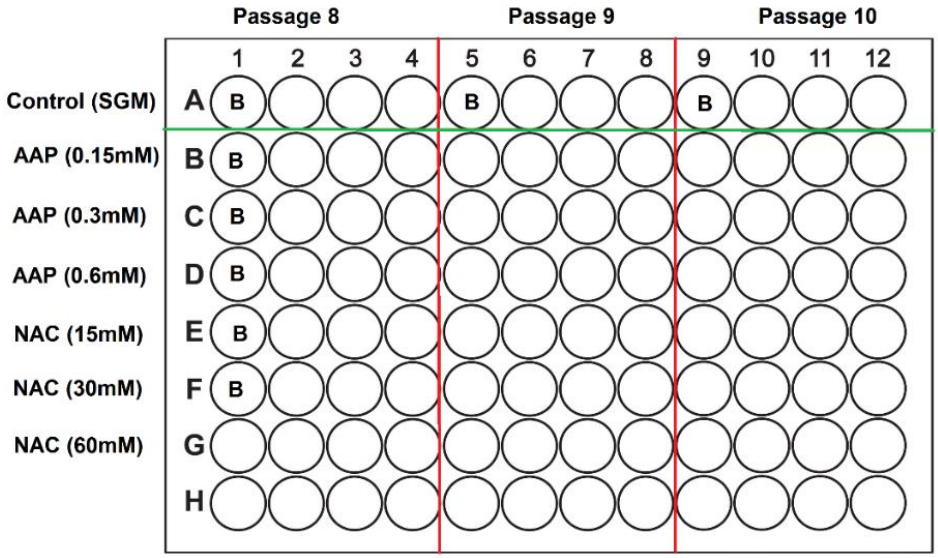

Figure 5.3 Layout of the 96 well plate and wells with treatment for BrdU assay. For each treatment condition, the assay was repeated on MSCs in x3 different passages (n=3) and for each repeat, triplicate wells were assessed. **B:** blank (background control), **mM (mmol):** millimole, **SGM:** standard growth medium.

5.2.5 Cell viability and in vitro toxicity assay

Cell viability after treatment with AAP and/or NAC was assessed using two methods: methyl-thiazolyl-tetrazolium (MTT) assay and crystal violet (CV) staining. Similar to the cellular proliferation assay (Fig. 5.3), cells were seeded into a 96 well plate (2000 cells/cm^2) in SGM (100 µl/well) and incubated for 24h at 37ºC to allow for cellular attachment. After 24h, all the medium from each well was aspirated and replaced with 100µl SGM containing either a high (0.6mM AAP or 60mM NAC), medium (0.3mM AAP or 30mM NAC), low (0.15mM AAP or 15mM NAC) or very low (7.5mM NAC) treatment dose. Plates were incubated at 37ºC for either 24h, 48h or 6 days with media being changed on day 3.

5.2.5.1 methyl-thiazolyl-tetrazolium (MTT) assay

The MTT (3-[4, 5-dimethylthiazol-2-yl]-2, 5-diphenyl tetrazolium bromide) assay measures cell viability through mitochondrial dehydrogenases. Mitochondrial dehydrogenases of viable cells cleave the tetrazolium ring, yielding purple formazan crystals. The crystals can be dissolved using a solubilization solution and the colour absorbance measured spectrophotometrically as an indication of the number of viable cells and thus the degree of cytotoxicity caused by the treatments (higher absorbance values indicates a greater amount of formazan formed and therefore more viable cells).

The following procedure was used for the methyl-thiazolyl-tetrazolium (MTT) assay (#SLBM0752V, Sigma-Aldrich®, St. Louis, USA): After 20h, 44h or 5 days and 20h of treatment (4 hours prior to

endpoint), medium was removed, the cells washed with washing solution and 100µl of DMEM (1% PenStrep) containing 10µl MTT label (M-6555 Sigma-Aldrich®, St. Louis, USA) added to each well. At the specified endpoints (after 4h of incubation in the presence of MTT), 100µl solubilization solution (M-8910 Sigma-Aldrich®, St. Louis, USA) was added and the plate incubated at room temperature for 5-10 min The absorbance values were read with the plate reader (Multiskan GO, Thermo Fisher, Finland) at 570 nm with a designated reference wavelength of 690 nm.

The MTT assay did, however, cross-react with NAC containing medium *(refer to results section 5.3.2, p.50)* and could thus only be used for the individual AAP treatments.

5.2.5.2 Crystal violet Staining

The Crystal violet Assay (hexamethyl pararosaniline chloride) was used as an alternative to determine the effect of individual NAC and combined NAC+AAP treatments on MSC viability (Feoktistova et al., 2016; Śliwka et al., 2016). Crystal violet is a simple histological stain that binds to the DNA and protein of adherent (live) cells and can be visualized using light microscopy or the colour absorbance can be spectrophotometrically measured. This characteristic can be used for the indirect quantification of cell death and to determine differences in proliferation upon stimulation with death-inducing agents compared to control. Crystal violet assay works independent from metabolism interactive additives or synergistic interaction, thus is identified as a replacement option for MTT assay when an antagonistic interaction prevents MTT measurement.

The seeding and treatment conditions were the same as described previously *(refer to section 5.2.5, p.47).* After treatment for either 24h, 48h or 6 days, all of the media was removed from each well and the cells washed with 150µl PBS (1x). The PBS was removed, and the cells fixed for 30 sec using 150µl methanol (Merck, Gauteng, RSA). After removal of the methanol, cells were washed once again (PBS 1x) and 150µl crystal violet working solution (0.01% in dH_2O) (Sigma-Aldrich®, Germany) added to each well and incubated for 5 min at room temperature. After staining, the crystal violet solution was removed, and the cells washed twice with PBS. One representative image was taken of each well using a light microscope (Olympus CKX41, CachN 10x/0.25 PhP objective). Following removal of the PBS, 100µl 70% ethanol (Merck, Gauteng, RSA) was added to dissolve the stain (shaking platform) (Heidolph, UNIMAX 1010) and the absorbance values were read with a plate reader (Multiskan GO, Thermo Fisher, Finland) at 570 nm.

5.2.6 Statistical analysis

All data values are presented as a mean ±standard error (mean±SE). Statistical analysis was performed using Statistica software (Version 13, StatSoft). Comparison of parameters (group x time) was evaluated by analysis of variance (Factorial ANOVA) followed by Tukey post hoc test. Statistical significance was accepted at $p<0.05$.

5.3 Results

5.3.1 The optimum individual dose of NAC or AAP to promote cellular proliferation

Compared to standard growth conditions (SGM set at 100%), of all the concentrations tested, the very low dose (7.5mM) of NAC had the most significant effect on the proliferation rate of MSCs over a period of 24h (187.2 ±12.9%) ($p<0.05$) and 48h (255.4 ±13.8%) ($p<0.05$) (Fig. 5.4A). Moreover, the high dose (0.6mM) of AAP significantly increased cellular proliferation after 24h (122.9 ±12.2%) ($p<0.05$) of treatment (Fig. 5.4B) compared to SGM. No significant differences were observed between treatment groups and SGM after 6 days in culture, this is likely due to contact inhibition after the cells reached confluency (>90% confluent on day 6).

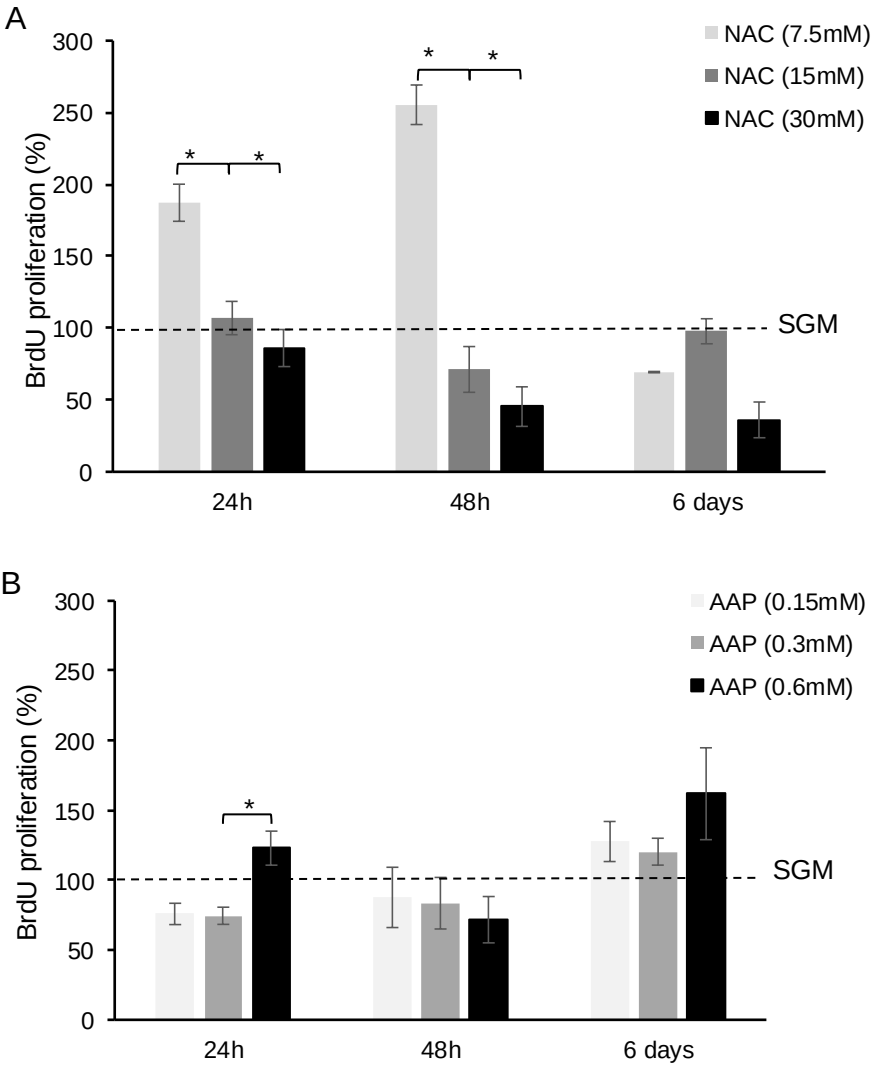

Figure 5.4 Proliferation rate of C3H10T1/2 cells after NAC and AAP treatment. A- The independent effect of NAC (7.5mM, 15mM, 30mM and 60mM) and **B-** AAP (0.15mM, 0.3mM, 0.6mM) on MSC proliferation (BrdU incorporation) over a period of 24h, 48h and 6 days. The assay was repeated on MSCs in x3 different passages (n=3) and for each repeat, triplicate wells were assessed. **Statistical analysis:** Values are presented as mean±SE with SGM (control) set at 100%. Factorial ANOVA with Tukey post hoc test (*****$p<0.05$).

5.3.2 The optimum individual dose of NAC or AAP to maintain cell viability

Due to excessive colour change (possible cross-reactivity) between MTT and NAC, the data obtained from the MTT assay for the individual NAC treatments could not be used. Upon further investigation, this information was also provided on the manufacturer's website (https://www.sigmaaldrich.com/catalog/product/sigma/a9165?lang=en&region=ZA). Refer to Figure 5.5 for a visual representation of the cross-reactivity that occurred on the plate during the performance of the assay. No significant difference was detected over time for any of the AAP treatment conditions (Fig. 5.6). However, a slight non-significant increase in the percentage (%) of viable cells was evident at 24h in the presence of AAP compared to control (Fig. 5.6). Because of the inconclusive data obtained from the MTT assay, the experiments were repeated using Crystal violet staining as an indicator of cell viability, triplicated (passages 8, 9, 10) biologically with three technical repeats for each.

Consistent with the MTT data, Crystal violet staining demonstrated that AAP (0.15mM, 0.3mM, 0.6mM) increased cell number compared to SGM during the first 24h of treatment and cell viability was maintained despite the presence of AAP over the 48h and 6-day culture period (Fig. 5.7). Quantification of Crystal Violet staining spectrophotometrically illustrated AAP sustained cell viability to a greater extent than SGM (Fig. 5.8).

Crystal violet staining furthermore confirmed that the high concentrations of NAC (15mM and 30mM) were cytotoxic (Fig. 5.9). Complete cell lysis occurred in the highest concentration of NAC (60mM). The very low dose of NAC (7.5mM) was the only tested concentration that could sustain cell viability to a similar extent than SGM over the 6-day culture period (Fig. 5.10).

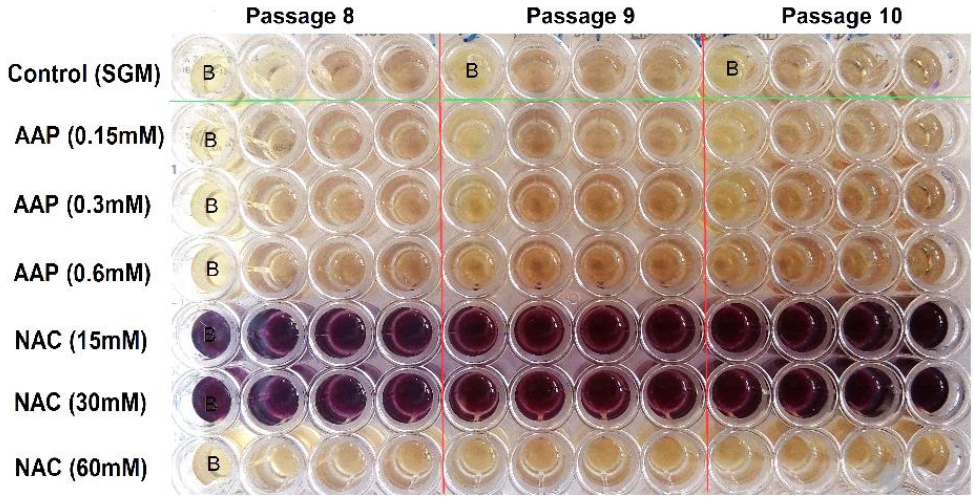

Figure 5.5 A representative image indicating cross-reactivity during the MTT assay. The reaction only appeared in NAC preconditioned wells containing viable cells (15mM and 30mM). No cross-reactivity was evident in the wells treated with NAC (60mM), due to complete cytotoxicity and cell lysis following treatment with a high concentration of NAC. A very low concentration of NAC (7.5mM) was therefore added to subsequent experiments. **mM (mmol):** millimole

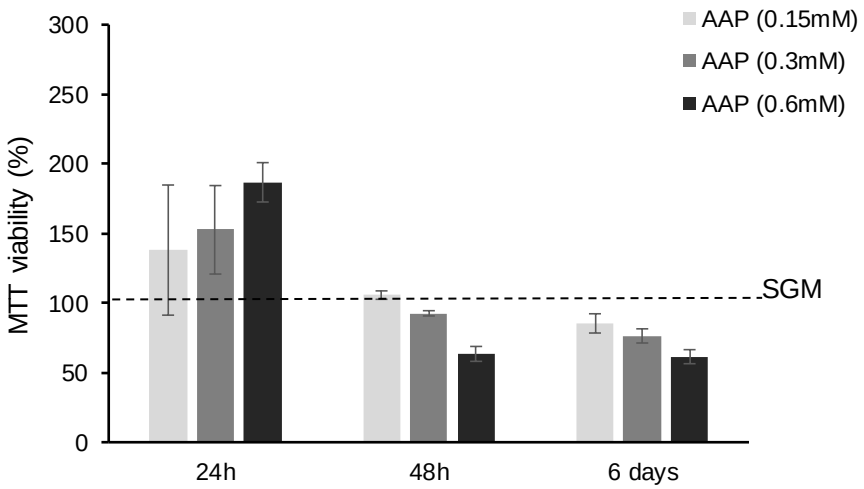

Figure 5.6 MSC viability following treatment with AAP. The independent effect of AAP (0.15mM, 0.3mM, 0.6mM) on MSC viability (MTT cell toxicity) over a period of 24h, 48h and 6 days. The assay was repeated on MSCs in x3 different passages (n=3) and for each repeat, triplicate wells were assessed. **Statistical analysis:** Values are presented as mean±SE with SGM (control) set at 100%. Factorial ANOVA with Tukey post hoc test (*****p<0.05).

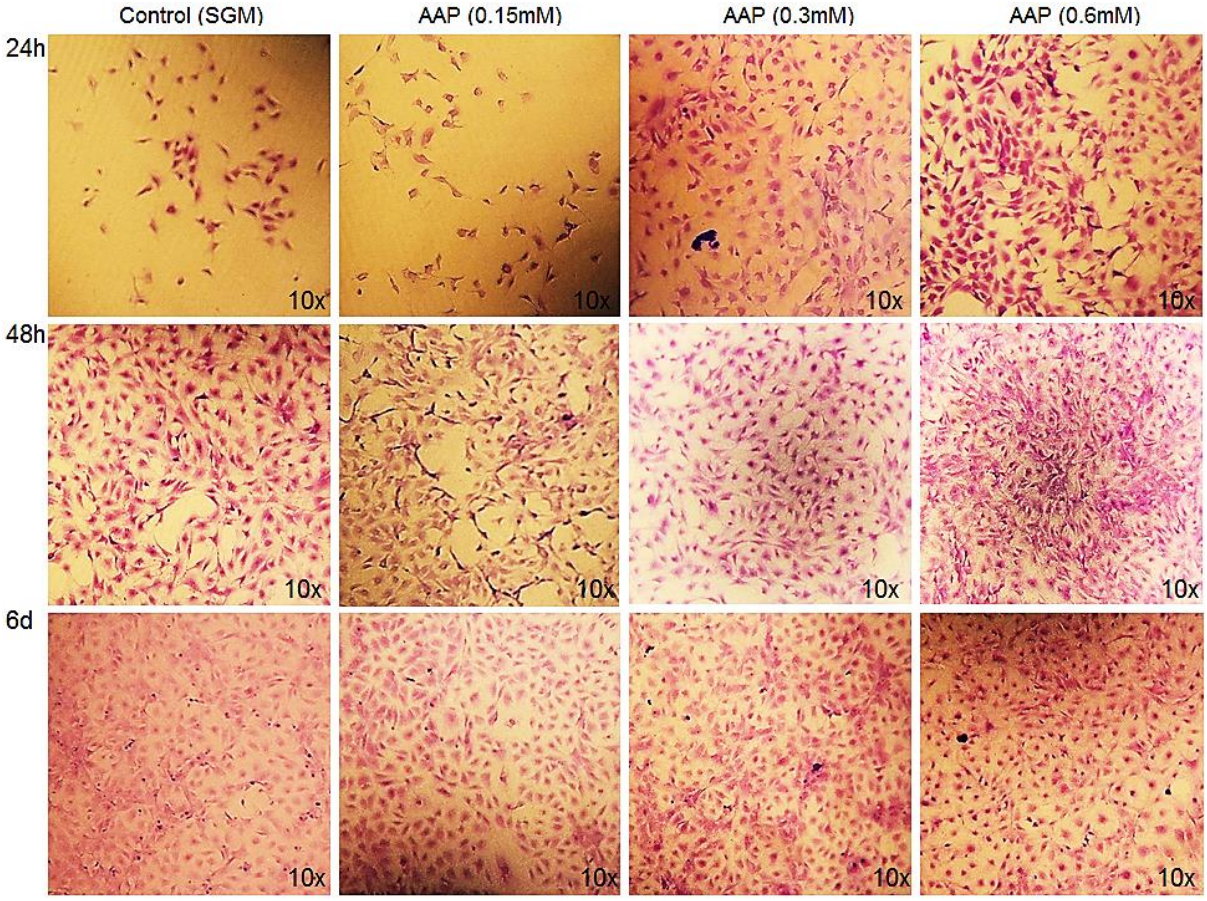

Figure 5.7 Representative images of crystal violet staining using a light microscope. Images were (10x/0.25 PhP objective) captured after 24h, 48h and 6 days of treatment with either AAP (0.15mM), AAP (0.3mM) or AAP (0.6mM). **mM (mmol):** millimole

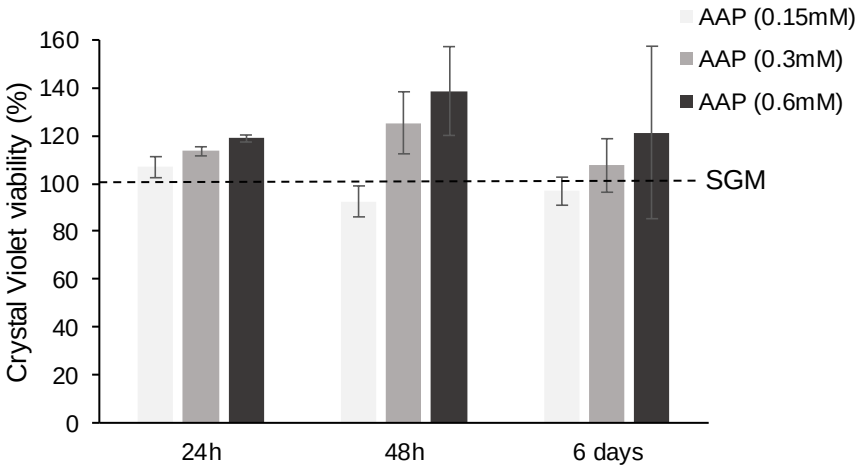

Figure 5.8 MSC viability following treatment with AAP. The independent effect of AAP (0.15mM, 0.3mM, 0.6mM) on MSC viability (CV staining) over a period of 24h, 48h and 6 days. The assay was repeated on MSCs in x3 different passages (n=3) and for each repeat, triplicate wells were assessed. **Statistical analysis:** Values are presented as mean±SE with SGM (control) set at 100%. Factorial ANOVA with Tukey post hoc test (*****p<0.05).

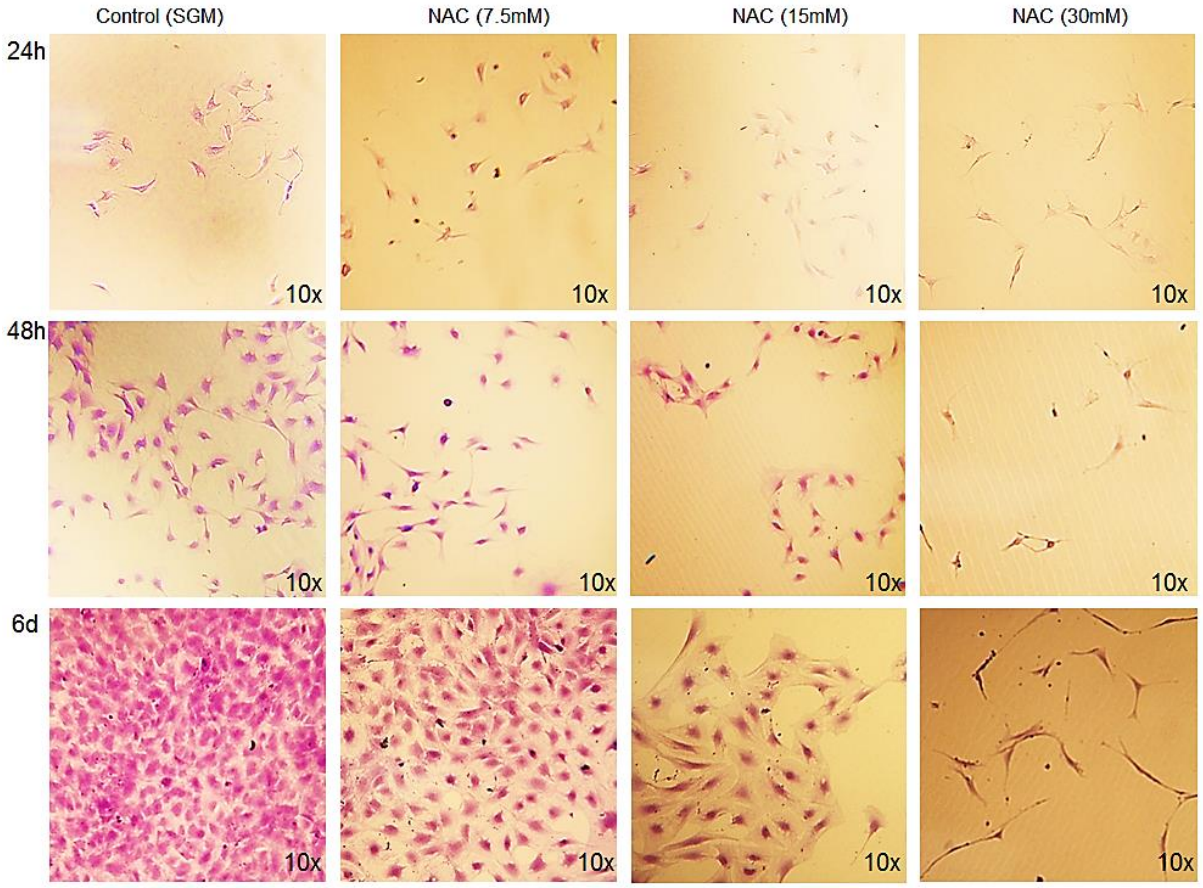

Figure 5.9 Representative images from each well after crystal violet staining using a light microscope. Images (10x/0.25 PhP objective) captured 24h, 48h and 6 days after treatment with NAC (7.5mM), NAC (15mM) and NAC (30mM) compared to control. **mM (mmol):** millimole

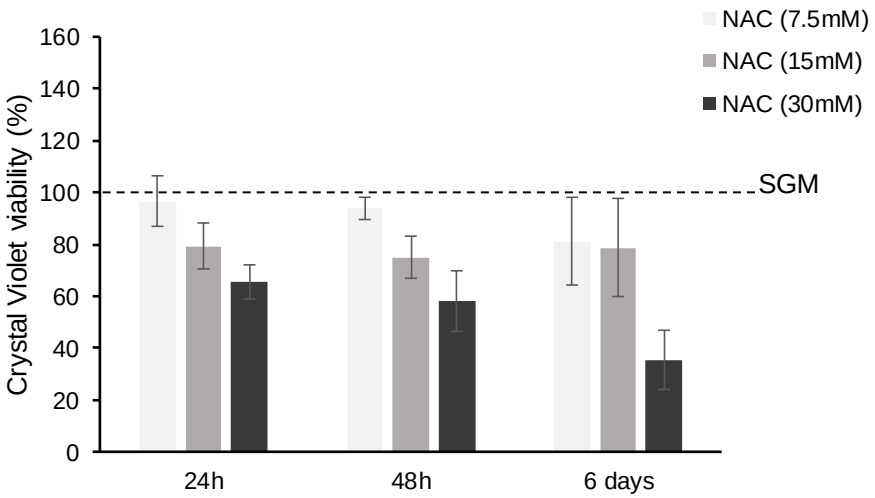

Figure 5.10 MSC viability following treatment with NAC. The independent effect of NAC (7.5mM, 15mM, and 30mM) on MSC viability (CV staining) over a period of 24h, 48h and 6 days. The assay was repeated on MSCs in x3 different passages (n=3) and for each repeat, triplicate wells were assessed. **Statistical analysis:** Values are presented as mean±SE with SGM (control) set at 100%. Factorial ANOVA with Tukey post hoc test (*****p<0.05).

5.3.3 Synergistic effect of AAP and NAC combinations on MSC viability

The synergistic effect of various combined treatment concentrations (NAC15mM+AAP0.6mM; NAC15mM+AAP0.3mM; NAC7.5mM+AAP0.6mM; NAC7.5mM+AAP0.3mM) on cell viability was assessed over a period of 6 days. Crystal violet staining demonstrated that all of the combinations tested could sustain cellular growth over the 6-day period (Fig. 5.11). Quantification of the crystal violet staining identified 7.5mM NAC + 0.6mM AAP as the optimum treatment concentrations. The data demonstrated that 7.5mM NAC + 0.6mM AAP significantly improved cell viability (122.6 ±4.8%) compared to SGM (p<0.05), whereas 7.5mM NAC + 0.3mM AAP maintained cell viability equivalent to control (104 ±12%) (Fig. 5.12).

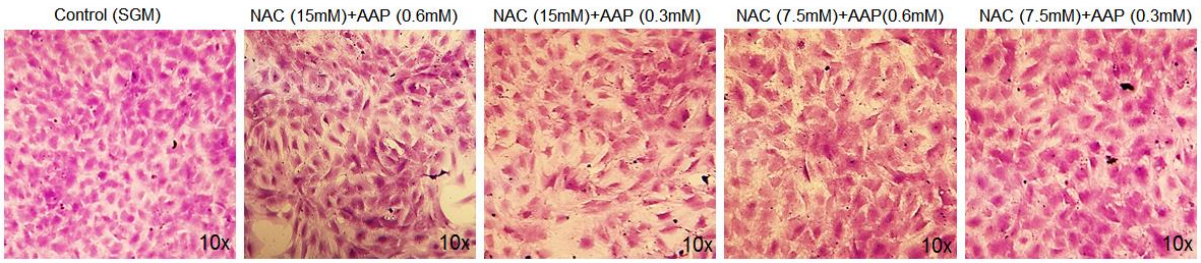

Figure 5.11 Representative pictures from each well after crystal violet staining. Images captured of each well containing AAP and NAC combined treatment over 6 days. **mM (mmol):** millimole

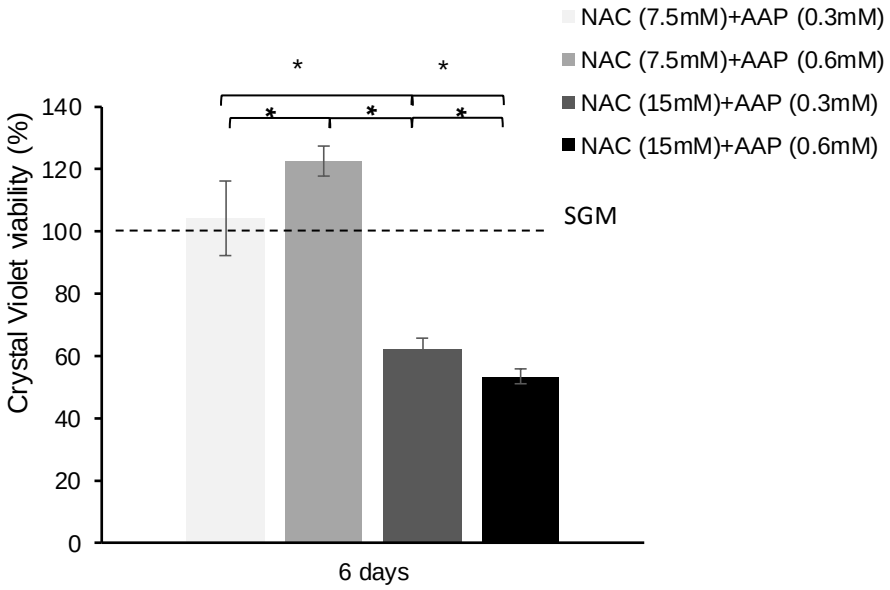

Figure 5.12 The synergistic effect of combined NAC and AAP treatment on cell viability (crystal violet staining) over a period of 6 days. The assay was repeated on MSCs in x3 different passages (n=3) and for each repeat, triplicate wells were assessed. **Statistical analysis:** Values are presented as mean±SE with SGM (control) set at 100%. One-way ANOVA with Tukey post hoc test (*****p<0.05).

5.4 Discussion

Mouse immortalized MSCs (C3H10T1/2) were used to determine the safest, non-toxic doses of NAC and AAP as potential agents to counteract MSCs impairment. These two substances have both antioxidant and anti-inflammatory properties, which act through several key pathways, to remove excessive intracellular oxidants and protect important organelles from ROS-induced damage (Bae et al., 2015; Sun et al., 2013). This protective effect is mediated by regulation of enzymes such as superoxide dismutase, catalase, glutathione peroxidase and *via* the action of non-enzymatic molecules (ergothioneine, vitamin C and microelements), which taking together prevent cellular senescence and apoptosis (Chen et al., 2017). This study demonstrated that under healthy (non-pathological) conditions, a combination of NAC (7.5mM) and AAP (0.6mM) was able to promote cellular proliferation and improve MSC viability over a period of 6 days in culture. Subsequent experiments will test the efficacy of this combined treatment regime to restore the molecular and functional responses of severely impaired diabetic MSCs.

As previously mentioned *(section 5.1, p.43),* the protective effect of either AAP or NAC added to standard culture conditions has already been assessed using human-derived MSCs. Potdar & D'souza (2010) demonstrated that 0.25mM ascorbic acid increased the proliferation rate and the expression of pluripotency markers (*Oct*4 and SOX2) in adipose tissue-derived stem cells (ADSCs) without affecting their phenotype or differentiation potential (Potdar and D'souza, 2010). Humans are strictly dependent on exogenous sources of ascorbic acid (also known as vitamin C) because of the

inability to synthesize the L-gulonolactone oxidase (GLO) enzyme (D'Aniello et al., 2017). Ascorbic acid is however not stable under standard culture conditions, whereas the 2-phosphate form (AAP) is a long-acting Vitamin C derivative that is more stable and better suited for cell culture conditions (Hata and Senoo, 1989). Using this long-acting derivative, AAP, various studies confirmed the observations of Patdar & D'souza (2010), illustrating that *in vitro* AAP treatment can maintain the stemness of MSCs and promote cell growth without negatively affecting their differentiation potential (Bae et al., 2015; Choi et al., 2008).

The growth promoting effect of AAP seemed to be dose dependent. Bae et al. (2015) tested various concentrations (0–0.5mM) of AAP on bone marrow-derived MSCs and demonstrated a dose-dependent effect with the highest proliferation rate achieved using a combination of 250µM (0.25mM) AAP and 1ng/ml FGF2. Similarly, Choi et al. (2008) investigated the effect of culture media supplemented with various concentrations (0–0.5mM) of AAP for 2 weeks, on bone marrow MSC proliferation, differentiation (adipocytes and osteoblasts) and ECM formation (collagen and glycosaminoglycan secretion) and also identified 250µM (0.25mM) as the optimum concentration (Bae et al., 2015; Choi et al., 2008). In this study, a concentration similar to the previously identified AAP concentration was selected as the medium dose (0.3mM) and then subsequently a higher and lower dose also tested. A higher concentration of AAP (0.6mM) was however identified as optimum for the use in our model. The protective mechanism of action of AAP is thought to involve a) counteracting the endogenous ROS production during *in vitro* expansion of MSCs and b) promoting the synthesis and secretion of ECM.

The excessive accumulation of intracellular ROS associated with hyperglycaemia or prolonged culture of cells results in increased oxidative stress and inflammation that can trigger cell death, *via* apoptosis (Kaneto et al., 2010; Pieme et al., 2017; Singh et al., 2009). ROS activated apoptosis is mediated through critical signalling pathways such as the nuclear factor kappa B (NFκB), the serine/threonine protein kinase (Akt) pathway and its downstream mammalian target of rapamycin complex 1 (mTORC1) (Fakhruddin et al., 2017; Volpe et al., 2018). In diabetes specifically, apoptosis can also be triggered through activation of Toll-Like Receptor 4 (TLR4) upstream of NFκB signalling (Volpe et al., 2018). Ascorbic acid exerts its biological function intracellularly and is transported into cells *via* sodium-coupled ascorbic acid transporters (SVCTs; SLC23), or in the case of dehydroascorbic acid by members of the glucose transporter (GLUT1; GLUT3; GLUT4) family (D'Aniello et al., 2017). Intracellularly, ascorbic acid reduces ROS production and has been shown to partially restore the levels of antioxidant enzymes such as catalase, SOD1 and 2, p-FOXO1 and p53. (Jeong and Cho, 2015). In addition to its protective role by reducing the levels of intracellular ROS, ascorbic acid also promotes collagen synthesis that forms a crucial part of the ECM (Bae et al., 2015; Choi et al., 2008; Hata and Senoo, 1989).

Within the stem cell niche, the ECM provide stem cells with specific signals to determine their activation status and fate, but also provides physical support within the microenvironment. This microenvironment can be influenced by several factors (chemical and structural) that subsequently

provides external stimuli inducing MSC proliferation and/or differentiation (Rojas-Ríos and González-Reyes, 2014). The ECM furthermore contains glycosaminoglycans (GAGs) and hyaluronic acid (HA) which offers a large water holding and growth factor binding capacity that significantly impacts cell adhesion, migration, differentiation, and morphogenesis (Votteler et al., 2010). This is supported by studies demonstrating that ascorbic acid-induced ECM deposition enhances the proliferation and migration capacity of MSCs (Kato et al., 2017; Prewitz et al., 2013).

NAC, on the other hand, is a glutathione (GSH) precursor that acts as a potent ROS inhibitor with anti-inflammatory properties (Li et al., 2015). Due to its ROS scavenging ability, NAC prevents oxidative stress and apoptosis by preventing the excessive accumulation of intracellular ROS (Ali et al., 2016; Berniakovich et al., 2012; Li et al., 2015). To date, numerous studies provide evidence in support of the cytoprotective effects of NAC on MSC function. In the presence of severe oxidative stress induced by exogenous H_2O_2 addition, gene expression analysis previously demonstrated that 30mM NAC treatment can protect diabetic mouse-derived MSCs against cellular damage through upregulation of pro-survival genes (Akt and *Bcl*-2) and downregulation of pro-apoptotic and stress-related genes (Caspase-3, *Bax*, *Bak*, *p53* and *p38*) (Ali et al., 2016). In support of this finding, Weinberg et al. (2014) indicated that 2mM NAC can prevent apoptosis in bone marrow MSCs-derived from a diabetic rat model (Weinberg et al., 2014) and Fan et al. (2011) demonstrated that 5mM NAC treatment in the presence of free radicals (alpha-phenyl-t-butyl nitrone) can protect MSCs against DNA damage and prolonged culture induced cellular senescence (Fan et al., 2011). In addition to its cytoprotective and growth promoting ability, NAC also has anti-inflammatory properties. These are related to NAC's ability to suppress proteasome activity and inhibit NFκB activation that subsequently limits the release of pro-inflammatory cytokines (Lasram et al., 2015).

In non-pathological models, previous studies have shown that combined treatment of NAC and AAP (NAC+AAP) accelerates cellular proliferation through suppression of cyclin-dependent kinase inhibitors whilst upregulating the pro-survival BCL2 protein (Li et al., 2015). Taking together, it is therefore hypothesized that the synergistic effect of AAP (antioxidant and ECM deposition) and NAC (ROS scavenging and anti-inflammatory) could provide a therapeutic compound with the potential to counteract stem cell dysfunction associated with the pathogenesis of diabetes. In this study, combined AAP and NAC treatment yielded better synergistic effects in terms of MSC proliferation and viability under standard culture conditions than either antioxidant alone, therefore warrants further testing in pathological conditions.

Chapter 6: Investigating the efficacy of antioxidant preconditioning to restore the molecular/paracrine and functional responses of bone marrow mesenchymal stem cells upon stimulation with diabetic wound fluid.

6.1 Introduction

Wound healing and the dysregulation thereof are complex physiological processes that currently have few effective treatment strategies, especially in multifactorial diseases like T2DM. The chronic inflammatory state of obesity and T2DM involves dysregulation of pro-inflammatory cytokines, chemokines, plasma levels of coagulating factors (fibrinogen and plasminogen activator inhibitor 1), acute-phase proteins, C-reactive protein (CRP) and apolipoproteins associated with high-density lipoprotein (HDL), such as serum amyloid A (Esser et al., 2014).

As described in previous chapters *(Chapters 2.2, p.10 and 4.1, p.30)* normal wound healing is dependent on the transition through the various stages of the healing process and that the cellular mediators of regeneration respond to changes in the paracrine signalling in the wound environment. Neutrophils and pro-inflammatory macrophages (M1) infiltrate the wound area during the early stages of healing (inflammatory phase). Under normal circumstances, this inflammatory process is inhibited, and healing continues by transitioning to the proliferation phase. The proliferative phase is characterized by the beginning of ECM formation, angiogenesis and re-epithelialization. Finally, the healing process is completed by remodelling and matrix reorganisation (Dreifke et al., 2015; Dulmovits and Herman, 2012; Martin and Nunan, 2015). Macrophages are a key component in this process and respond to paracrine signals and TLRs by either differentiating into an M1 pro-inflammatory phenotype (stimulation of TLR4) with antimicrobial activity and the ability to secrete inflammatory mediators such as IFNγ and TNFα; or differentiate to an M2 anti-inflammatory phenotype (stimulation of TLR3) that secretes growth promoting factors such as IL10 and TGFβ1. This switch from pro- to anti-inflammatory is essential to promote the transition into the reparative and remodelling stages of wound healing (Betancourt, 2013; Le Blanc and Davies, 2015). If the balance in the transition from M1 to M2 macrophages is disrupted (as is the case with dysregulation of inflammatory signals), healing will be impaired, and the wound may become chronic. In chronic diabetic wounds, a combination of microenvironmental factors, that include an excessive and delayed inflammatory response, ischemia, dysfunctional supporting cells and impaired angiogenesis hamper the natural progression through the stages of healing (Baltzis et al., 2014; Martin and Nunan, 2015).

Exogenously applied allogeneic (healthy) MSCs have a differentiation potential, immunosuppressive properties, and can impart anti-inflammatory effects, and could, therefore, restore the wound microenvironment through paracrine signalling by inducing the proliferative and remodelling phases of healing (Marfia et al., 2015; Zang et al., 2017). It has been shown that MSCs have a similar capacity to that of macrophages when it comes to phenotype and can polarize to become either pro-Inflammatory MSC1 (TLR4) or anti-Inflammatory MSC2 (TLR3) (Betancourt, 2013; Waterman et al., 2010). The compromised functionality of autologous MSCs in diabetes (due to long-term exposure to

pathological conditions and systematic changes in the stem cell niche), restricts their therapeutic potential (Shin and Peterson, 2012; van de Vyver, 2017) and might be related to their phenotype. The hostile chronic wound microenvironment may also influence the biological and metabolic vitality of healthy MSCs and as result negatively affect treatment outcomes (Li et al., 2007; Silva et al., 2015; Zhang et al., 2016a).

Taking together, these factors all contribute to the unpredictability of stem cell therapy for the treatment of diabetic wounds. The main purpose of this study was thus to (a) broaden our insight into the sensitivity of MSCs to pathological environments by assessing the molecular and paracrine responses of healthy and impaired diabetic MSCs to DWF and (b) to investigate the efficacy of antioxidant preconditioning in improving the functional responsiveness of these MSCs in the context of wound repair.

6.2 Material and Methods

6.2.1 Ethics approval statement

This study was approved by the animal research ethics committee at Stellenbosch University (#SU-3857, 15 June 2018) and complied with the South African Animal Protection Act (Act no 71, 1962). All experimental procedures were conducted according to the ethical guidelines and principles of the declaration of Helsinki *(Refer to Addendum A, p.115 for the ethical approval letters)*.

6.2.2 Overview of study design

Refer to Figure 6.1 below for an overview of the study design. All experiments were performed on MSCs derived from at least 3 animals per treatment group (n=3 biological repeats and x2 technical repeats). The specific treatment groups and detailed methodology is described in the sections below.

The treatment groups were as follow:

a) No treatment (baseline phenotype): MSCs expanded in Standard growth media (SGM) (±8 days) and only exposed to growth media.
b) DWF (baseline response): MSCs expanded in SGM (±8 days) followed by acute exposure to DWF for a period of 4h.
c) Antioxidant preconditioning (preconditioned phenotype): MSCs expanded in the presence of NAC+AAP (±8 days).
d) Antioxidant preconditioning + DWF (preconditioned response): MSCs expanded in the presence of N-acetylcysteine and Ascorbic acid 2-phosphate (NAC+AAP) (±8 days) followed by acute exposure to DWF for a period of 4h.

This study was therefore designed to assess the phenotype and responsiveness of MSCs on both molecular/paracrine as well as functional levels.

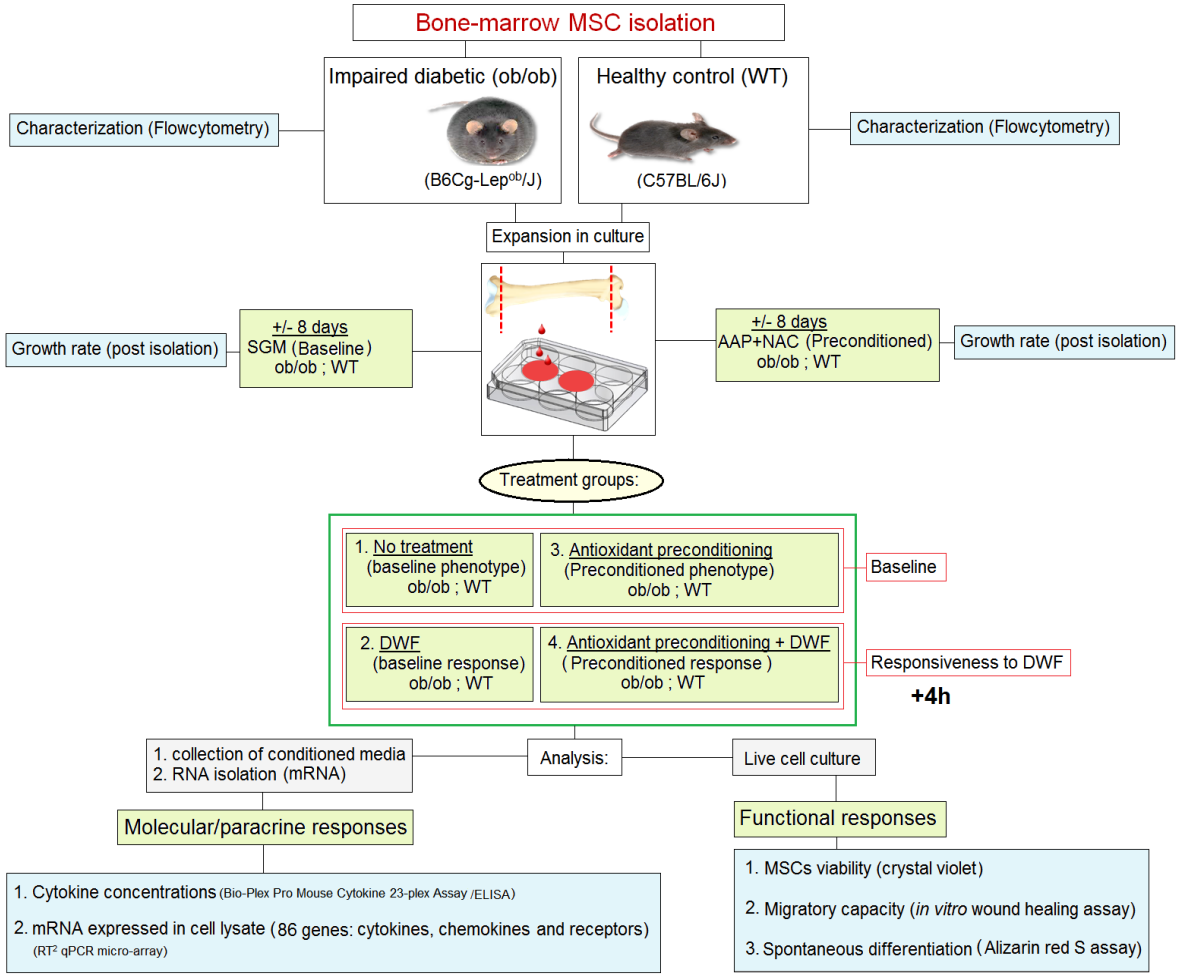

Figure 6.1 Overview of study design. The isolated bone marrow MSCs derived wild type or *ob/ob* mice were expanded in culture under either standard growth media (SGM) conditions (MSCs derived from left femur) or in the presence of antioxidants (preconditioning) (MSCs derived from right femur of the same mouse) prior to stimulation with diabetic wound fluid (DWF). The antioxidant preconditioning consisted of the optimum combined treatment with NAC (7.5mM) (Sigma-Aldrich®, St. Louis MO, USA) and AAP (0.6mM) (Sigma-Aldrich®, St. Louis MO, USA) as determined in *Chapter 5, p.43*. For the preconditioned MSCs, immediately following isolation, the isolation medium (first 96h) was supplemented with the antioxidants, with media being changed every 3-4 days. Following the expansion of cell number (80-90% confluent), MSCs (with and without preconditioning) were stimulated with DWF for a period of 4h. As determined in *Chapter 4, p.30*, the total protein concentration of the collected DWF was x3 fold less than that of FBS. For stimulation, the 10% FBS in the growth media was therefore replaced with 30% DWF.

6.2.3 Isolation and culture of bone marrow derived MSCs

Healthy control (source: wild type, C57BL/6J mice, weight 24.3±0.5g) (n=24) and impaired/ diabetic (source: obese pre-diabetic, B6 Cg-Lep^{ob}/J mice, weight 39.5±1.2g) (n=24) bone marrow-derived MSCs were isolated from the femurs of animals. Following euthanasia, the femurs were dissected out and the proximal and distal ends of each femur cut open in a sterile environment. Bone marrow aspirates were flushed into tissue culture plates (6-well plates, Nest Biotechnology Co., Ltd., USA)

using a 25-gauge needle and syringe containing isolation medium. Isolation medium consisted of DMEM with ultra-glutamine (4.5 g/L high glucose, BioWittaker, Lonza, Basel, Switzerland), containing 1% penicillin/streptomycin (BioWittaker, Lonza, Basel, Switzerland) and 20% FBS (Biochrom, Berlin, Germany). The bone marrow aspirates were maintained at 37°C, in 90% humidified air with 5% CO_2 to allow for plastic adherence of MSCs. After 96h, non-adherent cells were washed off with PBS and the media replaced with standard growth media (SGM). SGM consisted of DMEM with ultra-glutamine (4.5 g/L high glucose, BioWittaker, Lonza, Basel, Switzerland), containing 1% penicillin/streptomycin (BioWittaker, Lonza, Basel, Switzerland) and 10% FBS (Biochrom, Berlin, Germany). Media was changed every 3-4 days until the cells reached 80% confluence in passage 0 (Fig. 6.2).

For the functional response experiments, MSCs (with or without NAC+AAP preconditioning) (70% confluence; passage 0), were sub-cultured (passage 1) as follow: Cell culture medium was aspirated, and cells washed in pre-warmed PBS, adherent cells were detached from the wells (6-well plate) through enzymatic digestion using 1ml/well Accutase (StemPro®Accutase®, gibco®, USA). In the presence of Accutase, the plates were gently tapped and incubated for a maximum period of 5 min to allow for detachment. SGM (2ml) was added to inactivate the enzymatic activity and the cell suspension (3ml) transferred into 15ml Falcon tubes (Corning, Tarnaulipas, Mexico) and centrifuged at 1000 RPM for 5 min (Eppendorf centrifuge 5804, Germany). After centrifugation, the cell pellet was re-suspended in 1ml SGM. A cell count was performed on 20µl of the cell suspension using a haemocytometer as previously described *(refer to chapter 5.2.2, p.44)*. Seeding density (passage 1) differed according to each of the subsequent experiments as described in section 6.2.6 below (p.65).

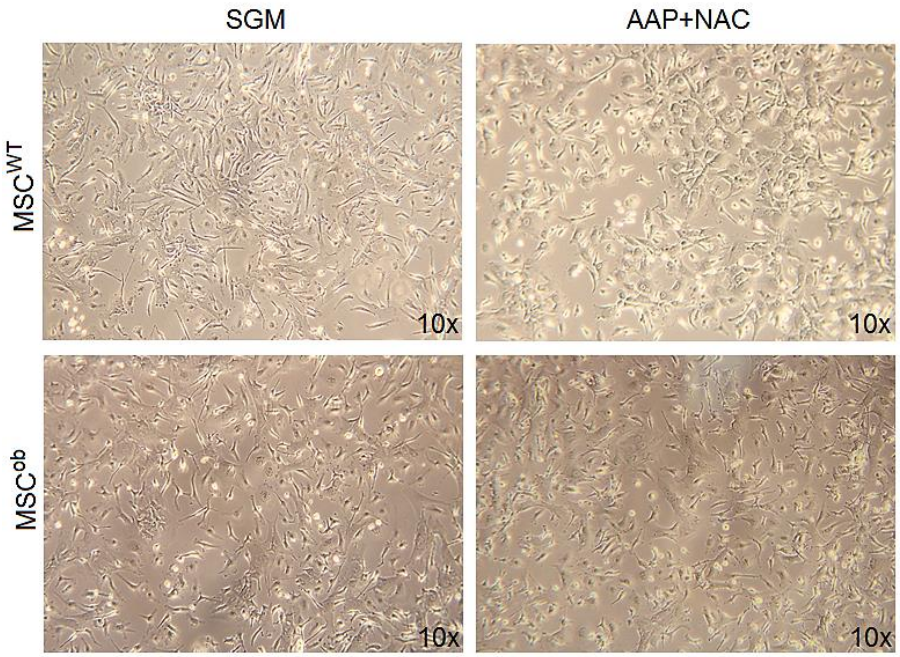

Figure 6.2 Representative images from isolated bone marrow stem cells. MSCs 8 days after isolation from healthy control and prediabetic obese mouse with and without preconditioning.

6.2.4 Flow cytometry characterization of isolated MSCs

MSCs (80% confluent; passage 0) were harvested through trypsinization, centrifuged at 1000 RPM for 5 min (Eppendorf centrifuge 5804, Germany), and resuspended in flow cytometry staining solution (PBS containing 20% FBS). Cell suspensions at a concentration of 1 x 10^6 cells per 100µL were co-labelled with rat anti-mouse monoclonal antibodies against the stem cell marker, Ly-6A/E (Sca-1) (PE conjugated, BD Pharmingen, USA) and the hematopoietic lineage marker, CD45 (FITC conjugated, BD Pharmingen, USA). Flow cytometry was performed on a BD FACS Calibre instrument using CellQuest software. A total of 15000 events were recorded prior to data analysis. Fluorescent compensation settings. were established through a compensation experiment using comp beads (BD™CompBead Plus Anti-Mouse Ig, k, BD Biosciences, USA). An unstained control sample was used as a negative control for gating purposes. Data analysis was performed using Flow Jo Vx (Treestar, Oregon, USA) software.

6.2.5 Analysis on Molecular/paracrine level

6.2.5.1 Collection and analysis of conditioned medium

After MSCs reached 80% confluence in passage 0, the growth media (with or without NAC+AAP) was replaced with serum-free media for a period of 24h. The complete serum-free growth media consists of Stem Pro MSC SFM basal media (Gibco, Life Technologies, USA), Stem Pro MSC SFM growth factor Supplement CST (Gibco, Life Technologies, USA), 2mM L-Glutamine (Gibco, Life Technologies, USA) and 5 µg/ml penicillin/streptomycin (BioWhittaker, Lonza, Basel, Switzerland). After 24h, the conditioned medium was collected, centrifuged to remove cellular debris and stored at -80˚C.

For stimulation with DWF, MSCs in treatment groups 2 and 4 (baseline and preconditioned response), were stimulated with SFM containing 30% DWF for 4h. Conditioned medium was collected (after stimulation/addition with DWF) and stored at -80˚C.

6.2.5.1.1 Multiplex bead array analysis

The cytokine concentrations (Eotaxin, G-CSF, GM-CSF, IFNγ, IL1α, IL1β, IL2, IL3, IL4, IL5, IL6, IL9, IL10, IL12(p40), IL12(p70), IL13, IL17A, KC, MCP1, MIP1α, MIP1β, RANTES, TNFα) within conditioned medium were assessed using the Bio-Plex Pro Mouse Cytokine 23-plex Assay (Bio-Plex Pro™ Mouse 23-plex, BIO-RAD, USA) according to the manufacturer's instruction, using a Multiplex reader (Bio-Plex® MAGPIX™ BIO-RAD, USA) and Bio-Plex Manager™ MP software. The Bio-Plex assay system is based on sandwich immunoassay, formatted on magnetic beads (Fluorescently dyed microspheres) with a distinct colour code to permit discrimination and are coated with a specific panel of antibodies. This assay simultaneously measures multiple analytics in a single sample indicating cytokines involved in inflammatory stage of healing.

6.2.5.1.2 Enzyme-linked Immunosorbent Assay (ELISA)

The mouse stromal-cell derived factor 1 (SDF1α)/ CXCL12 ELISA Kit (#RAB0125 Sigma-Aldrich®, USA) was used to determine SDF1α concentrations in conditioned medium according to the manufacturers' instructions. The ELISA is an enzyme-linked immunosorbent assay for the quantitative measurement of a target protein in biological samples. The assay employs a specific capture antibody coated on a 96 well plate. Standards and samples were pipetted into the wells, incubated and the target protein present in each sample bound to the wells by the immobilized antibody.

A streptavidin-HRP solution was added as the enzyme-linked antigen to detect the presence of and bind to the antibody in the sample. Then a colourless substrate solution was added to each well, which produced a colour to indicate the presence of the antibody/protein complex. Absorbance was read at 450nm (constant 37°C) using a standard spectrophotometer (Multiskan® GO plate reader, Thermo Fisher, Finland). Readings obtained from the spectrophotometer were exported into Thermo Scientific SkanIt® Software 3.2 for a detailed calculation of the concentration (pg/ml) of each sample using a linear standard curve.

6.2.5.2 RNA isolation and cDNA synthesis

Total RNA was isolated using the RNeasy RNA isolation kit (RNeasy® Mini Kit, QIAGEN, Germany) with on-column DNase digestion (RNase-Free DNase Set, QIAGEN, Germany) as per manufacturer's instructions. RNA quantification (ng/µl) and quality control were performed using the Eukaryote Total RNA Nano Series II Bioanalyzer (2100 Bioanalyzer, Agilent Technologies, Inc, USA). Total RNA (0.5µg) with integrity of above 9 (RIN>9) (Fig. 6.3) was used as a template for cDNA synthesis, using the RT^2 First Strand Kit (RT^2 First Strand Kit, QIAGEN, USA) that included a genomic DNA elimination step.

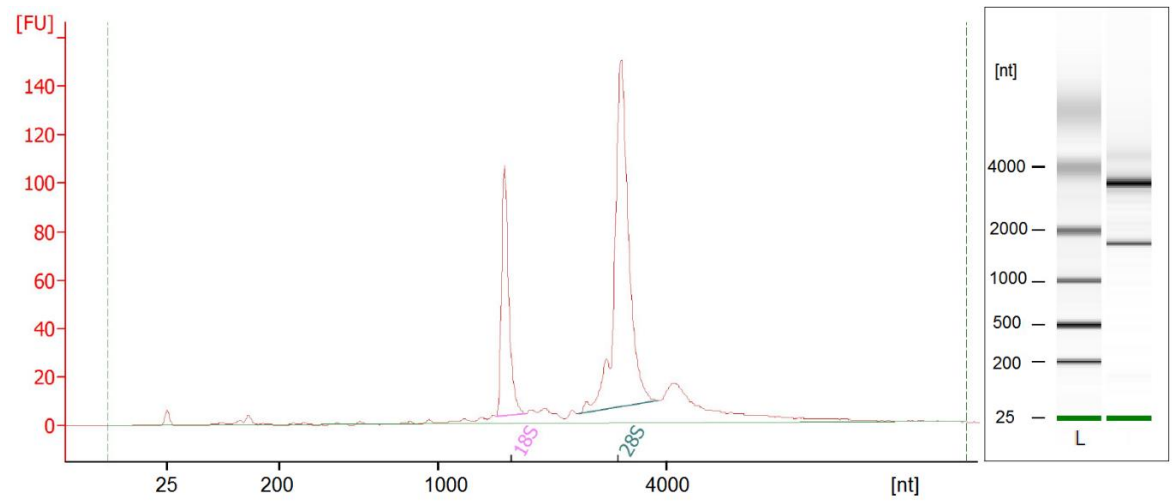

Figure 6.3 Representative image of a bioanalyzer gel and an electropherogram summary. RNA (0.5µg) with integrity of above 9 (RIN>9). **FU:** fluorescence units, **nt:** nucleotide.

6.2.5.2.1 RT² qPCR micro-array

cDNA samples for each treatment condition were analysed with a RT² Profiler PCR Inflammatory cytokines & receptors array (96-well plate format, RT² Profiler™ PCR Array, QIAGEN, USA) and RT² SYBR® Green Master-mix (ROX™ PCR Mastermix, QIAGEN, USA) using an ABI 7900HT Fast real-time PCR system (Applied Biosystems, Life technologies, USA) and SDS software (version 2.3, Life technologies, USA). Refer to Table 6.1 below for the full list of genes assessed.

The web-based PCR Profiler Array data analysis package was used for ΔΔCt based fold change calculations (QIAGEN web portal http://www.qiagen.com/geneglobe). Relative gene expression was calculated by comparison with the following housekeeping gene: heat shock protein 90α class B member 1 (Hsp90ab1; NM_008302). Hsp90ab1 was the most stable gene within the micro-array panel, with very little variation between samples. The PCR array analysis furthermore included a mouse genomic DNA contamination (MGDC; SA_00106), Reverse transcriptase (RTC; SA_00104) and Positive PCR (SA_00103) controls (PPC). Genes of interest were identified using Student's t-test of the replicate ΔΔCt values for each gene in the control and treatment groups. The level of significance was accepted at $p<0.05$.

Table 6.1 Represent detectable genes in RT² qPCR micro-array 96 well plate.

GenBank	*Symbol*	Description	GenBank	*Symbol*	Description	GenBank	*Symbol*	Description
NM_007926	*Aimp1*	Aminoacyl tRNA synthetase complex-interacting multifunctional protein 1	**NM_009969**	*Csf2*	Colony stimulating factor 2 (granulocyte-macrophage)	**NM_031167**	*IL1ra*	Interleukin 1 receptor antagonist
NM_007553	*Bmp2*	Bone morphogenetic protein 2	**NM_009971**	*Csf3*	Colony stimulating factor 3 (granulocyte)	**NM_021782**	*IL21*	Interleukin 21
NM_011329	*Ccl1*	Chemokine (C-C motif) ligand 1	**NM_009142**	*Cx3cl1*	Chemokine (C-X3-C motif) ligand 1	**NM_145636**	*IL27*	Interleukin 27
NM_011330	*Ccl11*	Chemokine (C-C motif) ligand 11	**NM_008176**	*Cxcl1*	Chemokine (C-X-C motif) ligand 1	**NM_008368**	*IL2rβ*	Interleukin 2 receptor, beta chain
NM_011331	*Ccl12*	Chemokine (C-C motif) ligand 12	**NM_021274**	*Cxcl10*	Chemokine (C-X-C motif) ligand 10	**NM_013563**	*IL2rγ*	Interleukin 2 receptor, gamma chain
NM_011332	*Ccl17*	Chemokine (C-C motif) ligand 17	**NM_019494**	*Cxcl11*	Chemokine (C-X-C motif) ligand 11	**NM_010556**	*IL3*	Interleukin 3
NM_011888	*Ccl19*	Chemokine (C-C motif) ligand 19	**NM_021704**	*Cxcl12*	Chemokine (C-X-C motif) ligand 12	**NM_133775**	*IL33*	Interleukin 33
NM_011333	*Ccl2*	Chemokine (C-C motif) ligand 2	**NM_018866**	*Cxcl13*	Chemokine (C-X-C motif) ligand 13	**NM_021283**	*IL4*	Interleukin 4
NM_016960	*Ccl20*	Chemokine (C-C motif) ligand 20	**NM_011339**	*Cxcl15*	Chemokine (C-X-C motif) ligand 15	**NM_010558**	*IL5*	Interleukin 5
NM_009137	*Ccl22*	Chemokine (C-C motif) ligand 22	**NM_009141**	*Cxcl5*	Chemokine (C-X-C motif) ligand 5	**NM_008370**	*IL5rα*	Interleukin 5 receptor, alpha
NM_019577	*Ccl24*	Chemokine (C-C motif) ligand 24	**NM_008599**	*Cxcl9*	Chemokine (C-X-C motif) ligand 9	**NM_010559**	*IL6rα*	Interleukin 6 receptor, alpha
NM_011337	*Ccl3*	Chemokine (C-C motif) ligand 3	**NM_009909**	*Cxcr2*	Chemokine (C-X-C motif) receptor 2	**NM_010560**	*IL6st*	Interleukin 6 signal transducer
NM_013652	*Ccl4*	Chemokine (C-C motif) ligand 4	**NM_009910**	*Cxcr3*	Chemokine (C-X-C motif) receptor 3	**NM_008371**	*IL7*	
NM_013653	*Ccl5*	Chemokine (C-C motif) ligand 5	**NM_007551**	*Cxcr5*	Chemokine (C-X-C motif) receptor 5	**NM_010735**	*Lta*	Lymphotoxin A
NM_009139	*Ccl6*	Chemokine (C-C motif) ligand 6	**NM_010177**	*Fasl*	Fas ligand (TNF superfamily, member 6)	**NM_008518**	*Ltb*	Lymphotoxin B
NM_013654	*Ccl7*	Chemokine (C-C motif) ligand 7	**NM_008337**	*Ifnγ*	Interferon gamma	**NM_010798**	*Mif*	Macrophage migration inhibitory factor
NM_021443	*Ccl8*	Chemokine (C-C motif) ligand 8	**NM_008348**	*IL10rα*	Interleukin 10 receptor, alpha	**NM_021524**	*Nampt*	Nicotinamide phosphoribosyl transferase
NM_011338	*Ccl9*	Chemokine (C-C motif) ligand 9	**NM_008349**	*IL10rβ*	Interleukin 10 receptor, beta	**NM_001013365**	*Osm*	Oncostatin M
NM_009912	*Ccr1*	Chemokine (C-C motif) receptor 1	**NM_008350**	*IL11*	Interleukin 11	**NM_019932**	*Pf4*	Platelet factor 4
NM_007721	*Ccr10*	Chemokine (C-C motif) receptor 10	**NM_008355**	*IL13*	Interleukin 13	**NM_009263**	*Spp1*	Secreted phosphoprotein 1
NM_009915	*Ccr2*	Chemokine (C-C motif) receptor 2	**NM_008357**	*IL15*	Interleukin 15	**NM_013693**	*Tnf*	Tumour necrosis factor
NM_009914	*Ccr3*	Chemokine (C-C motif) receptor 3	**NM_010551**	*IL16*	Interleukin 16	**NM_008764**	*Tnfrsf11b*	Tumour necrosis factor receptor superfamily, member 11b (osteoprotegerin)
NM_009916	*Ccr4*	Chemokine (C-C motif) receptor 4	**NM_010552**	*IL17a*	Interleukin 17A	**NM_009425**	*Tnfsf10*	Tumour necrosis factor (ligand) superfamily, member 10
NM_009917	*Ccr5*	Chemokine (C-C motif) receptor 5	**NM_019508**	*IL17b*	Interleukin 17B	**NM_011613**	*Tnfsf11*	Tumour necrosis factor (ligand) superfamily, member 11
NM_009835	*Ccr6*	Chemokine (C-C motif) receptor 6	**NM_145856**	*IL17f*	Interleukin 17F	**NM_023517**	*Tnfsf13*	Tumour necrosis factor (ligand) superfamily, member 13
NM_007720	*Ccr8*	Chemokine (C-C motif) receptor 8	**NM_010554**	*IL1α*	Interleukin 1 alpha	**NM_033622**	*Tnfsf13b*	Tumour necrosis factor (ligand) superfamily, member 13b
NM_011616	*Cd40lg*	CD40 ligand	**NM_008361**	*IL1β*	Interleukin 1 beta	**NM_009452**	*Tnfsf4*	Tumour necrosis factor (ligand) superfamily, member 4
NM_007778	*Csf1*	Colony stimulating factor 1 (macrophage	**NM_008362**	*IL1r1*	Interleukin 1 receptor, type I	**NM_009505**	*Vegfa*	Vascular endothelial growth factor A

Footnote: mRNA level expression of 84 genes and receptors of cytokines and chemokines.

6.2.6 Analysis of functional level

6.2.6.1 MSCs growth rate post isolation

Following isolation of MSCs, eight representative images (Fig. 6.4) was taken (EOS600D Canon digital camera) of each well (MSC^{WT} and MSC^{ob}) using a light microscope (Olympus CKX41, CachN 10x/0.25 PhP objective) on days 4, 8 and 12 post isolation. All images were captured at 10x magnification with the exact same microscope settings and light intensity. Cell confluency was quantified in each captured image using Image J software (version 1.46, NIH.gov, USA) according to the protocol developed by (Busschots et al., 2016).

Image J analysis: 1) After opening and selecting the appropriate image, image type was changed to 16bit, and background was processed to be changed to white. 2) This setting was then used to adjust the threshold. 3) By setting the measurement parameters; the percentage area (%) of each image covered by cells (confluency) was automatically calculated.

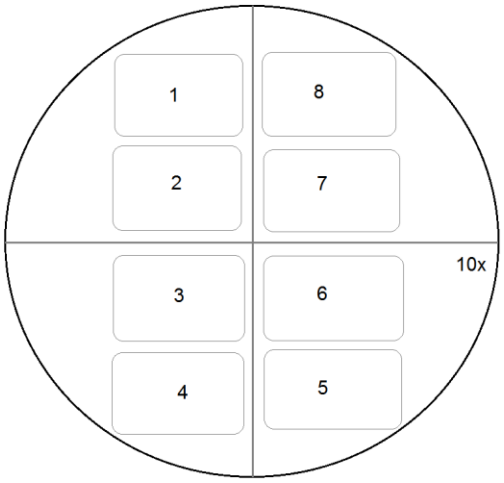

Figure 6.4 An illustration of area divided into eight zones for imaging in each well. Image was taken of each well using a light microscope (Olympus CKX41, CachN 10x/0.25 PhP objective).

6.2.6.2 Crystal Violet Staining

The Crystal violet assay (hexamethyl pararosaniline chloride) was used to determine cell viability (Feoktistova et al., 2016; Śliwka et al., 2016) in the four treatments groups. To assess cell viability, MSCs (passage 1) were seeded into a 96 well plate (~4.5 x 10^4 cells/well) in isolation medium containing 20% FBS (100 µl/well) and incubated for 48h at 37ºC until the cells reached 70% confluence. At this time point, all the media was aspirated from each well and cells treated as per the four treatment groups for either 24h, 48h or 96h. Crystal violet is a simple histological stain that binds to the DNA and protein of adherent (live) cells and can be visualized using light microscopy or the colour absorbance can be spectrophotometrically measured. This characteristic can be used for the indirect quantification of cell death and to determine differences in proliferation upon stimulation with

death-inducing agents compared to control. Crystal violet assay works independent from metabolism interactive additives or synergistic interaction, thus is identified as a replacement option for MTT assay when an antagonistic interaction prevents MTT measurement.

At the respective endpoints, the treatment media was removed from each well and cells washed with 150µl PBS (1x). Cells were then fixed for 30 sec using 150µl methanol (Merck, Gauteng, RSA). After removal of the methanol, cells were washed once again (PBS 1x) and 150µl crystal violet working solution (0.01% in dH_2O) (Sigma-Aldrich®, Germany) added to each well and incubated for 5 min at room temperature. After staining, the crystal violet solution was removed, and cells washed twice with PBS. Prior to extraction of the dye, one representative image was taken of each well using a light microscope (Olympus CKX41, CachN 10x/0.25 PhP objective). 100µl 70% Ethanol (Merck, Gauteng, RSA) was added to dissolve the stain (shaking platform) (Heidolph, UNIMAX 1010) and the absorbance values were read using a plate reader (Multiskan GO, Thermo Fisher, Finland) at 570 nm. The assay was performed on MSCs derived from at least 3 animals per group (repeated x3 times) for each time point, with each repeat containing x3 internal replicates (3 wells).

6.2.6.3 Migration assay

Cellular migration capacity was assessed using the live cell *in vitro* wound healing assay (Ibidi, Germany). Cell culture micro-well inserts containing 2 chambers were placed in a flat bottom plate (Gibco®CellStar®, Germany) (Fig. 6.5). MSCs were seeded at a density of ~9.0 x 10^4 cells per chamber in 70µl-90µl SGM (with or without AAP+NAC preconditioning) and incubated for 48h (37°C in a humidified environment, 5% CO_2) until the cells reached 90% confluence within each chamber. The culture insert was then removed by using sterile forceps to reveal a cell-free gap (wound) (Fig. 6.5) and the medium from each well replaced as per the four treatment groups.

The migration of cells into the cell-free gap was assessed over a period of 24h. At each time point (0h, 4h, 6h and 24h), four images (10x magnification, EOS600D Canon digital camera) were captured of the cell-free gap (wound area) using a light microscope (10x/0.25 PhP objective; Primovert, Zeiss, Germany). The cell-free area (µm²) was calculated using Image J software (version 1.46, NIH, USA) as follow: 1) appropriate image was selected and opened on Image J. 2) the image scale was set (distance in pixels =637.6; known distance =1, unit of length =mm). 3) Using the *freelance draw-line* tool the outer wound edges were traced, and the surface area (µm²) of the cell-free area calculated. The following formula was used to determine the percentage of wound closure over time:

$$\boldsymbol{wound\ closure}\ (\%) = \left[\frac{\boldsymbol{area\ 0h - area\ nh}}{\boldsymbol{area\ 0h}}\right] * \mathbf{100}$$

Area 'nh' represents the value obtained after the cell-free area was measured at the following time points: 0, 4, 6 or 24h. The assay was performed on MSCs derived from at least 3 animals (*ob/ob* and WT) per group (repeated x3 times) for each time point, with each repeat containing x2 internal replicates (2 inserts).

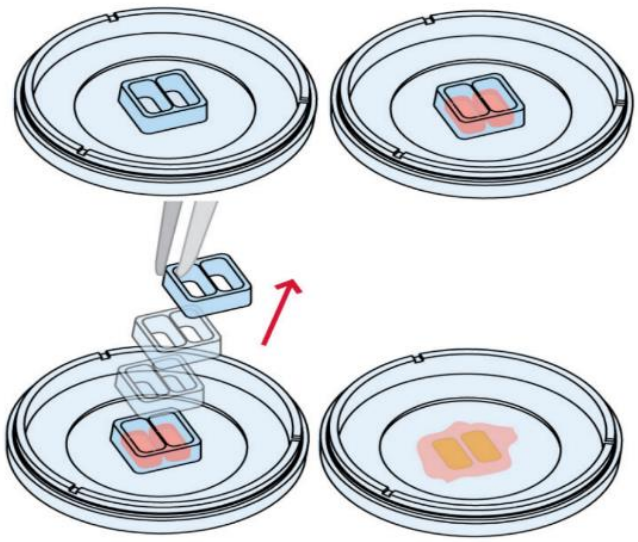

Figure 6.5 Illustration of procedure followed for the *in vitro* migration assay. 48h after seeding, insert was peeled off the culture plate by using sterile forceps and the medium from each well was aspirated.

After 24h in the migration chambers, in some of the treatment groups, the confluent areas of MSCs showed signs of morphological changes suggesting that spontaneous osteogenic differentiation occurred. To investigate this phenomenon, the MSCs were stained with Alizarin Red S (Amresco®, USA) to determine the presence of mineralization and Ca^{2+} deposition. At 24h, MSCs from all treatment groups were washed twice with PBS and fixed in 70% EtOH (v/v) for 5 min. Fixed cells were washed with dH_2O and stained overnight with 100mM Alizarin red S (pH 4.0–4.1) at room temperature. Unbound Alizarin red S was removed by washing three times with dH_2O and five representative images were taken per well using an Olympus light microscope (CKX41, CachN 10x/0.25 PhP objective, EOS600D Canon digital camera).

The percentage surface area stained positive for Alizarin Red was determined using ImageJ software (version 1.46, nih.gov) as follow: 1) appropriate image was selected and opened on Image J. 2) the image scale was set (distance in pixels =637.6; known distance =1, unit of length =mm). 3) using RGB stack, the greyscale image type and the green channel was selected. 4) the image threshold was adjusted to 50. 5) The measurement parameters were set, and the percentage surface area stained positive for Alizarin Red calculated.

6.2.7 Statistical analysis

Values are presented as mean ± standard error (mean±SE). Statistical analysis was performed using Statistica software (Statsoft, version 13). Factorial ANOVA with Tukey post hoc test was used to assess group, treatment and group x treatment effects. Genes of interest were identified using a Student's t-test of the replicate 2^ (ΔCt) values of each gene in the control and treatment groups. The level of significance was accepted at $p<0.05$.

6.3 Results

6.3.1 MSC^{ob} have an impaired growth rate post isolation compared to MSC^{WT}

Confluency over time post isolation was used as an indication of cellular growth rate. In MSCs derived from healthy control animals (MSC^{WT}), a significant effect of time ($p<0.05$) was evident with a steady growth curve (Fig. 6.6). The confluency of MSC^{WT} increased from 49.7±6.9% on day 4 to 69±1% on day 16 post isolation. Expansion of MSC^{WT} in the presence of antioxidants (preconditioning) slightly improved the growth rate of cells with 52.4±6.3% confluency on day 4 increasing to 77.9±4.7% on day 16 (Fig. 6.6 A). No significant difference was however detected in the confluency of MSC^{WT} with preconditioning compared to SGM at the same time point. Impaired growth was evident in MSCs derived from obese prediabetic animals (MSC^{ob}), with confluency remaining at 61.5±1% 16 days post isolation (Fig. 6.6 B). Expansion of MSC^{ob} in the presence of antioxidants was unable to restore cellular growth with confluency levels of 57±6% detected on day 16 post isolation (Fig. 6.6 B).

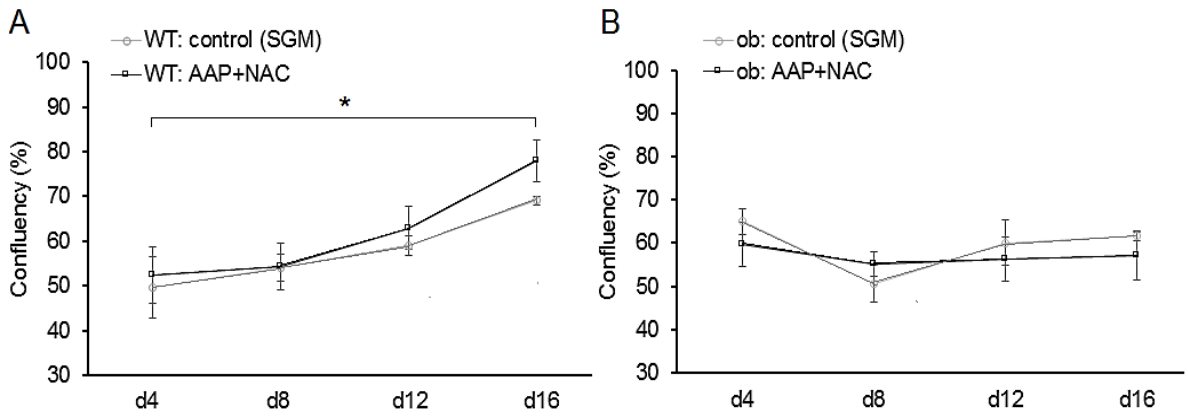

Figure 6.6 Confluency post isolation as an indication of the growth rate. A- MSC^{WT} and **B-** MSC^{ob} was isolated in SGM in the presence or absence of antioxidants and their growth rate was measured every 4 days for 16 days. MSC^{WT} showed a significant effect of time. All experiments were performed on MSCs derived from at least 3 animals per treatment group (n=3 biological repeats and x2 technical repeats). **Statistical analysis:** Factorial ANOVA with Tukey post hoc test. *$p<0.05$.

6.3.2 Flow cytometry characterization of isolated MSCs.

Flow cytometry surface marker characterization demonstrated that 88±4% of isolated bone marrow-derived cells expressed the stem cell marker, Sca1 (Fig. 6.7 A-C). A percentage of cells did however also express the hematopoietic lineage marker, CD45. Immediately, following isolation (passage 0), the bone marrow-derived stem cells therefore consisted of a heterogenous population of 60±3% MSCs (Sca1^{+}CD45^{-}) and 39±3% HSCs (Sca1^{+}CD45^{+}) (Fig. 6.7 A-D). There was no difference in

surface marker expression in the bone marrow MSCs derived from either WT control (MSC^{WT}) or *ob/ob* (MSC^{ob}) animals (Fig. 6.7 D).

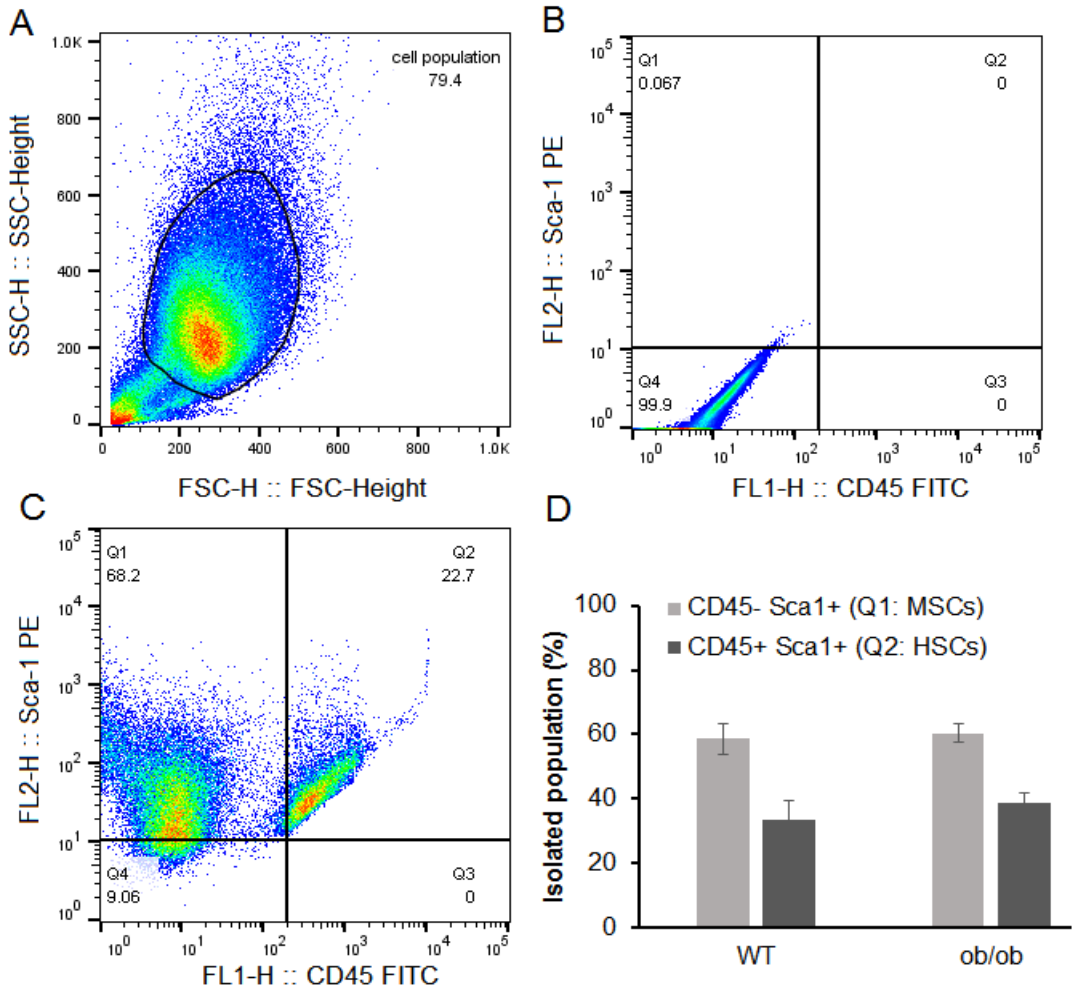

Figure 6.7 Characterization of healthy control and impaired/dysfunctional bone marrow derived MSCs. A– Flow cytometry dot plot demonstrating the forward (size) *vs* side (granularity) scatter of the isolated cells. **B, C–** The expression of Sca1 (PE) *vs* CD45 (FITC) in the unstained negative control sample (B) and bone marrow MSCs (C). Q1– MSCs expressing $Sca1^{+}CD45^{-}$; Q2– HSCs expressing $Sca1^{+}CD45^{+}$; Q3– Mature hematopoietic cells $Sca1^{-}CD45^{+}$; Q4- Cells expressing neither $Sca1^{-}$ nor $CD45^{-}$. **D–** Quantification of the percentage of MSCs and HSCs within the isolated populations (n=3). **Abbreviations: FITC:** Fluorescein isothiocyanate, **FSC:** forward scatter, **PE:** phycoerythrin, **Sca-1:** stem cell marker, **SSC:** side scatter.

6.3.3 Molecular and paracrine signalling at baseline and in response to stimulation with DWF

6.3.3.1 Secretome differences at baseline: MSC^{WT} vs MSC^{ob}.

The secretion of 24 cytokines from MSC^{WT} and MSC^{ob} were assessed at baseline with and without antioxidant preconditioning and the data presented in Table 6.2. From the 24 cytokines assessed within conditioned medium, significant differences ($p<0.05$) were detected at baseline (without stimulation with DWF) for 2 pro-inflammatory cytokines (TNFα, IFNγ) and 5 chemokines (KC, G-CSF, Eotaxin, MCP1, SDF1α) (Fig. 6.8).

Pro-inflammatory TNFα and IFNγ concentrations were significantly higher ($p<0.05$) in the conditioned medium collected from MSC^{ob} (TNFα 113±21 pg/ml; IFNγ 15±4 pg/ml) compared to MSC^{WT} (TNFα 40±14 pg/ml; IFNγ not detected) (Fig. 6.8 A, B). Pre-conditioning MSC^{ob} with antioxidants did downregulate the secretion of TNFα and IFNγ to levels comparable to that of MSC^{WT}. The chemokines KC, G-CSF and Eotaxin remained significantly higher ($p<0.05$) in the conditioned medium derived from MSC^{ob} (KC 778±151 pg/ml; G-CSF 67±12 pg/ml; Eotaxin 20±7 pg/ml) compared to MSC^{WT} (KC 353±50 pg/ml; G-CSF 10±8 pg/ml; Eotaxin not detected) regardless of pre-conditioning (Fig. 6.8 C-E). Pre-conditioning did promote MCP1 secretion in MSC^{ob} (1912±1772 pg/ml) ($p<0.05$) (Fig. 6.8 F), whereas only a small not significant increase (2571±901 pg/ml) was evident in MSC^{WT}. In contrast, SDF1α concentrations were significantly ($p<0.05$) less in the conditioned medium derived from MSC^{ob} (176±6 pg/ml) compared to MSC^{WT}; (203±3 pg/ml) (Fig. 6.8 G).

The data presented in Fig. 6.8 and Table 6.2 is indicating the restoration effects of AAP+NAC on impaired/dysfunctional MSC^{ob} compared to control at baseline (MSC^{WT} and MSC^{ob}) and antioxidative effects of these antioxidants on healthy MSCs was not a subject of these study.

Table 6.2 Cytokine secretome differences at baseline.

Secreted protein: Conditioned medium				
	Control		**Pre-conditioned**	
	MSC^{WT}	**MSC^{ob}**	**MSC^{WT}**	**MSC^{ob}**
Pro-inflammatory				
IL1α	-	4.0 (2.1)	-	-
IL1β	24 (8)	34 (7)	21 (11)	25 (5)
IL6	1 007 (254)	1 254 (514)	942 (316)	1 176 (263)
IL9	-	13 (12)	-	-
IL12(p40)	75 (22)	109 (11)	99 (10)	154 (31)
IL12(p70)	130 (70)	325 (65)	130 (70)	186 (61)
IL17A	-	-	-	-
IFNγ	**- [a]**	**15 (4) [a, c]**	-	**- [c]**
RANTES	127 (13)	226 (48)	122 (17)	229 (25)
TNFα	**40 (14) [a]**	**113 (21) [a, c]**	34 (19)	**51 (14) [c]**
Chemokines				
Eotaxin	**- [a]**	**20 (7) [a]**	**- [d]**	**9.1 (4.5) [d]**
G-CSF	**10 (8) [a]**	**67 (12) [a]**	**10 (7.5) [d]**	**30 (15) [d]**
GM-CSF	85 (32)	137 (22)	77 (40)	84 (17)
KC	**353 (50) [a]**	**778 (151) [a]**	**356 (48) [d]**	**578 (71) [d]**
MCP1	1 721 (113)	**5 171 (835) [c]**	**2 571 (901) [d]**	**12 912 (1 772) [c d]**
MIP1α	11 (2)	8.9 (0.4)	15 (4)	13 (0.4)
MIP1β	50 (2)	65 (4)	88 (36)	129 (11)
SDF1α	**203 (3)[a, d]**	**176 (6)[a]**	175 (4)	**173 (9)[d]**
Anti-inflammatory				
IL2	2.7 (2.6)	7.9 (2.7)	2.7 (2.6)	6.3 (3.5)
IL3	2.9 (1.7)	9.5 (1.6)	2.9 (1.7)	4.7 (1.8)
IL4	-	1.3 (1.2)	-	-
IL5	13 (7)	16 (2)	15 (6)	38 (8)
IL10	36 (7)	87 (8)	32 (11)	74 (19)
IL13	138 (25)	207 (37)	107 (55)	135 (23)

Footnote: Data is presented as mean (SE) in pg/ml. All experiments were performed on MSCs derived from at least 3 animals per treatment group (n=3 biological repeats and x2 technical repeats). **Statistical analysis:** Factorial ANOVA with Tukey post hoc test. Level of significance accepted at $p<0.05$. **Abbreviations:** **-** Not detected, **[a]** Significant difference at baseline (control) between MSC^{WT} and MSC^{ob}., **[b]** Significant difference in MSC^{WT} with and without preconditioning., **[c]** Significant difference in MSC^{ob} with and without preconditioning., **[d]** Significant difference between MSC^{WT} and MSC^{ob} with preconditioning.

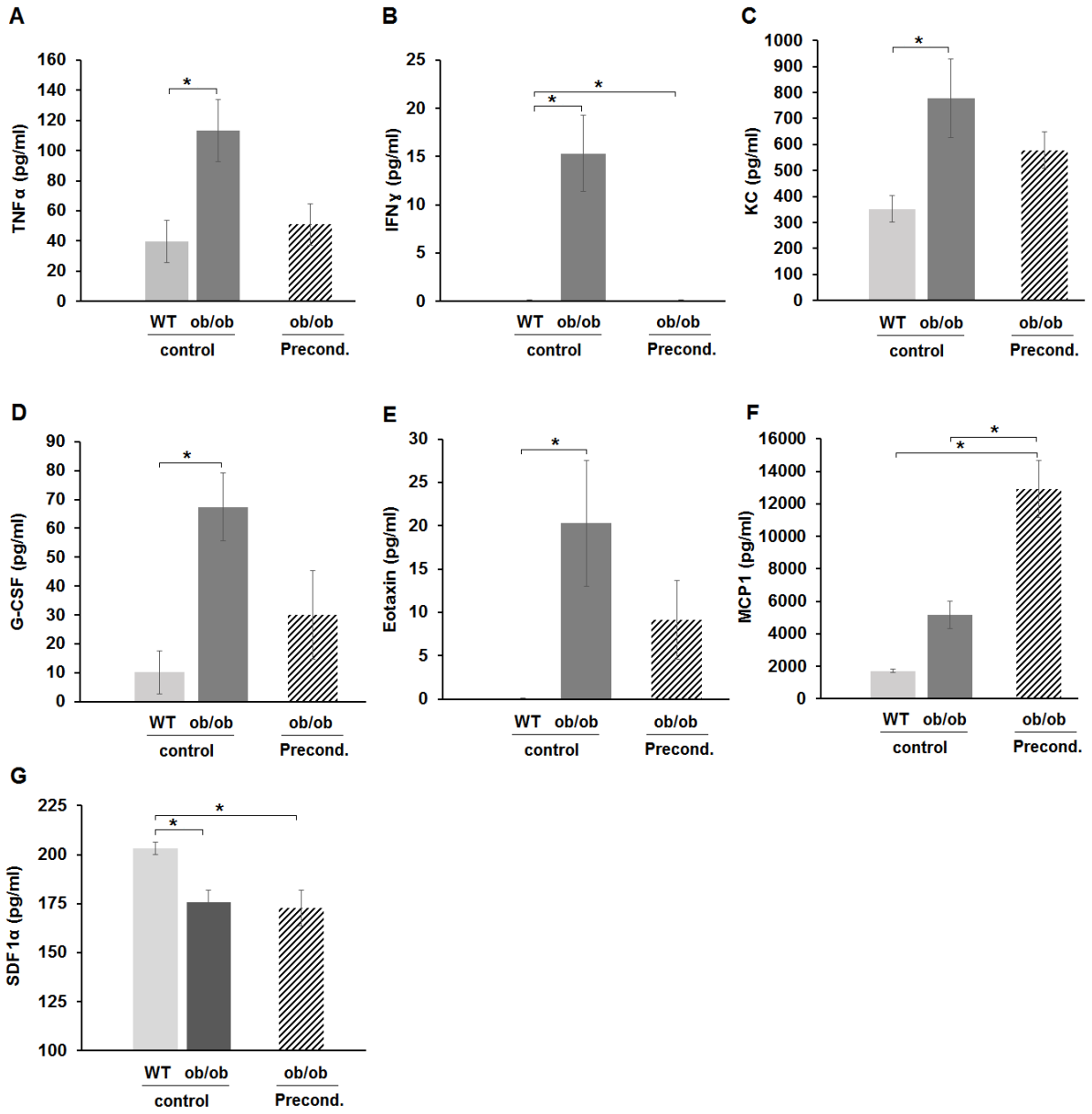

Figure 6.8 Differences in the baseline after preconditioning: healthy control MSC^{WT} *vs* impaired/dysfunctional MSC^{ob}. The cytokine concentrations in conditioned medium was assessed in MSC^{WT}, MSC^{ob} and preconditioned MSC^{ob}. **A-** Tumour necrosis factor alpha (TNFα) (pg/ml), **B-** Interferon (IFNγ) (pg/ml), **C-** KC (pg/ml), **D-** Granulocyte colony stimulating factor (G-CSF) (pg/ml), **E-** Eotaxin (pg/ml), **F-** Macrophage chemoattractant protein 1 (MCP1) (pg/ml), **G-** Stromal-cell derived factor 1 (SDF1α) (pg/ml). All experiments were performed on MSCs derived from at least 3 animals per treatment group (n=3 biological repeats and x2 technical repeats). **Statistical analysis:** Factorial ANOVA with Tukey post hoc test. *$p<0.05$.

6.3.3.2 Differences in the paracrine responsiveness following DWF stimulation: MSC^{WT} vs MSC^{ob}.

The cytokine concentrations following stimulation with DWF are presented in Table 6.3. The cytokine levels within DWF also is presented in the table and figures (DWF line) as background controls. Following stimulation with DWF, significant differences ($p<0.05$) were detected in concentrations of 2 chemokines (GM-CSF, Eotaxin), 3 pro-inflammatory cytokines (TNFα, IFNγ, IL9) and 4 anti-inflammatory cytokines (IL10, IL4, IL13, IL3) between groups (Fig. 6.9).

Similar to baseline, the chemokines GM-CSF and Eotaxin were detected at higher concentrations in MSC^{ob} (GM-CSF 486±26 pg/ml; Eotaxin 217±6 pg/ml) and preconditioned groups (GM-CSF 510±30 pg/ml; Eotaxin 229±9 pg/ml) following stimulation compared to MSC^{WT} (GM-CSF 399±10 pg/ml; Eotaxin 179±6 pg/ml) (Fig. 6.9 A-B). Despite these differences, the concentration of these chemokines post-stimulation was lower than that detected in DWF (Table 6.3).

Stimulation with DWF induced a much greater pro-inflammatory TNFα response in MSC^{ob} (20 441±1461 pg/ml) than MSC^{WT} (5 081±671 pg/ml); this excessive response in MSC^{ob} was dampened with preconditioning (9 190±487 pg/ml) (Fig. 6.9 C). Preconditioning furthermore increased the release of pro-inflammatory IFNγ and IL9 following stimulation with DWF in the MSC^{ob} (IFNγ 77±6 pg/ml; IL9 242±5 pg/ml) compared to MSC^{WT} (IFNγ 57±3 pg/ml; IL9 204±9 pg/ml) (Fig. 6.9 D-E).

A slight difference in the anti-inflammatory IL3, IL4 and IL13 response to DWF was evident between MSC^{ob} (IL3 38±1 pg/ml; IL4 65±3 pg/ml; IL13 745±7 pg/ml) and MSC^{WT} (IL3 33±1 pg/ml; IL4 53±1 pg/ml; IL13 617±14 pg/ml) (Fig. 6.9 F-I). IL4 in conditioned medium post-stimulation was however below the concentration detected in DWF (Table 6.3). Preconditioning significantly improved the secretion of anti-inflammatory IL10 post-stimulation in the MSC^{ob} group (MSC^{ob} 5 415±317 pg/ml; Preconditioned 10207±812 pg/ml; MSC^{WT} 6823±575 pg/ml) (Fig. 6.9 F).

The data presented in Fig. 6.9 and Table 6.3 indicates the restoration effects of AAP+NAC on impaired/dysfunctional MSC^{ob} compared to the responses observed in healthy control (MSC^{WT}). A limitation of the current study was not assessing the effect of preconditioning on the baseline phenotype of MSC^{WT}.

Table 6.3 Cytokine secretion profile in response to diabetic wound fluid (DWF).

Secreted protein: Response to DWF				
	DWF	**Control**		**Preconditioned**
		MSC^{WT}	**MSC^{ob}**	**MSC^{ob}**
Pro-inflammatory				
IL1α	6 992	2 737 (31)	2 640 (560)	2 974 (165)
IL1β	3 360	1 144 (22)	1 184 (125)	1 131 (133)
IL6	1 004	11 305 (2 119)	7 290 (3 240)	10 574 (3 827)
IL9	127	**204 (9)** [g]	**228 (4)** [f]	**242 (5)** [f, g]
IL12(p40)	4 962	2 944 (71)	3 051 (174)	2 934 (151)
IL12(p70)	598	1 030 (71)	1 068 (32)	1 064 (118)
IL17A	361	207 (6)	238 (19)	241 (20)
IFNγ	43	**57 (3)** [g]	68 (2)	**77 (6)** [g]
RANTES	128	3 971 (217)	5 376 (687)	12 833 (6 862)
TNFα	932	**5 081 (671)** [e]	**20 441 (1 461)** [e, f]	**9 190 (487)** [f]
Chemokines				
Eotaxin	572	**179 (6)** [e, g]	**217 (6)** [e]	**229 (9)** [g]
G-CSF	>47 590 [#]	14 160 (605)	14 942 (781)	15 484 (1 564)
GM-CSF	672	**399 (10)** [g]	486 (26)	**510 (30)** [g]
KC	>21 315 [#]	11 231 (3 397)	11 165 (1 767)	18 305 (5 378)
MCP1	18 568	35 772 (678)	34 706 (10 271)	35 432 (7 406)
MIP1α	>7 288 [#]	2 689 (257)	3 095 (493)	6 357 (2 603)
MIP1β	1187	18 344 (1 776)	26 690 (7 447)	31 905 (12 064)
Anti-inflammatory				
IL2	23	49 (1)	60 (1)	120 (19)
IL3	27	**33 (1)** [e*, g]	**38 (1)** [e*]	**39 (2)** [g]
IL4	91	**53 (1)** [e]	**65 (3)** [e]	60 (3)
IL5	27	53 (3)	66 (4)	95 (23)
IL10	263	**6 823 (575)** [g]	**5 415 (317)** [f]	**10 207 (812)** [f, g]
IL13	329	**617 (14)** [e, g]	**745 (7)** [e]	**747 (29)** [g]

Footnote: Data is presented as mean (SE) in pg/ml. The cytokine concentration existed in DWF is not subtracted from final cytokine concentrations. All experiments were performed on MSCs derived from at least 3 animals per treatment group (n=3 biological repeats and x2 technical repeats). **Statistical analysis:** Factorial ANOVA with Tukey post hoc test. Level of significance accepted at $p<0.05$. [#] the concentration of these chemokines was above the detection limit as indicated. [e] Significant difference between MSC^{WT} and MSC^{ob}., [e*] indicates $p=0.06$, [f] Significant difference in MSC^{ob} with and without preconditioning., [g] Significant difference between MSC^{WT} and MSC^{ob} with preconditioning.

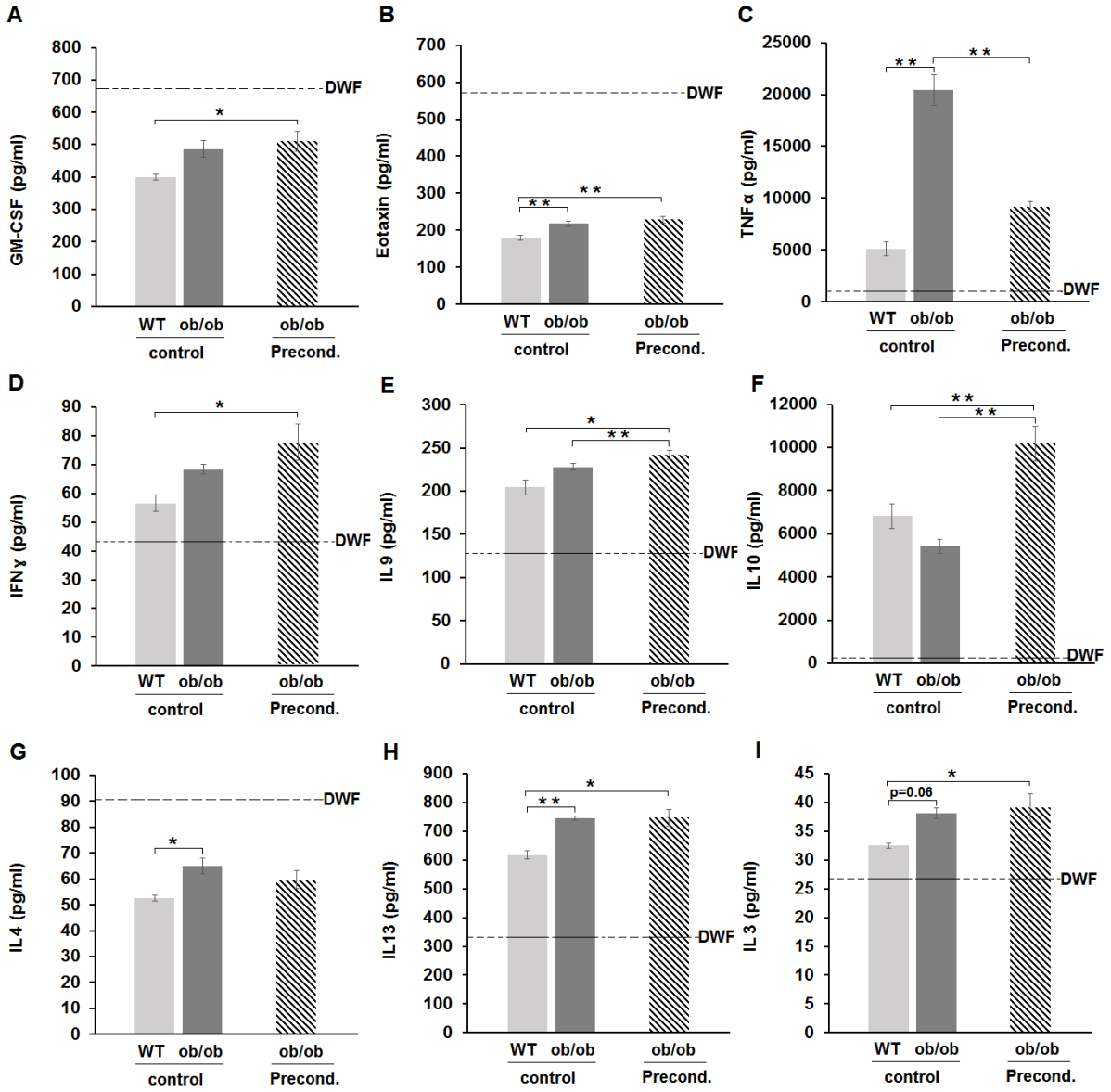

Figure 6.9 Differences in the paracrine responsiveness following DWF stimulation: healthy control MSC^{WT} *vs* impaired/dysfunctional MSC^{ob}. The cytokine concentrations in conditioned medium post stimulation with DWF was assessed in MSC^{WT}, MSC^{ob} and preconditioned MSC^{ob}. The cytokine concentration in DWF (DWF line) is not subtracted from final cytokine concentrations. **A-** Granulocyte macrophage colony stimulating factor (GM-CSF) (pg/ml), **B**- Eotaxin (pg/ml), **C-** Tumour necrosis factor alpha (TNFα) (pg/ml), **D**- Interferon gamma (IFNγ) (pg/ml), **E**- Interleukin 9 (IL9) (pg/ml), **F-** Interleukin 10 (IL10) (pg/ml), **G-** Interleukin 4 (IL4) (pg/ml), **H-** Interleukin 13 (IL13) (pg/ml), **I-** Interleukin 3 (IL3) (pg/ml). All experiments were performed on MSCs derived from at least 3 animals per treatment group (n=3 biological repeats and x2 technical repeats). **Statistical analysis:** Factorial ANOVA with Tukey post hoc test. *p<0.05. Abbr: DWF-diabetic wound fluid.

6.3.3.3 Gene expression (mRNA) differences at baseline and in response to stimulation with DWF: MSC^{WT} vs MSC^{ob}.

The mRNA expression pattern between groups is illustrated using a heatmap in Figure 6.10 A. For a summary of significant differences ($p<0.05$) in the mRNA expression profiles between groups refer to Figure 6.10 B. At baseline, under standard growth conditions, 31 genes were overexpressed (> 2-fold) and 39 genes under-expressed (> 2-fold) in MSC^{ob} *vs* MSC^{WT}. The overexpression of *Csf-1* (also known as M-CSF) was however the only significant difference ($p<0.05$) between the groups at baseline (Fig. 6.11 A). Overall, the preconditioning of MSC^{ob} downregulated the expression of 32 genes and upregulated the expression of 48 genes. The expression of *Csf1* in MSC^{ob} was downregulated with preconditioning to levels comparable to that observed in MSC^{WT}. Moreover, preconditioning induced the expression of *Ccl8* (also known as MCP2) ($p<0.05$) (Fig. 6.11 B).

When exposed to DWF (without preconditioning) both MSC^{WT} and MSC^{ob} responded by significantly ($p<0.05$) increasing the gene expression of macrophage chemoattractant proteins *Ccl2* (also known as MCP1) and *Ccl3* (also known as MIP1α) (Fig. 6.11 C, D). Furthermore, in MSC^{WT} DWF induced the expression ($p<0.05$) of 9 additional genes (*Ccl24, Ccl7, Cxcl10, Cxcl5, Cxcl9, IL15, IL1α, TNFα*) associated with pro-inflammatory chemotactic responses (Fig. 6.11 C). In contrast, MSC^{ob} responded by increasing ($p<0.05$) the expression of only 4 additional genes (*Cxcl1, IL11ra, IL27, Cxcl11*) (Fig. 6.11 D).

In response to DWF, the preconditioned MSC^{ob} population, significantly ($p<0.05$) upregulated the expression of TNFα, *Ccl12, Ccl17, Ccl19, Ccl2, Ccl3, Csf3, Cxcl11 and Mif* compared to baseline (Fig. 6.11 E); the expression of *Ccl7*, *Mif* and *Cxcl10* at MSC^{ob} was induced at baseline after exposure to DWF (Fig. 6.11 F).

The preconditioned MSC^{ob} furthermore had an increased expression of *Bmp2* (bone morphogenetic protein 2) in response to DWF compared to MSC^{WT} at baseline (Fig. 6.11 G) and increased the expression of *Vegfa* (vascular endothelial growth factor alpha) compared to baseline MSC^{WT} upon stimulation with DWF (Fig. 6.11 H). The difference in responses between the treatment groups is illustrated in Figure 6.10 B.

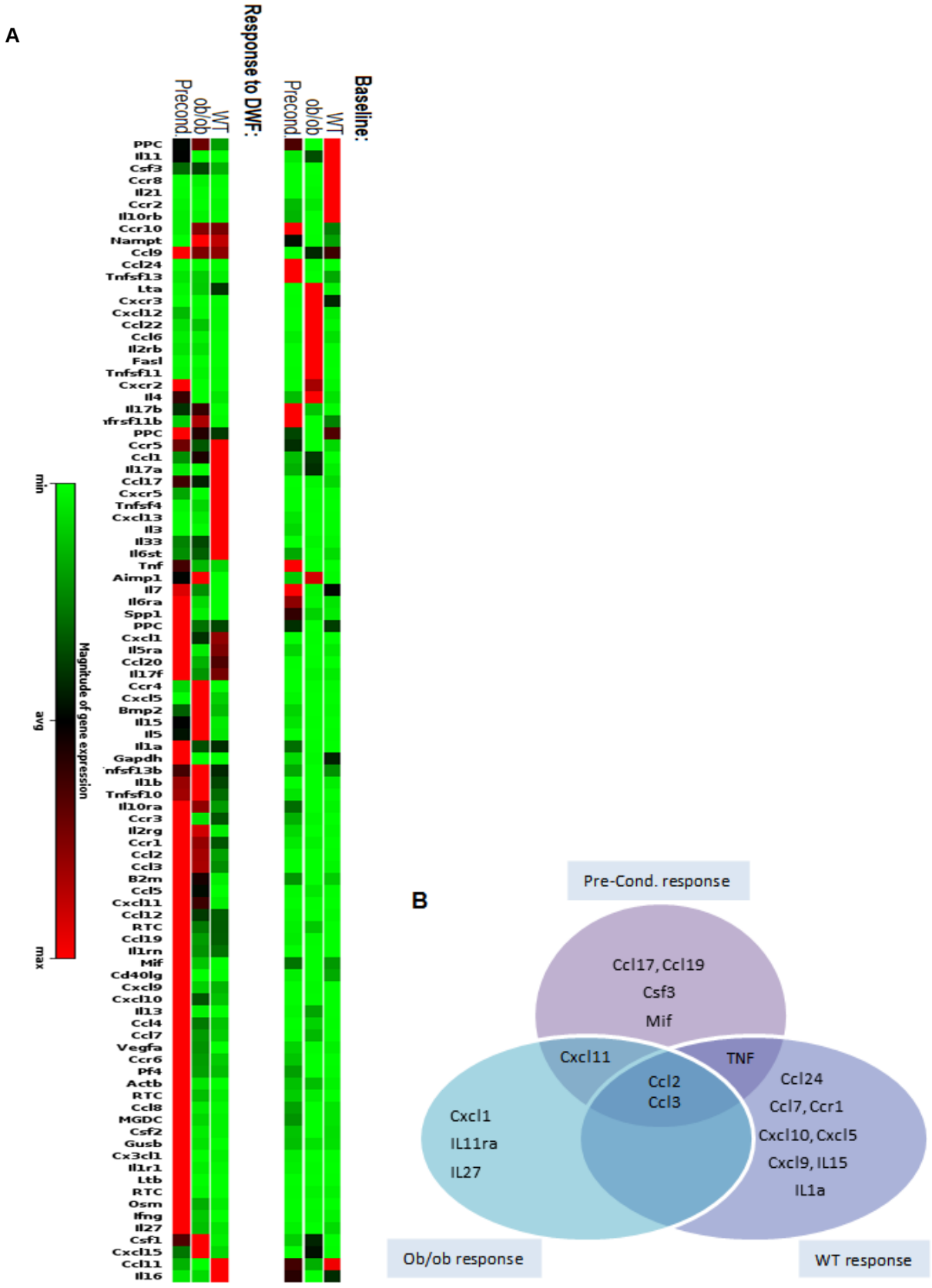

Figure 6.10 mRNA expression between groups and a summary of significant differences. A- Heat map of upregulated (red) and down-regulated (green) genes. **B-** Summary of the responsiveness of MSC^{WT}, MSC^{ob} and preconditioned MSC^{ob} to DWF (only genes that had a significant change in mRNA expression are indicated).

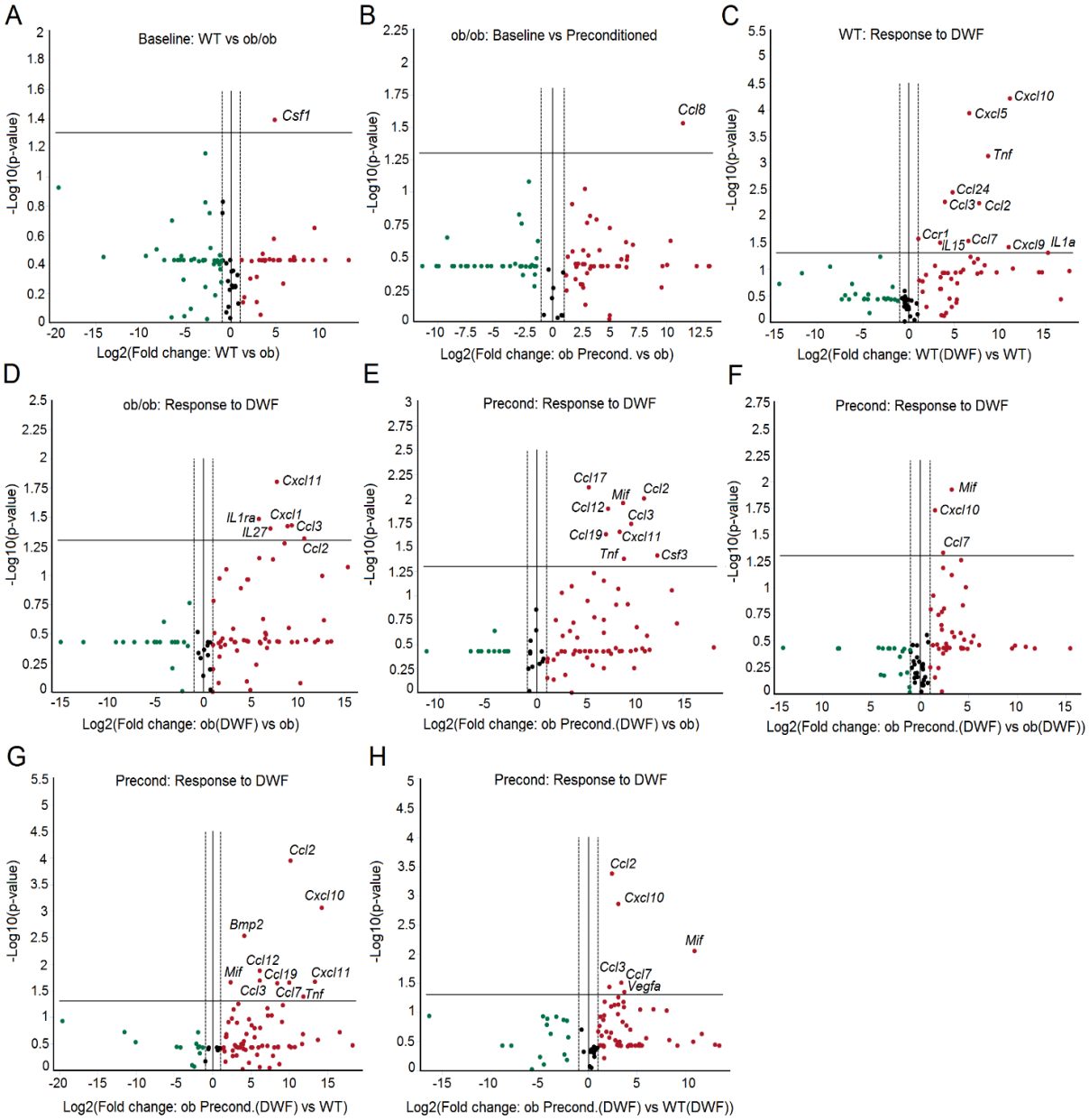

Figure 6.11 Gene expression differences in response to stimulation with DWF: healthy control MSC^{WT} *vs* impaired/dysfunctional MSC^{ob}. A-B- comparison of mRNA expression at baseline in MSC^{ob} *vs* MSC^{WT} (A) and in MSC^{ob} with and without antioxidant preconditioning (B) **C-** The gene expression responsiveness of MSC^{WT} to stimulation with DWF. **D-** The gene expression responsiveness of MSC^{ob} to stimulation with DWF, **E-F-G-H-** The gene expression response to preconditioning following stimulation with DWF in MSC^{ob} compared to baseline with and without DWF stimulation. All experiments were performed on MSCs derived from at least 3 animals per treatment group (n=3 biological repeats and x2 technical repeats). **Statistical analysis:** Genes of interest were identified using a Student's t-test of the replicate (n=3) 2^(ΔCt) values of each gene in the control and experimental groups. Red dot: upregulated, Black dot: unchanged and Green dot: down regulated.

6.3.4 MSC Function at baseline and in response to stimulation with DWF

6.3.4.1 Antioxidant preconditioning improves the viability of both MSC^{WT} and MSC^{ob}

Antioxidant preconditioning was able to improve cell viability under baseline conditions in both MSC^{WT} and MSC^{ob} compared to SGM (Fig. 6.12 and 6.13). Increase in cell viability was evident in preconditioned MSCs derived from healthy control animals (MSC^{WT}) over a period of 24h (3.6-fold, $p<0.05$), 48h (4.7-fold, $p<0.05$) and 96h (3.8-fold, $p<0.05$) (Fig. 6.13 A-C-E). Although less pronounced, increased viability was also evident in preconditioned MSCs derived from obese prediabetic animals (MSC^{ob}) at 24h (1.4-fold, $p<0.05$), 48h (1.3-fold, $p=0.06$) and 96h (1.5-fold, $p<0.05$) (Fig. 6.13 B-D-F). In the presence of DWF, the viability of MSCs was significantly ($p<0.05$) reduced (Fig. 6.13 A-F). Within the first 48h of exposure to DWF, preconditioning had a protective effect in MSC^{WT} with 2-fold (24h) and 1.9-fold (48h) higher viability rates than unconditioned MSCs (SGM) (Fig. 6.13 A, C). This protective effect was however not evident in preconditioned MSC^{ob} in the presence of DWF (Figure 6.13 B, D). Refer to Figure 6.12 for representative images illustrating crystal violet viability staining.

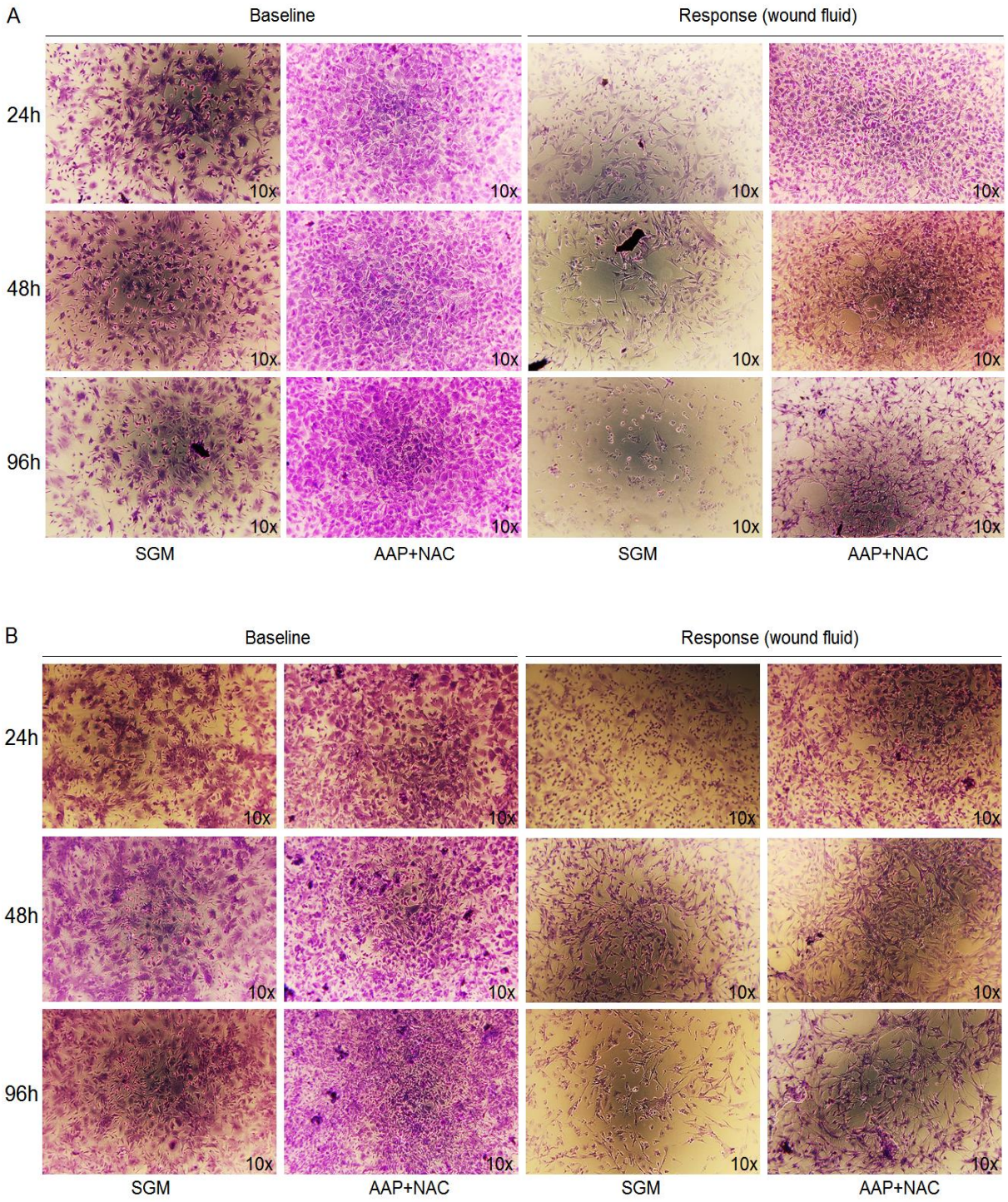

Figure 6.12 Representative images of crystal violet staining at baseline and response to DWF. A- $MSCs^{WT}$ and **B-** $MSCs^{ob}$ viability was analysed in four treatment groups at 24h, 48h and 96h after stimulation. Images were captured by a light microscope with 10x magnification. All experiments were performed on MSCs derived from at least 3 animals per treatment group (n=3 biological repeats and x3 technical repeats).

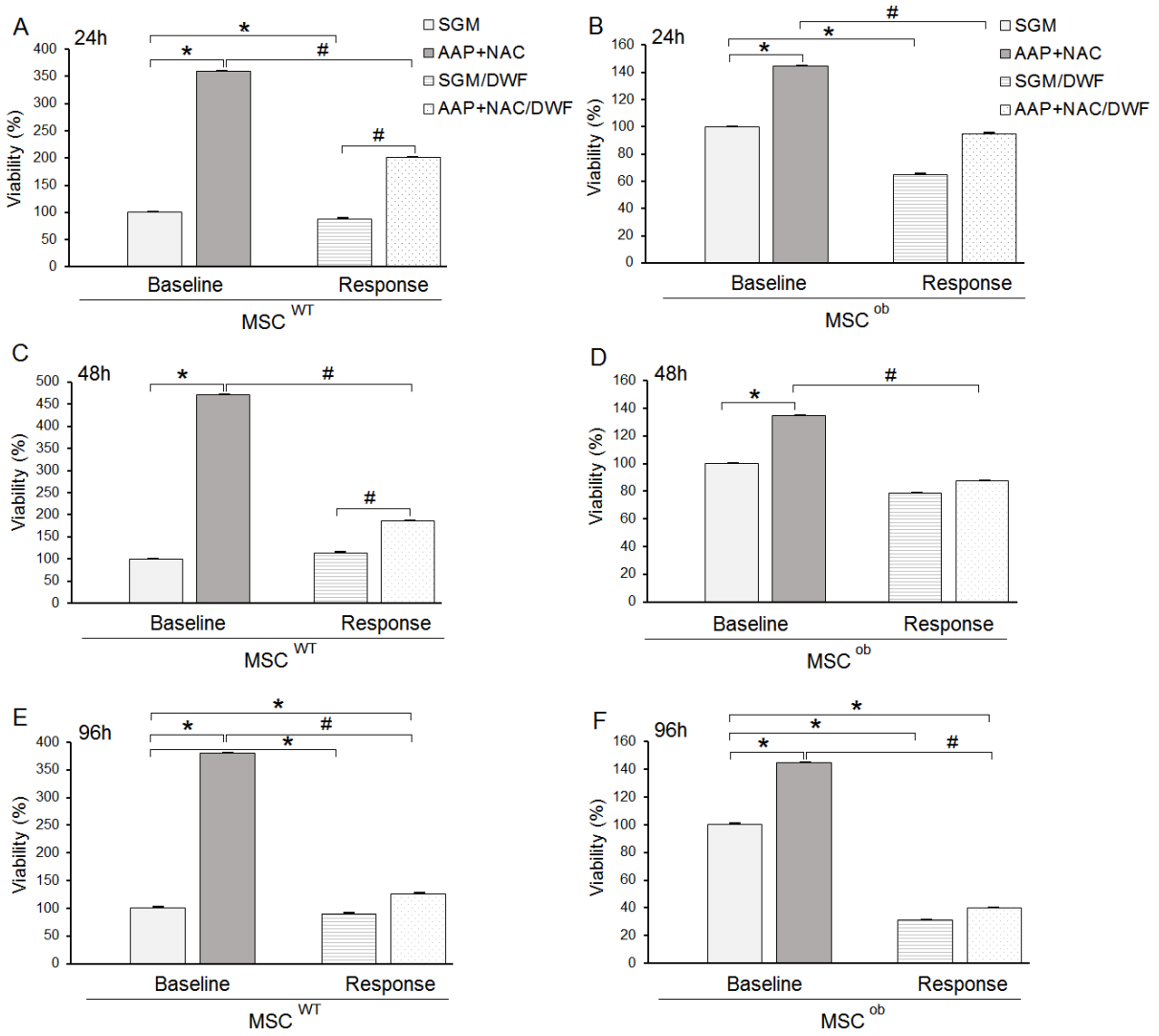

Figure 6.13 MSCs viability (%) in response to DWF with and without preconditioning. A-C-E- MSC^{WT} and **B-D-F-** MSC^{ob} viability was analysed in baseline phenotype (SGM), baseline response (SGM/DWF), preconditioned phenotype (AAP+NAC) and preconditioned response (AAP+NAC/DWF), 24h, 48h and 96h after stimulation. All experiments were performed on MSCs derived from at least 3 animals per treatment group (n=3 biological repeats and x3 technical repeats). **Statistical analysis:** Factorial ANOVA with Tukey post hoc test ($p<0.05$). * Significant differences compared to control. # Indicates significant differences between groups.

6.3.4.2 Diabetic wound fluid negatively affects the migration of MSC^{WT} and MSC^{ob}.

Under baseline conditions, significant wound closure ($p<0.05$) was evident at 24h in both unconditioned (SGM) (MSC^{WT} 26.1±2.5%; MSC^{ob} 39.6±3.8%) and preconditioned (MSC^{WT} 36.3±3.5%; MSC^{ob} 43.8±0.7%) MSCs (Fig. 6.15 A, C). In the presence of DWF at baseline, no effect of time was evident with the percentage of wound closure, however the closure remained <33% at 24h in all groups (Fig. 6.15 B, D). Despite slightly higher migration rates with antioxidant preconditioning, wound closure was not significantly improved in the presence of DWF compared to SGM (Fig. 6.15 B, D). Refer to Figure 6.14 for representative images of the wound healing assay used to assess MSC migration.

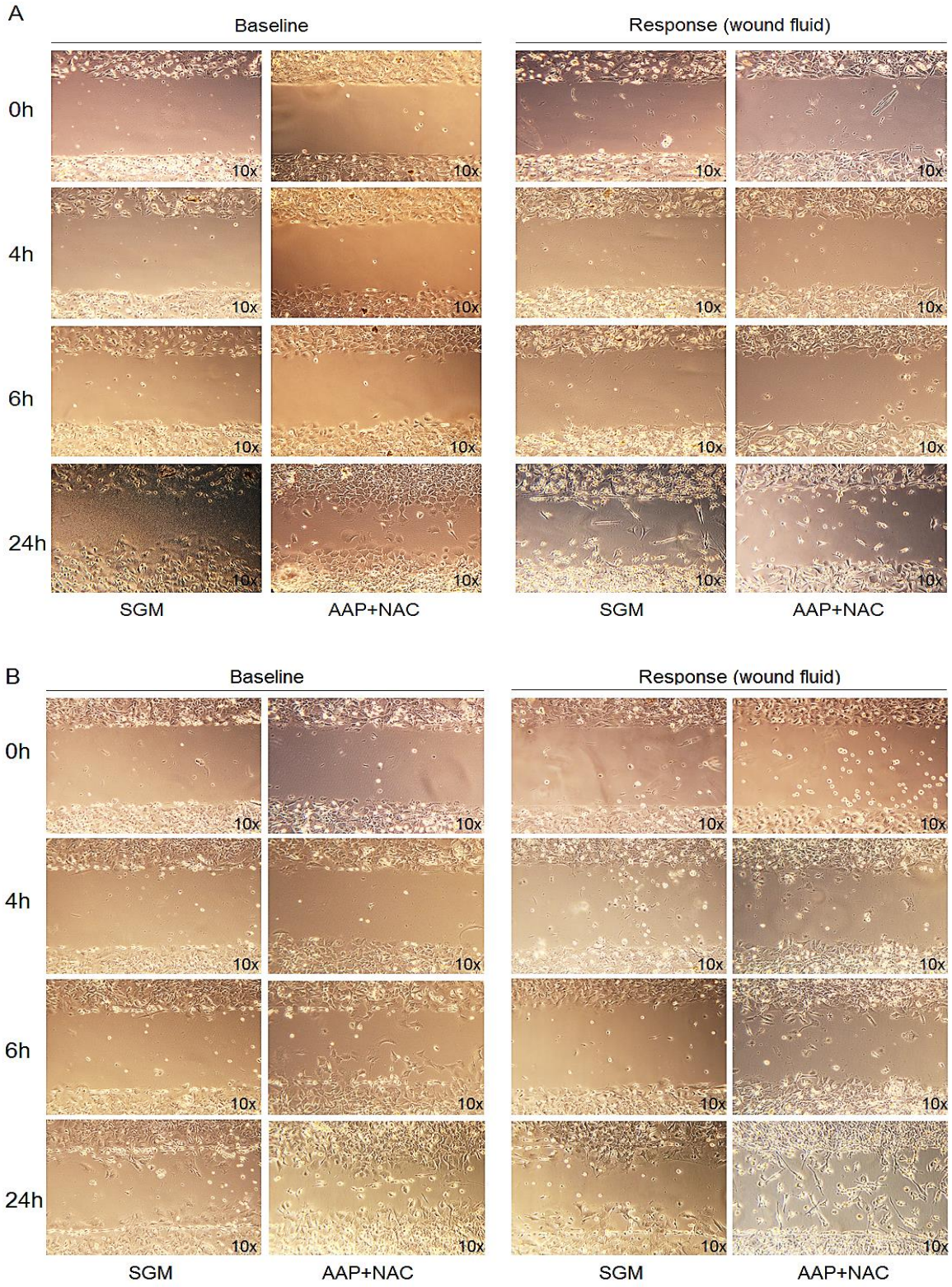

Figure 6.14 Representative images of migration assay at baseline and response to DWF. A- $MSCs^{WT}$ and **B-** $MSCs^{ob}$ *in vitro* healing were measured in four treatment group 4h, 6h and 24h after stimulation. All experiments were performed on MSCs derived from at least 3 animals per treatment group (n=3 biological repeats and x3 technical repeats).

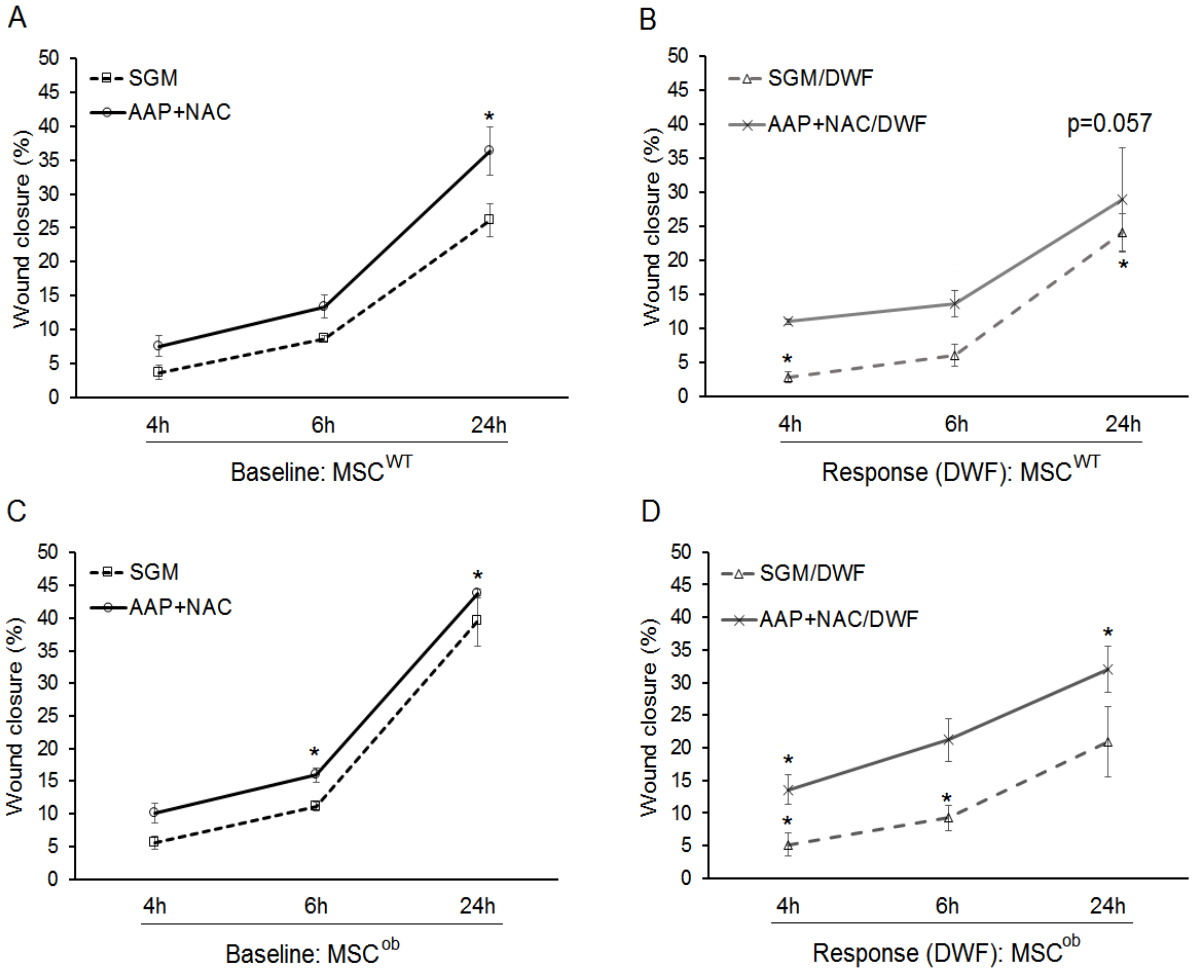

Figure 6.15 MSCs *in vitro* wound closure (%) in response to DWF with and without preconditioning. A-B- MSC^{WT} and **C-D-** MSC^{ob} migration towards gap closure was analysed in baseline phenotype (SGM), baseline response (SGM/DWF), preconditioned phenotype (AAP+NAC) and preconditioned response (AAP+NAC/DWF). All experiments were performed on MSCs derived from at least 3 animals per treatment group (n=3 biological repeats and x3 technical repeats). **Statistical analysis:** Factorial ANOVA with Tukey post hoc test ($p<0.05$). * Significant differences compared to control.

6.3.4.3 Antioxidant preconditioned MSC^{ob} spontaneously differentiate into bone in the presence of DWF.

Microscopy images revealed that preconditioned MSC^{ob} (>90% confluent) lay down extensive ECM that triggered spontaneous differentiation into the bone. This was confirmed using Alizarin Red S staining which illustrated a significant ($p<0.05$) increase in spontaneous Ca^{2+} deposits (3.8±2.9% of the surface area) formed by preconditioned MSC^{ob} in the presence of DWF (Fig. 6.16 B). In all other groups, Ca^{2+} deposits were <1% of the total surface area (Fig. 6.16 A, B). Refer to Figure 6.17 C for representative images of Alizarin Red staining.

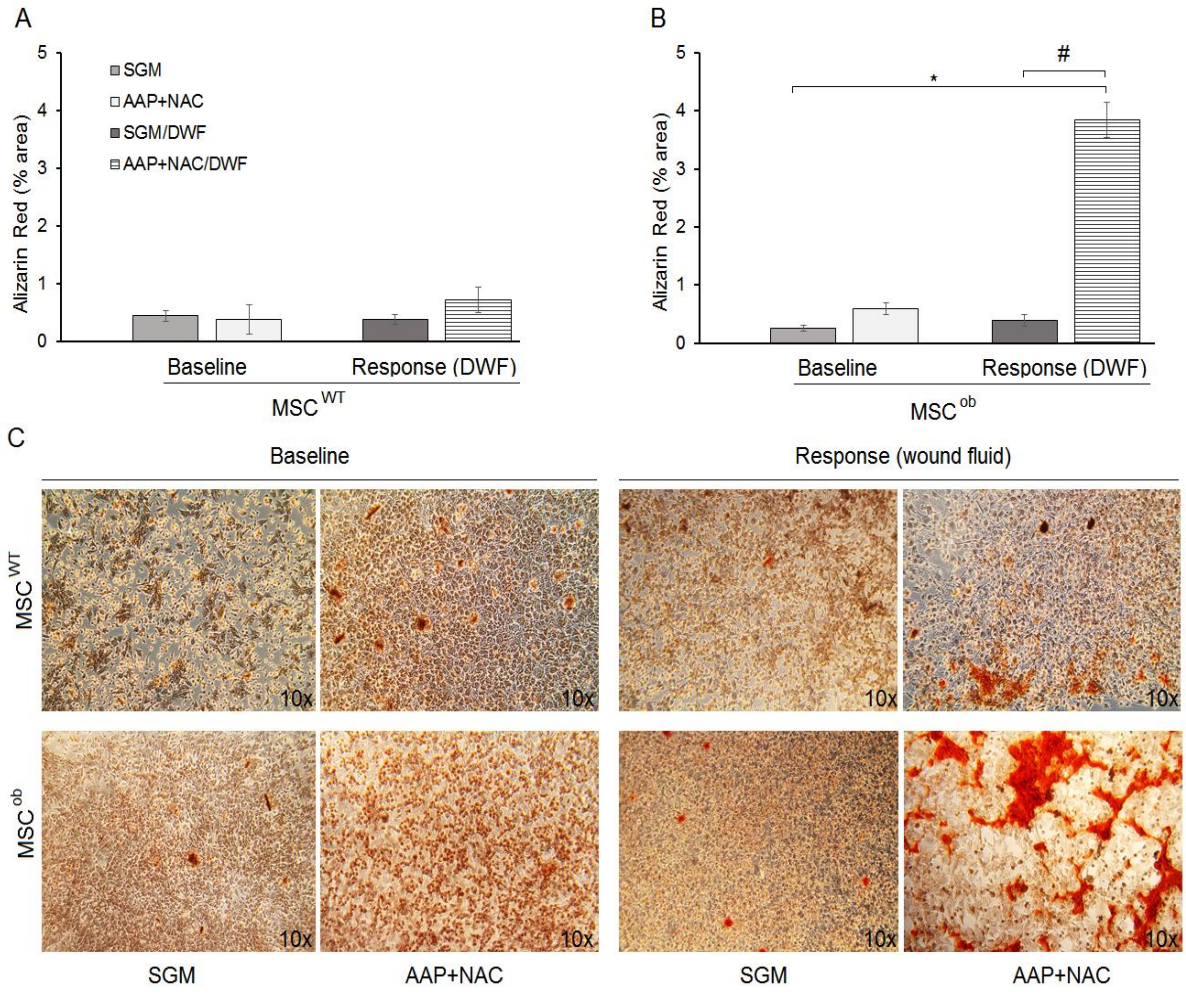

Figure 6.16 Mineralization in response to DWF with and without preconditioning. A- MSC^{WT} and **B-** MSC^{ob} percentage of mineralization was analysed in baseline phenotype (SGM), baseline response (SGM/DWF), preconditioned phenotype (AAP+NAC) and preconditioned response (AAP+NAC/DWF). **C-** Images from calcium deposits were captured by light microscopy with 10x magnification after staining. All experiments were performed on MSCs derived from at least 3 animals per treatment group (n=3 biological repeats and x3 technical repeats). **Statistical analysis:** Factorial ANOVA with Tukey post hoc test ($p<0.05$). * Significant differences compared to control. # Indicates significant differences between groups.

6.4 Discussion

Application of MSCs is a promising novel treatment in wound repair and regeneration (Ennis et al., 2013). However, in the context of diabetes, MSCs exhibit an altered secretome pattern due to pathological changes in their microenvironment and as a consequence autologous cell therapy in T2DM patients is mostly ineffective (Ribot et al., 2017; van de Vyver, 2017). The advancement of MSC therapy for the treatment of non-healing diabetic wounds is thus hampered by endogenous stem cell dysfunction and the limited viability of cells post-transplantation into the pathological wound environment (van de Vyver, 2017). There is *in vitro* evidence to support the growth-promoting and cytoprotective effects of some antioxidants such as NAC and AAP in a variety of models. To date, evidence indicating the positive effects of these antioxidants on MSC proliferation is however largely based on non-pathologic conditions, with only a few studies illustrating a protective effect against acute oxidative damage in a diabetic model (Ali et al., 2016; Weinberg et al., 2014; Yan et al., 2012). The novelty of this study lies in investigating the efficacy of combined NAC/AAP preconditioning to restore the function of impaired diabetic MSCs and in assessing its protective effects upon exposure of MSCs to DWF. In the context of this *ex vivo* study, wound fluid represented the extracellular fluid space within the micro-environment of a diabetic wound. Exposing healthy and impaired/dysfunctional bone marrow stem cells to DWF *in vitro* enabled an investigation into the functional and paracrine responsiveness of these cells on both molecular and protein level. This study is the first to demonstrate the efficacy of antioxidant preconditioning in restoring the paracrine function of impaired/dysfunctional stem cells towards that seen under control non-pathological conditions. This study furthermore demonstrates that expansion of primary bone marrow derived MSCs in the presence of combined NAC/AAP treatment improves the *ex vivo* viability of cells and has a slight protective effect against the toxicity of DWF. Despite improved viability, and a restored paracrine response, antioxidant preconditioning could however not rescue the proliferation and migration capacity of severely impaired diabetic MSCs.

Consistent with previous reports, a steady growth curve was evident in healthy control MSCs, whereas the *ex vivo* growth rate of MSCs derived from diabetic animals was severely impaired (van de Vyver, 2017; van de Vyver et al., 2016). Antioxidant preconditioning was able to significantly improve the viability of both healthy and impaired diabetic MSCs in culture. Therefore, MSC expansion in the presence of NAC/AAP may be an effective strategy to optimize cell viability in culture. Diabetic wound fluid (representative of the extrinsic wound environment post-transplantation) negatively impacted cell viability and confirmed the toxicity of a chronic wound environment. Although some studies have shown that DWF improves the proliferation and migration of stem cells (adipose tissue-derived) (Scherzed et al., 2011; Thamm et al., 2015), it is now known that wound fluid derived from acute and chronic wounds inversely influence stem cell function (Koenen et al., 2015). Koenen et al., 2015 demonstrated that acute wound fluid had a much stronger chemotactic impact on ADSCs than chronic wound fluid. The authors furthermore demonstrated that acute wound fluid stimulated proliferation whereas chronic wound fluid negatively affected proliferation (Koenen et al., 2015). This is consistent with our findings. Preconditioning did however have a slight protective effect in healthy

control MSCs during the first 48h of exposure to DWF. The mechanism of action underlying this protective effect is most likely related to the combined anti-inflammatory and ROS scavenging abilities of AAP and NAC *(as discussed in chapter 5, p.43).*

On molecular level, at baseline, the secretion of pro-inflammatory cytokines (TNFα, IFNγ) and chemokines (KC, G-CSF and Eotaxin) was more pronounced in the impaired/dysfunctional bone marrow stem cells. These factors all function to amplify the first stage of wound healing (inflammatory response), by recruiting neutrophils, lymphocytes, eosinophils and keratinocytes to the wounded area (Baltzis et al., 2014; Behm et al., 2012; Dreifke et al., 2015). Excessive inflammation prevents the transition into the proliferative stage of healing and as a consequence prevent regeneration. At the mRNA level, a similar pattern was observed, however only the overexpression of *csf1* was significant when comparing healthy *vs* dysfunctional stem cells and corresponded with higher chemokine (GM-CSF) levels detected in the conditioned medium. These and other chemokines were already present within the wound microenvironment (DWF) at very high concentrations and the additional release thereof is thus unwanted. Antioxidant preconditioning was able to reduce the secretion of pro-inflammatory TNFα and IFNγ at baseline but did not reduce chemokine secretion.

In the context of cell therapy, the paracrine responsiveness of stem cells to the wound microenvironment will determine their effectiveness in promoting healing (Heublein et al., 2015; Marfia et al., 2015; Mulder et al., 2012). The bone marrow stem cells (healthy and dysfunctional) responded by upregulating the gene expression and protein secretion of macrophage chemo-attractants, MCP1 (Ccl2) and MIP1α (Ccl3). In chronic diabetic wounds, a significant delay in macrophage infiltration related to a deficiency in Ccl2 has been demonstrated (Wood et al., 2014). Wood et al., 2014 furthermore indicated that acute Ccl2 treatment could restore the macrophage response and promote healing. This is supported by Yin et al., 2016 indicating that the use of scaffolds that actively release MCP1 promoted macrophage infiltration and improved wound healing in a mouse model of streptozotocin-induced diabetes (Wood et al., 2014; Yin et al., 2016). MCP1 is also known to influence the effector state of macrophages (Low et al., 2001), to mediate the angiogenic effect of TGFβ by recruiting vascular smooth muscle cells to the endothelium (Ma et al., 2007) and to recruit/improve the migration of bone marrow MSCs (Ishikawa et al., 2014). In this study, preconditioning further enhanced the MCP1 response of all the bone marrow stem cells.

Dysfunctional bone marrow stem cells did however have an excessive TNFα response to DWF. TNFα is a potent pro-inflammatory cytokine that amplifies inflammation through NFκB signalling (Liu, 2005). Persistent TNFα signalling is known to occur in diabetic wounds (Landis et al., 2010) and prevents the phenotype switch of macrophages form phagocytic (M1) to pro-regenerative (M2). Ashcroft et al., 2012 demonstrated that targeting TNFα in a mouse model (secretory leukocyte protease inhibitor null mice) of severely impaired wound healing-blunted leukocyte recruitment, reduced NFκB signalling, altered the M1/M2 macrophage balance and improved healing (Ashcroft et al., 2012). In the current study, antioxidant preconditioning of dysfunctional bone marrow stem cells blunted the TNFα response and improved the secretion of anti-inflammatory IL10.

IL10 activates the JAK/STAT3 pathway, which leads to upregulation of genes such as *Bcl*3 and miR-155 that impairs NFκB's ability in the production of TNFα (Hutchins et al., 2013; Monastero and Pentyala, 2017). Hyperinsulinemia in T2DM activates Akt/mTOR (mammalian target of rapamycin) signalling in regulator T cells and suppress their ability to reduce TNFα production from macrophages by inhibiting IL10 production and the overproduced TNFα is one of the major reasons of chronic inflammation (Han et al., 2014). Similar to IL10, both IL4 and IL13 have a key role in macrophage survival by activating PI3K/Akt/GSK3 pathway. They could activate macrophages and contribute to the differentiation of M2 macrophages, which are highly responsive to IL10 *via* this pathway. However PI3K/Akt/GSK3 regulation on IL10 does not seem to be directly involved in mediating the anti-inflammatory effects of this cytokine, but more substantially modulates the JAK/STAT pathway (Antoniv and Ivashkiv, 2011; Opal and DePalo, 2000). Taking together our data suggests that the combined *ex vivo* treatment of autologous stem cells with NAC and AAP could be an effective strategy to restore the paracrine function of impaired bone marrow stem cells prior to transplantation.

This anti-inflammatory effect of preconditioning, is related to NAC's ability to suppress proteasome activity and inhibit NFκB activation, subsequently limiting the release of pro-inflammatory cytokines (Lasram et al., 2015). Intracellularly, NAC together with AAP also reduces ROS production and has been shown to partially restore the levels of antioxidant enzymes such as catalase, superoxide dismutase (SOD) 1 and 2, p-FOXO1 and p53 (Jeong and Cho, 2015). Besides its protective role of reducing the levels of intracellular ROS, ascorbic acid also promotes the synthesis of collagen, a crucial part of the ECM (Bae et al., 2015; Choi et al., 2008; Hata and Senoo, 1989). The ECM provides physical support within the microenvironment and is a source of external stimuli (chemical and structural) that subsequently determine the activation status and fate (proliferation/differentiation) of stem cells (Rojas-Ríos and González-Reyes, 2014). This is supported by studies demonstrating that ascorbic acid-induced ECM deposition enhances the proliferation and migration capacity of cells (Bae et al., 2015; Choi et al., 2008; D'Aniello et al., 2017; Hata and Senoo, 1989).

Unfortunately, the combination of increased ECM deposition and the presence of high concentrations of inflammatory mediators such as TNFα within DWF, induced the spontaneous osteogenic differentiation of impaired diabetic MSCs in the present study. This unwanted phenomenon (spontaneous differentiation) was only evident under high cell densities (confluency) of preconditioned MSC^{ob} and could potentially inhibit the desired paracrine response of these cells.

The mechanism is likely related to BMP2 secretion in higher density cultures (Denker et al., 1999; Iwasaki et al., 1994) and cell-matrix/ cell-cell interactions (Long, 2001; Xue et al., 2013). It is well known that pro-inflammatory cytokines (present in high levels in DWF) enhance osteogenesis in MSCs by promoting MMPs (matrix metalloproteinase) (Almalki and Agrawal, 2016; Ben David et al., 2008; Croes et al., 2015; Li et al., 2016a) *via* PI3K/Akt signalling (Baker et al., 2015; Guntur et al., 2012), whilst other pathways such as extracellular signal-regulated kinase (ERK), p38 and WNT (Wingless-related integration site) signalling all regulate osteoblastic differentiation in MSCs (Silva et al., 2015) and could potentially be activated by the protein content of DWF (Löffler et al., 2013). This

taking together with increased collagen biosynthesis *(refer to section 5.4, p.54)* in the presence of ascorbic acid treatment (Mekala et al., 2013; Wang et al., 2006) might be responsible for triggering the spontaneous osteogenic differentiation of MSCs. This does not explain why the phenomenon was only evident in MSC^{ob} and not in MSC^{WT}, it might be related to excessive of pro-inflammatory signalling in MSC^{ob} but was beyond the scope of this study to determine and therefore warrants further investigation.

Taking together, this study gave insight into the molecular and paracrine responses of healthy and impaired diabetic MSCs in response to a chronic wound environment. It highlighted the skewing of the paracrine response towards a pro-inflammatory phenotype in impaired diabetic MSCs; antioxidant preconditioning could restore this excessive response. This study furthermore demonstrated that antioxidants can improve MSC viability in culture and have slight protective effects against pathological wound fluid. It is suggested that the combined *ex vivo* treatment of autologous MSCs with NAC and AAP might be an effective strategy to restore the paracrine responses of impaired bone marrow MSCs prior to transplantation.

Chapter 7: Conclusion & Future perspectives

Skin wound healing, in patients with certain underlying pathologies, is still a major concern for global healthcare, because the standard wound management methods are mostly ineffective in these conditions and limited alternative therapeutics and/or skin substitutes are available (Cerqueira et al., 2016). Failure in wound closure (non-healing) or excessive scarring are the likely outcomes of ineffective therapeutic approaches and is an undeniable reality, which in the past few years has prompted the development of more sophisticated strategies to deal with the problem. These novel strategies include artificial ECM-like matrices, growth factors, MSCs, anti-inflammatory agents, MSC-derived conditioned medium (CM) and/or extracellular vesicles (microvesicles, exosomes). These novel approaches all have great potential but their implementation in the clinical setting is hampered by a limited understanding of how reparative-cellular mediators are affected by and respond to pathological microenvironments. This study was the first to investigate not only how endogenous MSCs are affected by the pathogenesis of T2DM but also how the responsiveness of these cells upon exposure to DWF was altered on both molecular and paracrine level. Insight into these dysregulated responses provided the basis for identifying and testing the efficacy of two antioxidants to counteract/restore MSC function prior to their therapeutic use.

Physiological wound healing is a complex integrative process that involves a network of reparative cellular mediators (immune cells, stem/progenitor cells, keratinocytes, fibroblasts, epithelial cells, etc.), the ECM, nervous system and vascular system all of which is coordinated through paracrine signalling. The ability of MSCs to regulate the immune system (anti-inflammatory properties) and promote growth/regeneration by stimulating other cellular mediators, makes them an attractive therapeutic option for chronic wounds (Baltzis et al., 2014; Heublein et al., 2015; Marfia et al., 2015; Mulder et al., 2012). Unfortunately, in T2DM, a poor bone microenvironment which constitutes the MSC niche impairs the regenerative properties of endogenous MSCs and negatively affects their use for autologous cell therapy (Chang et al., 2015; Li et al., 2007; Zhang et al., 2016a).

The mechanisms underlying MSC impairment and the limited knowledge of MSC responses to environmental cues, therefore requires further investigation in basic animal models by creating such a milieu *ex vivo*, before autologous MSC therapies can advance successfully to the clinical setting (Otero-Viñas and Falanga, 2016; Satija et al., 2009).

One of the initial limitations in the advancement of stem cell therapy was the limited ability to track stem cells *in vivo* following transplantation. In 2013, Robert C. Caskey and Kenneth W. Liechty *(wound regeneration and repair, Gourdie and Myers, 2013; Chapter 6)* discussed the idea that in research focused on delayed healing, the ability to track specific cell types would dramatically improve our understanding of the cellular derangements in pathological conditions such as T2DM. To date, a variety of different transgenic mouse models has been developed and has significantly advanced our understanding of cell biology in numerous conditions. For example, Hayakawa et al. (2003) utilized

bone marrow from GFP (green fluorescent protein) chimera mice and transplanted these fluorescent cells into wounded C57BL/6 mice and was able to track the fate of the transplanted cells *in vivo*. Many of these animal models have added considerable value to our understanding of stem cell homing, but they, unfortunately, do not replicate the underlying pathological phenotype observed in patients (Gourdie and Myers, 2013; Hayakawa et al., 2003).

There are currently only a few diabetic animal models available for the study of chronic wounds, each with its own advantages and disadvantages. It is still common to use streptozotocin to induce diabetes in mice to study delayed wound healing. For example, Yin et al., 2016 studied the efficacy of bioengineered drug-eluting scaffolds to accelerate cutaneous wound healing in streptozotocin-induced diabetic mice. It should however be noted that this model is representative of type 1 diabetes and healing deficiencies are not as severe as is the case in obesity associated T2DM. Chen et al. *(wound regeneration and repair, Gourdie and Myers, 2013; Chapter 15)* suggested that despite slight deviations from the clinical setting, the splinted excisional wound model on leptin receptor-deficient diabetic (*db/db*) mice is a feasible way to study non-healing diabetic wounds. In this method, wound margin contraction by the *panniculus carnosus* layer is however prominent in the animals whereas human healing occurs through granulation tissue formation and re-epithelialization (Chen et al., 2013; Gourdie and Myers, 2013; Yin et al., 2016). This is however a limitation of most animal models.

A comparison in wound healing between a wild-type mouse with high-fat diet-induced obesity/pre-diabetes and an obese genetically modified mice (*ob/ob*) by Seitz et al., 2016, demonstrated that the *ob/ob* mouse model has more pronounced injury-induced inflammatory and tissue responses and therefore suggested that this could be a reliable option to investigate basic mechanisms of diabetes related skin repair (Seitz et al., 2010). The wild-type control (C57BL/6J) murine strain, was chosen because it shares a genetic background with the obese pre-diabetic (B6.Cg-Lepob/J) strain and is the most widely used inbred strain (Fang et al., 2019) (https://www.jax.org/strain/000632). In addition to choosing an appropriate animal model which suffer from the underlying diabetic pathology, the most appropriate wounding procedure should also be considered.

Reid et al., 2004 investigated the different procedures for creating incisional and excisional wounds and examined six parameters of wound healing. The authors used standard surgical models (head punch, back punch, back incisional, ear epithelial wound, transverse rectus abdominal myocutaneous flap and tube flap model) in transgenic and knockout animals to identify differences in the molecular pathways of healing in each of these models. Reid et al., 2004 concluded that to analyse ECM proteins, the incisional wound and tube flap procedures are the best options, but when measuring cell adhesion molecules and intracellular signalling most of the surgical approaches (incisional or excisional) would yield good results. Wong et al., 2011 did however suggest that full-thickness excisional wound models are a proper way to assess numerous components of wound healing *in vivo* (Reid et al., 2004; Wong et al., 2011).

Taking all of this into account, for the purpose of this research project, full-thickness excisional wounds on obese prediabetic mice (B6 Cg-Lep^{ob}/J) *(ob/ob)* was identified as an appropriate model to

use for harvesting diabetic wound fluid. Given the *wound contraction* limitation of all animal models, the *ob/ob* wound model was further optimized in this study by injecting NEP at the wound edges to prevent contraction and delay healing to more closely mimic DFUs in patients. Although healing was not completely prevented by this approach, the collected wound fluid was representative of an excessive persistent inflammatory microenvironment. This enabled the design of an *ex vivo* complex similar to actual wound conditions to investigate MSC responses to the pathological microenvironment in an *in vitro* setting.

Previous studies done by our group indicated that molecular pathways related to IL6/STAT3 signalling were dysregulated in functionally impaired MSCs derived from obese prediabetic mice under baseline conditions. The data suggested that the immune-modulatory properties of impaired diabetic MSCs might be skewed towards a pro-inflammatory profile (van de Vyver et al., 2016). In a patient based study, our group furthermore showed that systemic factors during metabolic disease progression contribute to the functional decline of MSCs (Seboko et al., 2018). Based on these findings, it was thus suggested that MSCs with a skewed gene expression profile to favour a pro-inflammatory environment would be unable to perform the imperative function of restoring the localized (wounded area) or systemic conditions needed for normal healing (van de Vyver, 2017). These initial studies did however not assess the secretome at baseline or the responsiveness of healthy vs impaired MSCs upon stimulation with environmental cues. Although the benefits of antioxidants (NAC and AAP) has already been shown in acute cell culture models, this research project was the first to test the efficacy of these factors to counteract functional impairments in diabetic MSCs.

These specific antioxidants were chosen because of their combined growth-promoting, ROS scavenging and anti-inflammatory properties that have the capacity to counteract the various components involved in the pathogenesis of T2DM namely: hyperglycaemia-associated AGEs accumulation that subsequently induces excessive oxidative stress and amplifies inflammation (Ashcroft et al., 2012; Liu, 2005) *(refer to section 2.1.3.3 & 2.1.3.4, p.8)* and affects MSCs function *(refer to section 2.4, p.20)*.

In agreement with our hypothesis, the data showed that MSC dysfunction involved disrupted paracrine signalling that is skewed towards a pro-inflammatory and destructive instead of a pro-regenerative phenotype. This was evident in the excessive pro-inflammatory TNFα response of impaired diabetic MSCs upon stimulation with DWF. Preconditioning with antioxidants could however dampen this excessive response and promoted the release of anti-inflammatory factors such as IL10. Suggesting that *ex vivo* treatment of autologous stem cells with NAC and AAP could potentially be an effective strategy to restore the paracrine function of impaired diabetic MSCs before transplantation.

It should however be noted that the paracrine response of MSCs is as dynamic as the microenvironment they are exposed to and depends on the MSC population's tissue of origin, heterogeneity, age of the donor, cell isolation protocol and the culture conditions used for testing (Ferreira et al., 2018). The data presented in this thesis should thus be interpreted within this context, especially since the cell population tested was heterogenous bone marrow-derived stem cells.

Nonetheless, the data indicated that in addition to a restored paracrine response, antioxidant preconditioning had a protective effect against the toxicity of DWF and could therefore be used as a potential strategy to improve the viability of both allogeneic and autologous MSCs post-transplantation. However, despite these clear beneficial effects of antioxidant preconditioning, it could not restore the proliferation and migration capacity of severely impaired diabetic MSCs.

The growth deficiencies therefore seem to be persistent despite the removal of these cells to a more optimal environment and is consistent with the findings of other studies (Frykberg and Banks, 2015; Shin and Peterson, 2012; van de Vyver et al., 2016). This has significant implications for preparing a sufficient number of cells for therapeutic administration purposes as their ability to expand in culture is limited. A modified culture system or additional treatment is thus still needed to improve the proliferation rate of impaired diabetic MSCs (Badiavas et al., 2007). Based on the literature the following additional ex vivo treatment strategies could be considered in conjunction with antioxidant preconditioning since their growth-promoting effects has already been shown in various in vitro models: FGF2, IGF1, BMP2, TGFβ, VEGF, PDGF, melatonin (Ferreira et al., 2018; Hu and Li, 2018; Peng et al., 2013). Furthermore, for transplantation purposes into chronic wounds, delivery mediums such as synthetic biomaterials that resemble the natural ECM could be an additional strategy to overcome the adhesion, proliferation and migration impairments of diabetic MSCs (Dash et al., 2013; Votteler et al., 2010).

To date, the delivery mediums that have been researched include natural and synthetic scaffolds (hydrogels, autologous bio-grafts and Nano-fibre scaffolds) or scaffold free-technologies (organoids, microtissues, spheroids) (Birbrair, 2017). However, due to the dynamic nature of the healing process, it might not be possible to deliver multiple combined therapeutic approaches at the same time to a patient in a cost-effective manner. Although the use of a combination of products in different categories could proof effective, the challenges and limitations, especially in low resource settings, should be taken into consideration. Challenges that need to be addressed include the time period of engrafted MSCs survival and their functional maintenance, the optimal dose, frequency and routes of MSC administration in different types of injuries and during different stages of diseases (Dash et al., 2013; Otero-Viñas and Falanga, 2016).

Given the persistent nature of the growth impairments, an alternative strategy is needed to utilize the secretome (conditioned medium) of antioxidant preconditioned MSCs with a restored paracrine function for therapeutic application.

MSC-derived CM contains various growth factors and tissue regenerative agents which can be manufactured, freeze-dried, packaged, and transported relatively easily without the negative risk of immune rejection in patients (Pawitan, 2014). The MSC secretome furthermore contains numerous extracellular vesicle (EVs) and exosomes that can be purified for therapeutic purposes (Di Rocco et al., 2016; Nawaz et al., 2016). There are, however, still various challenges in their production and separation, a lack of standardized quality assurance assays and limited reproducibility of *in vitro* and *in vivo* functional assays which need to be addressed (Witwer et al., 2019).

With the development of our theoretical understanding of the MSC impairment in diabetic patients at the cellular and molecular levels, it becomes clear that a more inclusive approach is needed to address multiple needs in the clinical setting. It furthermore, highlights the importance of understanding the diabetic wound microenvironment and the direct impact it has on the functionality of MSC. For instance, an increasing number of studies show phenotypic shifts in MSCs under different microenvironment conditions (Marfia et al., 2015; Si et al., 2011; Turinetto et al., 2016; Wang et al., 2013b).

Caution should thus be taken to avoid the premature implementation of MSC therapies in the clinical setting, especially since MSCs possess a mutual interaction with tumour cells and poses the risk of ectopic differentiation (Marfia et al., 2015; Si et al., 2011), as was evident in our data with the unwanted spontaneous osteogenic differentiation under high cell densities. Moreover, long-term culture of MSCs together with accelerated senescence increases the risk of genomic mutations, which could expose patients to more side effects, however the changes may be without possible malignant transformation (Marfia et al., 2015; Wang et al., 2013b).

Future research should thus focus on the expansion of our understanding of MSC functionality in hostile environments. This is of particular importance, especially since the repair and regeneration of tissues using minimally manipulated autologous stem cells represent the ultimate goal in regenerative medicine.

Reference List

Abdali, D., Samson, S.E., and Grover, A.K. (2015). How Effective Are Antioxidant Supplements in Obesity and Diabetes? Med Princ Pract *24*, 201–215.

Abderrahmani, A., Yengo, L., Caiazzo, R., Canouil, M., Cauchi, S., Raverdy, V., Plaisance, V., Pawlowski, V., Lobbens, S., Maillet, J., et al. (2018). Increased Hepatic PDGF-AA Signaling Mediates Liver Insulin Resistance in Obesity-Associated Type 2 Diabetes. Diabetes *67*, 1310–1321.

Abdullah, A., Peeters, A., de Courten, M., and Stoelwinder, J. (2010). The magnitude of association between overweight and obesity and the risk of diabetes: A meta-analysis of prospective cohort studies. Diabetes Research and Clinical Practice *89*, 309–319.

van Acker, K., Léger, P., Hartemann, A., Chawla, A., and Siddiqui, M.K. (2014). Burden of diabetic foot disorders, guidelines for management and disparities in implementation in Europe: a systematic literature review. Diabetes Metab. Res. Rev. *30*, 635–645.

Ahmad, J. (2016). The diabetic foot. Diabetes Metab Syndr *10*, 48–60.

Albiero, M., Avogaro, A., and Fadini, G.P. (2013). Restoring stem cell mobilization to promote vascular repair in diabetes. Vascul. Pharmacol. *58*, 253–258.

Albiero, M., Poncina, N., Ciciliot, S., Cappellari, R., Menegazzo, L., Ferraro, F., Bolego, C., Cignarella, A., Avogaro, A., and Fadini, G.P. (2015). Bone Marrow Macrophages Contribute to Diabetic Stem Cell Mobilopathy by Producing Oncostatin M. Diabetes *64*, 2957–2968.

Ali, F., Khan, M., Khan, S.N., and Riazuddin, S. (2016). N-Acetyl cysteine protects diabetic mouse derived mesenchymal stem cells from hydrogen-peroxide-induced injury: A novel hypothesis for autologous stem cell transplantation. Journal of the Chinese Medical Association *79*, 122–129.

Almalki, S.G., and Agrawal, D.K. (2016). Effects of matrix metalloproteinases on the fate of mesenchymal stem cells. Stem Cell Res Ther *7*, 129.

Amann, B., Luedemann, C., Ratei, R., and Schmidt-Lucke, J.A. (2009). Autologous bone marrow cell transplantation increases leg perfusion and reduces amputations in patients with advanced critical limb ischemia due to peripheral artery disease. Cell Transplant *18*, 371–380.

American diabetes association (2010). Diagnosis and Classification of Diabetes Mellitus. Diabetes Care *33*, S62–S69.

André-Lévigne, D., Modarressi, A., Pepper, M.S., and Pittet-Cuénod, B. (2017). Reactive Oxygen Species and NOX Enzymes Are Emerging as Key Players in Cutaneous Wound Repair. Int J Mol Sci *18*.

Andrews, K.L., Houdek, M.T., and Kiemele, L.J. (2015). Wound management of chronic diabetic foot ulcers: From the basics to regenerative medicine. Prosthet Orthot Int *39*, 29–39.

Antezana, M., Sullivan, S.R., Usui, M., Gibran, N., Spenny, M., Larsen, J., Ansel, J., Bunnett, N., and Olerud, J. (2002). Neutral endopeptidase activity is increased in the skin of subjects with diabetic ulcers. J. Invest. Dermatol. *119*, 1400–1404.

Antoniv, T.T., and Ivashkiv, L.B. (2011). Interleukin-10-induced gene expression and suppressive function are selectively modulated by the PI3K-Akt-GSK3 pathway. Immunology *132*, 567–577.

Arakawa, E., Hasegawa, K., Yanai, N., Obinata, M., and Matsuda, Y. (2000). A mouse bone marrow stromal cell line, TBR-B, shows inducible expression of smooth muscle-specific genes. FEBS Letters *481*, 193–196.

Argôlo Neto, N.M., Del Carlo, R.J., Monteiro, B.S., Nardi, N.B., Chagastelles, P.C., de Brito, A.F.S., and Reis, A.M.S. (2012). Role of autologous mesenchymal stem cells associated with platelet-rich plasma on healing of cutaneous wounds in diabetic mice. Clin. Exp. Dermatol. *37*, 544–553.

Ashcroft, G.S., Jeong, M.-J., Ashworth, J.J., Hardman, M., Jin, W., Moutsopoulos, N., Wild, T., McCartney-Francis, N., Sim, D., McGrady, G., et al. (2012). TNFα is a therapeutic target for impaired cutaneous wound healing. Wound Repair Regen *20*, 38–49.

Babon, J.J., and Nicola, N.A. (2012). The biology and mechanism of action of suppressor of cytokine signaling 3. Growth Factors *30*, 207–219.

Badiavas, E.V., and Falanga, V. (2003). Treatment of chronic wounds with bone marrow-derived cells. Arch Dermatol *139*, 510–516.

Badiavas, E.V., Ford, D., Liu, P., Kouttab, N., Morgan, J., Richards, A., and Maizel, A. (2007). Long-term bone marrow culture and its clinical potential in chronic wound healing. Wound Repair Regen *15*, 856–865.

Bae, S.H., Ryu, H., Rhee, K.-J., Oh, J.-E., Baik, S.K., Shim, K.Y., Kong, J.H., Hyun, S.Y., Pack, H.S., Im, C., et al. (2015). L-ascorbic acid 2-phosphate and fibroblast growth factor-2 treatment maintains differentiation potential in bone marrow-derived mesenchymal stem cells through expression of hepatocyte growth factor. Growth Factors *33*, 71–78.

Baker, N., Sohn, J., and Tuan, R.S. (2015). Promotion of human mesenchymal stem cell osteogenesis by PI3-kinase/Akt signaling, and the influence of caveolin-1/cholesterol homeostasis. Stem Cell Res Ther *6*, 238.

Baltzis, D., Eleftheriadou, I., and Veves, A. (2014). Pathogenesis and Treatment of Impaired Wound Healing in Diabetes Mellitus: New Insights. Adv Ther *31*, 817–836.

Behm, B., Babilas, P., Landthaler, M., and Schreml, S. (2012). Cytokines, chemokines and growth factors in wound healing. J Eur Acad Dermatol Venereol *26*, 812–820.

Bellan, M., Guzzaloni, G., Rinaldi, M., Merlotti, E., Ferrari, C., Tagliaferri, A., Pirisi, M., Aimaretti, G., Scacchi, M., and Marzullo, P. (2014). Altered glucose metabolism rather than naive type 2 diabetes mellitus (T2DM) is related to vitamin D status in severe obesity. Cardiovasc Diabetol *13*, 57.

Ben David, D., Reznick, A.Z., Srouji, S., and Livne, E. (2008). Exposure to pro-inflammatory cytokines upregulates MMP-9 synthesis by mesenchymal stem cells-derived osteoprogenitors. Histochem Cell Biol *129*, 589–597.

Berniakovich, I., Laricchia-Robbio, L., and Izpisua Belmonte, J.C. (2012). N-acetylcysteine protects induced pluripotent stem cells from in vitro stress: impact on differentiation outcome. The International Journal of Developmental Biology *56*, 729–735.

Betancourt, A.M. (2013). New Cell-Based Therapy Paradigm: Induction of Bone Marrow-Derived Multipotent Mesenchymal Stromal Cells into Pro-Inflammatory MSC1 and Anti-inflammatory MSC2 Phenotypes. In Mesenchymal Stem Cells-Basics and Clinical Application II, B. Weyand, M. Dominici, R. Hass, R. Jacobs, and C. Kasper, eds. (Berlin, Heidelberg: Springer Berlin Heidelberg), pp. 163–197.

Bhowmik, B., Afsana, F., Ahmed, T., Akhter, S., Choudhury, H.A., Rahman, A., Ahmed, T., Mahtab, H., and Azad Khan, A.K. (2015). Obesity and associated type 2 diabetes and hypertension in factory workers of Bangladesh. BMC Res Notes *8*, 460.

Birbrair, A. (2017). The Bone Marrow Microenvironment for Hematopoietic Stem Cells. In Stem Cell Microenvironments and Beyond, A. Birbrair, ed. (Cham: Springer International Publishing), pp. 5–19.

Busschots, S., O'Toole, S., J. O'Leary, J., and Stordal, B. (2016). Non-invasive and non-destructive measurements of confluence in cultured adherent cell lines. MethodsX *2*, 8–13.

Cantinieaux, D., Quertainmont, R., Blacher, S., Rossi, L., Wanet, T., Noël, A., Brook, G., Schoenen, J., and Franzen, R. (2013). Conditioned Medium from Bone Marrow-Derived Mesenchymal Stem Cells Improves Recovery after Spinal Cord Injury in Rats: An Original Strategy to Avoid Cell Transplantation. PLoS One *8*, e69515.

Cao, Y., Gang, X., Sun, C., and Wang, G. (2017). Mesenchymal Stem Cells Improve Healing of Diabetic Foot Ulcer. J Diabetes Res *2017*, 9328347.

Cederberg, H., Stančáková, A., Kuusisto, J., Laakso, M., and Smith, U. (2015). Family history of type 2 diabetes increases the risk of both obesity and its complications: is type 2 diabetes a disease of inappropriate lipid storage? J. Intern. Med. *277*, 540–551.

Cerqueira, M.T., Pirraco, R.P., and Marques, A.P. (2016). Stem Cells in Skin Wound Healing: Are We There Yet? Adv Wound Care (New Rochelle) *5*, 164–175.

Chang, T.-C., Hsu, M.-F., and Wu, K.K. (2015). High Glucose Induces Bone Marrow-Derived Mesenchymal Stem Cell Senescence by Upregulating Autophagy. PLoS One *10*, e0126537.

Chen, F., Liu, Y., Wong, N.-K., Xiao, J., and So, K.-F. (2017). Oxidative Stress in Stem Cell Aging. Cell Transplant *26*, 1483–1495.

Chen, J.S., Longaker, M.T., and Gurtner, G.C. (2013). Murine models of human wound healing. Methods Mol. Biol. *1037*, 265–274.

Chen, L., Tredget, E.E., Wu, P.Y.G., and Wu, Y. (2008). Paracrine Factors of Mesenchymal Stem Cells Recruit Macrophages and Endothelial Lineage Cells and Enhance Wound Healing. PLoS One *3*, e1886.

Chen, L., Tredget, E.E., Liu, C., and Wu, Y. (2009). Analysis of Allogenicity of Mesenchymal Stem Cells in Engraftment and Wound Healing in Mice. PLoS One *4*, e7119.

Cheng, M., Huang, K., Zhou, J., Yan, D., Tang, Y.-L., Zhao, T.C., Miller, R.J., Kishore, R., Losordo, D.W., and Qin, G. (2015). A critical role of Src family kinase in SDF-1/CXCR4-mediated bone-marrow progenitor cell recruitment to the ischemic heart. J Mol Cell Cardiol *81*, 49–53.

Choi, K.-M., Seo, Y.-K., Yoon, H.-H., Song, K.-Y., Kwon, S.-Y., Lee, H.-S., and Park, J.-K. (2008). Effect of ascorbic acid on bone marrow-derived mesenchymal stem cell proliferation and differentiation. Journal of Bioscience and Bioengineering *105*, 586–594.

Coughlan, M.T., Thorburn, D.R., Penfold, S.A., Laskowski, A., Harcourt, B.E., Sourris, K.C., Tan, A.L.Y., Fukami, K., Thallas-Bonke, V., Nawroth, P.P., et al. (2009). RAGE-Induced Cytosolic ROS Promote Mitochondrial Superoxide Generation in Diabetes. JASN *20*, 742–752.

Croes, M., Oner, F.C., Kruyt, M.C., Blokhuis, T.J., Bastian, O., Dhert, W.J.A., and Alblas, J. (2015). Proinflammatory Mediators Enhance the Osteogenesis of Human Mesenchymal Stem Cells after Lineage Commitment. PLoS One *10*, e0132781.

Dahlén, E.M., Tengblad, A., Länne, T., Clinchy, B., Ernerudh, J., Nystrom, F.H., and Östgren, C.J. (2014). Abdominal obesity and low-grade systemic inflammation as markers of subclinical organ damage in type 2 diabetes. Diabetes Metab. *40*, 76–81.

Dang, Z., Maselli, D., Spinetti, G., Sangalli, E., Carnelli, F., Rosa, F., Seganfreddo, E., Canal, F., Furlan, A., Paccagnella, A., et al. (2015). Sensory neuropathy hampers nociception-mediated bone marrow stem cell release in mice and patients with diabetes. Diabetologia *58*, 2653–2662.

D'Aniello, C., Cermola, F., Patriarca, E.J., and Minchiotti, G. (2017). Vitamin C in Stem Cell Biology: Impact on Extracellular Matrix Homeostasis and Epigenetics. Stem Cells International *2017*, 1–16.

Dash, N.R., Dash, S.N., Routray, P., Mohapatra, S., and Mohapatra, P.C. (2009). Targeting nonhealing ulcers of lower extremity in human through autologous bone marrow-derived mesenchymal stem cells. Rejuvenation Res *12*, 359–366.

Dash, S.N., Dash, N.R., Guru, B., and Mohapatra, P.C. (2013). Towards Reaching the Target: Clinical Application of Mesenchymal Stem Cells for Diabetic Foot Ulcers. Rejuvenation Research *17*, 40–53.

Davey, G.C., Patil, S.B., Loughlin, A., and Brien, T. (2014). Mesenchymal Stem Cell-Based Treatment for Microvascular and Secondary Complications of Diabetes Mellitus. Frontiers in Endocrinology *5*, Article 86.

Debin, L., Youzhao, J., Ziwen, L., Xiaoyan, L., Zhonghui, Z., and Bing, C. (2008). Autologous transplantation of bone marrow mesenchymal stem cells on diabetic patients with lower limb ischemia⋆⋆Supported by the Clinical Research Fund of Southwest Hospital at Third Military Medical University (SWH2005A109). Journal of Medical Colleges of PLA *23*, 106–115.

DeFuria, J., Belkina, A.C., Jagannathan-Bogdan, M., Snyder-Cappione, J., Carr, J.D., Nersesova, Y.R., Markham, D., Strissel, K.J., Watkins, A.A., Zhu, M., et al. (2013). B cells promote inflammation in obesity and type 2 diabetes through regulation of T-cell function and an inflammatory cytokine profile. Proc Natl Acad Sci U S A *110*, 5133–5138.

Delgado, A.V., McManus, A.T., and Chambers, J.P. (2005). Exogenous Administration of Substance P Enhances Wound Healing in a Novel Skin-Injury Model. Exp Biol Med (Maywood) *230*, 271–280.

Denker, A.E., Haas, A.R., Nicoll, S.B., and Tuan, R.S. (1999). Chondrogenic differentiation of murine C3H10T1/2 multipotential mesenchymal cells: I. Stimulation by bone morphogenetic protein-2 in high-density micromass cultures. Differentiation *64*, 67–76.

Denu, R.A., and Hematti, P. (2016). Effects of Oxidative Stress on Mesenchymal Stem Cell Biology. Oxid Med Cell Longev *2016*, 2989076.

Di Rocco, G., Baldari, S., and Toietta, G. (2016). Towards Therapeutic Delivery of Extracellular Vesicles: Strategies for In Vivo Tracking and Biodistribution Analysis. Stem Cells Int *2016*, 5029619.

Dinh, T., Tecilazich, F., Kafanas, A., Doupis, J., Gnardellis, C., Leal, E., Tellechea, A., Pradhan, L., Lyons, T.E., Giurini, J.M., et al. (2012). Mechanisms Involved in the Development and Healing of Diabetic Foot Ulceration. Diabetes *61*, 2937–2947.

Dominici, M., Le Blanc, K., Mueller, I., Slaper-Cortenbach, I., Marini, F., Krause, D., Deans, R., Keating, A., Prockop, D., and Horwitz, E. (2006). Minimal criteria for defining multipotent mesenchymal stromal cells. The International Society for Cellular Therapy position statement. Cytotherapy *8*, 315–317.

Dreifke, M.B., Jayasuriya, A.A., and Jayasuriya, A.C. (2015). Current wound healing procedures and potential care. Mater Sci Eng C Mater Biol Appl *48*, 651–662.

Drowley, L., Okada, M., Beckman, S., Vella, J., Keller, B., Tobita, K., and Huard, J. (2010). Cellular Antioxidant Levels Influence Muscle Stem Cell Therapy. Mol Ther *18*, 1865–1873.

Dulmovits, B.M., and Herman, I.M. (2012). Microvascular Remodeling and Wound Healing: A Role for Pericytes. Int J Biochem Cell Biol *44*, 1800–1812.

Duran-Jimenez, B., Dobler, D., Moffatt, S., Rabbani, N., Streuli, C.H., Thornalley, P.J., Tomlinson, D.R., and Gardiner, N.J. (2009). Advanced Glycation End Products in Extracellular Matrix Proteins Contribute to the Failure of Sensory Nerve Regeneration in Diabetes. Diabetes *58*, 2893–2903.

Ennis, W.J., Sui, A., and Bartholomew, A. (2013). Stem Cells and Healing: Impact on Inflammation. Adv Wound Care (New Rochelle) *2*, 369–378.

Esser, N., Legrand-Poels, S., Piette, J., Scheen, A.J., and Paquot, N. (2014). Inflammation as a link between obesity, metabolic syndrome and type 2 diabetes. Diabetes Research and Clinical Practice *105*, 141–150.

Fadini, G.P., de Kreutzenberg, S.V., Boscaro, E., Albiero, M., Cappellari, R., Kränkel, N., Landmesser, U., Toniolo, A., Bolego, C., Cignarella, A., et al. (2013a). An unbalanced monocyte polarisation in peripheral blood and bone marrow of patients with type 2 diabetes has an impact on microangiopathy. Diabetologia *56*, 1856–1866.

Fadini, G.P., Albiero, M., Seeger, F., Poncina, N., Menegazzo, L., Angelini, A., Castellani, C., Thiene, G., Agostini, C., Cappellari, R., et al. (2013b). Stem cell compartmentalization in diabetes and high cardiovascular risk reveals the role of DPP-4 in diabetic stem cell mobilopathy. Basic Res. Cardiol. *108*, 313.

Fadini, G.P., Albiero, M., Vigili de Kreutzenberg, S., Boscaro, E., Cappellari, R., Marescotti, M., Poncina, N., Agostini, C., and Avogaro, A. (2013c). Diabetes Impairs Stem Cell and Proangiogenic Cell Mobilization in Humans. Diabetes Care *36*, 943–949.

Fadini, G.P., Ciciliot, S., and Albiero, M. (2017). Concise Review: Perspectives and Clinical Implications of Bone Marrow and Circulating Stem Cell Defects in Diabetes. Stem Cells *35*, 106–116.

Fakhruddin, S., Alanazi, W., and Jackson, K.E. (2017). Diabetes-Induced Reactive Oxygen Species: Mechanism of Their Generation and Role in Renal Injury. J Diabetes Res *2017*, 8379327.

Falanga, V., Iwamoto, S., Chartier, M., Yufit, T., Butmarc, J., Kouttab, N., Shrayer, D., and Carson, P. (2007). Autologous Bone Marrow–Derived Cultured Mesenchymal Stem Cells Delivered in a Fibrin Spray Accelerate Healing in Murine and Human Cutaneous Wounds. Tissue Engineering *13*, 1299–1312.

Fan, G., Wen, L., Li, M., Li, C., Luo, B., Wang, F., Zhou, L., and Liu, L. (2011). Isolation of mouse mesenchymal stem cells with normal ploidy from bone marrows by reducing oxidative stress in combination with extracellular matrix. BMC Cell Biol *12*, 30.

Fang, J.-Y., Lin, C.-H., Huang, T.-H., and Chuang, S.-Y. (2019). In Vivo Rodent Models of Type 2 Diabetes and Their Usefulness for Evaluating Flavonoid Bioactivity. Nutrients *11*, 530.

Farrell, E., O'Brien, F.J., Doyle, P., Fischer, J., Yannas, I., Harley, B.A., O'Connell, B., Prendergast, P.J., and Campbell, V.A. (2006). A collagen-glycosaminoglycan scaffold supports adult rat mesenchymal stem cell differentiation along osteogenic and chondrogenic routes. Tissue Eng. *12*, 459–468.

Feoktistova, M., Geserick, P., and Leverkus, M. (2016). Crystal Violet Assay for Determining Viability of Cultured Cells. Cold Spring Harb Protoc *2016*, pdb.prot087379.

Ferreira, J.R., Teixeira, G.Q., Santos, S.G., Barbosa, M.A., Almeida-Porada, G., and Gonçalves, R.M. (2018). Mesenchymal Stromal Cell Secretome: Influencing Therapeutic Potential by Cellular Pre-conditioning. Front. Immunol. *9*.

Finegood, D.T. (2003). Obesity, inflammation and type II diabetes. International Journal of Obesity *27*, S4–S5.

Firneisz, G. (2014). Non-alcoholic fatty liver disease and type 2 diabetes mellitus: The liver disease of our age? World J Gastroenterol *20*, 9072–9089.

Fivenson, D.P., Faria, D.T., Nickoloff, B.J., Poverini, P.J., Kunkel, S., Burdick, M., and Strieter, R.M. (1997). Chemokine and inflammatory cytokine changes during chronic wound healing. Wound Repair Regen *5*, 310–322.

Frykberg, R.G., and Banks, J. (2015). Challenges in the Treatment of Chronic Wounds. Advances in Wound Care *4*, 560–582.

Gallagher, K.A., Joshi, A., Carson, W.F., Schaller, M., Allen, R., Mukerjee, S., Kittan, N., Feldman, E.L., Henke, P.K., Hogaboam, C., et al. (2015). Epigenetic Changes in Bone Marrow Progenitor Cells Influence the Inflammatory Phenotype and Alter Wound Healing in Type 2 Diabetes. Diabetes *64*, 1420–1430.

Gillis, J., Gebremeskel, S., Phipps, K.D., MacNeil, L.A., Sinal, C.J., Johnston, B., Hong, P., and Bezuhly, M. (2015). Effect of N-Acetylcysteine on Adipose-Derived Stem Cell and Autologous Fat Graft Survival in a Mouse Model. Plast. Reconstr. Surg. *136*, 179e–188e.

Glenn, J.D., and Whartenby, K.A. (2014). Mesenchymal stem cells: Emerging mechanisms of immunomodulation and therapy. World J Stem Cells *6*, 526–539.

Goetsch, K.P., and Niesler, C.U. (2011). Optimization of the scratch assay for in vitro skeletal muscle wound healing analysis. Anal. Biochem. *411*, 158–160.

Golay, A., and Ybarra, J. (2005). Link between obesity and type 2 diabetes. Best Practice & Research Clinical Endocrinology & Metabolism *19*, 649–663.

Goren, I., Kämpfer, H., Podda, M., Pfeilschifter, J., and Frank, S. (2003). Leptin and wound inflammation in diabetic ob/ob mice: differential regulation of neutrophil and macrophage influx and a potential role for the scab as a sink for inflammatory cells and mediators. Diabetes *52*, 2821–2832.

Gourdie, R.G., and Myers, T.A. (2013). Murine Models of Human Wound Healing. In Wound Regeneration and Repair: Methods and Protocols, (Humana Press), pp. 265–276.

van Greevenbroek, M.M.J., Schalkwijk, C.G., and Stehouwer, C.D.A. (2013). Obesity-associated low-grade inflammation in type 2 diabetes mellitus: causes and consequences. Neth J Med *71*, 174–187.

Gulati, S., and Misra, A. (2017). Abdominal obesity and type 2 diabetes in Asian Indians: dietary strategies including edible oils, cooking practices and sugar intake. European Journal of Clinical Nutrition *71*, 850–857.

Guntur, A.R., Rosen, C.J., and Naski, M.C. (2012). N-cadherin adherens junctions mediate osteogenesis through PI3K signaling. Bone *50*, 54–62.

Guo, Y., Lin, C., Xu, P., Wu, S., Fu, X., Xia, W., and Yao, M. (2016). AGEs Induced Autophagy Impairs Cutaneous Wound Healing via Stimulating Macrophage Polarization to M1 in Diabetes. Sci Rep *6*, 36416.

Han, J.M., Patterson, S.J., Speck, M., Ehses, J.A., and Levings, M.K. (2014). Insulin Inhibits IL-10–Mediated Regulatory T Cell Function: Implications for Obesity. The Journal of Immunology *192*, 623–629.

Hardwicke, J.T., Hart, J., Bell, A., Duncan, R., Thomas, D.W., and Moseley, R. (2011). The effect of dextrin-rhEGF on the healing of full-thickness, excisional wounds in the (db/db) diabetic mouse. J Control Release *152*, 411–417.

Hata, R., and Senoo, H. (1989). L-ascorbic acid 2-phosphate stimulates collagen accumulation, cell proliferation, and formation of a three-dimensional tissuelike substance by skin fibroblasts. J. Cell. Physiol. *138*, 8–16.

Haw, J.S., Galaviz, K.I., Straus, A.N., Kowalski, A.J., Magee, M.J., Weber, M.B., Wei, J., Narayan, K.M.V., and Ali, M.K. (2017). Long-term Sustainability of Diabetes Prevention Approaches: A Systematic Review and Meta-analysis of Randomized Clinical Trials. JAMA Intern Med *177*, 1808–1817.

Hayakawa, J., Migita, M., Ueda, T., Shimada, T., and Fukunaga, Y. (2003). Generation of a Chimeric Mouse Reconstituted with Green Fluorescent Protein-Positive Bone Marrow Cells: A Useful Model for Studying the Behavior of Bone Marrow Cells in Regeneration In Vivo | SpringerLink. Int J Hematol. *77*, 456–462.

Herder, C., and Roden, M. (2011). Genetics of type 2 diabetes: pathophysiologic and clinical relevance. European Journal of Clinical Investigation *41*, 679–692.

Heublein, H., Bader, A., and Giri, S. (2015). Preclinical and clinical evidence for stem cell therapies as treatment for diabetic wounds. Drug Discovery Today *20*, 703–717.

Hocking, A.M., and Gibran, N.S. (2010). Mesenchymal stem cells: Paracrine signaling and differentiation during cutaneous wound repair. Experimental Cell Research *316*, 2213–2219.

Honczarenko, M., Le, Y., Swierkowski, M., Ghiran, I., Glodek, A.M., and Silberstein, L.E. (2006). Human bone marrow stromal cells express a distinct set of biologically functional chemokine receptors. Stem Cells *24*, 1030–1041.

Horwitz, E.M., Andreef, M., and Frassoni, F. (2006). Mesenchymal Stromal Cells. Curr Opin Hematol *13*, 419–425.

Hou, C., Shen, L., Huang, Q., Mi, J., Wu, Y., Yang, M., Zeng, W., Li, L., Chen, W., and Zhu, C. (2013). The effect of heme oxygenase-1 complexed with collagen on MSC performance in the treatment of diabetic ischemic ulcer. Biomaterials *34*, 112–120.

Hu, C., and Li, L. (2018). Preconditioning influences mesenchymal stem cell properties in vitro and in vivo. J Cell Mol Med *22*, 1428–1442.

Huang, S., Xu, L., Sun, Y., Wu, T., Wang, K., and Li, G. (2015a). An improved protocol for isolation and culture of mesenchymal stem cells from mouse bone marrow. Journal of Orthopaedic Translation *3*, 26–33.

Huang, T., Qi, Q., Zheng, Y., Ley, S.H., Manson, J.E., Hu, F.B., and Qi, L. (2015b). Genetic Predisposition to Central Obesity and Risk of Type 2 Diabetes: Two Independent Cohort Studies. Diabetes Care *38*, 1306–1311.

Hurrle, S., and Hsu, W.H. (2017). The etiology of oxidative stress in insulin resistance. Biomed J *40*, 257–262.

Hutchins, A.P., Diez, D., and Miranda-Saavedra, D. (2013). The IL-10/STAT3-mediated anti-inflammatory response: recent developments and future challenges. Brief Funct Genomics *12*, 489–498.

IDF, 8th edition (2017). Diabetes Atlas-Facts & figures.

Isakson, M., de Blacam, C., Whelan, D., McArdle, A., and Clover, A.J.P. (2015). Mesenchymal Stem Cells and Cutaneous Wound Healing: Current Evidence and Future Potential. Stem Cells Int *2015*, 831095.

Ishikawa, M., Ito, H., Kitaori, T., Murata, K., Shibuya, H., Furu, M., Yoshitomi, H., Fujii, T., Yamamoto, K., and Matsuda, S. (2014). MCP/CCR2 Signaling Is Essential for Recruitment of Mesenchymal Progenitor Cells during the Early Phase of Fracture Healing. PLoS One *9*.

Iwasaki, M., Nakahara, H., Nakase, T., Kimura, T., Takaoka, K., Caplan, A.I., and Ono, K. (1994). Bone morphogenetic protein 2 stimulates osteogenesis but does not affect chondrogenesis in osteochondrogenic differentiation of periosteum-derived cells. Journal of Bone and Mineral Research *9*, 1195–1204.

J. O'Gorman, D., and Krook, A. (2011). Exercise and the Treatment of Diabetes and Obesity - ClinicalKey. Med Clin N Am *95*, 953–969.

Jain, P., Perakath, B., Jesudason, M.R., and Nayak, S. (2011). The effect of autologous bone marrow-derived cells on healing chronic lower extremity wounds: results of a randomized controlled study. Ostomy Wound Manage *57*, 38–44.

Januszyk, M., Sorkin, M., Glotzbach, J.P., Vial, I.N., Maan, Z.N., Rennert, R.C., Duscher, D., Thangarajah, H., Longaker, M.T., Butte, A.J., et al. (2014). Diabetes Irreversibly Depletes Bone Marrow–Derived Mesenchymal Progenitor Cell Subpopulations. Diabetes *63*, 3047–3056.

Järbrink, K., Ni, G., Sönnergren, H., Schmidtchen, A., Pang, C., Bajpai, R., and Car, J. (2016). Prevalence and incidence of chronic wounds and related complications: a protocol for a systematic review. Syst Rev *5*, 152.

Javazon, E.H., Keswani, S.G., Badillo, A.T., Crombleholme, T.M., Zoltick, P.W., Radu, A.P., Kozin, E.D., Beggs, K., Malik, A.A., and Flake, A.W. (2007). Enhanced epithelial gap closure and increased angiogenesis in wounds of diabetic mice treated with adult murine bone marrow stromal progenitor cells. Wound Repair and Regeneration *15*, 350–359.

Jeong, S.-G., and Cho, G.-W. (2015). Endogenous ROS levels are increased in replicative senescence in human bone marrow mesenchymal stromal cells. Biochem. Biophys. Res. Commun. *460*, 971–976.

Jhamb, S., Vangaveti, V.N., and Malabu, U.H. (2016). Genetic and molecular basis of diabetic foot ulcers: Clinical review. Journal of Tissue Viability *25*, 229–236.

Jiang, J., and Papoutsakis, E.T. (2013). Stem-Cell Niche Based Comparative Analysis of Chemical and Nano-mechanical Material Properties Impacting Ex Vivo Expansion and Differentiation of Hematopoietic and Mesenchymal Stem Cells. Advanced Healthcare Materials *2*, 25–42.

Joost, H.-G., and Schürmann, A. (2014). The genetic basis of obesity-associated type 2 diabetes (diabesity) in polygenic mouse models. Mamm Genome *25*, 401–412.

Kahn, S.E., Cooper, M.E., and Del Prato, S. (2014). Pathophysiology and treatment of Type 2 diabetes: Perspectives on the past, present and future. Lancet *383*, 1068–1083.

Kaneto, H., Katakami, N., Matsuhisa, M., and Matsuoka, T. (2010). Role of Reactive Oxygen Species in the Progression of Type 2 Diabetes and Atherosclerosis. Mediators Inflamm *2010*, 453892.

Karaderi, T., Drong, A.W., and Lindgren, C.M. (2015). Insights into the Genetic Susceptibility to Type 2 Diabetes from Genome-Wide Association Studies of Obesity-Related Traits. Curr Diab Rep *15*, 83.

Karimabad, M.N., and Hassanshahi, G. (2015). Significance of CXCL12 in type 2 diabetes mellitus and its associated complications. Inflammation *38*, 710–717.

Katagi, M., Terashima, T., Okano, J., Urabe, H., Nakae, Y., Ogawa, N., Udagawa, J., Maegawa, H., Matsumura, K., Chan, L., et al. (2014). Hyperglycemia induces abnormal gene expression in hematopoietic stem cells and their progeny in diabetic neuropathy. FEBS Lett *588*, 1080–1086.

Kato, J., Kamiya, H., Himeno, T., Shibata, T., Kondo, M., Okawa, T., Fujiya, A., Fukami, A., Uenishi, E., Seino, Y., et al. (2014). Mesenchymal stem cells ameliorate impaired wound healing through enhancing keratinocyte functions in diabetic foot ulcerations on the plantar skin of rats. Journal of Diabetes and Its Complications *28*, 588–595.

Kato, Y., Iwata, T., Washio, K., Yoshida, T., Kuroda, H., Morikawa, S., Hamada, M., Ikura, K., Kaibuchi, N., Yamato, M., et al. (2017). Creation and Transplantation of an Adipose-derived Stem Cell (ASC) Sheet in a Diabetic Wound-healing Model. J Vis Exp *126*, e54539.

Katsumoto, K., and Kume, S. (2013). The Role of CXCL12-CXCR4 Signaling Pathway in Pancreatic Development. Theranostics *3*, 11–17.

Kim, S.S., Song, C.K., Shon, S.K., Lee, K.Y., Kim, C.H., Lee, M.J., and Wang, L. (2009). Effects of human amniotic membrane grafts combined with marrow mesenchymal stem cells on healing of full-thickness skin defects in rabbits. Cell Tissue Res. *336*, 59–66.

Kim, Y., Keogh, J.B., and Clifton, P.M. (2017). Effects of Two Different Dietary Patterns on Inflammatory Markers, Advanced Glycation End Products and Lipids in Subjects without Type 2 Diabetes: A Randomised Crossover Study. Nutrients *9*, 336.

Kirana, S., Stratmann, B., Prante, C., Prohaska, W., Koerperich, H., Lammers, D., Gastens, M.H., Quast, T., Negrean, M., Stirban, O.A., et al. (2012). Autologous stem cell therapy in the treatment of limb ischaemia induced chronic tissue ulcers of diabetic foot patients. Int. J. Clin. Pract. *66*, 384–393.

Kitaori, T., Ito, H., Schwarz, E.M., Tsutsumi, R., Yoshitomi, H., Oishi, S., Nakano, M., Fujii, N., Nagasawa, T., and Nakamura, T. (2009). Stromal cell–derived factor 1/CXCR4 signaling is critical for the recruitment of mesenchymal stem cells to the fracture site during skeletal repair in a mouse model. Arthritis & Rheumatism *60*, 813–823.

Klimczak, A., and Kozlowska, U. (2016). Mesenchymal Stromal Cells and Tissue-Specific Progenitor Cells: Their Role in Tissue Homeostasis. Stem Cells Int *2016*, 4285215.

Ko, K.I., Coimbra, L.S., Tian, C., Alblowi, J., Kayal, R.A., Einhorn, T.A., Gerstenfeld, L.C., Pignolo, R.J., and Graves, D.T. (2015). Diabetes reduces mesenchymal stem cells in fracture healing through a TNFα-mediated mechanism. Diabetologia *58*, 633–642.

Koenen, P., Spanholtz, T.A., Maegele, M., Stürmer, E., Brockamp, T., Neugebauer, E., and Thamm, O.C. (2015). Acute and chronic wound fluids inversely influence adipose-derived stem cell function: molecular insights into impaired wound healing. International Wound Journal *12*, 10–16.

Kume, S., Kato, S., Yamagishi, S., Inagaki, Y., Ueda, S., Arima, N., Okawa, T., Kojiro, M., and Nagata, K. (2005). Advanced glycation end-products attenuate human mesenchymal stem cells and prevent cognate differentiation into adipose tissue, cartilage, and bone. J. Bone Miner. Res. *20*, 1647–1658.

Kusuma, G.D., Carthew, J., Lim, R., and Frith, J.E. (2017). Effect of the Microenvironment on Mesenchymal Stem Cell Paracrine Signaling: Opportunities to Engineer the Therapeutic Effect. Stem Cells Dev. *26*, 617–631.

Kwon, D.S., Gao, X., Liu, Y.B., Dulchavsky, D.S., Danyluk, A.L., Bansal, M., Chopp, M., McIntosh, K., Arbab, A.S., Dulchavsky, S.A., et al. (2008). Treatment with bone marrow-derived stromal cells accelerates wound healing in diabetic rats. International Wound Journal *5*, 453–463.

Landis, R.C., Evans, B.J., Chaturvedi, N., and Haskard, D.O. (2010). Persistence of TNFα in diabetic wounds. Diabetologia *53*, 1537–1538.

Lasram, M.M., Dhouib, I.B., Annabi, A., El Fazaa, S., and Gharbi, N. (2015). A review on the possible molecular mechanism of action of N-acetylcysteine against insulin resistance and type-2 diabetes development. Clin. Biochem. *48*, 1200–1208.

Laurent Maranda, E., Rodriguez-Menocal, L., and V. Badiavas, E. (2016). Role of Mesenchymal Stem Cells in Dermal Repair in Burns and Diabetic Wounds. Current Stem Cell Research & Therapy *12*, 61–70.

Le Blanc, K., and Davies, L.C. (2015). Mesenchymal stromal cells and the innate immune response. Immunol. Lett. *168*, 140–146.

Leal, E.C., Carvalho, E., Tellechea, A., Kafanas, A., Tecilazich, F., Kearney, C., Kuchibhotla, S., Auster, M.E., Kokkotou, E., Mooney, D.J., et al. (2015). Substance P Promotes Wound Healing in Diabetes by Modulating Inflammation and Macrophage Phenotype. The American Journal of Pathology *185*, 1638–1648.

Leary, S., Underwood, W., Anthony, R., Cartner, S., Golab, G.C., and Patterson-Kane, E. (2013). AVMA Guidelines for the Euthanasia of Animals: 2013 Edition (1931 N. Meacham Road Schaumburg, IL 60173: American Veterinary Medical Association).

Lee, J. (2013). Adipose tissue macrophages in the Development of Obesity-induced Inflammation, Insulin Resistance and Type 2 Diabetes. Arch Pharm Res *36*, 208–222.

Lee, I.-M., Shiroma, E.J., Lobelo, F., Puska, P., Blair, S.N., and Katzmarzyk, P.T. (2012). Impact of Physical Inactivity on the World's Major Non-Communicable Diseases. Lancet *380*, 219–229.

Lewellis, S.W., and Knaut, H. (2012). Attractive Guidance: How the chemokine SDF1/CXCL12 guides different cells to different locations. Semin Cell Dev Biol *23*, 333–340.

Li, C., Li, G., Liu, M., Zhou, T., and Zhou, H. (2016a). Paracrine effect of inflammatory cytokine-activated bone marrow mesenchymal stem cells and its role in osteoblast function. Journal of Bioscience and Bioengineering *121*, 213–219.

Li, C.-J., Sun, L.-Y., and Pang, C.-Y. (2015). Synergistic Protection of N-Acetylcysteine and Ascorbic Acid 2-Phosphate on Human Mesenchymal Stem cells Against Mitoptosis, Necroptosis and Apoptosis. Scientific Reports *5*, 9819.

Li, H., Fu, X., Ouyang, Y., Cai, C., Wang, J., and Sun, T. (2006). Adult bone-marrow-derived mesenchymal stem cells contribute to wound healing of skin appendages. Cell Tissue Res. *326*, 725–736.

Li, Y., Zhang, W., Chang, L., Han, Y., Sun, L., Gong, X., Tang, H., Liu, Z., Deng, H., Ye, Y., et al. (2016b). Vitamin C alleviates aging defects in a stem cell model for Werner syndrome. Protein Cell *7*, 478–488.

Li, Y.-M., Schilling, T., Benisch, P., Zeck, S., Meissner-Weigl, J., Schneider, D., Limbert, C., Seufert, J., Kassem, M., Schütze, N., et al. (2007). Effects of high glucose on mesenchymal stem cell proliferation and differentiation. Biochem. Biophys. Res. Commun. *363*, 209–215.

Lin, H.-Y., Weng, S.-W., Chang, Y.-H., Su, Y.-J., Chang, C.-M., Tsai, C.-J., Shen, F.-C., Chuang, J.-H., Lin, T.-K., Liou, C.-W., et al. (2018a). The Causal Role of Mitochondrial Dynamics in Regulating Insulin Resistance in Diabetes: Link through Mitochondrial Reactive Oxygen Species. Oxid Med Cell Longev *2018*, 7514383.

Lin, J.-D., Hsu, C.-H., Wu, C.-Z., Hsieh, A.-T., Hsieh, C.-H., Liang, Y.-J., Chen, Y.-L., Pei, D., and Chang, J.-B. (2018b). Effect of body mass index on diabetogenesis factors at a fixed fasting plasma glucose level. PLoS One *13*, e0189115.

Lin, T.-M., Tsai, J.-L., Lin, S.-D., Lai, C.-S., and Chang, C.-C. (2005). Accelerated growth and prolonged lifespan of adipose tissue-derived human mesenchymal stem cells in a medium using reduced calcium and antioxidants. Stem Cells Dev. *14*, 92–102.

Ling, L., Gu, S., Cheng, Y., and Ding, L. (2018). bFGF promotes Sca-1+ cardiac stem cell migration through activation of the PI3K/Akt pathway. Mol Med Rep *17*, 2349–2356.

Litwinoff, E., del Pozo, C.H., Ramasamy, R., and Schmidt, A. (2015). Emerging Targets for Therapeutic Development in Diabetes and Its Complications: The RAGE Signaling Pathway. Clin Pharmacol Ther *98*, 135–144.

Liu, Z.G. (2005). Molecular mechanism of TNF signaling and beyond. Cell Res. *15*, 24–27.

Löffler, M., Schmohl, M., Schneiderhan-Marra, N., and Beckert, S. (2011). Wound Fluid Diagnostics in Diabetic Foot Ulcers. pp. 47–70.

Löffler, M.W., Schuster, H., Bühler, S., and Beckert, S. (2013). Wound fluid in diabetic foot ulceration: more than just an undefined soup? Int J Low Extrem Wounds *12*, 113–129.

Long, M.W. (2001). Osteogenesis and Bone-Marrow-Derived Cells. Blood Cells, Molecules, and Diseases *27*, 677–690.

Low, Q.E.H., Drugea, I.A., Duffner, L.A., Quinn, D.G., Cook, D.N., Rollins, B.J., Kovacs, E.J., and DiPietro, L.A. (2001). Wound Healing in MIP-1α−/− and MCP-1−/− Mice. Am J Pathol *159*, 457–463.

Lu, D., Chen, B., Liang, Z., Deng, W., Jiang, Y., Li, S., Xu, J., Wu, Q., Zhang, Z., Xie, B., et al. (2011). Comparison of bone marrow mesenchymal stem cells with bone marrow-derived mononuclear cells for treatment of diabetic critical limb ischemia and foot ulcer: a double-blind, randomized, controlled trial. Diabetes Res. Clin. Pract. *92*, 26–36.

Lu, Y.-Q., Lu, Y., Li, H.-J., and Cheng, X.-B. (2012). Effect of advanced glycosylation end products (AGEs) on proliferation of human bone marrow mesenchymal stem cells (MSCs) in vitro. In Vitro Cell. Dev. Biol. Anim. *48*, 599–602.

Lucas, D. (2017). The Bone Marrow Microenvironment for Hematopoietic Stem Cells. Adv. Exp. Med. Biol. *1041*, 5–18.

Luft, V.C., Schmidt, M.I., Pankow, J.S., Couper, D., Ballantyne, C.M., Young, J.H., and Duncan, B.B. (2013). Chronic inflammation role in the obesity-diabetes association: a case-cohort study. Diabetol Metab Syndr *5*, 31.

M. Nathan, D. (2009). International Expert Committee Report on the Role of the A1C Assay in the Diagnosis of Diabetes. Diabetes Care *32*, 1327–1334.

Ma, J., Wang, Q., Fei, T., Han, J.-D.J., and Chen, Y.-G. (2007). MCP-1 mediates TGF-beta-induced angiogenesis by stimulating vascular smooth muscle cell migration. Blood *109*, 987–994.

Mancuso, P., Raman, S., Glynn, A., Barry, F., and Murphy, J.M. (2019). Mesenchymal Stem Cell Therapy for Osteoarthritis: The Critical Role of the Cell Secretome. Front. Bioeng. Biotechnol. *7*, 9.

Mangialardi, G., and Madeddu, P. (2016). Bone Marrow-Derived Stem Cells: a Mixed Blessing in the Multifaceted World of Diabetic Complications. Curr Diab Rep *16*, 43.

Mangialardi, G., Spinetti, G., Reni, C., and Madeddu, P. (2014). Reactive Oxygen Species Adversely Impacts Bone Marrow Microenvironment in Diabetes. Antioxid Redox Signal *21*, 1620–1633.

Marfia, G., Navone, S.E., Di Vito, C., Ughi, N., Tabano, S., Miozzo, M., Tremolada, C., Bolla, G., Crotti, C., Ingegnoli, F., et al. (2015). Mesenchymal stem cells: potential for therapy and treatment of chronic non-healing skin wounds. Organogenesis *11*, 183–206.

Markakis, K., Bowling, F.L., and Boulton, A.J.M. (2016). The diabetic foot in 2015: an overview. Diabetes/Metabolism Research and Reviews *32*, 169–178.

Martin, P., and Nunan, R. (2015). Cellular and molecular mechanisms of repair in acute and chronic wound healing. Br J Dermatol *173*, 370–378.

Martínez, J.A., Milagro, F.I., Claycombe, K.J., and Schalinske, K.L. (2014). Epigenetics in Adipose Tissue, Obesity, Weight Loss, and Diabetes12. Adv Nutr *5*, 71–81.

de Mayo, T., Conget, P., Becerra-Bayona, S., Sossa, C.L., Galvis, V., and Arango-Rodríguez, M.L. (2017). The role of bone marrow mesenchymal stromal cell derivatives in skin wound healing in diabetic mice. PLoS One *12*, e0177533.

McFarlin, K., Gao, X., Liu, Y.B., Dulchavsky, D.S., Kwon, D., Arbab, A.S., Bansal, M., Li, Y., Chopp, M., Dulchavsky, S.A., et al. (2006). Bone marrow-derived mesenchymal stromal cells accelerate wound healing in the rat. Wound Repair Regen *14*, 471–478.

Mehrbani Azar, Y., Green, R., Niesler, C.U., and van de Vyver, M. (2018). Antioxidant Preconditioning Improves the Paracrine Responsiveness of Mouse Bone Marrow Mesenchymal Stem Cells to Diabetic Wound Fluid. Stem Cells and Development *27*, 1646–1657.

Mekala, N.K., Baadhe, R.R., Rao Parcha, S., and Prameela Devi, Y. (2013). Enhanced proliferation and osteogenic differentiation of human umbilical cord blood stem cells by L-ascorbic acid, in vitro. Curr Stem Cell Res Ther *8*, 156–162.

Metallo, C.M., Mohr, J.C., Detzel, C.J., Pablo, J.J. de, Wie, B.J.V., and Palecek, S.P. (2007). Engineering the Stem Cell Microenvironment. Biotechnology Progress *23*, 18–23.

Mohammadzadeh, L., Samedanifard, S.H., Keshavarzi, A., Alimoghaddam, K., Larijani, B., Ghavamzadeh, A., Ahmadi, A.S., Shojaeifard, A., Ostadali, M.R., Sharifi, A.M., et al. (2013). Therapeutic outcomes of transplanting autologous granulocyte colony-stimulating factor-mobilised peripheral mononuclear cells in diabetic patients with critical limb ischaemia. Exp. Clin. Endocrinol. Diabetes *121*, 48–53.

Moissoglu, K., Majumdar, R., and Parent, C.A. (2014). Cell Migration: Sinking in a Gradient. Current Biology *24*, R23–R25.

Monastero, R.N., and Pentyala, S. (2017). Cytokines as Biomarkers and Their Respective Clinical Cutoff Levels. Int. J. of Inflammation *2017*, 4309485.

Moore, K.A., and Lemischka, I.R. (2006). Stem Cells and Their Niches. Science *311*, 1880–1885.

Mulder, G.D., Lee, D.K., and Jeppesen, N.S. (2012). Comprehensive review of the clinical application of autologous mesenchymal stem cells in the treatment of chronic wounds and diabetic bone healing. Int Wound J *9*, 595–600.

Murphy, M.B., Moncivais, K., and Caplan, A.I. (2013). Mesenchymal stem cells: environmentally responsive therapeutics for regenerative medicine. Exp Mol Med *45*, e54.

Mutsaers, S.E., Bishop, J.E., McGrouther, G., and Laurent, G.J. (1997). Mechanisms of tissue repair: from wound healing to fibrosis. Int. J. Biochem. Cell Biol. *29*, 5–17.

Narita, Y., Yamawaki, A., Kagami, H., Ueda, M., and Ueda, Y. (2008). Effects of transforming growth factor-beta 1 and ascorbic acid on differentiation of human bone-marrow-derived mesenchymal stem cells into smooth muscle cell lineage. Cell Tissue Res *333*, 449–459.

Nawaz, M., Fatima, F., Vallabhaneni, K.C., Penfornis, P., Valadi, H., Ekström, K., Kholia, S., Whitt, J.D., Fernandes, J.D., Pochampally, R., et al. (2016). Extracellular Vesicles: Evolving Factors in Stem Cell Biology. Stem Cells Int *2016*, 1073140.

Noor, S., Zubair, M., and Ahmad, J. (2015). Diabetic foot ulcer—A review on pathophysiology, classification and microbial etiology. Diabetes & Metabolic Syndrome: Clinical Research & Reviews *9*, 192–199.

Nowotny, K., Jung, T., Höhn, A., Weber, D., and Grune, T. (2015). Advanced Glycation End Products and Oxidative Stress in Type 2 Diabetes Mellitus. Biomolecules *5*, 194–222.

Okura, T., Ueta, E., Nakamura, R., Fujioka, Y., Sumi, K., Matsumoto, K., Shoji, K., Matsuzawa, K., Izawa, S., Nomi, Y., et al. (2017). High Serum Advanced Glycation End Products Are Associated with Decreased Insulin Secretion in Patients with Type 2 Diabetes: A Brief Report. J Diabetes Res *2017*, 5139750.

Opal, S.M., and DePalo, V.A. (2000). Anti-inflammatory cytokines. Chest *117*, 1162–1172.

Otero-Viñas, M., and Falanga, V. (2016). Mesenchymal Stem Cells in Chronic Wounds: The Spectrum from Basic to Advanced Therapy. Adv Wound Care (New Rochelle) *5*, 149–163.

Ozdemir, D., and Feinberg, M.W. (2019). MicroRNAs in diabetic wound healing: Pathophysiology and therapeutic opportunities. Trends in Cardiovascular Medicine *29*, 131–137.

Padilla, J., Vieira-Potter, V.J., Jia, G., and Sowers, J.R. (2015). Role of Perivascular Adipose Tissue on Vascular Reactive Oxygen Species in Type 2 Diabetes: A Give-and-Take Relationship. Diabetes *64*, 1904–1906.

Paul, J. (2018). Role of Inflammation in Obesity and Diabetes. Journal of Obesity and Metabolism *1*, 1–3.

Pawitan, J.A. (2014). Prospect of Stem Cell Conditioned Medium in Regenerative Medicine. Biomed Res Int *2014*, 965849.

Peng, Y., Huang, S., Wu, Y., Cheng, B., Nie, X., Liu, H., Ma, K., Zhou, J., Gao, D., Feng, C., et al. (2013). Platelet Rich Plasma Clot Releasate Preconditioning Induced PI3K/AKT/NFκB Signaling Enhances Survival and Regenerative Function of Rat Bone Marrow Mesenchymal Stem Cells in Hostile Microenvironments. Stem Cells Dev *22*, 3236–3251.

Pérez, L.M., de Lucas, B., and Gálvez, B.G. (2018). Unhealthy Stem Cells: When Health Conditions Upset Stem Cell Properties. Cell. Physiol. Biochem. *46*, 1999–2016.

Phinney, D.G., and Pittenger, M.F. (2017). MSC-Derived Exosomes for Cell-Free Therapy. Stem Cells *35*, 851–858.

Pieme, C.A., Tatangmo, J.A., Simo, G., Biapa Nya, P.C., Ama Moor, V.J., Moukette Moukette, B., Tankeu Nzufo, F., Njinkio Nono, B.L., and Sobngwi, E. (2017). Relationship between hyperglycemia, antioxidant capacity and some enzymatic and non-enzymatic antioxidants in African patients with type 2 diabetes. BMC Res Notes *10*.

Pinney, D.F., and Emerson, C.P. (1989). 10T1/2 cells: an in vitro model for molecular genetic analysis of mesodermal determination and differentiation. Environ. Health Perspect. *80*, 221–227.

Polonsky, K.S., and Burant, C.F. (2016). Type 2 Diabetes Mellitus. In Williams Textbook of Endocrinology, (Philadelphia, PA: Elsevier), pp. 1385–1450.

Potdar, P.D., and D'souza, S.B. (2010). Ascorbic acid induces proliferation of human subcutaneous adipose tissue derived mesenchymal stem cells with upregulation of embryonic stem cell pluripotency markers Oct4 and SOX 2. Hum Cell *23*, 152–155.

Prewitz, M.C., Seib, F.P., von Bonin, M., Friedrichs, J., Stißel, A., Niehage, C., Müller, K., Anastassiadis, K., Waskow, C., Hoflack, B., et al. (2013). Tightly anchored tissue-mimetic matrices as instructive stem cell microenvironments. Nat. Methods *10*, 788–794.

Procházka, V., Gumulec, J., Jalůvka, F., Šalounová, D., Jonszta, T., Czerný, D., Krajča, J., Urbanec, R., Klement, P., Martinek, J., et al. (2010). Cell Therapy, a New Standard in Management of Chronic Critical Limb Ischemia and Foot Ulcer. Cell Transplant *19*, 1413–1424.

Qi, M., Zhou, Q., Zeng, W., Wu, L., Zhao, S., Chen, W., Luo, C., Shen, M., Zhang, J., and Tang, C.-E. (2018). Growth factors in the pathogenesis of diabetic foot ulcers. Front Biosci (Landmark Ed) *23*, 310–317.

Qian, H., Le Blanc, K., and Sigvardsson, M. (2012). Primary Mesenchymal Stem and Progenitor Cells from Bone Marrow Lack Expression of CD44 Protein. J Biol Chem *287*, 25795–25807.

Qing, C. (2017). The molecular biology in wound healing & non-healing wound. Chinese Journal of Traumatology *20*, 189–193.

Ra'em, T., and Cohen, S. (2012). Microenvironment design for stem cell fate determination. Adv. Biochem. Eng. Biotechnol. *126*, 227–262.

Raghavan, S., Pachucki, M.C., Chang, Y., Porneala, B., Fox, C.S., Dupuis, J., and Meigs, J.B. (2016). Incident Type 2 Diabetes Risk is Influenced by Obesity and Diabetes in Social Contacts: a Social Network Analysis. J Gen Intern Med *31*, 1127–1133.

Rajkovic, N., Zamaklar, M., Lalic, K., Jotic, A., Lukic, L., Milicic, T., Singh, S., Stosic, L., and Lalic, N.M. (2014). Relationship between Obesity, Adipocytokines and Inflammatory Markers in Type 2 Diabetes: Relevance for Cardiovascular Risk Prevention. Int J Environ Res Public Health *11*, 4049–4065.

Ravari, H., Hamidi-Almadari, D., Salimifar, M., Bonakdaran, S., Parizadeh, M.R., and Koliakos, G. (2011). Treatment of non-healing wounds with autologous bone marrow cells, platelets, fibrin glue and collagen matrix. Cytotherapy *13*, 705–711.

Rehmann, M.S., Luna, J.I., Maverakis, E., and Kloxin, A.M. (2016). Tuning microenvironment modulus and biochemical composition promotes human mesenchymal stem cell tenogenic differentiation. J Biomed Mater Res A *104*, 1162–1174.

Reid, R.R., Said, H.K., Mogford, J.E., and Mustoe, T.A. (2004). The future of wound healing: pursuing surgical models in transgenic and knockout mice. J. Am. Coll. Surg. *199*, 578–585.

Restaino, R.M., Deo, S.H., Parrish, A.R., Fadel, P.J., and Padilla, J. (2017). Increased monocyte derived reactive oxygen species in type 2 diabetes: Role of endoplasmic reticulum stress. Exp Physiol *102*, 139–153.

Rezabakhsh, A., Cheraghi, O., Nourazarian, A., Hassanpour, M., Kazemi, M., Ghaderi, S., Faraji, E., Rahbarghazi, R., Avci, Ç.B., Bagca, B.G., et al. (2017). Type 2 Diabetes Inhibited Human Mesenchymal Stem Cells Angiogenic Response by Over-Activity of the Autophagic Pathway. J. Cell. Biochem. *118*, 1518–1530.

Ribot, J., Caliaperoumal, G., Paquet, J., Boisson-vidal, C., Petite, H., and Anagnostou, F. (2017). Type 2 diabetes alters mesenchymal stem cell secretome composition and angiogenic properties. J Cell Mol Med *21*, 349–363.

Ridiandries, A., Tan, J.T.M., and Bursill, C.A. (2018). The Role of Chemokines in Wound Healing. Int J Mol Sci *19*, 3217.

Ridzuan, N., John, C.M., Sandrasaigaran, P., Maqbool, M., Liew, L.C., Lim, J., and Ramasamy, R. (2016). Preliminary study on overproduction of reactive oxygen species by neutrophils in diabetes mellitus. World J Diabetes *7*, 271–278.

Ring, B.D., Scully, S., Davis, C.R., Baker, M.B., Cullen, M.J., Pelleymounter, M.A., and Danilenko, D.M. (2000). Systemically and topically administered leptin both accelerate wound healing in diabetic ob/ob mice. Endocrinology *141*, 446–449.

Risérus, U., Willett, W.C., and Hu, F.B. (2009). Dietary fats and prevention of type 2 diabetes. Prog Lipid Res *48*, 44–51.

Rodrigues, K.F., Pietrani, N.T., Sandrim, V.C., Vieira, C.M.A.F., Fernandes, A.P., Bosco, A.A., and Gomes, K.B. (2015). Association of a Large Panel of Cytokine Gene Polymorphisms with Complications and Comorbidities in Type 2 Diabetes Patients. J Diabetes Res *2015*, 605965.

Rodríguez-Rodero, S., Menéndez-Torre, E., Fernández-Bayón, G., Morales-Sánchez, P., Sanz, L., Turienzo, E., González, J.J., Martinez-Faedo, C., Suarez-Gutiérrez, L., Ares, J., et al. (2017). Altered intragenic DNA methylation of HOOK2 gene in adipose tissue from individuals with obesity and type 2 diabetes. PLoS One *12*, e0189153.

Rojas-Ríos, P., and González-Reyes, A. (2014). Concise Review: The Plasticity of Stem Cell Niches: A General Property Behind Tissue Homeostasis and Repair. STEM CELLS *32*, 852–859.

Saisho, Y. (2014). Glycemic Variability and Oxidative Stress: A Link between Diabetes and Cardiovascular Disease? Int J Mol Sci *15*, 18381–18406.

Saki, N., Jalalifar, M.A., Soleimani, M., Hajizamani, S., and Rahim, F. (2013). Adverse Effect of High Glucose Concentration on Stem Cell Therapy. Int J Hematol Oncol Stem Cell Res *7*, 34–40.

Sasaki, M., Abe, R., Fujita, Y., Ando, S., Inokuma, D., and Shimizu, H. (2008). Mesenchymal stem cells are recruited into wounded skin and contribute to wound repair by transdifferentiation into multiple skin cell type. J. Immunol. *180*, 2581–2587.

Sassoli, C., Zecchi-Orlandini, S., and Formigli, L. (2012). Trophic Actions of Bone Marrow-Derived Mesenchymal Stromal Cells for Muscle Repair/Regeneration. Cells *1*, 832–850.

Satija, N.K., Singh, V.K., Verma, Y.K., Gupta, P., Sharma, S., Afrin, F., Sharma, M., Sharma, P., Tripathi, R.P., and Gurudutta, G.U. (2009). Mesenchymal stem cell-based therapy: a new paradigm in regenerative medicine. J. Cell. Mol. Med. *13*, 4385–4402.

Schellenberg, E.S., Dryden, D.M., Vandermeer, B., Ha, C., and Korownyk, C. (2013). Lifestyle interventions for patients with and at risk for type 2 diabetes: a systematic review and meta-analysis. Ann. Intern. Med. *159*, 543–551.

Scherzed, A., Hackenberg, S., Froelich, K., Radeloff, A., Technau, A., Kessler, M., Hagen, R., Rak, K., Koehler, C., and Kleinsasser, N. (2011). The effect of wound fluid on adipose-derived stem cells in vitro: a study in human cell materials. Tissue Eng Part C Methods *17*, 809–817.

Schiffer, T.A., and Friederich-Persson, M. (2017). Mitochondrial Reactive Oxygen Species and Kidney Hypoxia in the Development of Diabetic Nephropathy. Front Physiol *8*, 211.

Schmohl, M., Beckert, S., Joos, T.O., Königsrainer, A., Schneiderhan-Marra, N., and Löffler, M.W. (2012). Superficial wound swabbing: a novel method of sampling and processing wound fluid for subsequent immunoassay analysis in diabetic foot ulcerations. Diabetes Care *35*, 2113–2120.

Schultz, G.S., Davidson, J.M., Kirsner, R.S., Bornstein, P., and Herman, I.M. (2011). Dynamic Reciprocity in the Wound Microenvironment. Wound Repair Regen *19*, 134–148.

Schürmann, C., Goren, I., Linke, A., Pfeilschifter, J., and Frank, S. (2014). Deregulated unfolded protein response in chronic wounds of diabetic ob/ob mice: a potential connection to inflammatory and angiogenic disorders in diabetes-impaired wound healing. Biochem. Biophys. Res. Commun. *446*, 195–200.

Schuster, D.P. (2010). Obesity and the development of type 2 diabetes: the effects of fatty tissue inflammation. Diabetes Metab Syndr Obes *3*, 253–262.

Scott, R.A., Fall, T., Pasko, D., Barker, A., Sharp, S.J., Arriola, L., Balkau, B., Barricarte, A., Barroso, I., Boeing, H., et al. (2014). Common genetic variants highlight the role of insulin resistance and body fat distribution in type 2 diabetes, independently of obesity. Diabetes *63*, 4378–4387.

Seboko, A.M., Conradie, M.M., Kruger, M.J., Ferris, W.F., Conradie, M., and van de Vyver, M. (2018). Systemic Factors During Metabolic Disease Progression Contribute to the Functional Decline of Adipose Tissue-Derived Mesenchymal Stem Cells in Reproductive Aged Females. Front. Physiol. *9*, 1812.

Seida, J.C., Mitri, J., Colmers, I.N., Majumdar, S.R., Davidson, M.B., Edwards, A.L., Hanley, D.A., Pittas, A.G., Tjosvold, L., and Johnson, J.A. (2014). Effect of Vitamin D3 Supplementation on Improving Glucose Homeostasis and Preventing Diabetes: A Systematic Review and Meta-Analysis. J Clin Endocrinol Metab *99*, 3551–3560.

Seitz, O., Schürmann, C., Hermes, N., Müller, E., Pfeilschifter, J., Frank, S., and Goren, I. (2010). Wound Healing in Mice with High-Fat Diet- or ob Gene-Induced Diabetes-Obesity Syndromes: A Comparative Study. Exp Diabetes Res *2010*, 476969.

Sen, C.K., Gordillo, G.M., Roy, S., Kirsner, R., Lambert, L., Hunt, T.K., Gottrup, F., Gurtner, G.C., and Longaker, M.T. (2009). Human Skin Wounds: A Major and Snowballing Threat to Public Health and the Economy. Wound Repair Regen *17*, 763–771.

Shin, L., and Peterson, D.A. (2012). Impaired Therapeutic Capacity of Autologous Stem Cells in a Model of Type 2 Diabetes. STEM CELLS Translational Medicine *1*, 125–135.

Si, Y.-L., Zhao, Y.-L., Hao, H.-J., Fu, X.-B., and Han, W.-D. (2011). MSCs: Biological characteristics, clinical applications and their outstanding concerns. Ageing Research Reviews *10*, 93–103.

Silva, J.C., Sampaio, P., Fernandes, M.H., and Gomes, P.S. (2015). The Osteogenic Priming of Mesenchymal Stem Cells is Impaired in Experimental Diabetes. Journal of Cellular Biochemistry *116*, 1658–1667.

da Silva Meirelles, L., Fontes, A.M., Covas, D.T., and Caplan, A.I. (2009). Mechanisms involved in the therapeutic properties of mesenchymal stem cells. Cytokine & Growth Factor Reviews *20*, 419–427.

Sindhu, S., Akhter, N., Kochumon, S., Thomas, R., Wilson, A., Shenouda, S., Tuomilehto, J., and Ahmad, R. (2018). Increased Expression of the Innate Immune Receptor TLR10 in Obesity and Type-2 Diabetes: Association with ROS-Mediated Oxidative Stress. Cell. Physiol. Biochem. *45*, 572–590.

Singh, S.R. (2012). Stem cell niche in tissue homeostasis, aging and cancer. Curr. Med. Chem. *19*, 5965–5974.

Singh, P.P., Mahadi, F., Roy, A., and Sharma, P. (2009). Reactive oxygen species, reactive nitrogen species and antioxidants in etiopathogenesis of diabetes mellitus type-2. Indian J Clin Biochem *24*, 324–342.

Singh, V.P., Bali, A., Singh, N., and Jaggi, A.S. (2014). Advanced Glycation End Products and Diabetic Complications. Korean J Physiol Pharmacol *18*, 1–14.

Slagter, S.N., van Vliet-Ostaptchouk, J.V., van Beek, A.P., Keers, J.C., Lutgers, H.L., van der Klauw, M.M., and Wolffenbuttel, B.H.R. (2015). Health-Related Quality of Life in Relation to Obesity Grade, Type 2 Diabetes, Metabolic Syndrome and Inflammation. PLoS One *10*, e0140599.

Śliwka, L., Wiktorska, K., Suchocki, P., Milczarek, M., Mielczarek, S., Lubelska, K., Cierpiał, T., Łyżwa, P., Kiełbasiński, P., Jaromin, A., et al. (2016). The Comparison of MTT and CVS Assays for the Assessment of Anticancer Agent Interactions. PLOS ONE *11*, e0155772.

Soghra Bahmanpour, P. (2016). Effects of Platelet-Rich Plasma & Platelet-Rich Fibrin with and without Stromal Cell-Derived Factor-1 on Repairing Full-Thickness Cartilage Defects in Knees of Rabbits. Iranian Journal of Medical Sciences *41*, 507.

Song, L., Nicolas, L., and Ngan, H. (2017). Mesenchymal stem cells for tissue regeneration. In Engineering Stem Cells for Tissue Regeneration, (World Scientific), pp. 1–27.

Sorg, H., Tilkorn, D.J., Hager, S., Hauser, J., and Mirastschijski, U. (2017). Skin Wound Healing: An Update on the Current Knowledge and Concepts. Eur Surg Res *58*, 81–94.

Spenny, M.L., Muangman, P., Sullivan, S.R., Bunnett, N.W., Ansel, J.C., Olerud, J.E., and Gibran, N.S. (2002). Neutral endopeptidase inhibition in diabetic wound repair. Wound Repair and Regeneration *10*, 295–301.

Spinetti, G., Cordella, D., Fortunato, O., Sangalli, E., Losa, S., Gotti, A., Carnelli, F., Rosa, F., Riboldi, S., Sessa, F., et al. (2013). Global Remodeling of the Vascular Stem Cell Niche in Bone Marrow of Diabetic Patients. Circ Res *112*, 510–522.

Staiano, A.E., Harrington, D.M., Johannsen, N.M., Newton, R.L., Sarzynski, M.A., Swift, D.L., and Katzmarzyk, P.T. (2015). Uncovering Physiological Mechanisms for Health Disparities in Type 2 Diabetes. Ethn Dis *25*, 31–37.

Stallmeyer, B., Pfeilschifter, J., and Frank, S. (2001). Systemically and topically supplemented leptin fails to reconstitute a normal angiogenic response during skin repair in diabetic ob/ob mice. Diabetologia *44*, 471–479.

Stephen, J., Bravo, E.L., Colligan, D., Fraser, A.R., Petrik, J., and Campbell, J.D.M. (2016). Mesenchymal stromal cells as multifunctional cellular therapeutics - a potential role for extracellular vesicles. Transfus. Apher. Sci. *55*, 62–69.

Stern, M.M., Myers, R.L., Hammam, N., Stern, K.A., Eberli, D., Kritchevsky, S.B., Soker, S., and Van Dyke, M. (2009). The influence of extracellular matrix derived from skeletal muscle tissue on the proliferation and differentiation of myogenic progenitor cells ex vivo. Biomaterials *30*, 2393–2399.

Stoff, A., Rivera, A.A., Banerjee, N.S., Moore, S.T., Numnum, T.M., Espinosa-de-los-Monteros, A., Richter, D.F., Siegal, G.P., Chow, L.T., Feldman, D., et al. (2009). Promotion of Incisional Wound Repair By Human Mesenchymal Stem Cell Transplantation. Exp Dermatol *18*, 362–369.

Strissel, K.J., Denis, G.V., and Nikolajczyk, B.S. (2014). Immune Regulators of Inflammation in Obesity-Associated Type 2 Diabetes and Coronary Artery Disease. Curr Opin Endocrinol Diabetes Obes *21*, 330–338.

Sun, L.-Y., Pang, C.-Y., Li, D.-K., Liao, C.-H., Huang, W.-C., Wu, C.-C., Chou, Y.-Y., Li, W.W., Chen, S.-Y., Liu, H.-W., et al. (2013). Antioxidants cause rapid expansion of human adipose-derived mesenchymal stem cells via CDK and CDK inhibitor regulation. Journal of Biomedical Science *20*, 53.

Tfayli, H., and Arslanian, S. (2009). Pathophysiology of type 2 diabetes mellitus in youth: the evolving chameleon. Arq Bras Endocrinol Metabol *53*, 165–174.

Thamm, O.C., Theodorou, P., Stuermer, E., Zinser, M.J., Neugebauer, E.A., Fuchs, P.C., and Koenen, P. (2015). Adipose-derived stem cells and keratinocytes in a chronic wound cell culture model: the role of hydroxyectoine. International Wound Journal *12*, 387–396.

Tomić, M., Ljubić, S., Kaštelan, S., Gverović Antunica, A., Jazbec, A., and Poljičanin, T. (2013). Inflammation, Haemostatic Disturbance, and Obesity: Possible Link to Pathogenesis of Diabetic Retinopathy in Type 2 Diabetes. Mediators Inflamm *2013*, 818671.

Touma, C., and Pannain, S. (2011). Does lack of sleep cause diabetes? Cleve Clin J Med *78*, 549–558.

Townsend, C.M., Beauchamp, R.D., Evers, B.M., and Mattox, K.L. (2016). Regenerative Medicine. In Sabiston Textbook of Surgery E-Book, (Elsevier Health Sciences), pp. 163–172.

Trengove, N.J., Langton, S.R., and Stacey, M.C. (1996). Biochemical analysis of wound fluid from nonhealing and healing chronic leg ulcers. WR and Regen *4*, 234–239.

Trengove, N.J., Bielefeldt-Ohmann, H., and Stacey, M.C. (2000). Mitogenic activity and cytokine levels in non-healing and healing chronic leg ulcers. Wound Repair and Regeneration *8*, 13–25.

Turinetto, V., Vitale, E., and Giachino, C. (2016). Senescence in Human Mesenchymal Stem Cells: Functional Changes and Implications in Stem Cell-Based Therapy. Int J Mol Sci *17*, 1164.

Turner, A.J., Isaac, R.E., and Coates, D. (2001). The neprilysin (NEP) family of zinc metalloendopeptidases: genomics and function. Bioessays *23*, 261–269.

Ulus, A.T., Pınarli, F.A., Sonmez, D., Yesilyurt, A., and Delibasi, T. (2014). The Contralateral Extremity has Also Benefit from the Locally Administered Bone Marrow-Derived Mononuclear Cells and Cord Blood Serum in Diabetic Ischemic Wound Healing. Stem Cell Rev and Rep *10*, 97–102.

Uribarri, J., Cai, W., Ramdas, M., Goodman, S., Pyzik, R., Chen, X., Zhu, L., Striker, G.E., and Vlassara, H. (2011). Restriction of Advanced Glycation End Products Improves Insulin Resistance in Human Type 2 Diabetes. Diabetes Care *34*, 1610–1616.

Van Pham, P., Tran, N.Y., Phan, N.L.-C., Vu, N.B., and Phan, N.K. (2016). Vitamin C stimulates human gingival stem cell proliferation and expression of pluripotent markers. In Vitro Cell.Dev.Biol.-Animal *52*, 218–227.

Venkiteswaran, G., Lewellis, S.W., Wang, J., Reynolds, E., Nicholson, C., and Knaut, H. (2013). Generation and dynamics of an endogenous, self-generated signaling gradient across a migrating tissue. Cell *155*, 09046.

Vlassara, H., and Uribarri, J. (2014). Advanced Glycation End Products (AGE) and Diabetes: Cause, Effect, or Both? Curr Diab Rep *14*, 453.

Volmer-Thole, M., and Lobmann, R. (2016). Neuropathy and Diabetic Foot Syndrome. Int J Mol Sci *17*, 917.

Volpe, C.M.O., Villar-Delfino, P.H., dos Anjos, P.M.F., and Nogueira-Machado, J.A. (2018). Cellular death, reactive oxygen species (ROS) and diabetic complications. Cell Death Dis *9*, 119.

Votteler, M., Kluger, P.J., Walles, H., and Schenke-Layland, K. (2010). Stem Cell Microenvironments - Unveiling the Secret of How Stem Cell Fate is Defined. Macromolecular Bioscience *10*, 1302–1315.

van de Vyver, M. (2017). Intrinsic Mesenchymal Stem Cell Dysfunction in Diabetes Mellitus: Implications for Autologous Cell Therapy. Stem Cells Dev. *26*, 1042–1053.

van de Vyver, M., Niesler, C., Myburgh, K.H., and Ferris, W.F. (2016). Delayed wound healing and dysregulation of IL6/STAT3 signalling in MSCs derived from pre-diabetic obese mice. Mol. Cell. Endocrinol. *426*, 1–10.

Walker, C.G., Solis-Trapala, I., Holzapfel, C., Ambrosini, G.L., Fuller, N.R., Loos, R.J.F., Hauner, H., Caterson, I.D., and Jebb, S.A. (2015). Modelling the Interplay between Lifestyle Factors and Genetic Predisposition on Markers of Type 2 Diabetes Mellitus Risk. PLoS One *10*, e0131681.

Wan, X.-C., Liu, C.-P., Li, M., Hong, D., Li, D.-M., Chen, H.-X., and Li, J.-C. (2008). Staphylococcal enterotoxin C injection in combination with ascorbic acid promotes the differentiation of bone marrow-derived mesenchymal stem cells into osteoblasts in vitro. Biochemical and Biophysical Research Communications *373*, 488–492.

Wang, J., and Knaut, H. (2014). Chemokine signaling in development and disease. Development *141*, 4199–4205.

Wang, Q., Zhu, H., Zhou, W.-G., Guo, X.-C., Wu, M.-J., Xu, Z.-Y., Jiang, J., Shen, C., and Liu, H.-Q. (2013a). N-acetylcysteine-pretreated human embryonic mesenchymal stem cell administration protects against bleomycin-induced lung injury. Am. J. Med. Sci. *346*, 113–122.

Wang, Y., Singh, A., Xu, P., Pindrus, M.A., Blasioli, D.J., and Kaplan, D.L. (2006). Expansion and osteogenic differentiation of bone marrow-derived mesenchymal stem cells on a vitamin C functionalized polymer. Biomaterials *27*, 3265–3273.

Wang, Y., Zhang, Z., Chi, Y., Zhang, Q., Xu, F., Yang, Z., Meng, L., Yang, S., Yan, S., Mao, A., et al. (2013b). Long-term cultured mesenchymal stem cells frequently develop genomic mutations but do not undergo malignant transformation. Cell Death & Disease *4*, e950.

Waterman, R.S., Tomchuck, S.L., Henkle, S.L., and Betancourt, A.M. (2010). A New Mesenchymal Stem Cell (MSC) Paradigm: Polarization into a Pro-Inflammatory MSC1 or an Immunosuppressive MSC2 Phenotype. PLoS One *5*, e10088.

Wei, F.L., Qu, C.Y., Song, T.L., Ding, G., Fan, Z.P., Liu, D.Y., Liu, Y., Zhang, C.M., Shi, S., and Wang, S.L. (2012). Vitamin C Treatment Promotes Mesenchymal Stem Cell Sheet Formation and Tissue Regeneration by Elevating Telomerase Activity. J Cell Physiol *227*, 3216–3224.

Weinberg, E., Maymon, T., and Weinreb, M. (2014). AGEs induce caspase-mediated apoptosis of rat BMSCs via TNFα production and oxidative stress. J Mol Endocrinol *52*, 67–76.

Witwer, K., Van Balkom, B., Bruno, S., Choo, A., Dominici, M., Gimona, M., F. Hill, A., De Kleijn, D., Koh, M., Lai, R.C., et al. (2019). Defining mesenchymal stromal cell (MSC)-derived small extracellular vesicles for therapeutic applications. Journal of Extracellular Vesicles *8*, 1609206.

Wong, V.W., Sorkin, M., Glotzbach, J.P., Longaker, M.T., and Gurtner, G.C. (2011). Surgical Approaches to Create Murine Models of Human Wound Healing. Journal of Biomedicine and Biotechnology *2011*, 969618.

Wood, S., Jayaraman, V., Huelsmann, E.J., Bonish, B., Burgad, D., Sivaramakrishnan, G., Qin, S., DiPietro, L.A., Zloza, A., Zhang, C., et al. (2014). Pro-Inflammatory Chemokine CCL2 (MCP-1) Promotes Healing in Diabetic Wounds by Restoring the Macrophage Response. PLoS One *9*, e91574.

World Health Organization (1999). Definition, diagnosis and classification of diabetes mellitus and its complications: report of a WHO consultation. Part 1, Diagnosis and classification of diabetes mellitus (Geneva: Geneva: World Health Organization).

Wu, Y., Wang, J., Scott, P.G., and Tredget, E.E. (2007a). Bone marrow-derived stem cells in wound healing: a review. Wound Repair and Regeneration *15*, S18–S26.

Wu, Y., Chen, L., Scott, P.G., and Tredget, E.E. (2007b). Mesenchymal stem cells enhance wound healing through differentiation and angiogenesis. Stem Cells *25*, 2648–2659.

Xi, B., Takeuchi, F., Meirhaeghe, A., Kato, N., Chambers, J.C., Morris, A.P., Cho, Y.S., Zhang, W., Mohlke, K.L., Kooner, J.S., et al. (2014). Associations of genetic variants in/near BMI-associated genes with type 2 diabetes: A systematic meta-analysis. Clin Endocrinol (Oxf) *81*, 702–710.

Xue, R., Li, J.Y.-S., Yeh, Y., Yang, L., and Chien, S. (2013). Effects of matrix elasticity and cell density on human mesenchymal stem cells differentiation. Journal of Orthopaedic Research *31*, 1360–1365.

Yager, D.R., Kulina, R.A., and Gilman, L.A. (2007). Wound Fluids: A window into the wound environment? Int J Low Extrem Wounds *6*, 262–272.

Yan, J., Tie, G., Wang, S., Messina, K.E., DiDato, S., Guo, S., and Messina, L.M. (2012). Type 2 Diabetes Restricts Multipotency of Mesenchymal Stem Cells and Impairs Their Capacity to Augment Postischemic Neovascularization in db/db Mice. J Am Heart Assoc *1*, e002238.

Yang, K., Wang, X.Q., He, Y.S., Lu, L., Chen, Q.J., Liu, J., and Shen, W.F. (2010). Advanced glycation end products induce chemokine/cytokine production via activation of p38 pathway and inhibit proliferation and migration of bone marrow mesenchymal stem cells. Cardiovasc Diabetol *9*, 66.

Yeboah, A., Maguire, T., Schloss, R., Berthiaume, F., and Yarmush, M.L. (2017). Stromal Cell-Derived Growth Factor-1 Alpha-Elastin Like Peptide Fusion Protein Promotes Cell Migration and Revascularization of Experimental Wounds in Diabetic Mice. Adv Wound Care (New Rochelle) *6*, 10–22.

Yin, H., Ding, G., Shi, X., Guo, W., Ni, Z., Fu, H., and Fu, Z. (2016). A bioengineered drug-Eluting scaffold accelerated cutaneous wound healing In diabetic mice. Colloids Surf B Biointerfaces *145*, 226–231.

Yoshikawa, T., Mitsuno, H., Nonaka, I., Sen, Y., Kawanishi, K., Inada, Y., Takakura, Y., Okuchi, K., and Nonomura, A. (2008). Wound Therapy by Marrow Mesenchymal Cell Transplantation. Plastic and Reconstructive Surgery *121*, 860–877.

Zaccardi, F., Webb, D.R., Yates, T., and Davies, M.J. (2016). Pathophysiology of type 1 and type 2 diabetes mellitus: a 90-year perspective. Postgraduate Medical Journal *92*, 63–69.

Zang, L., Hao, H., Liu, J., Li, Y., Han, W., and Mu, Y. (2017). Mesenchymal stem cell therapy in type 2 diabetes mellitus. Diabetology & Metabolic Syndrome *9*, 36.

Zhang, B., Liu, N., Shi, H., Wu, H., Gao, Y., He, H., Gu, B., and Liu, H. (2016a). High glucose microenvironments inhibit the proliferation and migration of bone mesenchymal stem cells by activating GSK3β. Journal of Bone and Mineral Metabolism *34*, 140–150.

Zhang, P., Li, J., Qi, Y., Zou, Y., Liu, L., Tang, X., Duan, J., Liu, H., and Zeng, G. (2016b). Vitamin C promotes the proliferation of human adipose-derived stem cells via p53-p21 pathway. Organogenesis *12*, 143–151.

Zhang, Y., Liu, J., Yao, J., Ji, G., Qian, L., Wang, J., Zhang, G., Tian, J., Nie, Y., Zhang, Y.Edi., et al. (2014). Obesity: Pathophysiology and Intervention. Nutrients *6*, 5153–5183.

Zhao, R., Liang, H., Clarke, E., Jackson, C., and Xue, M. (2016). Inflammation in Chronic Wounds. Int J Mol Sci *17*, 2085.

Zimmerlin, L., Park, T.S., Zambidis, E.T., Donnenberg, V.S., and Donnenberg, A.D. (2013). Mesenchymal stem cell secretome and regenerative therapy after cancer. Biochimie *95*, 05010.

Zisa, D., Shabbir, A., Mastri, M., Taylor, T., Aleksic, I., McDaniel, M., Suzuki, G., and Lee, T. (2011). Intramuscular VEGF activates an SDF1-dependent progenitor cell cascade and an SDF1-independent muscle paracrine cascade for cardiac repair. American Journal of Physiology - Heart and Circulatory Physiology *301*, H2422–H2432.

Addenda

Addendum A: Ethical approval letters

UNIVERSITEIT•STELLENBOSCH•UNIVERSITY
jou kennisvennoot • your knowledge partner

Approved Protocol

Date: 30 – June – 2017

PI Name: Van De Vyver, Mari M

Protocol #: SU-ACUD17-00016

Title: Development of a chronic wound model using B6.Cg-Lepob/J obese diabetic and C57BL/6J wild-type control mice: Characterizing cellular changes that impair regenerative potential of wound-derived fibroblasts and endogenous mesenchymal stem cells.

Dear Mari Van De Vyver, the Response to Modification, was reviewed on 23-June-2017 by the Research Ethics Committee: Animal Care and Use via committee review procedures and was approved. Please note that this clearance is only valid for a period of twelve months. Ethics clearance of protocols spanning more than one year must be renewed annually through submission of a progress report, up to a maximum of three years.

Applicants are reminded that they are expected to comply with accepted standards for the use of animals in research and teaching as reflected in the South African National Standards 10386: 2008. The SANS 10386: 2008 document is available on the Division for Research Developments website www.sun.ac.za/research.

As provided for in the Veterinary and Para-Veterinary Professions Act, 1982. It is the principal investigator's responsibility to ensure that all study participants are registered with or have been authorised by the South African Veterinary Council (SAVC) to perform the procedures on animals, or will be performing the procedures under the direct and continuous supervision of a SAVC-registered veterinary professional or SAVC-registered para-veterinary professional, who are acting within the scope of practice for their profession.

Please remember to use your protocol number, SU-ACUD17-00016 on any documents or correspondence with the REC: ACU concerning your research protocol. Please note that the REC: ACU has the prerogative and authority to ask further questions, seek additional information, require further modifications or monitor the conduct of your research. Any event not consistent with routine expected outcomes that results in any unexpected animal welfare issue (death, disease, or prolonged distress) or human health risks (zoonotic disease or exposure, injuries) must be reported to the committee, by creating an Adverse Event submission within the system.

We wish you the best as you conduct your research. If you have any questions or need further help, please contact the REC: ACU secretariat at wabeukes@sun.ac.za or 021 808 9003.

Sincerely, REC: ACU Secretariat

Research Ethics Committee: Animal Care and Use

UNIVERSITEIT
STELLENBOSCH
UNIVERSITY

Amendment Approval

Date: 15 June 2018

PI Name: Dr. Mari Van de Vyver

Protocol #:3857

Title: Development of a chronic wound model using B6.Cg-Lepob/J obese diabetic and C57BL/6J wild-type control mice: Characterizing cellular changes that impair regenerative potential of wound-derived fibroblasts and endogenous mesenchymal stem cells.

Dear Mari Van de Vyver ,

The Development of a chronic wound model using B6.Cg-Lepob/J obese diabetic and C57BL/6J wild-type control mice: Characterizing cellular changes that impair regenerative potential of wound-derived fibroblasts and endogenous mesenchymal stem cells - amendment. , was reviewed on 13 June 2018 by the Research Ethics Committee: Animal Care and Use via committee review procedures and was approved. Please note that this clearance is only valid for a period of twelve months. Ethics clearance of protocols spanning more than one year must be renewed annually through submission of a progress report, up to a maximum of three years.

New Co-workers:

Kiara Boodhoo (MSc student) and Dr Dalene de Swardt (Postdoc)

Applicants are reminded that they are expected to comply with accepted standards for the use of animals in research and teaching as reflected in the South African National Standards 10386: 2008. The SANS 10386: 2008 document is available on the Division for Research Developments website www.sun.ac.za/research.

As provided for in the Veterinary and Para-Veterinary Professions Act, 1982. It is the principal investigator's responsibility to ensure that all study participants are registered with or have been authorised by the South African Veterinary Council (SAVC) to perform the procedures on animals, or will be performing the procedures under the direct and continuous supervision of a SAVC-registered veterinary professional or SAVC-registered para-veterinary professional, who are acting within the scope of practice for their profession.

Please remember to use your protocol number 3857 on any documents or correspondence with the REC: ACU concerning your research protocol.

Please note that the REC: ACU has the prerogative and authority to ask further questions, seek additional information, require further modifications or monitor the conduct of your research.

Any event not consistent with routine expected outcomes that results in any unexpected animal welfare issue (death, disease, or prolonged distress) or human health risks (zoonotic disease or exposure, injuries) must be reported to the committee, by creating an Adverse Event submission within the system.

We wish you the best as you conduct your research.

If you have any questions or need further help, please contact the REC: ACU Secretariat at wabeukes@sun.ac.za or 021 808 9003.

Sincerely,

Winston Beukes

REC: ACU Secretariat

Research Ethics Committee: Animal Care and Use

Addendum B: Published Article

STEM CELLS AND DEVELOPMENT
Volume 27, Number 23, 2018

DOI: 10.1089/scd.2018.0145

ORIGINAL RESEARCH REPORT

Antioxidant Preconditioning Improves the Paracrine Responsiveness of Bone Marrow Mesenchymal Stem Cells to Diabetic Wound Fluid

Yashar Mehrbani Azar,[1] Robyn Green,[1] Carola Ulrike Niesler,[2] and Mari van de Vyver[1]

Mesenchymal stem cells (MSCs) are a promising therapeutic tool for the treatment of nonhealing diabetic wounds. The pathological nature of the niche microenvironment limits the use of autologous cell therapy in diabetic patients. Prolonged exposure of endogenous MSCs to a pathological microenvironment in vivo reduces their ability to respond to environmental cues. This study investigated the effectiveness of ex vivo antioxidant treatment [*N*-acetylcysteine (7.5 mM NAC) and Ascorbic acid 2-phosphate (0.6 mM AAP)] to restore the paracrine function of diabetic MSCs. Healthy control [bone marrow stem cells derived from wild-type mice (SC^{WT})] (source: wild-type C57BL/6J mice) ($n = 12$) and impaired/dysfunctional [bone marrow stem cells derived from ob/ob mice (SC^{ob})] (source: obese diabetic, B6.Cg-Lep^{ob}/J mice) ($n = 12$) MSCs were isolated. Ex vivo treatment groups (SC^{WT} vs. SC^{ob}) were as follows: (1) no treatment (baseline phenotype), (2) stimulated with diabetic wound fluid (DWF) (baseline response), (3) antioxidant preconditioning (preconditioned phenotype), and (4) antioxidant preconditioned with subsequent stimulation with DWF (preconditioned response). The paracrine responsiveness on both the molecular (mRNA expression of 80 cytokines and receptors, qPCR microarray) and protein (23-plex bead-array Luminex assay) level was assessed. At baseline, 31 genes were overexpressed ($> \times 2$-fold) and 39 genes were underexpressed ($> \times 2$-fold) in SC^{ob} versus SC^{WT}. In conditioned media, significant differences ($P < 0.05$) were detected at baseline for two proinflammatory cytokines [tumor necrosis factor alpha (TNFα) and interferon gamma (IFNγ)], four chemokines [keratinocyte chemoattractant (KC), granulocyte colony-stimulating factor (GCSF), Eotaxin, and macrophage chemoattractant protein (MCP1)], and one anti-inflammatory cytokine [interleukin 10 (IL10)]. Following stimulation with DWF, significant differences ($P < 0.05$) were detected in the secretion of two chemokines [granulocyte macrophage colony-stimulating factor (GMCSF) and Eotaxin], three proinflammatory cytokines (TNFα, IFNγ, and IL9), and four anti-inflammatory cytokines (IL10, IL4, IL13, and IL3). Antioxidant preconditioning significantly dampened the excessive TNFα response observed in SC^{ob} and improved the secretion of IL10. Taken together these data suggest that the combined ex vivo treatment of autologous stem cells with NAC and AAP could potentially be an effective strategy to restore the paracrine function of impaired diabetic MSCs before transplantation.

Keywords: TNFα, IL10, cytokines, mesenchymal stem cells, wound healing, diabetes

Introduction

Obesity and type 2 diabetes mellitus (DM) are regarded as chronic low-level inflammatory states that, in combination with hyperglycemic conditions, cause severe co-morbidities such as nonhealing wounds. Lower extremity wounds [such as diabetic foot ulcers (DFU)], which affect the musculoskeletal system and skin, occur in 4%–10% of diabetic patients and have a 20%–80% recurrence rate [1–4]; DFUs are currently the leading cause for lower limb amputations globally.

Mesenchymal stem cell (MSC) therapies aimed at improving wound healing are widely pursued in preclinical trials. This is due to the immune-modulatory, growth-promoting, and anti-inflammatory properties that MSCs possess [3,5–7]. However, in this respect, the use of autologous stem cells from patients with DM are not as effective in promoting healing as those from nondiabetic controls [8]. Based on the findings from various in vitro studies, it is now known that DM alters the characteristics of endogenous MSCs to such an extent that the changes remain evident, despite removal of these cells to a more optimal in vitro environment [8,9]. Bone marrow stem

[1]Division of Endocrinology, Department of Medicine, Faculty of Medicine and Health Sciences, Stellenbosch University, Cape Town, South Africa.
[2]Discipline of Biochemistry, School of Life Sciences, University of Kwazulu-Natal, Scottsville, South Africa.

cells derived from a DM microenvironment have impaired viability, have refractory mobility, and are unable to close an in vitro wound effectively [9–12]. The mechanism underlying these impairments is, however, not yet clear. Furthermore, it is unknown if these impairments can be reversed using in vitro treatments, and if so, whether preconditioned MSCs will retain a repaired status when reintroduced to the pathological microenvironment in vivo.

Wound healing is a complex process that consists of four main phases: hemostasis, inflammation (destructive/phagocytic), proliferation (extracellular matrix formation, angiogenesis, and reepithelialization), and remodeling (matrix reorganization) [13,14]. The inflammatory phase is essential for the phagocytosis of bacteria, dead cells, and tissue debris. This phase is characterized by immune cell (neutrophil/M1 macrophage) infiltration and the presence of proinflammatory signaling molecules [15]. If the transition from M1 (proinflammatory) to M2 (proregenerative) macrophages does not occur timeously, healing is impaired, and the wound may become chronic. This is the case with diabetic ulcers, where a combination of factors, including an excessive and delayed inflammatory response, dysfunctional supporting cells (fibroblasts, keratinocytes, and epithelial cells), ischemia, impaired angiogenesis, and neuropathy, prevents the wound from transitioning into the proliferative and remodeling phases [5,15,16]. The paracrine properties of exogenously applied allogeneic (healthy) bone marrow stem cells have been shown to restore the wound microenvironment by inducing the proliferative and remodeling phases of healing through anti-inflammatory and proregenerative signaling [7]. Bone marrow stem cells isolated from pathological environments (such as those existing during DM) lose their ability to promote repair. We hypothesize that prolonged exposure of autologous MSCs to a pathological microenvironment in vivo reduces the ability of these cells to respond to environmental cues and thereby effect repair. Assessing whether the paracrine (cytokine) responsiveness of MSCs is skewed toward a prodestructive or proregenerative response could potentially be used as diagnostic parameters to predict the degree of MSC dysfunction in a diabetic patient.

The pathogenesis of DM, which contributes to the functional decline of stem cells, is driven by hyperglycemia (advanced glycation end products), chronic inflammation, and oxidative stress [8]. Ascorbic acid 2-phosphate (AAP) and *N*-acetylcysteine (NAC) are antioxidants that have been shown to preserve the ''stemness'' of healthy MSCs during prolonged culture, by preventing apoptosis and promoting proliferation, telomerase activity, and increasing intracellular levels of antioxidant enzymes such as superoxide dismutase [17–20]. It is hypothesized that these protective agents could potentially be used to restore the function of impaired autologous stem cells.

This study therefore investigated whether in vitro antioxidant preconditioning could restore the paracrine function of impaired diabetic bone marrow stem cells. To achieve this, an in vivo murine model of impaired wound healing was established, and diabetic wound fluid collected. The paracrine (secretome; extracellular) and molecular (intracellular) responsiveness of healthy and impaired/dysfunctional stem cells were then assessed at baseline and following ex vivo exposure to diabetic wound fluid. The successful restoration of the paracrine function of impaired/diabetic stem cells ex vivo before use for autologous cell therapy could improve the predictability of cell therapy in diabetic ulcer patients in the clinical setting.

Materials and Methods

This study was approved by the animal research ethics committee (SU-ACUD17-000016) at Stellenbosch University and complied with the South African Animal Protection Act (Act no. 71, 1962). All experimental procedures were conducted according to the ethical guidelines and principles of the declaration of Helsinki.

Induction of full-thickness wounds and collection/analysis of wound fluid

Full-thickness excisional wounds were induced dorsally on obese prediabetic mice (B6.Cg-Lep^{ob}/J) (ob/ob) with subcutaneous injections of recombinant neutral endopeptidase (NEP) to (1) prevent wound contraction and (2) more closely mimic diabetic ulcers in patients [21,22].

Seven ($n=7$) ob/ob mice (8-week old; weight 43 ± 2 g) were anesthetized using isoflurane (Safeline Pharmaceuticals Pty, Ltd., SA) gas. Dorsal hair was shaved, washed with povidone-iodine and a local anesthetic, and 2% lignocaine (7 mg/kg; Bodene Pty, Ltd., SA) applied before making two identical contralateral full-thickness skin excisions (including the underlying *panniculus carnosus*) (6 mm^2) (Fig. 1). Immediately postwounding and on day 7, NEP (0.3 μg/mL; enzyme activity 50 pmol/h/μg) (SRP6450, Neprilysin/CD10; Sigma-Aldrich, St. Louis, MO) was injected subcutaneously at the wound edges to prevent skin contraction and further delay healing. The enzyme activity of the injected NEP is equivalent to that observed in the foot ulcers of diabetic patients [21,22]. Postsurgery pain (3 days) was managed by adding acetaminophen (300 mg/kg) (GSK, Cape Town, SA) to the drinking water of individually housed animals. Both excisional wounds were covered by a vapor-permeable polyurethane film (Hydrofilm; Paul Hartmann AG, Heidenheim, Germany) and the accumulated exudate (diabetic wound fluid, DWF) harvested by needle puncture [23,24] at 7, 14, and 21 days postwounding. At these time points, DWF was collected by injecting 100 μL sterile saline onto the wounds and then collecting the wound exudate together with the saline. The collected DWF was pooled, sterile filtered, and centrifuged to eliminate all debris and stored at −80°C. Note: on day 14 postwounding, the start of reepithelialization was evident, and wounds were therefore reopened (by removing the epithelial layer) at this time point, following the collection of the DWF.

The total protein concentration of the sterile filtered DWF (9.6 μg/mL) was determined to be threefold less than the total amount of protein in fetal bovine serum (FBS) (27.9 μg/mL) using a standard Bradford assay with BSA (Hyclone BSA; Thermo, Logan) as control (Supplementary Fig. S1; Supplementary Data are available online at www.liebertpub.com/scd). For the in vitro experiments, bone marrow-derived stem cells (SCs) were therefore stimulated with media containing 30% DWF [600 μL DWF + 1,400 μL Dulbecco's modified Eagle's medium (DMEM) with ultraglutamine containing 1% penicillin/streptomycin], while control growth media contained the standard 10% FBS. The

FIG. 1. Full-thickness excisional diabetic wound model. **(A)** The weight of the B6.Cg-Lep^{ob}/J (ob/ob) mice over time after initial wounding (day 0) and rewounding (day 14). **(B)** Representative images of contralateral dorsal full-thickness excisional wounds that were induced on ob/ob mice. Images were taken immediately (day 0) and on days 7, 14, and 21 postwounding. **(C)** Percentage wound closure (%). Wound surface area at each time point was determined using ImageJ software (version 1.46, nih.gov) and the percentage wound closure calculated using the following formula: (wound area d0 – wound area dn)/(wound area d0) × 100. Statistical analysis: data are presented as (mean ± SE). Repeated-measures ANOVA with Bonferroni post hoc test. $^{**}P < 0.01$. Color images available online at www.liebertpub.com/scd

total protein content in the media used to stimulate SCs with DWF was thus equivalent to that of standard growth media. The cytokine concentrations within DWF were determined using a Bio-Plex Pro Mouse Cytokine 23-plex assay (No. M60009RDPD; Bio-Rad, Hercules, CA) [Eotaxin, granulocyte colony-stimulating factor (GCSF), granulocyte macrophage colony-stimulating factor (GMCSF), interferon gamma (IFNγ), interleukin (IL)1α, IL1β, IL2, IL3, IL4, IL5, IL6, IL9, IL10, IL12 (p40), IL12 (p70), IL13, and IL17A, keratinocyte chemoattractant (KC), macrophage chemoattractant protein (MCP1) (MCAF), macrophage inflammatory protein (MIP)1α, MIP1β, RANTES, and tumor necrosis factor alpha (TNFα)] as per manufacturer's instructions.

As a parallel control, to assess whether wound closure was truly delayed in our diabetic wound model, acute wounds (without NEP injection) were induced on six ($n = 6$) healthy control mice (C57BL6/J) (8-week old; weight 25 ± 0.2 g) using the same procedure as described above. Complete macroscopic wound closure and significant healing were evident in the control animals on day 7 (Supplementary Fig. S2).

Determination of the safest, nontoxic doses of NAC and AAP for in vitro antioxidant preconditioning

The dose-response experiment was performed using a mouse MSC line (C3H/10T1/2, clone 8, ATCC ccl-226) (passage 5–7) as part of the refinement criteria of this study to limit the required number of animals. MSCs were cultured in standard growth media (SGM) consisting of DMEM with ultra-glutamine (4.5 g/L high-glucose DMEM; BioWittaker, Lonza, Basel, Switzerland) containing 10% FBS (Biochrom, Berlin, Germany) and 1% penicillin/streptomycin (BioWittaker, Lonza). Cells were maintained at 37°C, in 90% humidified air with 5% CO_2. The effect of different doses of NAC (7.5, 15, and 30 mM) (Sigma-Aldrich, St. Louis, MO) or AAP (0.15, 0.3, 0.6 mM) (Sigma-Aldrich, St. Louis, MO) on MSC proliferation (BrdU ELISA; Roche, Basel, Switzerland) was assessed over a period of 24 and 48 h, respectively. This was done to determine the optimum dose of each individual antioxidant. To assess the synergistic effect of the optimum doses, the survival rate of MSCs following exposure to the combined antioxidant treatment was determined over a period of 6 days using Crystal Violet staining (0.01% in dH_2O) (Sigma-Aldrich, Steinheim, Germany) [25].

Isolation and characterization of bone marrow-derived SCs

Healthy control (source: wild type, C57BL/6J mice, weight 23.6 ± 0.9 g) ($n = 12$) and impaired/dysfunctional bone marrow-derived SCs (source: obese diabetic, B6.Cg-Lep^{ob}/J mice, weight 37.2 ± 1.7 g) ($n = 12$) were isolated as previously described [9]. Briefly, following sacrifice of the animals, the femurs were dissected out and the proximal and distal ends of each femur cut open in a sterile environment. Bone marrow aspirates were flushed into tissue culture plates (six-well plates; Nest Biotechnology, NJ) using a 25-gauge needle and syringe containing growth media with 20% FBS (Biochrom). Growth media consisted of DMEM with ultra-glutamine (4.5 g/L high glucose; BioWittaker, Lonza), containing 1% penicillin/streptomycin (BioWittaker, Lonza). Bone marrow aspirates were maintained at 37°C, in 90% humidified air with 5% CO_2. After 96 h, nonadherent cells were washed off with phosphate-buffered saline (PBS) and the media replaced with SGM containing 10% FBS (Biochrom). Media were then changed every 3–4 days until the cells reached confluence in passage 0. All subsequent experiments were performed on SCs derived from at least three animals per group ($n = 3$ biological repeats).

SCs (90% confluent; passage 0) were harvested through trypsinization and resuspended in flow cytometry staining solution (PBS containing 20% FBS). Cell suspensions at a concentration of 1×10^6 cells per 100 μL were co-labeled with rat anti-mouse monoclonal antibodies against the stem cell marker, Ly-6A/E (Sca-1) (PE conjugated; BD Pharmingen, San Diego, CA) and the hematopoietic lineage marker, CD45 (FITC conjugated; BD Pharmingen). Flow cytometry was performed on a BD FACSCalibur instrument using CellQuest software. A total of 15,000 events were recorded before data

analysis. Fluorescent compensation settings were established through a compensation experiment using comp beads (BD™CompBead Plus Anti-Mouse Ig, k; BD Biosciences, San Jose, CA). An unstained control sample was used as a negative control for gating purposes. Data analysis was performed using Flow Jo Vx (Treestar, OR) software.

For all subsequent experiments, the isolated bone marrow SCs were expanded in culture under either standard growth media (control) conditions or in the presence of antioxidant preconditioning before stimulation with DWF.

In vitro treatment conditions and study design

Antioxidant preconditioning consisted of combined treatment with NAC (7.5 mM) (Sigma-Aldrich, St. Louis, MO) and AAP (0.6 mM) (Sigma-Aldrich, St. Louis, MO) added to the growth media (SGM), with media being changed every 3–4 days until the cells reached 80% confluence. The inflammatory phenotype and paracrine responsiveness of healthy versus impaired SCs (with and without preconditioning) to environmental cues were assessed following ex vivo exposure to DWF. For the treatment of SCs with DWF, the FBS (10%) in the growth media was replaced by DWF (30%) with an equivalent total protein concentration. The treatment groups were as follows: (1) no treatment (baseline phenotype): SCs expanded in standard growth media (±8 days) and only exposed to growth media, (2) DWF: SCs expanded in standard growth media (±8 days) followed by acute exposure to DWF for a period of 4 h, (3) antioxidant preconditioning: SCs expanded in the presence of NAC/AAP (±8 days), And (4) antioxidant preconditioning+DWF: SCs expanded in the presence of NAC/AAP (±8 days) followed by acute exposure to DWF for a period of 4 h. Refer to Supplementary Fig. S3 for an overview of the study design and treatment groups.

Collection and analysis of conditioned media

After MSCs reached 80% confluence, the growth media (with or without NAC/AAP) were replaced with serum-free media for a period of 24 h. The complete serum-free growth media consists of Stem Pro MSC SFM basal media (No. A10334-01; Gibco, Life Technologies), Stem Pro MSC SFM growth factor Supplement CTS (A10333-01; Gibco, Life Technologies), 2 mM L-Glutamine (No. 25030-081; Gibco, Life Technologies), and 5 μg/mL penicillin/streptomycin (No. DE17-6026; BioWhittaker, Lonza). After 24 h, the conditioned media were collected, centrifuged to remove cellular debris, and stored at −80°C. The cytokine concentrations within conditioned media were assessed using the Bio-Plex Pro Mouse Cytokine 23-plex Assay (No. M60009RDPD; Bio-Rad) [Eotaxin, GCSF, GMCSF, IFNγ, IL1α, IL1β, IL2, IL3, IL4, IL5, IL6, IL9, IL10, IL12 (p40), IL12 (p70), IL13, and IL17A, KC, MCP1 (MCAF), MIP1α, MIP1β, RANTES, and TNFα] according to the manufacturer's instruction, using a Multiplex reader (MAGPIX; Bio-Rad) and Bio-Plex Manager™ MP software.

RNA isolation, cDNA synthesis, and RT2 qPCR microarray

Total RNA was isolated using the RNeasy RNA isolation kit (Qiagen, Berlin, Germany) with on-column DNAse digestion (Qiagen). RNA quantification and quality control were performed using the Eukaryote Total RNA Nano Series II (2100 Bioanalyzer; Agilent Technologies, Inc., Santa Clara, CA). Total RNA (0.5 μg) with an integrity of above 9 (RIN >9) was used as a template for cDNA synthesis, using the RT^2 First Strand Kit (Qiagen) that includes a genomic DNA elimination step. cDNA samples for each treatment condition were analyzed with an RT^2 Profiler polymerase chain reaction (PCR) inflammatory cytokine and receptor array (96-well plate format; Qiagen) and RT^2 SYBR Green Master-mix (Rox PCR Master mix; Qiagen) using an ABI 7900HT Fast real-time PCR system (Applied Biosystems, Life technologies), and SDS software (version 2.3; Life technologies). The web-based PCR Profiler Array data analysis package was used for ΔΔCt-based fold change calculations (Qiagen, www.qiagen.com). Relative gene expression was calculated by comparison with the following housekeeping gene: heat shock protein 90α class B member 1 (Hsp90ab1) (NM_008302). The PCR array analysis furthermore included a mouse genomic DNA contamination (SA_00106), reverse transcriptase (SA_00104), and positive PCR (SA_00103) controls. Genes of interest were identified using Student's *t*-test of the replicate ΔΔCt values for each gene in the control and treatment groups. The level of significance was accepted at $P < 0.05$.

Statistical analysis

Values are presented as mean ± standard error (mean ± SE). Statistical analysis was performed using Statistica software (Statsoft, version 13). Repeated-measures ANOVA with Bonferroni post hoc test was used to assess animal weight and wound closure over time. Factorial ANOVA with Tukey post hoc test was used to assess group, treatment, and group × treatment effects. Genes of interest were identified using a Student's *t*-test of the replicate $2^{(\Delta Ct)}$ values of each gene in the control and treatment groups. The level of significance was accepted at $P < 0.05$.

Results

Full-thickness excisional diabetic wound model: collected wound fluid is representative of the in vivo microenvironment of an inflammatory diabetic wound

No weight loss was apparent in the wounded animals (start weight: 43 ± 2 g; end weight: 41 ± 7 g) for the duration of the study (Fig. 1A). Impaired wound closure (macroscopic) was evident in the ob/ob animals over the initial recovery period of 14 days (day 0 to 7: 33% ± 7% wound closure; day 0 to 14: 77% ± 4% wound closure) as well as in the subsequent period after rewounding (day 14 to 21: 48% ± 7% wound closure) (Fig. 1B, C). In contrast, significant wound closure was evident after only 7 days in the WT control animals (Supplementary Fig. S1). Wound fluid was collected and analyzed as indication of the clinical condition of the wound. The DWF collected from the ob/ob animals had a cytokine profile that mimics the clinical characteristics of a nonhealing diabetic wound. Refer to Table 1 for the quantification of cytokine concentrations detected in the DWF. Proinflammatory cytokines (IL1α, IL1β, IL6, IL12p40, IL12p70, IL17A, RANTES, and TNFα) and chemokines

Table 1. Cytokine Secretion Profile in Response to Diabetic Wound Fluid

	Secreted protein: response to DWF			
		Control		*Preconditioned*
	DWF	*SC^{WT}*	*SC^{ob}*	*SC^{ob}*
Proinflammatory				
IL1α	6,992	2,737 (31)	2,640 (560)	2,974 (165)
IL1β	3,360	1,144 (22)	1,184 (125)	1,131 (133)
IL6	1,004	11,305 (2,119)	7,290 (3,240)	10,574 (3,827)
IL9	127	204 (9)[a]	228 (4)[b]	242 (5)[a,b]
IL12p40	4,962	2,944 (71)	3,051 (174)	2,934 (151)
IL12p70	598	1,030 (71)	1,068 (32)	1,064 (118)
IL17A	361	207 (6)	238 (19)	241 (20)
IFNγ	43	57 (3)[a]	68 (2)	77 (6)[a]
RANTES	128	3,971 (217)	5,376 (687)	12,833 (6,862)
TNFα	932	5,081 (671)[c]	20,441 (1,461)[b,c]	9,190 (487)[b]
Chemokines				
Eotaxin	572	179 (6)[a,c]	217 (6)[c]	229 (9)[a]
GCSF	>47,590[d]	14,160 (605)	14,942 (781)	15,484 (1,564)
GMCSF	672	399 (10)[a]	486 (26)	510 (30)[a]
KC	>21,315[d]	11,231 (3,397)	11,165 (1,767)	18,305 (5,378)
MCP1	18,568	35,772 (678)	34,706 (10,271)	35,432 (7,406)
MIP1α	>7,288[d]	2,689 (257)	3,095 (493)	6,357 (2,603)
MIP1β	1,187	18,344 (1,776)	26,690 (7,447)	31,905 (12,064)
Anti-inflammatory				
IL2	23	49 (1)	60 (1)	120 (19)
IL3	27	33 (1)[a,c]*	38 (1)[c]*	39 (2)[a]
IL4	91	53 (1)[c]	65 (3)[c]	60 (3)
IL5	27	53 (3)	66 (4)	95 (23)
IL10	263	6,823 (575)[a]	5,415 (317)[b]	10,207 (812)[a,b]
IL13	329	617 (14)[a,c]	745 (7)[c]	747 (29)[a]

Data are presented as mean (SE) in pg/mL. Statistical analysis: factorial ANOVA with Tukey post hoc test. Level of significance accepted at $P<0.05$.
[a]Significant difference between SC^{WT} and SC^{ob} with preconditioning.
[b]Significant difference in SC^{ob} with and without preconditioning.
[c]Significant difference between SC^{WT} and SC^{ob}. [c]*Indicates $P=0.06$.
[d]The concentration of these chemokines was above the detection limit as indicated.
GCSF, granulocyte colony-stimulating factor; GMCSF, granulocyte macrophage colony-stimulating factor; IFNγ, interferon gamma; IL, interleukin; KC, keratinocyte chemoattractant; MCP, macrophage chemoattractant protein; MIP, macrophage inflammatory protein; SC^{ob}, bone marrow stem cells derived from ob/ob mice; SC^{WT}, bone marrow stem cells derived from wild-type mice; TNFα, tumor necrosis factor alpha.

(Eotaxin, GCSF, GMCSF, MCP1, MIP1α, and MIP1β) were present in high concentrations, whereas anti-inflammatory cytokines (IL2, IL3, IL4, IL5, IL9, and IL10) had much lower levels within the DWF.

The safest nontoxic doses of NAC and AAP for in vitro antioxidant preconditioning

Compared to standard growth conditions, of all the concentrations tested (NAC 7.5, 15, and 30 mM; AAP 0.15, 0.3, and 0.6 mM), 7.5 mM NAC had the most significant effect on the proliferation rate of MSCs over a period of 24 h (~2-fold increase) ($P<0.05$) and 48 h (~2.5-fold increase) ($P<0.05$) (Fig. 2A, B). Similarly, 0.6 mM AAP was shown to promote MSC proliferation over a period of 24 h (~1.3-fold increase) compared to standard growth conditions (Fig. 2A, B). The combined treatments of 7.5 mM NAC and 0.6 mM AAP maintained cell viability over a period of 6 days (Fig. 2C) and were thus identified as the optimum concentrations for preconditioning.

Characterization of healthy control (source: wild type, C57BL/6J mice) and impaired/dysfunctional (source: obese diabetic, B6.Cg-Lep^{ob}/J mice) bone marrow-derived SCs

Flow cytometry surface marker characterization demonstrated that 88% ± 4% of isolated bone marrow-derived cells expressed the stem cell marker, Sca1 (Fig. 3A–C). A percentage of cells did, however, also express the hematopoietic lineage marker, CD45. Immediately, following isolation (passage 0), the bone marrow-derived SCs therefore consisted of a heterogenous population of 60% ± 3% MSCs ($Sca1^+CD45^-$) and 39% ± 3% hematopoietic stem cells ($Sca1^+CD45^+$) (Fig. 3A–D). There was no difference in surface marker expression in the bone marrow SCs derived from either WT control (SC^{WT}) or ob/ob (SC^{ob}) animals (Fig. 3D). SC^{ob} had impaired viability and growth with fewer cells visible 96 h postisolation compared to their SC^{WT} counterparts at the same time point (Fig. 3E, F).

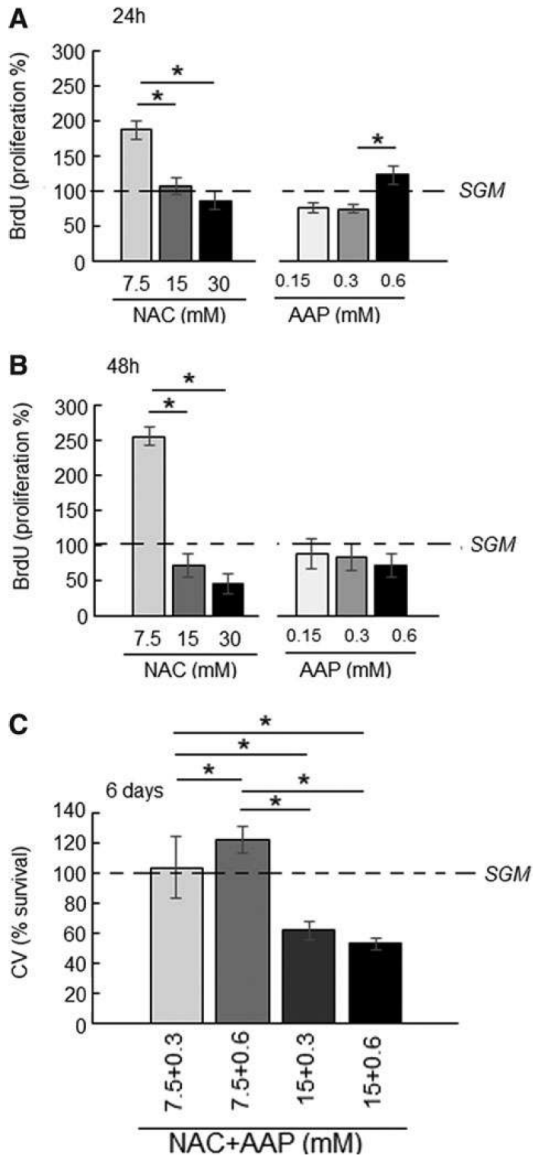

FIG. 2. Safest, nontoxic dosages of NAC and AAP. **(A, B)** The independent effect of NAC (7.5, 15, and 30 mM) and AAP (0.15, 0.3, and 0.6 mM) on MSC proliferation (BrdU incorporation) over a period of 24 h **(A)** and 48 h **(B)**. **(C)** The synergistic effect of combined NAC and AAP treatment on cell viability (crystal violet staining) over a period of 6 days. Statistical analysis: data (mean ± SE) are presented as percentage with SGM (control) set at 100. Factorial ANOVA with Tukey post hoc test. *$P < 0.05$. AAP, ascorbic acid 2-phosphate, CV, crystal violet; NAC, *N*-acetylcysteine; SGM, standard growth media.

Secretome differences at baseline: healthy control (SC^{WT}) versus impaired/dysfunctional (SC^{ob})

The secretion of 23 cytokines from SC^{WT} and SC^{ob} was assessed at baseline with and without antioxidant preconditioning (Table 2). Of the 23 cytokines assessed within conditioned media, significant differences ($P < 0.05$) were detected at baseline (without stimulation) for two proinflammatory cytokines (TNFα and IFNγ), four chemokines (KC, GCSF, Eotaxin, and MCP1), and one anti-inflammatory cytokine (IL10).

Proinflammatory TNFα and IFNγ concentrations were significantly higher ($P < 0.05$) in the conditioned media derived from SC^{ob} (TNFα 2.9-fold higher; IFNγ 15 ± 4 pg/mL) compared to SC^{WT} (IFNγ not detected). Preconditioning SC^{ob} with antioxidants did, however, downregulate the secretion of TNFα and IFNγ to levels comparable to that of SC^{WT}. The chemokines KC, GCSF, and Eotaxin remained significantly higher ($P < 0.05$) in the conditioned media derived from SC^{ob} (KC 2.2-fold higher; GCSF 6.7-fold higher; Eotaxin 20 ± 7 pg/mL) compared to SC^{WT} (Eotaxin not detected), regardless of preconditioning. Preconditioning did, however, promote MCP1 secretion in SC^{ob} (2.5-fold increase) ($P < 0.05$), whereas only a small increase (1.5-fold, not significant) was evident in SC^{WT}. The anti-inflammatory cytokine, IL10, tended to be higher (2.4-fold) ($P = 0.06$) in the conditioned media derived from SC^{ob} compared to SC^{WT} and was unaffected by preconditioning.

Gene expression (mRNA) differences at baseline and in response to stimulation with DWF: healthy control (SC^{WT}) versus impaired/dysfunctional (SC^{ob})

At baseline, under standard growth conditions, 31 genes were overexpressed (>2-fold) and 39 genes underexpressed (>2-fold) in the SC^{ob} versus SC^{WT} (Fig. 4A). The overexpression of colony-stimulating factor (Csf1) (also known as MCSF) (29-fold) was, however, the only significant difference ($P < 0.05$) between the groups at baseline (Fig. 4A, C). Overall, preconditioning of SC^{ob} downregulated the expression of 32 genes and upregulated the expression of 48 genes (Fig. 4B). The expression of Csf1 in SC^{ob} was downregulated with preconditioning to levels comparable to that observed in SC^{WT} (Fig. 4C). Preconditioning induced the expression of Ccl8 (also known as MCP2) ($P < 0.05$), which was previously undetectable in SC^{ob} (Fig. 4B, D).

When exposed to DWF, both the SC^{WT} and SC^{ob} responded by significantly ($P < 0.05$) increasing the gene expression of macrophage chemoattractant proteins, ccl2 (also known as MCP1) and ccl3 (also known as MIP1α) (Fig. 4E–H). In SC^{WT}, DWF furthermore induced the expression ($P < 0.05$) of nine additional genes (ccl24, ccl7, ccr1, cxcl10, cxcl5, cxcl9, IL15, IL1α, and TNF) associated with proinflammatory chemotactic responses. In contrast, SC^{ob} responded by increasing ($P < 0.05$) the expression of only four additional genes (cxcl1, IL11rn, IL27, and cxcl11) (Fig. 4F, H). Preconditioning did, however, restore the TNF response ($P < 0.05$) and induced the expression of ccl17, ccl19, csf3, macrophage inhibitory factor (Mif), and B2m (Fig. 4G, H) in SC^{ob}. A summary of the relevant molecular responses ($P < 0.05$) within these groups is indicated in Fig. 4H.

Differences in the paracrine responsiveness following DWF stimulation: healthy control (SC^{WT}) versus impaired/dysfunctional (SC^{ob})

Following stimulation with DWF, significant differences ($P < 0.05$) were detected in the conditioned media

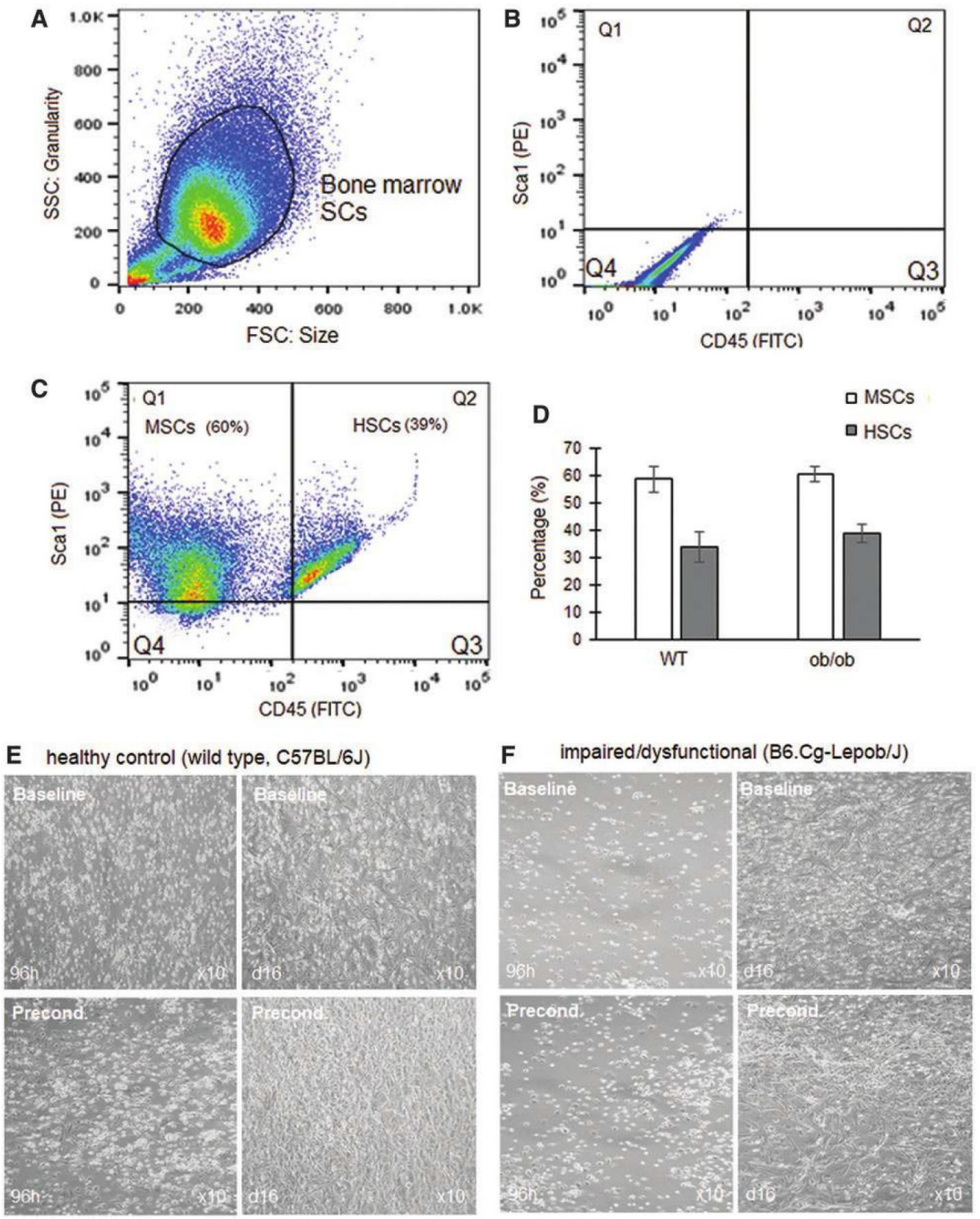

FIG. 3. Characterization of healthy control (source: wild type, C57BL/6J mice) and impaired/dysfunctional (source: obese diabetic, B6.Cg-Lep^{ob}/J mice) bone marrow-derived SCs. **(A)** Representative flow cytometry dot plot demonstrating the forward (size) versus side (granularity) scatter of the isolated cells. **(B, C)** The expression of Sca1 (PE) versus CD45 (FITC) in unstained negative control sample **(B)** and bone marrow SCs **(C)**. Q1—MSCs expressing Sca1^{+}CD45^{-}; Q2—HSCs expressing Sca1^{+}CD45^{+}; Q3—Mature hematopoietic cells Sca1^{-}CD45^{+}; Q4—Cells expressing neither Sca1^{-} nor CD45^{-}. **(D)** Quantification of the percentage MSCs and HSCs within the isolated population. **(E, F)** Representative images of the healthy control **(E)** and impaired/dysfunctional **(F)** bone marrow SCs with and without antioxidant preconditioning at 96 h and day 16 postisolation. Statistical analysis: data are presented as (mean ± SE). Factorial ANOVA with Tukey post hoc test. HSC, hematopoietic stem cells; MSCs, mesenchymal stem cells; Precond, antioxidant preconditioning. Color images available online at www.liebertpub.com/scd

Table 2. Cytokine Secretome Differences at Baseline

	Secreted protein: conditioned media			
	Control		*Preconditioned*	
	SC^{WT}	SC^{ob}	SC^{WT}	SC^{ob}
Proinflammatory				
IL1α	—	4.0 (2.1)	—	—
IL1β	24 (8)	34 (7)	21 (11)	25 (5)
IL6	1,007 (254)	1,254 (514)	942 (316)	1,176 (263)
IL9	—	13 (12)	—	—
IL12p40	75 (22)	109 (11)	99 (10)	154 (31)
IL12p70	130 (70)	325 (65)	130 (70)	186 (61)
IL17A	—	—	—	—
IFNγ	—[a]	15 (4)[a,c]	—	—[c]
RANTES	127 (13)	226 (48)	122 (17)	229 (25)
TNFα	40 (14)[a]	113 (21)[a,c]	34 (19)	51 (14)[c]
Chemokines				
Eotaxin	—[a]	20 (7)[a]	—[d]	9.1 (4.5)[d]
GCSF	10 (8)[a]	67 (12)[a]	10 (7.5)[d]	30 (15)[d]
GMCSF	85 (32)	137 (22)	77 (40)	84 (17)
KC	353 (50)[a]	778 (151)[a]	356 (48)[d]	578 (71)[d]
MCP1	1,721 (113)	5,171 (835)[c]	2,571 (901)[d]	12,912 (1 772)[c,d]
MIP1α	11 (2)	8.9 (0.4)	15 (4)	13 (0.4)
MIP1β	50 (2)	65 (4)	88 (36)	129 (11)
Anti-inflammatory				
IL2	2.7 (2.6)	7.9 (2.7)	2.7 (2.6)	6.3 (3.5)
IL3	2.9 (1.7)	9.5 (1.6)	2.9 (1.7)	4.7 (1.8)
IL4	—	1.3 (1.2)	—	—
IL5	13 (7)	16 (2)	15 (6)	38 (8)
IL10	36 (7)[a]*	87 (8)[a]*	32 (11)	74 (19)
IL13	138 (25)	207 (37)	107 (55)	135 (23)

Data are presented as mean (SE) in pg/mL. Statistical analysis: factorial ANOVA with Tukey post hoc test. Level of significance accepted at $P < 0.05$.
[a]Significant difference at baseline (control) between SC^{WT} and SC^{ob}. [a]*Indicates $P = 0.06$.
[b]Significant difference in SC^{WT} with and without preconditioning.
[c]Significant difference in SC^{ob} with and without preconditioning.
[d]Significant difference between SC^{WT} and SC^{ob} with preconditioning.
—, not detected.

concentrations of two chemokines [GMCSF and Eotaxin (also known as ccl11)], three proinflammatory cytokines (TNFα, IFNγ, and IL9), and four anti-inflammatory cytokines (IL10, IL4, IL13, and IL3) between groups (SC^{WT} vs. SC^{ob} vs. preconditioned SC^{ob}) (Fig. 5 and Table 1).

Similar to baseline, the chemokines GMCSF and Eotaxin in conditioned media were detected at higher concentrations in SC^{ob} (GMCSF 486 ± 26 pg/mL and Eotaxin 217 ± 6 pg/mL) and preconditioned groups (GMCSF 510 ± 30 pg/mL and Eotaxin 229 ± 9 pg/mL), following stimulation compared to SC^{WT} (GMCSF 399 ± 10 pg/mL and Eotaxin 179 ± 6 pg/mL) (Fig. 5A, B). Despite these differences, the concentration of these chemokines poststimulation was lower than that detected in DWF (Table 1).

Stimulation with DWF induced a much greater proinflammatory TNFα response in SC^{ob} (20,441 ± 1,461 pg/mL) than SC^{WT} (5,081 ± 671 pg/mL); this excessive response in SC^{ob} was dampened with preconditioning (9,190 ± 487 pg/mL) (Fig. 5C). Preconditioning furthermore increased the release of proinflammatory IFNγ and IL9 following stimulation with DWF in the SC^{ob} (IFNγ 77 ± 6 pg/mL and IL9 242 ± 5 pg/mL) compared to SC^{WT} (IFNγ 57 ± 3 pg/mL and IL9 204 ± 9 pg/mL) (Fig. 5D, E).

A slight difference in the anti-inflammatory IL3, IL4, and IL13 response to DWF was evident between SC^{ob} (IL3 38 ± 1 pg/mL; IL4 65 ± 3 pg/mL; and IL13 745 ± 7 pg/mL) and SC^{WT} (IL3 33 ± 1 pg/mL; IL4 53 ± 1 pg/mL; and IL13 617 ± 14 pg/mL) (Fig. 5F–I). IL4 in conditioned media poststimulation was, however, below the concentration detected in DWF (Table 1). Preconditioning significantly improved the secretion of anti-inflammatory IL10 poststimulation in the SC^{ob} group (SC^{ob} 5,415 ± 317 pg/mL; Precond 10,207 ± 812 pg/mL; SC^{WT} 6,823 ± 575 pg/mL) (Fig. 5F).

Discussion

Tissue repair and regeneration using endogenous stem cells represents the ultimate goal in regenerative medicine; however, the pathological nature of the in vivo microenvironment has hampered the use of autologous cell therapy in diabetic patients. This study demonstrated that bone marrow stem cells derived from an obese diabetic microenvironment have a skewed inflammatory phenotype; this may contribute to their inability to perform the imperative function of restoring the localized (wounded area) conditions needed for normal healing. Wound fluid is generated by enhanced capillary leakage

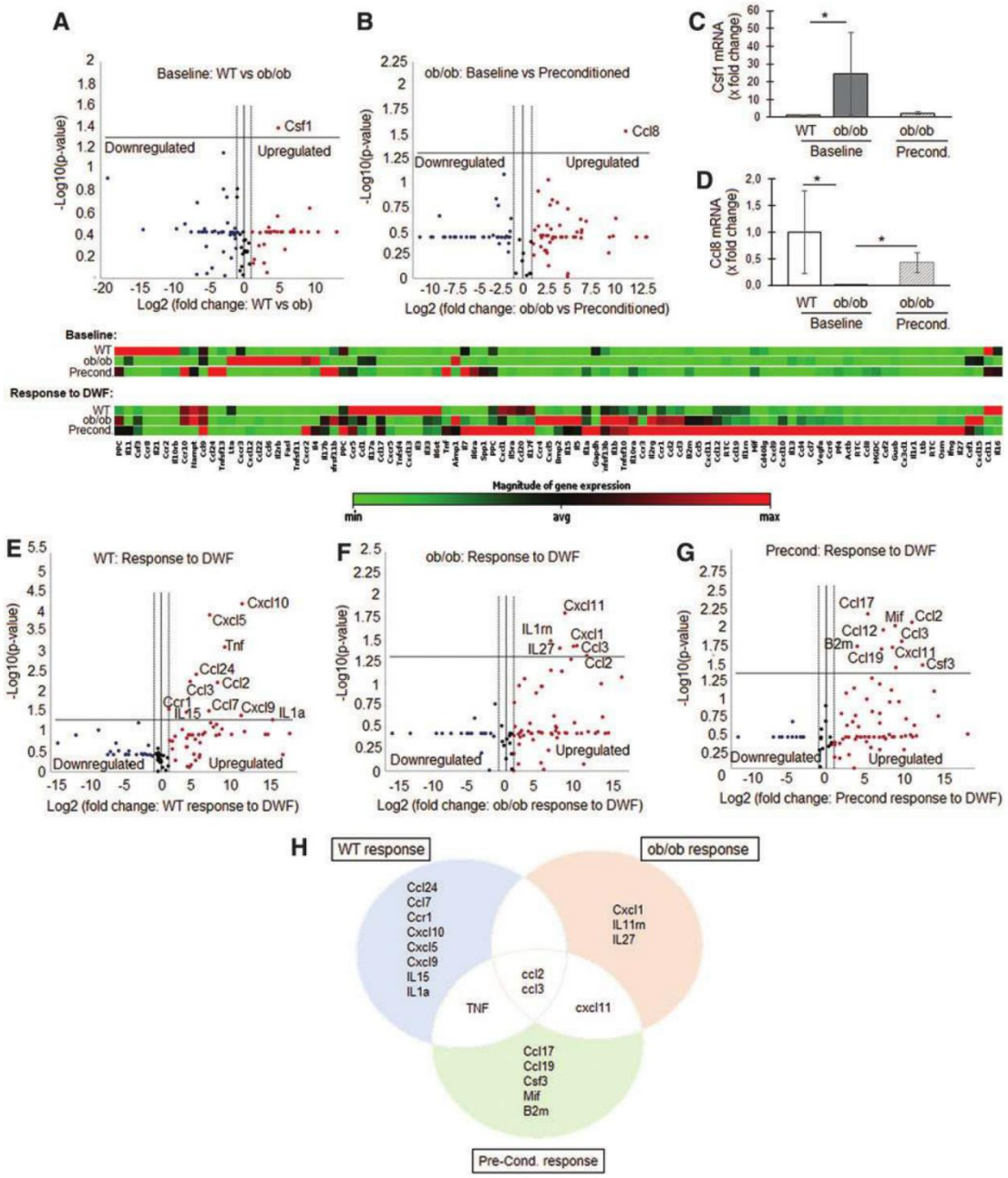

FIG. 4. Gene expression differences at baseline and in response to stimulation with DWF: healthy control (SC^{WT}) versus impaired/dysfunctional (SC^{ob}). **(A, B)** A comparison of mRNA expression at baseline in SC^{ob} versus SC^{WT} **(A)** and in SC^{ob} with and without antioxidant preconditioning **(B)**. **(C, D)** Quantification of Csf1 **(C)** and ccl8 **(D)** mRNA (×fold difference compared to control) at baseline within the respective groups. **(E)** The gene expression responsiveness of SC^{WT} to stimulation with DWF. **(F)** The gene expression responsiveness of SC^{ob} to stimulation with DWF. **(G)** The gene expression response of preconditioned SC^{ob} following stimulation with DWF. **(H)** Summary of the responsiveness of SC^{WT}, SC^{ob}, and preconditioned SC^{ob} to DWF (only genes that had a significant change in mRNA expression is indicated). Statistical analysis: genes of interest were identified using a Student's *t*-test of the replicate ($n=3$) $2^{(\Delta Ct)}$ values of each gene in the control and experimental groups. $^*P<0.05$. Csf, colony-stimulating factor; SC^{ob}, bone marrow stem cells derived from ob/ob mice; SC^{WT}, bone marrow stem cells derived from wild-type mice. Color images available online at www.liebertpub.com/scd

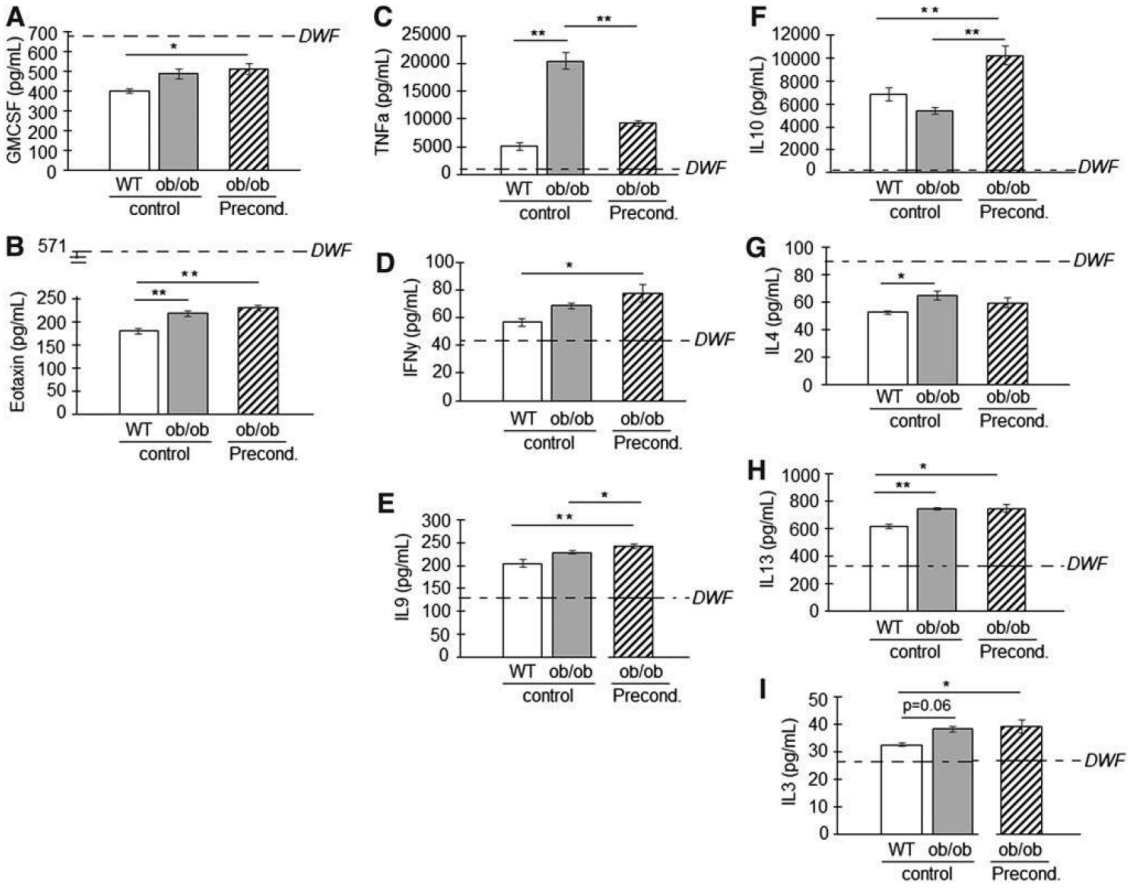

FIG. 5. Differences in the paracrine responsiveness following DWF stimulation: healthy control (SC^{WT}) versus impaired/dysfunctional (SC^{ob}). The cytokine concentrations in conditioned media poststimulation with DWF were assessed in SC^{WT}, SC^{ob}, and preconditioned SC^{ob}. **(A)** GMCSF (pg/mL), **(B)** Eotaxin (pg/mL), **(C)** TNFα (pg/mL), **(D)** IFNγ (pg/mL), **(E)** IL9 (pg/mL), **(F)** IL10 (pg/mL), **(G)** IL4 (pg/mL), **(H)** IL13 (pg/mL), and **(I)** IL3 (pg/mL). Statistical analysis: factorial ANOVA with Tukey post hoc test. $^*P < 0.05$. DWF, wound fluid; GMCSF, granulocyte macrophage colony-stimulating factor; IFNγ, interferon gamma; IL, interleukin; TNFα, tumor necrosis factor alpha.

and local activity of a variety of resident and migratory cell types that react to a breach in the skin barrier. The composition of wound fluid is therefore broadly assumed to reflect the clinical condition of a wound [26,27]. In the context of this ex vivo study, wound fluid therefore represented the extracellular fluid space within the microenvironment of a diabetic wound. Exposing healthy and impaired/dysfunctional bone marrow stem cells to DWF in vitro enabled an investigation into the paracrine responsiveness of these cells on both molecular and protein level. This study was furthermore the first to demonstrate the efficacy of antioxidant preconditioning in restoring the paracrine function of impaired/dysfunctional stem cells toward that seen under control nonpathological conditions.

Although the ob/ob animal model has been used in numerous studies investigating diabetes-related impaired wound healing [28–31], the endogenous stem cells derived from these animals have not yet been characterized. At baseline, the secretion of proinflammatory cytokines (TNFα, IFNγ) and chemokines (KC, GCSF, and Eotaxin) was more pronounced in the impaired/dysfunctional bone marrow stem cells. These factors all function to amplify the first stage of a wound (inflammatory response), by recruiting neutrophils, lymphocytes, eosinophils, and keratinocytes to the wounded area [5,13,32]. At the mRNA level, a similar pattern was observed; however, only the overexpression of csf1 was significant between healthy versus dysfunctional stem cells and corresponded with higher chemokine (GMCSF) levels detected in the conditioned media. These and other chemokines were already present within the wound microenvironment (DWF) at very high concentrations and the additional release thereof is thus unwanted. Antioxidant preconditioning was able to reduce the secretion of proinflammatory TNFα and IFNγ at baseline, but did not reduce chemokine secretion.

In the context of cell therapy, the paracrine responsiveness of stem cells to the wound microenvironment will determine their effectiveness in promoting healing [3,6,7]. The bone marrow stem cells (healthy and dysfunctional)

responded by upregulating the gene expression and protein secretion of macrophage chemoattractants MCP1 (ccl2) and MIP1α (ccl3). In chronic diabetic wounds, a significant delay in macrophage infiltration related to a deficiency in ccl2 has been demonstrated [33]. Wood et al. [33] furthermore indicated that acute ccl2 treatment could restore the macrophage response and promote healing. This is supported by Yin et al. [34], indicating that the use of scaffolds that actively release MCP1 promoted macrophage infiltration and improved wound healing in a mouse model of streptozotocin-induced diabetes. MCP1 is also known to influence the effector state of macrophages [35], to mediate the angiogenic effect of transforming growth factor beta (TGFβ) by recruiting vascular smooth muscle cells to the endothelium [36], and to recruit/improve the migration of bone marrow MSCs [37]. In this study, preconditioning further enhanced the MCP1 response of all the bone marrow stem cells.

Dysfunctional bone marrow stem cells did, however, have an excessive TNFα response to DWF. TNFα is a potent proinflammatory cytokine that amplifies inflammation through NFκB signaling [38]. Persistent TNFα signaling is known to occur in diabetic wounds [39] and prevents the phenotype switch of macrophages form phagocytic (M1) to pro-regenerative (M2). Ashcroft et al. [40] demonstrated that targeting TNFα in a mouse model (secretory leukocyte protease inhibitor null mice) of severely impaired wound healing-blunted leukocyte recruitment reduced NFκB signaling, altered the M1/M2 macrophage balance, and improved healing. In this study, antioxidant preconditioning of dysfunctional bone marrow stem cells blunted the TNFα response and improved the secretion of anti-inflammatory IL10.

Taken together, these data suggest that the combined ex vivo treatment of autologous stem cells with NAC and AAP could be an effective strategy to restore the paracrine function of impaired bone marrow stem cells before transplantation. This study was, however, done with acute exposure to the pathological microenvironment and future studies should assess whether these cells will retain their restored ability over longer periods of exposure.

Acknowledgments

This research was supported by grants from the National Research Foundation (NRF) (grant no. 105921) and the Harry Crossley foundation. YMA received bursaries from the NRF and the Faculty of Medicine and Health Sciences, Stellenbosch University. We would like to thank Prof. K.H. Myburgh for her insight and role as mentor.

Author Disclosure Statement

No competing financial interests exist.

References

1. van Acker K, P Léger, A Hartemann, A Chawla and MK Siddiqui. (2014). Burden of diabetic foot disorders, guidelines for management and disparities in implementation in Europe: a systematic literature review. Diabetes Metab Res Rev 30:635–645.
2. Ahmad J. (2016). The diabetic foot. Diabetes Metab Syndr 10:48–60.
3. Mulder GD, DK Lee and NS Jeppesen. (2012). Comprehensive review of the clinical application of autologous mesenchymal stem cells in the treatment of chronic wounds and diabetic bone healing. Int Wound J 9:595–600.
4. Wild S, G Roglic, A Green, R Sicree and H King. (2004). Global prevalence of diabetes: estimates for the year 2000 and projections for 2030. Diabetes Care 27:1047–1053.
5. Baltzis D, I Eleftheriadou and A Veves. (2014). Pathogenesis and treatment of impaired wound healing in diabetes mellitus: new insights. Adv Ther 31:817–836.
6. Heublein H, A Bader and S Giri. (2015). Preclinical and clinical evidence for stem cell therapies as treatment for diabetic wounds. Drug Discov Today 20:703–717.
7. Marfia G, SE Navone, C Di Vito, N Ughi, S Tabano, M Miozzo, C Tremolada, G Bolla, C Crotti, et al. (2015). Mesenchymal stem cells: potential for therapy and treatment of chronic non-healing skin wounds. Organogenesis 11:183–206.
8. van de Vyver M. (2017). Intrinsic mesenchymal stem cell dysfunction in diabetes mellitus: implications for autologous cell therapy. Stem Cells Dev 26:1042–1053.
9. van de Vyver M, C Niesler, KH Myburgh and WF Ferris. (2016). Delayed wound healing and dysregulation of IL6/STAT3 signalling in MSCs derived from pre-diabetic obese mice. Mol Cell Endocrinol 426:1–10.
10. Shin L and DA Peterson. (2012). Impaired therapeutic capacity of autologous stem cells in a model of type 2 diabetes. Stem Cells Transl Med 1:125–135.
11. Silva JC, P Sampaio, MH Fernandes and PS Gomes. (2015). The osteogenic priming of mesenchymal stem cells is impaired in experimental diabetes. J Cell Biochem 116: 1658–1667.
12. Zhang B, N Liu, H Shi, H Wu, Y Gao, H He, B Gu and H Liu. (2016). High glucose microenvironments inhibit the proliferation and migration of bone mesenchymal stem cells by activating GSK3β. J Bone Miner Metab 34:140–150.
13. Dreifke MB, AA Jayasuriya and AC Jayasuriya. (2015). Current wound healing procedures and potential care. Mater Sci Eng C Mater Biol Appl 48:651–662.
14. Dulmovits BM and IM Herman. (2012). Microvascular remodeling and wound healing: a role for pericytes. Int J Biochem Cell Biol 44:1800–1812.
15. Martin P and R Nunan. (2015). Cellular and molecular mechanisms of repair in acute and chronic wound healing. Br J Dermatol 173:370–378.
16. Pence BD and JA Woods. (2014). Exercise, obesity, and cutaneous wound healing: evidence from rodent and human studies. Adv Wound Care (New Rochelle) 3:71–79.
17. Ali F, M Khan, SN Khan and S Riazuddin. (2016). N-Acetyl cysteine protects diabetic mouse derived mesenchymal stem cells from hydrogen-peroxide-induced injury: a novel hypothesis for autologous stem cell transplantation. J Chin Med Assoc 79:122–129.
18. Bae SH, H Ryu, K-J Rhee, J-E Oh, SK Baik, KY Shim, JH Kong, SY Hyun, HS Pack, et al. (2015). L-ascorbic acid 2-phosphate and fibroblast growth factor-2 treatment maintains differentiation potential in bone marrow-derived mesenchymal stem cells through expression of hepatocyte growth factor. Growth Factors 33:71–78.
19. Jeong S-G and G-W Cho. (2015). Endogenous ROS levels are increased in replicative senescence in human bone marrow mesenchymal stromal cells. Biochem Biophys Res Commun 460:971–976.

20. Zheng C, B Sui, C Hu and Y Jin. (2015). [Vitamin C promotes in vitro proliferation of bone marrow mesenchymal stem cells derived from aging mice]. Nan Fang Yi Ke Da Xue Xue Bao 35:1689–1693.
21. Antezana M, SR Sullivan, M Usui, N Gibran, M Spenny, J Larsen, J Ansel, N Bunnett and J Olerud. (2002). Neutral endopeptidase activity is increased in the skin of subjects with diabetic ulcers. J Invest Dermatol 119:1400–1404.
22. Spenny ML, P Muangman, SR Sullivan, NW Bunnett, JC Ansel, JE Olerud and NS Gibran. (2002). Neutral endopeptidase inhibition in diabetic wound repair. Wound Repair Regen 10:295–301.
23. Löffler MW, H Schuster, S Bühler and S Beckert. (2013). Wound fluid in diabetic foot ulceration: more than just an undefined soup? Int J Low Extrem Wounds 12:113–129.
24. Schmohl M, S Beckert, TO Joos, A Königsrainer, N Schneiderhan-Marra and MW Löffler. (2012). Superficial wound swabbing: a novel method of sampling and processing wound fluid for subsequent immunoassay analysis in diabetic foot ulcerations. Diabetes Care 35:2113–2120.
25. Feoktistova M, P Geserick and M Leverkus. (2016). Crystal violet assay for determining viability of cultured cells. Cold Spring Harb Protoc 2016:pdb.prot087379.
26. Staiano-Coico L, PJ Higgins, SB Schwartz, AJ Zimm and J Goncalves. (2000). Wound fluids: a reflection of the state of healing. Ostomy Wound Manage 46:85S–93S; quiz:94S–95S.
27. Yager DR, RA Kulina and LA Gilman. (2007). Wound fluids: a window into the wound environment? Int J Low Extrem Wounds 6:262–272.
28. Goren I, E Müller, J Pfeilschifter and S Frank. (2006). Severely impaired insulin signaling in chronic wounds of diabetic ob/ob mice: a potential role of tumor necrosis factor-alpha. Am J Pathol 168:765–777.
29. Ring BD, S Scully, CR Davis, MB Baker, MJ Cullen, MA Pelleymounter and DM Danilenko. (2000). Systemically and topically administered leptin both accelerate wound healing in diabetic ob/ob mice. Endocrinology 141:446–449.
30. Schürmann C, I Goren, A Linke, J Pfeilschifter and S Frank. (2014). Deregulated unfolded protein response in chronic wounds of diabetic ob/ob mice: a potential connection to inflammatory and angiogenic disorders in diabetes-impaired wound healing. Biochem Biophys Res Commun 446:195–200.
31. Stallmeyer B, J Pfeilschifter and S Frank. (2001). Systemically and topically supplemented leptin fails to reconstitute a normal angiogenic response during skin repair in diabetic ob/ob mice. Diabetologia 44:471–479.
32. Behm B, P Babilas, M Landthaler and S Schreml. (2012). Cytokines, chemokines and growth factors in wound healing. J Eur Acad Dermatol Venereol 26:812–820.
33. Wood S, V Jayaraman, EJ Huelsmann, B Bonish, D Burgad, G Sivaramakrishnan, S Qin, LA DiPietro, A Zloza, C Zhang and SH Shafikhani. (2014). Pro-inflammatory chemokine CCL2 (MCP-1) promotes healing in diabetic wounds by restoring the macrophage response. PLoS One 9:e91574.
34. Yin H, G Ding, X Shi, W Guo, Z Ni, H Fu and Z Fu. (2016). A bioengineered drug-Eluting scaffold accelerated cutaneous wound healing In diabetic mice. Colloids Surf B Biointerfaces 145:226–231.
35. Low QE, IA Drugea, LA Duffner, DG Quinn, DN Cook, BJ Rollins, EJ Kovacs and LA DiPietro. (2001). Wound healing in MIP-1alpha(–/–) and MCP-1(–/–) mice. Am J Pathol 159:457–463.
36. Ma J, Q Wang, T Fei, J-DJ Han and Y-G Chen. (2007). MCP-1 mediates TGF-beta-induced angiogenesis by stimulating vascular smooth muscle cell migration. Blood 109: 987–994.
37. Ishikawa M, H Ito, T Kitaori, K Murata, H Shibuya, M Furu, H Yoshitomi, T Fujii, K Yamamoto and S Matsuda. (2014). MCP/CCR2 signaling is essential for recruitment of mesenchymal progenitor cells during the early phase of fracture healing. PLoS One 9:e104954.
38. Liu ZG. (2005). Molecular mechanism of TNF signaling and beyond. Cell Res 15:24–27.
39. Landis RC, BJ Evans, N Chaturvedi and DO Haskard. (2010). Persistence of TNFalpha in diabetic wounds. Diabetologia 53:1537–1538.
40. Ashcroft GS, M-J Jeong, JJ Ashworth, M Hardman, W Jin, N Moutsopoulos, T Wild, N McCartney-Francis, D Sim, et al. (2012). Tumor necrosis factor-alpha (TNF-α) is a therapeutic target for impaired cutaneous wound healing. Wound Repair Regen 20:38–49.

Address correspondence to:
Dr. Mari van de Vyver
Division of Endocrinology
Department of Medicine
Faculty of Medicine and Health Sciences
Stellenbosch University
Cape Town 8000
South Africa

E-mail: vandevyverm@sun.ac.za

Received for publication July 19, 2018
Accepted after revision August 30, 2018
Prepublished on Liebert Instant Online September 6, 2018